UNIVERSITY OF SOUTHAMPTON

FACULTY OF MEDICINE, HEALTH AND BIOLOGICAL SCIENCES

School of Medicine

# The Regulation of Tight Junctions in Colonic Epithelial Cells by Inflammation and Related Cytokines

**Dr Shyam Prasad MA, MB BS, MRCP(UK)**

Thesis for the degree of Doctor of Philosophy

October 2005

# CORRECTION SHEET

UNIVERSITY OF SOUTHAMPTON

ABSTRACT

FACULTY OF MEDICINE, HEALTH AND BIOLOGICAL SCIENCES

SCHOOL OF MEDICINE

Doctor of Philosophy

**The Regulation of Tight Junctions in Colonic Epithelial Cells by Inflammation and Related Cytokines**

**by Shyam Prasad**

The inflammatory bowel diseases (IBD) are associated with an increase in the permeability of the intestinal mucosa. This contributes to the diarrhoea that forms the predominant symptom of active disease. It also facilitates the mucosal penetration of bacterial and food antigens, which stimulate inappropriate or exaggerated immune responses, resulting in inflammation. Tight junctions (TJs) regulate the mucosal barrier by sealing the paracellular space between epithelial cells. Evidence points to disruptions of TJ structure and function in IBD. TJs consist of the transmembrane proteins occludin, junctional adhesion molecules and the claudins. These are linked to large intracellular proteins such as zonula occludens-1 (ZO-1), which themselves are bound to the cell's actin cytoskeleton. Of these constituents, the claudins are of particular interest because each is purported to confer a pattern of resistance or permeability to small ions on the paracellular space. For example, claudin 2 has been demonstrated to confer a high permeability to small cations. This thesis examines the hypothesis that cytokines important in the pathogenesis of IBD impair the barrier function of the intestinal epithelium by inducing alterations in the regulation of TJ proteins.

The expression of TJ proteins in IBD and normal colonic epithelia was examined by immunohistochemistry, western blotting and quantitative reverse transcriptase-mediated polymerase chain reaction. Claudin 2 was strongly expressed in inflamed epithelia, whilst being barely detectable in normal colon. In contrast, claudins 3 and 4, occludin and ZO-1 were highly expressed in normal colon, but were reduced or redistributed in the surface epithelium of many IBD cases. To functionally test the effects of inflammatory cytokines implicated in the pathogenesis of IBD, the T84 cell line was cultured on collagen S-coated, semi-permeable supports to model the epithelial barrier. Measurements of transepithelial electrical resistance (TER) and the passage of uncharged dextran were utilised to monitor permeability. The expression of claudins 2, 3 and 4 was studied by immunofluorescence and western blotting. TER increased over 15 days, correlating positively with the incorporation of claudins 3 and 4 into the TJ, but negatively with the amount of claudin 2 detected. Claudin 2 expression did not correlate with either proliferation or junctional reorganisation after calcium ion depletion and replenishment. Interleukin-(IL-)13 and combined interferon-gamma and tumour necrosis factor-alpha (IFNγ/TNFα) increased permeability to dextran and reduced TER. IFNγ/TNFα led to decreases in claudins 2 and 3 and the redistribution of claudin 4, whereas IL-13 dramatically increased claudin 2 mRNA and protein expression, with little effect on claudins 3 and 4. The effects of IL-13 on TER and claudin 2 mRNA and protein levels could be inhibited by co-incubation with Ly294002, an inhibitor of phosphatidylinositol-3-kinase.

This is the first demonstration that IBD is associated with alterations in claudin expression, particularly an increase in claudin 2. Similar alterations can be induced *in vitro* by cytokines. Thus, cytokine-induced alterations in claudin expression may contribute to the pathogenesis and symptoms of IBD.

# CONTENTS

## FIGURES

# ACKNOWLEDGEMENTS

Firstly, I would like to acknowledge my supervisors, Dr Jane Collins and Professor Tom MacDonald.

Secondly, I would like to acknowledge those whose work contributed to this thesis: Dr Katri Kaukinen, who performed the immunohistochemical staining for the claudins; Roberto Mingrino, who isolated the tissue epithelial cells from one case used in Western blotting and four cases used in qRT-PCR, and who performed the RNA extraction from tissue epithelial cells.

Thirdly, I wish to thank those whose assistance proved invaluable in the successful generation of results: Penny Johnson, who taught me the procedure for immunohistochemistry; Kate Hayes, who demonstrated to me the techniques of cell culture, transepithelial resistance measurement and immunofluorescence staining; Roger Alston, who taught me the skills of successful confocal microscopy; Dr Robert Powell, who showed me the route to successful qRT-PCR.

Fourthly, I wish to acknowledge and emphasise the profound debt of gratitude I owe to my wife, Katriina Knight, whose support and forbearance not only provided a perfect atmosphere in which to develop this work, but also illustrated those traits of character which can lead one to mental poise and equanimity. I dedicate this thesis to you and to our child, Ashok, whose birth we will forever recall as the most joyful moment of this period.

# ABBREVIATIONS

| | |
|---|---|
| AAD | amino-actinomycin D |
| ABC | active beta-catenin |
| AJ | adherens junction |
| ANOVA | One-Way Analysis of Variance |
| APC | adenomatous polyposis coli |
| ATP | adenosine triphosphate |
| BCA | bicinchoninic acid |
| BSA | bovine serum albumin |
| C- | carboxy- |
| CAR | cell adhesion recognition |
| CARD | caspase recruitment domain |
| CD | Crohn's disease |
| CDK | cell division kinase |
| Cdx | caudal-related homeodomain |
| CK2 | casein kinase 2 |
| cDNA | complementary deoxyribonucleic acid |
| CRB1 | Crumbs 1 |
| CT | calculated threshold |
| DJ | desmosome |
| DMEM | Dulbecco's Modified Eagle Medium |
| DMSO | dimethyl sulphoxide |
| DNA | deoxyribonucleic acid |
| dNTP | deoxyribonucleoside triphosphates |
| D-PBS | Dulbecco's phosphate-buffered saline |
| DPX | xylene/dibutyl phthalate |
| DTT | dithiothreitol |
| EDTA | ethylenediaminetetraacetic acid |
| EGF | epidermal growth factor |
| ELISA | enzyme-linked immunosorbant assay |
| EMSA | electromobility shift assay |
| ERK | extracellular signal-related |
| F-actin | filamentous actin |
| FBS | fetal bovine serum |
| FITC | fluorescein isothiocyanate |

| | |
|---|---|
| GAPDH | glyceraldehyde 3-phosphate dehydrogenase |
| GFP | green fluorescent protein |
| GMA | glycol methacrylate |
| GSK | glycogen synthase kinase |
| GTP | guanosine triphosphate |
| HBSS | Hank's Balanced Salt Solution |
| HK | housekeeping genes |
| HNF | hepatocyte nuclear factor |
| HRP | horseradish peroxidase |
| IBD | inflammatory bowel disease |
| IFN | interferon |
| Ig | immunoglobulin |
| IL | interleukin |
| IRS | insulin receptor substrate |
| JAK | Janus kinases |
| JAM | junctional adhesion molecule |
| kDa | kilodalton |
| LASER | light amplification by stimulated emission of radiation |
| LDH | lactate dehydrogenase |
| LFA-1 | lymphocyte-function-associated protein 1 |
| Lef | lymphoid-enhancing factor |
| M | moles per litre |
| MAGI | membrane-associated guanylate kinase-inverted |
| MAGUK | membrane-associated guanylate kinase homologue |
| MAPK | mitogen-activated protein kinase |
| MDCK | Madin-Darby Canine Kidney |
| MDP | muramyl dipeptide |
| mM | millimoles per litre |
| mRNA | messenger ribonucleic acid |
| MUPP1 | multi-PDZ domain protein 1 |
| μM | micromoles per litre |
| N- | amino- |
| NADH | nicotinamide adenine dinucleotide |
| NCBI | national center for biotechnology information |
| NFkB | nuclear factor kappa B |
| NKT | natural-killer T |

| | |
|---|---|
| nM | nanomoles per litre |
| NSAID | non-steroidal anti-inflammatory drugs |
| PAGE | polyacrylamide gel electrophoresis |
| Pals | protein associated with Lin-seven |
| PAR | partitioning-defective |
| PATJ | PALS1-associated tight junction protein |
| PBS | phosphate-buffered saline |
| PBS-T | phosphate-buffered saline-Tween |
| PCR | Polymerase Chain Reaction |
| PDK | phosphatidylinositol-3,4,5-triphosphate-dependent kinase |
| PDZ | post-synaptic density-90/discs large/ZO-1 |
| PEG | polyethylene glycol |
| PI3K | phosphatidylinositol 3-kinase |
| PLC | phospholipase C |
| PRR | pattern-recognition receptor |
| PVDF | polyvinylidene difluoride |
| RNA | ribonucleic acid |
| RT | reverse transcriptase |
| SAF-B | scaffold attachment factor-B |
| SDS | sodium dodecyl sulphate |
| SH3 | Src homology 3 |
| SEM | standard error of the mean |
| STAT | signal transducer and activator of transcription |
| TBS | Tris-buffered saline solution |
| TCF | T-cell factor |
| TER | transepithelial electrical resistance |
| TGF-β | transforming growth factor-beta |
| Th | T-helper |
| TJ | tight junction |
| $T_m$ | melting temperature |
| TNF | tumour necrosis factor |
| TPA | 12-O-tetradecanoylphorbol-13-acetate |
| UBC | ubiquitin C |
| UC | ulcerative colitis |
| ZO | zonula occludens |
| ZONAB | ZO-1-associated nucleic acid-binding protein |

# CHAPTER 1

# INTRODUCTION

# 1.1 BACKGROUND

## 1.1.1 THE DISEASES

### 1.1.1.1 INTRODUCTION

Inflammatory disorders of the intestine are responsible for an enormous burden of disease worldwide. Gastrointestinal infections are responsible for millions of deaths each year, particularly amongst children and the elderly. However in the United Kingdom and the West death or long-term sequelae are uncommon following infection, and it is chronic, non-infectious, inflammatory disease that contributes predominantly to the overall morbidity due to intestinal disease. Coeliac disease, or gluten enteropathy, is the commonest, but the suffering it causes is slight as the causes are known and effective treatment is available. Inflammatory bowel disease causes a degree of suffering matched by few others disorders, particularly as current therapies are only partially efficacious. In addition, some patients have disease refractory to current treatment strategies. IBD forms the main focus of this thesis.

### 1.1.1.2 INFLAMMATORY BOWEL DISEASE

Inflammatory bowel disease (IBD) describes a group of disorders of the digestive tract that includes Crohn's disease (CD) and ulcerative colitis (UC). The similarities between these diseases, both clinically and pathologically, make distinguishing between them sometimes difficult; ten per cent of IBD cases acquire the term 'indeterminate colitis' for at least part of their course (Farmer et al., 2000; Meucci et al., 1999; Russel et al., 1998; Shivananda et al., 1991; Shivananda et al., 1996). Both disorders are thought to be due to an abnormal response to a component of the intestinal bacterial flora in a genetically predisposed host (Farrell and Peppercorn, 2002; Shanahan, 2002). This abnormal response may be a dysregulated immune response or loss of tolerance to bacterial antigens, or an abnormal increase in gut permeability due to exogenous or endogenous factors (see below). IBD is characterised by chronic relapsing inflammation of the intestine, resulting in the symptoms of diarrhoea, urgency to pass blood and/or mucus per rectum, abdominal pain, anorexia, weight loss and fever. Numerous extra-intestinal or systemic features may occur, for example arthritis, sacro-iliitis, erythema

nodosum and other rashes, iritis and other ocular inflammations, sclerosing cholangitis and liver disease. IBD is also associated with many other (predominantly autoimmune) diseases (Snook et al., 1989). Long-term extensive colonic inflammation is associated with a substantially increased risk of malignant change, particularly in UC (Langholz et al., 1992; Munkholm et al., 1993).

The prevalence of UC is about 160 per 100,000 and that of CD about 50 per 100,000. It is estimated that there are 100-200,000 sufferers in the UK. The incidence of CD has risen five-fold in northern Europe over the last fifty years, whilst that of UC has only risen slightly (Barton et al., 1989; Kyle, 1992; Rose et al., 1988). The reasons for this are unclear. IBD presents most commonly amongst young adults, particularly CD, and males and females are equally affected.

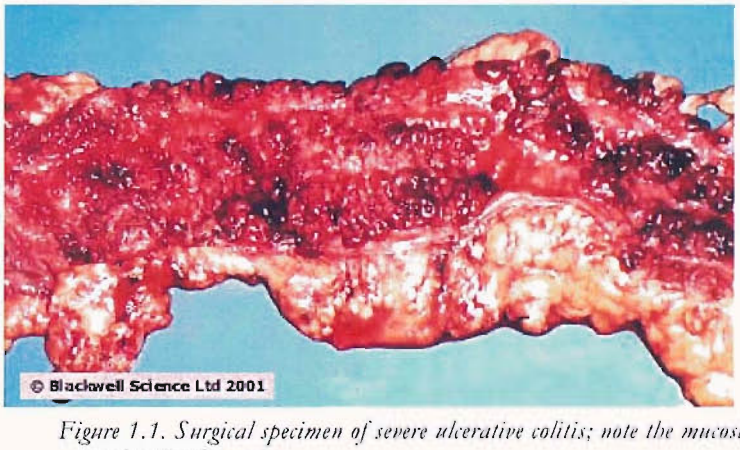


*Figure 1.1. Surgical specimen of severe ulcerative colitis; note the mucosal necrosis and pseudopolyp formation*

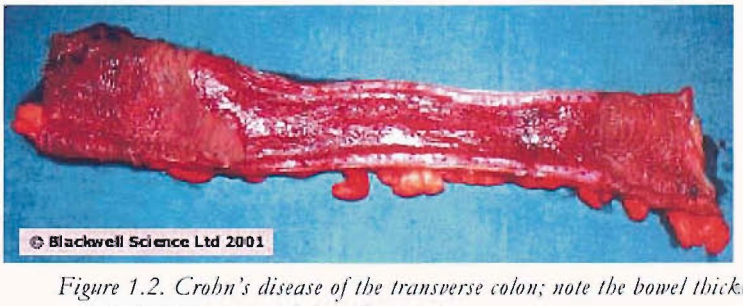


*Figure 1.2. Crohn's disease of the transverse colon; note the bowel thickening and the discontinuous nature of the inflammation.*

### 1.1.1.3 PATHOLOGY OF ULCERATIVE COLITIS

UC is characterised by continuous inflammation extending proximally from the rectum but confined to the colon (Ament, 1975; Shepherd, 1991; Wright, 1970). The inflammation is superficial, affecting the mucosa and occasionally the submucosa. Fine or linear ulceration is a common feature, and the infiltrated lamina propria becomes oedematous and haemorrhagic. The inflammatory infiltrate consists mainly of polymorphs, plasma cells, lymphocytes and eosinophils. Gland destruction and crypt abscesses are common. Damage to epithelial cells is associated with epithelial cell proliferation, leading to an overall increase in cell turnover. Apoptosis also contributes to epithelial cell loss. Long-standing disease may lead to the formation of hyperplastic, inflamed mucosa (pseudopolyps; see figure 1.1), and sometimes epithelial dysplasia or cancer.

### 1.1.1.4 PATHOLOGY OF CROHN'S DISEASE

Crohn's disease may occur anywhere in the gastrointestinal tract, although the most common pattern is an ileocolitis (Ament, 1975; Tanaka and Riddell, 1990). The disease is often discontinuous. The bowel is thickened and fibrosed (figure 1.2) due to a transmural inflammation, and strictures can thus form. Aphthous, large, or deep fissuring ulcers are common, and fistula formation to skin, other organs or other intestinal segments may result. The inflammatory infiltrate consists mainly of lymphocytes, tissue macrophages and plasma cells, and in half of cases granulomas form. There is marked tissue destruction but the mucosal architecture is relatively well preserved.

### 1.1.1.5 AETIO-PATHOGENESIS OF IBD

As stated earlier, two important components in the aetiology of IBD are a genetic predisposition and an abnormal immune or inflammatory response to bacterial antigens. However, these components are likely to be closely linked, and it is more helpful to conceptualise the disease as the result of a series of linked processes, any of which may be dysfunctional in a given case and lead to an exaggerated response. This concept is

illustrated in figure 1.3. One or more environmental triggers on a predisposing genetic background lead to a vicious cycle of exaggerated or uncontrolled immune responses to bacterial antigens. This causes a perturbation of the epithelial barrier, which results in further exposure of the immune system to the luminal bacterial flora.

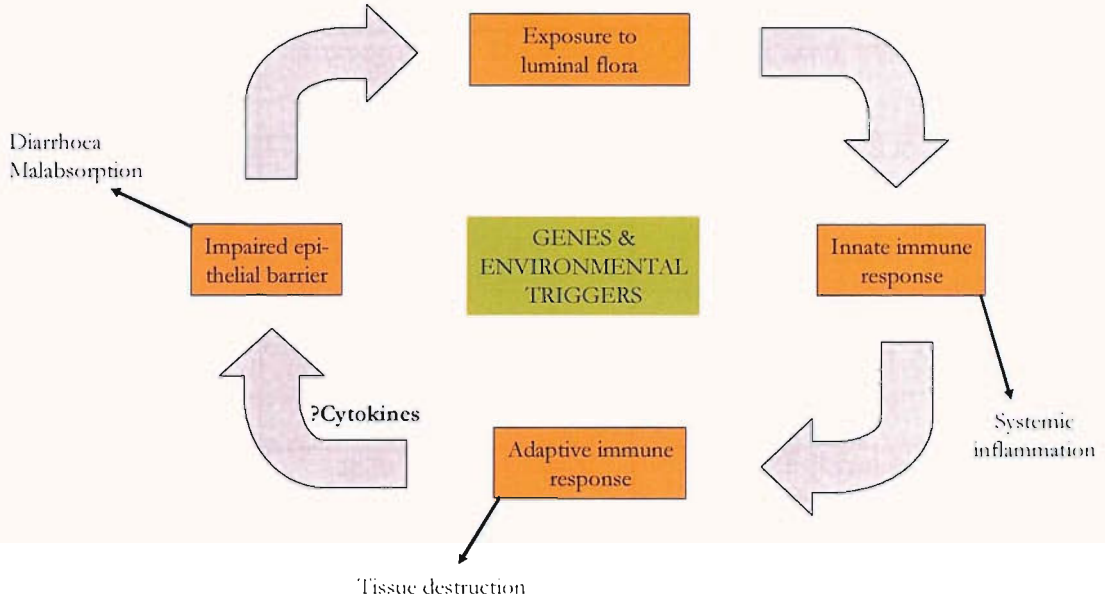


*Figure 1.3. Diagram to illustrate the vicious cycle of the pathogenesis of IBD.*

### *1.1.1.5.1 Genetics of IBD*

Although there is an inherited predisposition to IBD, this does not follow a Mendelian pattern (Bonen and Cho, 2003). UC carries a ten-fold increased risk among first-degree relatives of patients, for example, but no increased risk among spouses (Farrell and Peppercorn, 2002). The concordance rate for monozygotic twins is 44% for CD, 6-14% for UC, but 4% for dizygotic twins (Orholm et al., 2000; Thompson et al., 1996; Tysk et al., 1988). The genes that predispose to IBD have not been fully described. Several loci within the genome have been shown to associate with IBD (Bonen and Cho, 2003). Although CD and UC share some susceptibility genes, some loci associate with CD rather than UC. Others associate with different distributions of CD within the gastrointestinal tract, with different pathological features of CD (fibrosis

and stenosis versus inflammation and fistulation), or with an aggressive clinical course (Bonen and Cho, 2003). Many of the candidate genes at these loci are related to aspects of the inflammatory or immune responses; the major loci are summarised in table 1.1. Efforts are currently underway to delineate which are the important genes and mutations at each site, and how much they contribute to the pathogenesis.

| IBD locus designation | Chromosomal Location | Diagnoses | Candidate genes within or near locus |
|---|---|---|---|
| *IBD1* | 16q12 | CD | NOD2 |
| *IBD2* | 12q13 | UC | VDR, IFN-γ |
| *IBD3* | 6p13 | UC > CD | MHC I and II, TNF-α |
| *IBD4* | 14q11 | CD | TCR α/δ complex |
| *IBD5* | 5q31–33 | CD | OCTN, IL-3, IL-4, IL-5, IL-13, CSF-2 |
| *IBD6* | 19p13 | CD, UC | ICAM-1, C3, TBXA2R, LTB4H |
| Other loci | 1p36 | CD, UC | TNF-R family, CASP9 |
| Other loci | 7q | UC > CD | MUC-3 |
| Other loci | 3p | UC > CD | HGFR, EGFR, GNA12 |
| Other loci | 10q23 | CD | DLG5 |
| Other loci | 9q32-33 | CD, UC | TLR4 |

*Table 1.1. Major susceptibility loci in IBD. VDR, vitamin D receptor; IFN, interferon; MHC, Major Histocompatibility Complex; TNF, tumour necrosis factor; TCR, T-cell receptor; OCTN, organic cation transporter cluster; IL, interleukin; CSF, cerebrospinal fluid; ICAM, intercellular adhesion molecule 1; TBXA2R, thromboxane A2 receptor; LTBH4H, leukotriene B4 hydroxylase; TNF-R, TNF receptor; CASP, caspase; MUC3, mucin 3; HGFR, hepatocyte growth factor; EGFR, epidermal growth factor; GNA12, inhibitory guanine nucleotide-binding protein; DLG5, discs-large 5; TLR4, toll-like receptor 4. Adapted from Bonen and Cho (2003).*

Evidence strongly implicates variants in the gene for NOD2/CARD15 on chromosome 16 in a small proportion (approximately 18%) of the genetic predisposition to Crohn's disease (Hampe et al., 2001; Hugot et al., 2001; Ogura et al., 2001). This gene is expressed within monocytes, epithelial cells and Paneth cells, where it encodes a cytosolic pattern-recognition receptor (PRR) to muramyl dipeptide (MDP, a bacterial cell wall component) (Inohara et al., 2003; Tanabe et al., 2004). The current model of NOD2 suggests that its role in recognising MDP is to limit the activation of

nuclear factor kappa B (NFkB) by Toll-like Receptor 2 (another PRR for MDB) (Netea et al., 2004; O'Neill, 2004; Van Heel et al., 2001). NFkB is a key transcriptional factor in the initiation of immune and inflammatory responses (Mahida and Johal, 2001; Schreiber et al., 1998). Furthermore, epithelial cells carrying a mutated form of NOD2 are less able to resist invasion by bacteria in experimental systems (Hisamatsu et al., 2003).

Very recently further gene mutations have been associated with IBD. These include the cation transporter genes OCTN 1 and 2 (Peltekova et al., 2004), TLR4 (Franchimont et al., 2004), which encodes another bacterial pattern-recognition receptor and, interestingly, DLG5 (Stoll et al., 2004). Whereas the mutations in TLR4 and DLG5 appear to associate independently with both CD and UC, mutations in the OCTN genes only confer an increased risk of CD. This risk is increased further in those who also carry a mutation in NOD2, giving a relative risk of approximately 10 if a mutation is carried in both. Similarly, the association of mutations in DLG5 with IBD as a whole or CD in particular is stronger in the presence of a mutation in NOD2, although no relative risks are quoted. DLG5 encodes a protein containing several protein-protein binding domains (Wakabayashi et al., 2003). It has recently been co-immunoprecipitated with β-catenin (Wakabayashi et al., 2003), a component of the adherens junction (see 1.2.2.3), but its cellular location and function in humans are not yet known. However DLG5 homologues in other species are involved in processes such as cell polarity and control of proliferation (Humbert et al., 2003). Its similarity to other proteins involved in the structure and function of the epithelial permeability barrier has led to speculation that dlg5 defects may contribute to altered epithelial permeability (Stoll et al., 2004).

It is therefore unlikely that a single gene or gene cluster is responsible for the entire genetic contribution to IBD, but more probable that several distinct alleles carried by an individual combine to predispose to a particular disease pattern. Some of these genes, such as DLG5, may be associated with defects in the function of the epithelial barrier. Furthermore, these multiple predispositions may underlie the greater-than-expected concordance for site and clinical type of CD within particular families, suggesting multiple, distinct forms of the disease (Bayless et al., 1996).

#### *1.1.1.5.2 Environmental Precipitants and Risk Factors in IBD*

The environmental triggers for IBD are not well-described. Nevertheless, there is strong evidence to support the idea that the use of Non-Steroidal Anti-Inflammatory Drugs (NSAIDs) can provoke exacerbations of IBD and, possibly, its initial onset. These drugs are known from human and animal studies to disturb gut barrier function and lead to an increase in its permeability (Bjarnason and MacPherson, 1994).

Cigarette smoking is associated with an increased risk of CD, but a reduced risk of UC (Danese et al., 2004). However, the mechanisms underlying this are unknown.

Psychological stress is cited as a potential trigger of exacerbations by up to 40% of UC patients and stress has been shown to precipitate relapses of colitis in some animal models (Danese et al., 2004; Hollander, 2003). Studies have shown that stress can increase intestinal permeability in rodents (Kiliaan et al., 1998; Meddings and Swain, 2000; Soderholm and Perdue, 2001).

#### *1.1.1.5.3 The Intestinal Bacterial Flora in IBD*

Numerous lines of evidence implicate the luminal bacterial flora in the onset of IBD. For example, all of the rodent models of IBD require luminal bacteria to develop the phenotype (Blumberg et al., 1999; Wirtz and Neurath, 2000). Human IBD occurs mostly in the regions of the alimentary canal with the highest bacterial concentrations (Sartor, 1997). Diversion of the faecal stream proximal to an area of inflammation can lead to its resolution (Shanahan, 2002), implicating the luminal contents. Sometimes antibiotics can be helpful in ameliorating flares of IBD (Turunen et al., 1998).

Evidence points to a loss of tolerance towards otherwise harmless enteric bacteria in active IBD (Duchmann et al., 1995). Although less than half of the four hundred or more species of bacteria in the intestinal lumen have been characterised, studies in rodents (Madsen et al., 2000; Rath et al., 1996; Rath et al., 1999; Rath et al., 2001) and on human tissue (Edmiston, Jr. et al., 1982; Hartley et al., 1992; Hudson et al., 1984; Poxton et al., 1997; Swidsinski et al., 2002) strongly suggest the predominant species in the colons of cases of IBD do not differ from those found in normals. Recently, however, adherent-invasive types of *E.coli* have been detected at a much higher frequency in the mucosa of patients with active IBD than in normal controls

(Darfeuille-Michaud et al., 1998; Darfeuille-Michaud et al., 2004; Glasser et al., 2001; Martin et al., 2004). Others have found much higher mucosal concentrations of bacteria in general in IBD (Swidsinski et al., 2002). The *E.coli* strains isolated from IBD mucosa may display an enhanced ability to activate NFkB in intestinal epithelial cells (La Ferla et al., 2004). However, it is not yet clear if this is due to differences in the bacterial flora, differences in the resistance of the epithelium or mucosa generally, or an effect of inflammation on mucosal resistance.

#### *1.1.1.5.4 Immunological Defects in IBD*

There are many proposed immunological defects in IBD (Monteleone and MacDonald, 2000; Shanahan, 2002). It is not known if these are primary defects or if they occur in response to initiation of the disease process by, for example, a defective mucosal barrier. These abnormal responses, however, lead to the common clinical and pathological features of IBD, such as systemic inflammation, tissue destruction and fibrosis.

From the numerous rodent models of intestinal inflammation and many studies of patient-derived material, a large body of sometimes conflicting evidence has emerged on the immunological impairments found in IBD. The impairments fall into three main categories, which are not mutually exclusive. Firstly, it is proposed that the innate immune system (antigen-presenting cells, macrophages, natural killer cells and epithelial cells) is defective in some way (Korzenik and Dieckgraefe, 2000). Either it fails to resist luminal bacteria, leading to excessive and prolonged activation of the adaptive immune system, or excessive signalling within the cells of the innate immune system leads to excessive recruitment and activation of the adaptive immune system. Secondly, it has been suggested that there is an exaggerated response by the adaptive immune system to the normal stimuli it receives continuously (James, 1988). The mucosal immune system develops in tandem with the absorptive surface and the luminal bacteria (MacDonald, 2003), and it is said to be normally in a state of controlled activation (Pickard et al., 2004). In IBD this level of activation is proposed to be heightened (James, 1988). Thirdly, it has been proposed that the normal regulatory mechanisms for controlling or suppressing the responses of the adaptive immune system are defective in IBD, leading to an exaggerated response to a minor or innocuous stimulus, or to loss of the usual tolerance to commensal bacterial antigen (James et al., 1987; Strober and James, 1986).

Evidence to support defective innate immunity includes the genetic mutations in PRRs described earlier. Furthermore, some children with defects of phagocyte function, such as chronic granulomatous disease or glycogen storage disease type 1b, develop a CD-like enteritis that is ameliorated by boosting phagocyte function (Winkelstein et al., 2000). The therapeutic agent Granulocyte-Monocyte Colony Stimulating Factor (GM-CSF), which boosts bone marrow production of phagocytes, is currently in phase 3 of development as a treatment in IBD (Dieckgraefe and Korzenik, 2002). In addition, if one considers the intestinal epithelium to form part of the innate immune system, there is strong evidence to support impairment of epithelial barrier function in the pathogenesis of IBD (discussed in 1.3).

Much of the evidence strongly supports the second contention of an exaggerated adaptive immune response to enteric antigens. This evidence derives from three main sources: studies of tissue and cells derived from human patients, studies on rodent models of disease, and, more recently, studies of the effects in human patients of inhibiting specific cytokines using monoclonal antibodies. A large body of evidence supports the idea that the proinflammatory cytokine Tumour Necrosis Factor-alpha (TNFα) is a key factor in IBD. TNFα is produced mainly by macrophages, which are found in excess in the lamina propria in disease. The number of TNFα-positive cells, the amount of TNFα produced after stimulation of lamina propria cells ex vivo, the mucosal concentration of TNFα and the abundancy of TNFα transcripts are all elevated in IBD (Andus et al., 1993; MacDonald et al., 1990; Masuda et al., 1995; Murch et al., 1993; Nielsen et al., 1993; Reinecker et al., 1993; Woywodt et al., 1994). Furthermore, an antibody specific for TNFα, recently introduced as a therapeutic agent in CD, has produced dramatic improvements in the majority of those who receive it (Gordon and MacDonald, 2003). However, at least 20% of patients are refractory to this intervention and many patients relapse, suggesting that other pathways can develop to sustain the inflammation.

In the case of CD, T lymphocytes that display a T-helper-1 phenotype appear to play a prominent role. T-helper 1 ($Th_1$) differentiation, which is driven by macrophage-derived interleukin-(IL-)12, is associated with the secretion of a repertoire of cytokines, such as interferon-gamma (IFNγ) and interleukin-2 (IL-2), that are thought to be key to the development of cell-mediated immunity (Strober et al., 2002). The number of IFNγ-positive cells and the abundancy of IFNγ transcripts have been shown to be elevated in

the intestinal mucosa in both CD and UC (Breese et al., 1993). The amount of IFNγ produced after stimulation of lamina propria T-helper cells *ex vivo* is also significantly higher in CD than in controls (Fais et al., 1991; Fuss et al., 1996), although this has not been demonstrated in UC. The number of cells secreting IL-2 and the abundancy of transcripts are also increased in CD, but not in UC (Mullin et al., 1992). Collectively, this evidence supports the notion of CD being perpetuated by $Th_1$-type mechanisms.

Although there is a massive infiltration of T cells into the lamina propria in UC, their role is not well understood. It has been suggested that UC is a $Th_2$-mediated disease (Strober et al., 2003). This is a T-cell differentiation pathway commonly seen in responses to parasites. It is associated with the secretion of certain cytokines, such as IL-4, IL-5 and IL-13, and with antibody-mediated responses (Strober et al., 2002). In support of the latter, there is a large plasma cell infiltrate in UC (Kett et al., 1987). Furthermore, production of antibodies specific for self or bacterial antigens is common in UC (Das et al., 1993; Saxon et al., 1990), but it is not clear whether these antibodies are pathogenic. In relation to $Th_2$-type cytokines, however, there is little evidence that IL-4 levels are increased in UC (Fuss et al., 1996). Modest elevations in secreted IL-5 have been demonstrated when lamina propria T cells from UC patients are stimulated *ex vivo* (Fuss et al., 1996). However, much more interest has been generated by the possible role of IL-13 in the pathogenesis of UC. Oxazolone-induced colitis, a murine model of inflammation closely resembling UC, results from the induction of IL-13-producing natural-killer T (NKT) cells, a subset of lamina propria lymphocytes (Heller et al., 2002). Blockade of IL-13 or elimination of NKT cells can prevent the colitis from developing. The chronic inflammation of the colitis that develops in IL-10-deficient mice is also associated with elevated production of IL-13 by lamina propria mononuclear cells (Spencer et al., 2002). In human IBD IL-13 mRNA is considerably more abundant in UC mucosa than in normal mucosa (Inoue et al., 1999). However, attempts to measure IL-13 protein levels by enzyme-linked immunosorbant assays (ELISAs) on supernatants of cultured biopsies have not shown increases over normal (Kadivar et al., 2004; Vainer et al., 2000), although this may be a feature of the methodology. Indeed, a recent study has shown clearly that stimulation of a subset of NKT cells from UC cases induces them to produce substantially greater amounts of IL-13 compared to controls (Fuss et al., 2004). These cells were cytotoxic to a cultured epithelial cell line and this cytotoxicity was augmented by IL-13.

Significantly increased expression of the inflammatory cytokine IL-17 has recently been demonstrated in the mucosa and serum of patients with UC and CD (Fujino et al., 2003; Nielsen et al., 2003). IL-17 is thought to be important in mucosal inflammation and is secreted predominantly by T cells (particularly memory cells) and monocytes/macrophages (Jovanovic et al., 1998; Yao et al., 1995). Its receptor is found on many cell types, including epithelial cells (Yao et al., 1997). IL-17 strongly induces genes associated with inflammation (e.g. IL-6) and enhances the proinflammatory responses induced by TNFα (Jovanovic et al., 1998). Like TNFα, it seems to work by activating NFκB (Awane et al., 1999). However, in colonic subepithelial myofibroblasts IL-17 can downregulate responses to TNFα (Andoh et al., 2002).

In recent years some investigators have challenged the traditional Th1-Th2 paradigm and instead proposed new models involving both clusters of cytokines. In these models the inflammatory process is separated into two phases – an initial inductive phase and a subsequent effector phase characterised by chronic inflammation. It has been proposed that Th1 and Th2 pathways and cytokines may be involved in each phase, either concomitantly or sequentially (Cominelli, 2004; Reuter and Pizarro, 2004).

The third contention outlined above was that there is a defect in the regulation of immune responses in IBD. Whereas in most people immune responses to self-antigens or their bacterial flora are suppressed, it has been proposed that these mechanisms are defective in IBD. The two major mechanisms involved are induction of oral tolerance, by which reactive effector T-cell clones are deleted or made anergic (unresponsive), or suppression of immune responses by a separate subset of regulatory T-cells. Oral tolerance is very difficult to study in humans as it is induced mainly in young childhood. Nevertheless a single study has supported the idea of loss of tolerance by showing that CD patients' T-cells proliferate and produce cytokines in response to extracts of their own flora in vitro, whereas control T-cells do not (Duchmann et al., 1995).

The best-described regulatory T-cell is the $CD4^+CD25^+$ T-cell (Sakaguchi et al., 1995). $CD4^+CD25^+$ cells are specific for self-antigens (Jordan et al., 2001) and produce cell-surface and secretory TGF-β after stimulation (Nakamura et al., 2001). TGF-β is a key inhibitor of immune responses and appears to interfere with successful NFkB signalling, for example that stimulated by TNFα (MacDonald and Monteleone,

unpublished). In CD lamina propria mononuclear cells appear to be unresponsive to TGF-β, and levels of Smad7, a known repressor of TGF-β signalling, are elevated (Monteleone et al., 2001). Interfering with Smad7 expression in vitro appears to restore successful TGF-β-stimulated suppression of cytokine secretion (Monteleone et al., 2001).

#### *1.1.1.5.5 Summary*

One of the consequences of an exaggerated immuno-inflammatory response, from whatever cause, may be an impairment of gut barrier function (Almer et al., 1993). Furthermore, a defective gut barrier may lead to greater access of the bacterial flora to the cells of the immune system and a still heightened immune reponse, thus setting off a vicious cycle. As discussed earlier, impaired barrier function may be both the mechanism by which certain environmental agents (NSAIDs, stress) provoke episodes of IBD, and the phenotype generated by one or more of the genetic predispositions to IBD (e.g. DLG5). This barrier function is performed by the intestinal epithelium. Its structure, function, regulation and impairment in IBD are discussed below.

## 1.2 THE INTESTINAL EPITHELIAL BARRIER

### 1.2.1 OVERVIEW

The intestine is lined by a single layer of billions of tightly adherent cells. It forms a barrier that is selectively permeable to the toxins, pathogens and macromolecules of the 'external' world of the gut lumen. A number of proteins are involved in connecting cells together to maintain and regulate this barrier (so-called 'gate' function). These proteins aggregate into discrete junctions at the lateral cell membrane, visible by electron and light microscopy (reviewed in Knust and Bossinger, 2002). These include the tight junction (or zonula occludens), adherens junction (or zonula adherens), desmosome, and gap junction (see figure 1.4) (Collins, 2002). Furthermore, tight junctions prevent lateral movement of lipids and glycoproteins within the outer leaflet of the cell membrane and thus cause a degree of compartmentalisation within the lateral membrane (so-called 'fence' function) (Matter and Balda, 2003; Schneeberger and Lynch, 2004). Tight junction and adherens junction-mediated adhesion is dynamic and can be relaxed when necessary, for example when cells proliferate and migrate to repair a wound, and these junctions are bound to the actin cytoskeleton (Jamora and Fuchs, 2002; Schneeberger and Lynch, 2004). In the face of significant frictional forces from luminal contents and the stresses induced by continual peristaltic movements, significant cohesive strength is imparted to the layer by the binding of desmosomes to the keratin intermediate filament system (Garrod et al., 2002). Gap junctions are responsible for electrical coupling within entire sheets of cells by allowing small ions to pass between them (Evans and Martin, 2002). Finally, growing evidence has recently emerged of a role for junctional components in cellular signalling processes, particularly outside-in signalling (Balda and Matter, 2003; Green and Gaudry, 2000; Jamora and Fuchs, 2002).

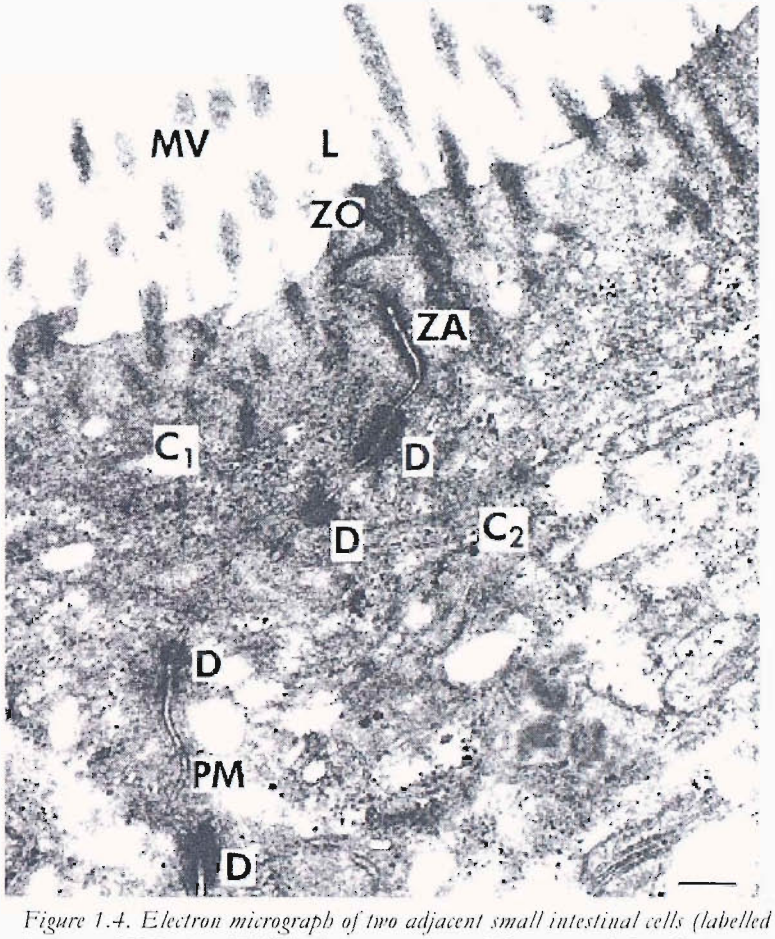


*Figure 1.4. Electron micrograph of two adjacent small intestinal cells (labelled $C_1$ and $C_2$). L:lumen;MV:microvilli;PM:plasma membrane;ZO:zona occludens;ZA:zona adherens;D:desmosome. (Reproduced with permission of Dr J.E.Collins)*

## 1.2.2 STRUCTURE AND FUNCTION OF THE JUNCTIONS

### 1.2.2.1 STRUCTURE OF THE TIGHT JUNCTION

A feature common to epithelial cell-cell junctions is their division into integral membrane proteins, which adhere to the same or similar proteins displayed by adjacent cells, and cytoplasmic proteins, which form the links between the transmembrane proteins and the cytoskeleton. The subapical zonular junctional complex comprises the tight junction (TJ), which seals the paracellular space (Matter and Balda, 2003; Schneeberger and Lynch, 2004), and the adherens junction (AJ), which is adhesive (Jamora and Fuchs, 2002; Nagafuchi, 2001). The major integral membrane proteins of the TJ include the claudin family, occludin and Junctional Adhesion Molecule. The cytoplasmic, junction-associated proteins include the membrane-associated guanylate kinase homologues (MAGUK proteins) ZO-1, ZO-2 and ZO-3, cingulin and a growing list of other molecules (Gonzalez-Mariscal et al., 2003; Schneeberger and Lynch, 2004). Some important features of these proteins are discussed below.

#### *1.2.2.1.1 Claudins*

The claudin multi-gene family comprises at least 23 members (Katoh and Katoh, 2003; Turksen and Troy, 2004; Tsukita and Furuse, 2000a). They encode proteins of approximately 23kDa whose proposed common structure is illustrated in figure 1.5. Hydrophilicity analysis led to the proposed four transmembrane domain structure (Furuse et al., 1998a). A carboxy-terminal tyrosine-valine motif binds the MAGUK proteins ZO-1, ZO-2 and ZO-3 (Itoh et al., 1999a), thus anchoring the claudins within the TJ. Claudins 1 and 8 have also been shown to bind the MAGUK protein MUPP1 (Hamazaki et al., 2002; Jeansonne et al., 2003), but little is known about the function of MUPP1 or the significance of this interaction. The carboxy-terminus of claudin 1 can interact with the eighth PDZ domain of PALS1-associated tight junction protein (PATJ) (Roh et al., 2002a). This protein interacts with protein associated with Lin-seven (Pals1) and Crumbs 1 (CRB1) to form a TJ complex involved in epithelial cell polarity (Roh et al., 2002b).

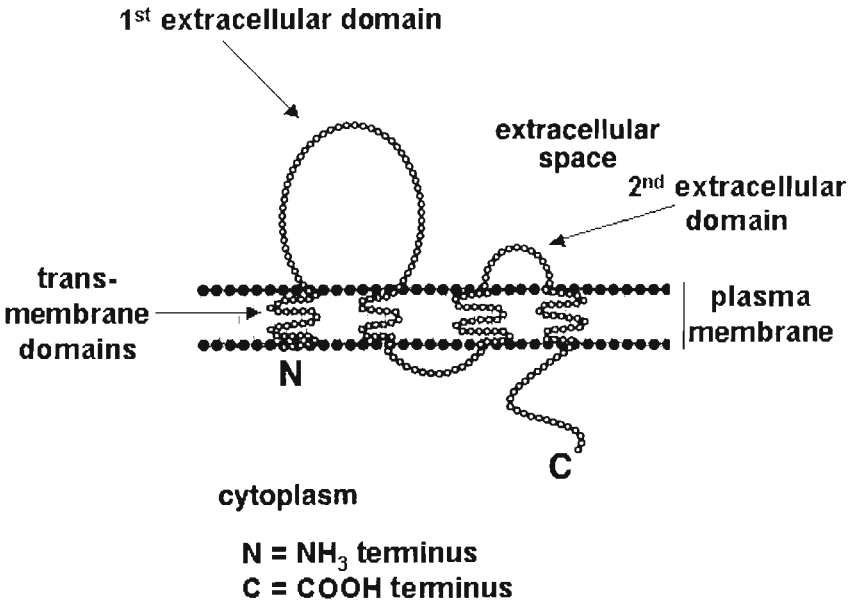


*Figure 1.5. Diagrammatic representation of claudin molecule (modified from Tsukita and Furuse, 2000b).*

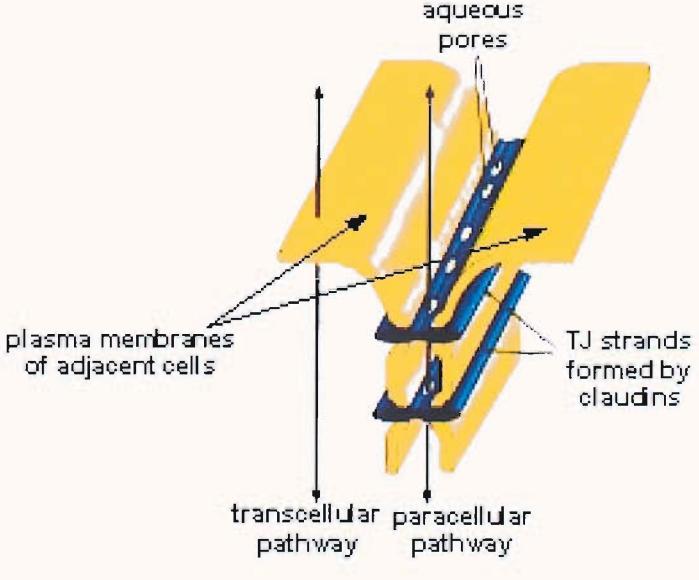


*Figure 1.6. Model of TJ strands and pores formed by the claudins of two adjacent cells (adapted from Tsukita and Furuse, 2000b).*

Claudins transfected into cultured cells are incorporated into pre-existing TJs (Furuse et al., 1998a). In L-fibroblasts, which lack TJs, they are incorporated into cell-cell contact sites that strongly resemble, by freeze-fracture electron microscopy, the strand pattern of other TJs (Furuse et al., 1998b). They are thus thought to form the key component of the proposed strand structure of the TJ. Their adhesive nature was confirmed in these studies (Kubota et al., 1999), as was the suggestion that different claudin types on adjacent cells can also interact with each other (eg claudins 1 and 3) (Furuse et al., 1999).

The fact that both ions and inert molecules pass to varying degrees between adjacent cells (paracellular permeability pathway) led to the proposal that within these strands are small, regulated pores (Tsukita and Furuse, 2000b)(see figure 1.6). A suggestion that claudins form the physical basis of these pores also arose from the observation that the condition of hereditary renal magnesium wasting (familial hypomagnesemia with hypercalciuria and nephrocalcinosis) is caused by mutations in the gene encoding claudin 16 (Simon et al., 1999; Weber et al., 2001), which is only found in the thick ascending loop of Henle.

Evidence has emerged that claudins are a major factor in establishing epithelial barrier function. For example, claudin 1 transfected Madin-Darby Canine Kidney (MDCK) cells generate a higher electrical resistance across the cell monolayer and are more resistant to the paracellular passage of uncharged probes of different size (Inai et al., 1999). Furthermore, it is becoming clear that certain claudins can influence the ionic selectivity of the paracellular pathway. Thus, overexpression of human claudin 4 in MDCK cells increases the electrical resistance across the monolayer by specifically reducing sodium ion permeability, without affecting permeability to chloride ions or inert molecules (Van Itallie et al., 2001). That the proposed extracellular domains of a claudin molecule determine its electrophysiological properties is neatly illustrated by a study in which the electrical charges of selected extracellular amino acids were reversed in two different claudins by site-directed mutagenesis. Substituting a negative for a positive charge at position 65 in the first extracellular domain of claudin-4 increased paracellular sodium ion permeability; substituting positive for negative charges at three positions in the first extracellular domain of claudin-15 reversed paracellular charge selectivity from a preference for sodium ions to one for chloride ions (Colegio et al., 2002).

The function of claudin 2 has been of interest since it was demonstrated that transfection of its gene into MDCK-C7 cells (which express claudins 1 and 4 but not 2) led to a dramatic drop in transepithelial electrical resistance (TER). This was associated with high cation (sodium, potassium) but unchanged anion (chloride) permeabilities. In other words, claudin 2 conferred a cation-leaky phenotype to the cells without affecting permeabilities to anions and uncharged molecules (Amasheh et al., 2002). Further evidence for the role of the extracellular domains in these functions came from a study of chimeric proteins, formed by the interchange of the extracellular domains of claudins 2 and 4 (Colegio et al., 2003). When transfected into leaky MDCK II cells, each of the chimeras displayed the properties attributed to the claudin from which its extracellular domains originated. Thus the claudin 4 extracellular domains increased TER and reduced cation permeability despite being expressed in molecules containing claudin 2 transmembrane and intracellular domains. In other words, cation resistance is a feature of the extracellular domains of claudin 4. This group has also demonstrated that introducing claudin 4 into a cation-selective cell line, such as MDCK II, decreases cation-permeability, whereas claudin 2 has no effect; conversely, introducing claudin 2 into an anion-selective cell line, such as LLC-PK1, increases cation-permeability, whereas claudin 4 has no effect (Van Itallie et al., 2003).

The roles of the other domains in claudin function are beginning to be elucidated. A recent study, in which chimeras of claudins 2 and 4 containing exchanged tail domains were constructed and expressed in MDCK II cells, showed that these domains are responsible for the relative stability of the individual claudins (Van Itallie et al., 2004). The half-life of either intact claudin 2 or a claudin 4 chimera that contained the tail of claudin 2 was greater than 12 hours, whereas the half-life of intact claudin 4 was approximately 4 hours. The longer half-life conferred on claudin 4 by the tail of claudin 2 led to an increase in both its protein level and its physiological influence (cation resistance).

Some evidence has emerged of variations in the pattern of claudin expression between tissues (Tsukita and Furuse, 2002). Indeed, in the kidney tubule a different repertoire of claudins is found within each different segment, perhaps reflecting their different electrophysiological features (Kiuchi-Saishin et al., 2002). In the normal rat colon the predominant species are claudins 3 and 4 at the surface and claudins 2, 3 and 5 in the crypts; in the small intesine are found claudins 3, 4 and 5 at the surface and

claudins 2, 3 and 5 in the crypts (Rahner et al., 2001). However, no published studies have comprehensively examined the expression of these claudin subtypes in the human intestinal epithelium. Claudins 1, 3, 4 and 5 have been observed in the human colon in a study that used western blotting to detect expression in whole mucosal biopsies (Burgel et al., 2002). In addition the expression of claudin 4 in these biopsy samples was shown to be reduced in an inflammatory condition known as collagenous colitis; increases in claudin 2 expression were observed in some cases, although this did not reach statistical significance (Burgel et al., 2002). Very recently, the human intestinal epithelial expression of claudins 1 (Zeissig et al., 2004) and 2 (Escaffit et al., 2004) has been confirmed.

Recently, murine models of claudin mutation (claudin 1 knockout mice, Furuse et al., 2002) and claudin overexpression (claudin 6 transgenic mice, Turksen and Troy, 2002) have been generated. Both defects were fatal soon after birth, ostensibly due to dehydration caused by the loss of skin barrier function. The intestines of these animals were not examined. Such models have not yet been generated for claudins 2 to 5.

#### *1.2.2.1.2 Occludin*

Occludin is a 65kDa protein predicted to contain two extracellular loops, four transmembrane domains and intracellular amino- and carboxy- termini (Furuse et al., 1993). It is depicted diagrammatically in figure 1.7.

The binding partners of occludin are numerous and suggest an important role for it within the TJ. Direct binding to ZO-1 and ZO-2 (Furuse et al., 1994) and ZO-3 (Haskins et al., 1998) occurs via its carboxy-(C-)terminal cytoplasmic region, and it is this region that targets it to the TJ (Matter and Balda, 1998; Mitic et al., 1999). However, more recent evidence has suggested that the second extracellular domain is also required for localisation at the TJ (Medina et al., 2000). The specific site on murine occludin that binds to ZO-1 has recently been localised to a 19 amino acid site at the C-terminus, which binds to two sites on ZO-1 – the guanylate kinase domain and its adjacent hinge region (Schmidt et al., 2004 and see 1.2.2.1.4). *In vitro* occludin has been shown to bind directly to filamentous actin (Wittchen et al., 1999). It may also interact with proteins of the gap junction, as binding to transfected human connexin-32 has been demonstrated experimentally for murine occludin (Kojima et al., 1999). VAP-33, a protein implicated

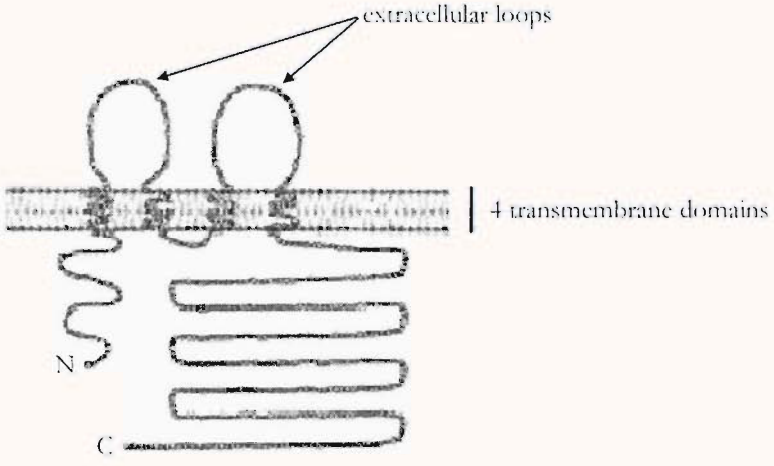


*Figure 1.7. Diagram of occludin structure; N – amino terminal; C – carboxy terminal. (Adapted from Furuse et al., 1993).*

in vesicle docking and fusion, has also been shown to bind occludin, although the implications of this are unclear (Lapierre et al., 1999). The E3 ubiquitin-protein ligase Itch has been shown to bind both *in vivo* and *in vitro* to the amino-terminus of occludin and to be involved in its ubiquitination (Traweger et al., 2002a). Occludin has also been co-immunoprecipitated with the non-receptor tyrosine kinase c-yes (Chen and Lu, 2003) and the regulatory (p85) subunit of phosphatidylinositol-3-kinase (Nusrat et al., 2000; Sheth et al., 2003; Sheth et al., 2003), which may therefore play roles in its regulation. Indeed, a single study has shown that disruption of TJs in Caco2 cells by oxidative stress is associated with the co-localisation and increased co-immunoprecipitation of occludin and this p85 subunit (Nusrat et al., 2000; Sheth et al., 2003).

Occludin was the first transmembrane TJ protein to be described (Furuse et al., 1993). It was isolated from rats using antibodies raised against an unknown membrane antigen of chicken liver (Furuse et al., 1993) and was proposed initially to contribute to both the adhesive and barrier properties of TJs (Balda et al., 1996a; McCarthy et al., 1996). Indeed, expression of occludin in fibroblasts that lack it can confer adhesiveness (Van Itallie and Anderson, 1997). This requires the presence of ZO-1 and so does not occur in L-fibroblasts, which lack ZO-1. Adhesion in this study could be disrupted by the addition of synthetic peptides corresponding to the first extracellular sequence of occludin. A subsequent study showed that the resealing of disrupted TJs in A6 cells could also be prevented by synthetic peptides homologous to the first extracellular

sequence (Lacaz-Vieira et al., 1999). A similar study in the Xenopus kidney epithelial cell line A6 has shown the same for the second extracellular sequence (Wong and Gumbiner, 1997), and the transfection of occludin mutants into MDCK cells has also suggested a crucial role for this sequence in the successful co-localisation of occludin with ZO-1 at the TJ (Medina et al., 2000). Recent work in endothelial cells has suggested that the amino acid sequence responsible for this disruption is a four residue motif (LYHY) found in the second extracellular domain of all mammalian species examined (Blaschuk et al., 2002).

Early work had also shown that the transfection of occludin into MDCK cells led to an increase in electrical resistance across the cells, suggesting a role in regulating the permeability to ions (Balda et al., 1996a). However, expression of occludin mutants that lacked the carboxy-terminus was associated with a marked increase in the paracellular flux of small molecular weight tracers, with no effect seen on electrical resistance (Balda et al., 1996a). This suggested that the regulation of ionic and small molecular permeabilities was separable, with a crucial role for occludin in the latter. Furthermore, in MDCK cells (Balda et al., 2000) and in the murine epithelial cell line CSG 120/7 (Bamforth et al., 1999), expression of mutant and chimeric occludins has shown both extracellular domains and the amino-terminus to be involved in the regulation of paracellular permeability.

The above evidence had suggested that occludin had crucial roles in regulating TJ adhesion and paracellular permeability. However, the generation of murine embryonic stem cells lacking the ability to synthesise occludin led to the formation of occludin-deficient epithelium that was structurally identical to wild-type epithelium; functionally, the epithelium maintained its ability to prevent the passage of a low molecular mass tracer through the paracellular pathway (Saitou et al., 1998). This was strong evidence that occludin was not necessary to form strand structures, recruit ZO-1 and function as a barrier. Furthermore, a mouse line that carried a null mutation in the occludin gene was viable and displayed no gross external phenotypic abnormality (Saitou et al., 2000). The intestinal epithelial barrier function appeared normal electrophysiologically. However there were several histological abnormalities in other tissues; for example, the gastric epithelium was inflamed and hyperplastic, the males were sterile and the females did not suckle their young well. Occludin was therefore not necessary for the generation of TJs but appeared to have a significant influence on proliferation and possible

differentiation. These mice were not subjected to any challenge, such as a gastrointestinal infection, so more subtle functions of occludin in relation to gut inflammation could not be elucidated. Other findings have suggested that the role of occludin may be regulatory rather than, or as well as, structural. There is a body of evidence to suggest this regulatory function relates to either or both of two properties of the molecule: its phosphorylation state and structural variation derived from alternative splicing of mRNA. This evidence is discussed later.

#### *1.2.2.1.3 Junctional Adhesion Molecule*

The family of JAM proteins (molecular weight 35-39kDa) are members of the immunoglobulin superfamily (Martin-Padura et al., 1998; Liu et al., 2000a; Williams et al., 1999), consisting of two V-type immunoglobulin domains. Four members have thus far been described (Bazzoni, 2003; Hirabayashi et al., 2003). They have no ability to reconstitute TJ strands in culture and may be important in maintaining the TJ seal during trafficking of blood cells through endothelia and epithelia; in this context they have been shown to bind to the beta integrin LFA-1, which is involved in the migration of leukocytes through endothelia (Ostermann et al., 2002). Furthermore, an antibody to human JAM-2 has been demonstrated to block the transmigration of primary human peripheral blood leukocytes across cultured human umbilical vein endothelial cells (Johnson-Leger et al., 2002). In the mouse preimplantation embryo, JAM-1 was recently shown to be expressed at cell-cell contact sites early in the eight-cell stage and before any other TJ protein or E-cadherin. Its role appeared to be in regulating the timing of blastocoel cavity formation after compaction and adhesion had occurred (Thomas et al., 2004).

Within TJs JAM is bound via its carboxy-terminus to the PDZ3 domain of ZO-1 (see below) (Ebnet et al., 2000), to PAR3 (a homologue of a cell polarity protein in the nematode *C. elegans)* (Ebnet et al., 2001), and to the protein AF-6 (Ebnet et al., 2000). It also binds to the amino-terminus of cingulin and to occludin (Bazzoni et al., 2000), and JAM-4 can bind to membrane-associated guanylate kinase-inverted-1 (MAGI-1) (Hirabayashi et al., 2003).

Recently, the crystal structure of human JAM-1 has been elucidated, confirming the Ig-like domain structure and its ability to form homotypic dimers (Prota et al., 2003).

Interestingly, this dimerisation is inhibited by the binding of a reovirus, which uses JAM-1 as its cellular receptor (Forrest et al., 2003).

#### *1.2.2.1.4 Zonula Occludens-1*

Zonula Occludens-1 (ZO-1) is a large (225kDa) multi-domain non-transmembrane TJ protein (Anderson et al., 1988; Stevenson et al., 1986), outlined diagrammatically in figure 1.8.


*Figure 1.8. Domain structure of ZO-1. PDZ – Postsynaptic density/Discs large/ZO-1 domain; SH3 – Src homology 3 domain; H – Hinge region; GuK – Guanylate kinase-like domain; α – Alpha domain*

ZO-1 is described as a Membrane-Associated Guanylate Kinase (MAGUK) protein, although its guanylate kinase domain is predicted to be non-functional and to take part in protein-protein binding, along with its PDZ and SH3 domains. It is homologous to two other MAGUKs found at TJs (ZO-2 and ZO-3), but most is known about ZO-1 (Gonzalez-Mariscal et al., 2003).

Its structural role in TJs can be inferred from its multiple binding partners. It binds to the three best-described transmembrane TJ protein classes: to occludin via its guanylate kinase and hinge regions (Fanning et al., 1998; Furuse et al., 1994; Schmidt et al., 2004); to JAM via its second and third PDZ domains (Bazzoni et al., 2000; Ebnet et al., 2000); and to the C-terminal tyrosine-valine motif of claudins via its first PDZ domain (Itoh et al., 1999a). Like occludin, the adherens junction protein alpha-catenin (see 1.2.2.3) can also bind to ZO-1 via its guanylate kinase and hinge regions (Mueller et al., 2004). The proline-rich C-terminal half of ZO-1 binds to F-actin (Fanning et al., 1998); this actin-binding region has been further localised to a 220 amino acid region (Fanning et al., 2002). It is thus well-placed to link the transmembrane structures of the

TJ to the actin cytoskeleton. Its interactions with ZO-2 (Itoh et al., 1999b) and ZO-3 (Haskins et al., 1998) via its second PDZ domain suggest that it forms a crucial part of a scaffold of proteins at the TJ plaque (Wittchen et al., 1999).

Mouse epithelial cell clones lacking ZO-1 expression were recently generated (Umeda et al., 2004). In confluent cultures the TJs appeared normal, with increased ZO-2 expression suggesting redundancy between it and ZO-1. However, the formation of new TJs after calcium depletion and replenishment was markedly delayed (as assessed by the recruitment of claudins and occludin and barrier establishment), suggesting a crucial role for ZO-1 in TJ assembly (Umeda et al., 2004).

The other binding partners of ZO-1 suggest that its role may be more than simply structural. ZO-1 binds to or interacts with many other proteins, some of whose functions are only just being elucidated. For example, ZO-1 interacts with the small GTPase, rab13, which is homologous to the yeast Sec4 protein that is involved in the regulation of membrane traffic and endocytosis (Zahraoui et al., 1994). An intimate association between ZO-1 and rab13 has also been demonstrated during the development of the mouse preimplantation embryo (Sheth et al., 2000a, and see 1.2.2.2.2). The role of small GTPases in the regulation of TJs is discussed further in 1.2.2.2.3. In MDCK cells ZO-1 interacts closely with the protein AF-6, a target of Ras. Activated Ras not only inhibits this interaction, but also disturbs cell-cell contacts and reduces the amount of both ZO-1 and AF-6 found at the membrane (Yamamoto et al., 1997; Yamamoto et al., 1999). Also in MDCK cells, inhibition of the mitogen-activated protein kinase (MAPK) pathway leads to the accumulation of tyrosine-phosphorylated ZO-1 and occludin at the membrane and the assembly of functional TJs (Chen et al., 2000). Recently, inhibition of the same pathway in T84 cells has been shown to prevent the dislocation of ZO-1 and occludin induced by an activator of protein kinase C (Weiler et al., 2004). A G protein, Gα 12, has also been demonstrated to bind to the SH3 domain of ZO-1 and increase the paracellular permeability of MDCK cells (Meyer et al., 2002). These findings suggest not only that ZO-1 is a crucial structural component of TJs, but also that its accumulation at the membrane is regulated, and that this correlates with epithelial barrier function.

### *1.2.2.1.5 Other Tight Junction Proteins*

The number of TJ proteins now described is large and growing, and reviewed com-

| PDZ-containing | Interacting Partners |
|---|---|
| MAGI-1 | JAM-4 |
| MAGI-2 | PTEN |
| MAGI-3 | RTPTβ, PTEN |
| MUPP-1 | Claudins 1 and 8, JAM-1 |
| PAR-3 | JAM-1, PAR-6, Apkc |
| PAR-6 | PAR-3, aPKC, PALS-1, mLgl |
| PALS-1 | PATJ, Crumbs |
| PATJ | ZO-3, Claudin 1, PALS-1 |
| mDlg | 4.1R |
| Scrib | |
| Non-PDZ-containing | Interacting Partners |
| Cingulin | JAM-1, ZO-1, ZO-2, ZO-3 |
| Symplekin | Colocalizes with ZO-1 at TJ; also present in nucleus |
| HuASH1 | |
| GEF-H1 | |
| aPKC | PAR-3, PAR-6 |
| PP2A | |
| Heterotrimeric G proteins | ZO-1, ZO-2 |
| Rab3b, Rab13 | |
| Sec6/Sec8 | |
| PTEN | MAGI-2, MAGI-3 |
| 7H6 | |

*Table 1.2. Summary of TJ-associated proteins not discussed in detail in the main text, divided into PDZ-containing and non-PDZ-containing; known interaction partners for each are also listed.*

prehensively in several reviews (e.g. Gonzalez-Mariscal et al., 2003). A list of those not discussed in detail is provided in table 1.2, together with their known interaction

partners. Knowledge of many of these, such as cingulin, symplekin, 7H6 and pilt, is limited (Citi et al., 1988; Cordenonsi et al., 1999; Kawabe et al., 2001; Keon et al., 1996; Zhong et al., 1993). Molecules involved in intracellular vesicle trafficking, such as rab3b, rab13 and homologues of yeast SEC6 and –8 gene products are also found at TJs (Grindstaff et al., 1998; Weber et al., 1994; Zahraoui et al., 1994; Weber et al., 1994). A recently described protein, ZO-1-associated nucleic acid-binding protein (ZONAB), is discussed in more detail later.

### 1.2.2.2 REGULATION OF TIGHT JUNCTIONS

#### *1.2.2.2.1 Phosphorylation*

Phosphorylation of ZO-1 has been proposed to be a means of regulating TJ function, and thus paracellular permeability. This was first suggested by the observation that ZO-1 from a low-resistance strain of MDCK cells contained about twice as much phosphate as that from a high-resistance strain (Stevenson et al., 1989), despite the strains having similar levels of ZO-1 (Stevenson et al., 1988). ATP depletion of MDCK cells leads to the disruption of TJs, reduced localisation of ZO-1 at the membrane and decreased overall phosphorylation of ZO-1 (Gopalakrishnan et al., 1998). ATP repletion leads both to TJ reassembly and to tyrosine phosphorylation of ZO-2 and ZO-3, though not ZO-1 (Tsukamoto and Nigam, 1999). Intact Rho GTPase activity ameliorates the effects of ATP depletion (Gopalakrishnan et al., 1998). ZO-1 may be a target for protein kinase C (Stuart and Nigam, 1995) and, in A431 epidermal cells, exposure to epidermal growth factor (EGF) leads to both transient tyrosine phosphorylation and redistribution to the TJ of ZO-1 (Van Itallie et al., 1995). EGF stimulates phospholipase C-gamma (PLC-gamma) and selective inhibition of this PLC isoform in MDCK cells leads to decreased TER and hyperphosphorylation of ZO-1, ZO-2 and occludin (Ward et al., 2002). The SH3 domain of ZO-1 binds to a serine kinase that phosphorylates a region C-terminal to the SH3 domain, but the function of this is as yet unknown (Balda et al., 1996b). Together, these observations suggest an association between the phosphorylation status of ZO-1 and TJ assembly.

The phosphorylation state of occludin may relate to its function (Sakakibara et al., 1997). Bands of protein of multiple weights are elicited when occludin is

immunoprecipitated or detected by western blotting, and these can be resolved to lower weight bands by phosphatase treatment (Sakakibara et al., 1997; Wong, 1997). Hyperphosphorylated occludin in these studies was associated with NP-40 and Triton X-100 insolubility and staining of TJs by immunofluorescence. Rho GTPase induces the phosphorylation of occludin, and this is associated with its localisation at TJs and barrier formation in MDCK cells (Gopalakrishnan et al., 1998). Calcium depletion of MDCK cells disrupts cell-cell contacts and opens TJs, and reintroduction of calcium ions reverses this. In this model, prolonged calcium depletion leads to both the disappearance of occludin from cell-cell contacts, with its appearance in the cytoplasm, and its dephosphorylation (Farshori and Kachar, 1999). Recently, calcium-repletion in this model has been shown to lead to tyrosine phosphorylation of occludin, which was temporally associated with an increase in TER, and which could be completely abolished by inhibiting the nonreceptor tyrosine kinase c-Yes (Chen et al., 2002). Furthermore, treatment of an MDCK cell monolayer with the phorbol ester 12-O-tetradecanoylphorbol-13-acetate (TPA), which activates protein kinase C, leads to discontinuities in the TJ strand network, as seen by freeze-fracture electron microscopy, and to reduced phosphorylation of occludin (Farshori and Kachar, 1999). This is also seen in LLC-PK1 cells, where it was suggested that TPA leads to downstream activation of a serine/threonine phosphatase (Clarke et al., 2000). Indeed, such a serine/threonine phosphatase has subsequently been described (Nunbhakdi-Craig et al., 2002). Occludin has also been shown to be a direct target for protein kinase C at a serine residue near the carboxy terminus (Andreeva et al., 2001). ATP depletion of MDCK cells also leads to perturbation of TJs and loss of the permeability barrier, with recovery after ATP repletion within three hours. TJ disassembly in this model is also associated with dephosphorylation of occludin (and other TJ components), but reassembly, as in the calcium-depletion/repletion model, requires intact tyrosine kinase activity and is associated with tyrosine phosphorylation of occludin (Tsukamoto and Nigam, 1999). A similar finding has been described in another model of MDCK cell TJ disassembly/reassembly, namely, Ras transformation followed by mitogen-activated protein kinase treatment (Chen et al., 2000). In T84 cells, recruitment of TJ components, including hyperphosphorylated occludin, into the TJ protein complex can be induced by cytokines such as IL-15 (Nishiyama et al., 2001). On the other hand, infection of intestinal epithelial cells by enteropathogenic E.coli is associated with dephosphorylation of occludin and its shift from TJs to an intracellular compartment,

which can be prevented by a serine/threonine phosphatase inhibitor (Simonovic et al., 2000). In another model of TJ formation, the development of the mouse blastocyst, occludin phosphorylation is associated with its conversion from Triton X-100 solubility to insolubility; this has been suggested to regulate its association with the α+ isoform of ZO-1 (see 1.2.2.2.2) and membrane assembly (Sheth et al., 2000b). This collective evidence implicates the phosphorylation of occludin, probably at tyrosine residues, as a key step in its localisation at the membrane and in the assembly of TJs; the disassembly of TJs appears to be associated with the dephosphorylation of occludin, possibly at key serine and threonine residues, leading to its loss from TJs.

#### *1.2.2.2.2 Alternative Splicing of mRNA*

Several isoforms of ZO-1 have been described, resulting from alternative mRNA splicing at at least three sites (known as α, β and γ). In relation to the α domain, about which most is known, two isoforms of ZO-1 are formed: one form containing an 80 amino acid domain (α+) and the other lacking it (α-) (Willott et al., 1992). In mature tissues the α- isoform is restricted to the highly specialised and dynamic junctions of endothelial cells, Sertoli cells and renal podocytes, whereas the α+ isoform is found in all other epithelial tissues (Balda and Anderson, 1993). In the mouse embryo it has been known for some time that, at the time of compaction (8-cell stage), ZO-1 localises in a punctate fashion to the lateral membrane contact sites, whereas by the 32-cell stage it localises to junctions that have become zonular (belt-like) (Fleming and Hay, 1991). A subsequent study by the same group (Sheth et al., 1997) has demonstrated that the punctate junctions contain the α- isoform, but the subsequent formation of the zonular junctions is associated with the assembly of the α+ isoform at the membrane from an initial perinuclear location; occludin remains closely associated with the α+ isoform at both its perinuclear and subsequent junctional locations. Indeed, it appears that at the 8-cell stage ZO-1α- is expressed along the lateral membrane in a single junction complex containing elements of both TJs (ZO-1) and AJs (alpha- and beta-catenin). At compaction, rab13 relocates to this complex and co-localises precisely with ZO-1, suggesting a role for rab13 in regulating this event. The separation of the TJ and AJ proteins into separate junctions coincides with the membrane expression of ZO-1α+

and occludin, the establishment of a functional TJ seal and the beginning of blastocoel formation at the 32-cell stage (Sheth et al., 2000a).

The gene for occludin, on chromosome 5, yields several mRNA bands when northern blotted, suggesting the possibility of several products by alternative splicing (Saitou et al., 1997). This was first confirmed in MDCK cells, in which a form of occludin was described that contained an extra amino-terminal 56 amino acid insertion (Muresan et al., 2000). An exon coding for this was found in the appropriate position within the occludin gene. Both forms were coexpressed in T84 cells and mouse intestine, but the functional significance of this isoform is unknown. Recently, a variant of occludin that lacks the fourth transmembrane domain and immediate carboxy-terminal flanking region was described in human tissues, embryos and cell lines (Ghassemifar et al., 2002). Low level expression was described at the edges of subconfluent or wounded confluent Caco2 cell monolayers, suggesting a possible role in regulating occludin function. Another recent study has confirmed that the fourth transmembrane domain is required for the targeting of occludin to the TJ and its co-localisation with ZO-1; the absence of this domain led to the relocalisation of the carboxy-terminus extracellularly (Mankertz et al., 2002).

#### *1.2.2.2.3 Small GTPases*

A variety of small GTPases have been located at the TJ (Gonzalez-Mariscal et al., 2003). Several of these, such as rab3B (Weber et al., 1994) and rab13 (Zahraoui et al., 1994), are homologous to polarity-regulating GTPases in yeasts, but in epithelia they also regulate TJ formation (Marzesco et al., 2002). Overexpression of a constitutively active form of rab13 delays the formation of functional TJs and the localisation of claudin 1 to the TJ in MDCK cells (Marzesco et al., 2002) and impairs the transport of claudin 1 in non-polarised fibroblasts (Yamamoto et al., 2003). The mechanisms are unclear but may involve the inhibition of Protein Kinase A (Kohler et al., 2004). A recent study also suggested that rab13 may be mediating a continuous endocytosis and recycling to the surface of occludin (Morimoto et al., 2004). The association of rab13 with ZO-1 at the time of compaction of the 8-cell mouse preimplantation embryo has been discussed earlier (see 1.2.2.2.2).

As mentioned earlier, the GTPases RhoA and Rac1 are associated with the accumulation of ZO-1 and occludin at the TJ (Gopalakrishnan et al., 1998; Jou et al.,

1998). Activation of Rho in MDCK cells that have already developed TJs is, however, associated with an increase in paracellular permeability (Benais-Pont et al., 2003). Confusingly, a series of experiments involving the transfection into MDCK cells of constitutively active or dominant negative forms of RhoA, Rac1 and Cdc42 showed the system to be more complicated, with both active and inactive forms of each GTPase being able to redistribute certain TJ proteins (including the claudins) away from the TJ (Bruewer et al., 2004). The relevance of these findings to regulatory processes in vivo remains unclear.

#### *1.2.2.2.4 Regulation of Other Genes*

There is emerging evidence to suggest that ZO-1 may be involved in regulating the transcription of other genes. In MDCK, LLC-PK1 and CV-1 cells, ZO-1 has been demonstrated in the nuclei of both subconfluent cells and cells at the edge of wounds (Gottardi et al., 1996). In the same study, ZO-1 was demonstrated in the nuclei of paraffin-embedded canine intestinal epithelial cells, but only at the tips of villi. Furthermore, ZO-1 contains nuclear sorting signals (Gonzalez-Mariscal et al., 1999) and a nuclear export signal (Islas et al., 2002)

In MDCK cells, ZO-1 has been immunoprecipitated with a protein termed ZO-1-associated nucleic acid-binding protein (ZONAB), which is homologous to Y-box transcription factors (Balda and Matter, 2000). ZONAB co-localised with ZO-1 at the membrane, but was also detected in the nucleus without detectable ZO-1. It was shown to bind to the promoter of the gene coding for ErbB-2, a tyrosine kinase co-receptor important for epithelial differentiation and morphogenesis (Niemann et al., 1998), and to promoter elements of several cell-cycle regulators. Confluent cells contained large amounts of membrane ZO-1, but small amounts of endogenous ZONAB. Artificially overexpressing ZONAB in these cells inhibited ErbB-2 promoter activity. Subconfluent cells on the other hand already contained large amounts of ZONAB; transfecting them with more ZONAB did not further inhibit ErbB-2 promoter activity, whereas overexpression of ZO-1 stimulated ErbB-2 promoter activity and was proposed to achieve this by sequestering ZONAB at the membrane. This is the first demonstration that membrane ZO-1, by regulating the amount of nuclear ZONAB available for nuclear binding, directly regulates the expression of at least one gene involved in epithelial differentiation and morphogenesis. In addition, ZONAB has recently been

shown to bind directly to the cell division kinase (CDK) 4 in MDCK cells (Balda et al., 2003); by regulating the nuclear accumulation of CDK4, it appears to be able to regulate cell density and proliferation.

ZO-2 has been demonstrated in the nuclei of renal tubular cells (Gonzalez-Mariscal et al., 2000). The same group has shown that both ZO-2 and ZO-3 contain a nuclear export signal (Islas et al., 2002). Furthermore, nuclear localisation of ZO-2 could be induced in cell culture by creating a wound and thus impairing cell-cell contacts; this ZO-2 derived from a pre-existing pool rather than from de novo synthesis (Islas et al., 2002). Recently, nuclear ZO-2, but not ZO-1, has been shown to associate with a DNA-binding protein, known as scaffold attachment factor-B (SAF-B), via its PDZ-1 region, at least in MDCK and LLC-PK1 cells (Traweger et al., 2002b). It has also been shown to associate with Jun, Fos and C/EPB transcription factors at both the nucleus and TJ (Betanzos et al., 2004). This has not been demonstrated for ZO-1, however, suggesting that ZO-1 and ZO-2 do not serve overlapping functions in this respect.

#### 1.2.2.3 ADHERENS JUNCTION

The adherens junction is closely apposed to the tight junction, being sited immediately below it in the terminal bar complex of epithelial cells (Farquhar and Palade, 1965). E-cadherin, its adhesive, homophilic, transmembrane protein, is bound on the cytoplasmic side by alpha-, beta- and gamma-catenin (Ozawa et al., 1989; Perry et al., 1999a; Wijnhoven et al., 2000). These proteins have been much investigated because of their roles in compaction and blastocyst formation in the preimplantation embryo (Larue et al., 1994; Riethmacher et al., 1995), and because of their roles in proliferation and carcinogenesis in the adult colonic epithelium (Wijnhoven et al., 2000). E-cadherin adhesion is essential for epithelial differentiation (Larue et al., 1994; Riethmacher et al., 1995), and it appears to be required for the assembly of TJs (see below). Its expression also enhances the assembly of desmosomes (DJs) (Gumbiner et al., 1988). At early cell-cell contact sites in cultured mouse epithelial cells E-cadherin has been shown to bind to ZO-1 within a single, hybrid and punctate cell-cell junction (Ando-Akatsuka et al., 1999). Separate TJs and AJs form when ZO-1 and E-cadherin are sorted out from this hybrid by their subsequent binding to occludin and catenins respectively (Ando-Akatsuka et al., 1999). This resembles the development of separate

TJs and AJs from a single hybrid junction containing both ZO-1α- and catenins in the mouse preimplantation embryo (Fleming et al., 2000). Here, E-cadherin mediated adhesion is also permissive for TJ separation, maturation and sealing, which occurs when occludin and ZO-1α+ are expressed at the membrane (Sheth et al., 2000a).

The structure of E-cadherin is described in detail in several reviews (e.g. Malhotra, 1996). Basically, it contains five extracellular domains, with a putative cell adhesion recognition (CAR) tripeptide on the first and outermost domain that is specific to each cadherin, even across species (Malhotra, 1996). Adhesion between cadherin-bearing cells is calcium-dependent and with E-cadherin it is homophilic (Nagar et al., 1996).

The genes encoding human and murine E-cadherin have been cloned and they contain sequences promoting epithelial specific transcription (Behrens et al., 1991; Hennig et al., 1996). Studies of the factors regulating transcription and translation of this gene have implicated various transcription factors in its activation (Hennig et al., 1996; Batsche et al., 1998; Hosono et al., 2000), and several mechanisms in its repression (Rodrigo et al., 1999; Batlle et al., 2000; Tamura et al., 2000).

Enhancement of E-cadherin expression is associated with clustering of beta- and gamma-catenin at the membrane (Troyanovsky, 1999), whereas reduced E-cadherin expression can release the catenins from the AJ (Nelson and Nusse, 2004). In addition, the catenins can shuttle to the nucleus and regulate the transcription of other genes (Polakis, 2000). The level of cytosolic β-catenin (i.e. unbound to E-cadherin) is tightly regulated by its forming a complex with APC and axin, which allows it to be phosphorylated at four amino-terminal residues by glycogen synthase kinase 3-beta (GSK3β) and casein kinase 1, thus designating it for ubiquitinaton (Giles et al., 2003). If this complex cannot form because of a mutation to one of these components, or a signal is delivered via the Wnt pathway to inhibit GSK3β (van Noort et al., 2002), hypophosphorylated (or 'active') β-catenin is stabilised and allowed to enter the nucleus, where it binds to the T-cell factor (TCF) family of transcription factors (Nelson and Nusse, 2004). This β-catenin-TCF complex can increase the transcription of many pro-proliferative genes and genes involved in tissue remodelling (e.g. matrix metalloproteinase-7, fibronectin) (Giles et al., 2003; Polakis, 2000).

β-catenin is the mammalian orthologue of the Arm protein in Drosophila and consists largely of 12 tandemly arranged 42 amino acid sequences known as arm repeats (Giles et al., 2003). These arm repeats mediate its protein-protein interactions and facilitate its nuclear localisation (Giles et al., 2003).

Several other proteins are associated with the AJ (Nagafuchi, 2001). Alpha-catenin interacts with other F-actin-binding proteins, such as vinculin and α-actinin. In addition, hepatocyte growth factor and epidermal growth factor receptors are concentrated at AJs (Nagafuchi, 2001).

## 1.3 THE INTESTINAL EPITHELIAL BARRIER IN INFLAMMATORY BOWEL DISEASE

### 1.3.1 *IN VIVO* STUDIES

The assessment of intestinal permeability in patients is commonly performed by measuring the urinary excretion of two orally administered water-soluble markers. One marker is typically small and is thought to permeate well through normal mucosa, whereas the second is larger and minimally permeates the normal mucosa. The ratio of excretion of the second to the first marker will thus increase if the mucosa becomes more leaky and permeable. Typical combinations include mannitol plus lactose, or $^{51}$Cr-ethylenediaminetetraacetic acid ($^{51}$Cr-EDTA) plus PEG 400. These measurements have been performed in a variety of clinical settings (Unno and Fink, 1998).

In IBD there is considerable evidence for an increase in mucosal permeability, as measured by these methods, in both CD and UC (Almer et al., 1993; Andre et al., 1988; Hollander et al., 1986; Secondulfo et al., 2001; Soderholm et al., 1999; Teahon et al., 1992; Zuckerman and Watts, 1993). Some evidence exists for the utility of repeated measurements in assessing disease activity and prognosis (Teahon et al., 1991). It has been more difficult to demonstrate that increased permeability precedes disease onset, which would suggest an aetiological role, but a case report suggests this (Irvine and Marshall, 2000). This describes a child of a patient with CD, who was shown to have elevated permeability but no sign of IBD on thorough investigation, but who developed CD several years later. Studies of first-degree relatives of patients with CD, who are at particularly high risk of subsequently developing the disease, have consistently demonstrated a minority (10-20%) to have abnormally high permeability (Hollander et al., 1986; May et al., 1993; Secondulfo et al., 2001; Soderholm et al., 1999; Teahon et al., 1992). This suggests a genetic basis or contribution to this abnormality, whereas studies in spouses of cases suggest possible transmissible or dietary factors (Breslin et al., 2001; Soderholm et al., 1999). Other studies have also demonstrated an abnormal increase in permeability in response to NSAIDs among some first-degree relatives of patients (Hilsden et al., 1996; Zamora et al., 1999). NSAIDs are known to provoke relapses of IBD in some patients. Overall, this evidence suggests that an elevated baseline permeability, or an exaggerated response to provoking environmental agents, may predispose some people to develop IBD. Whether this predisposition is genetically

determined or transmissible remains to be determined. Once inflammation is established, however, an increase in intestinal permeability is readily detected.

### 1.3.2 *EX VIVO* STUDIES

Diarrhoea is a predominant symptom in IBD, and it is caused by an imbalance between absorption and secretion. An impaired epithelial barrier may lead to increased loss of electrolytes and water into the lumen, and thus contribute to the diarrhoea (so-called 'leak-flux' diarrhoea). Three ways in which this impairment in barrier function may arise are, firstly, via inherent or reactive changes in the structure of intercellular junctions; secondly, via apoptosis, leading to functional loss of barrier function; and, thirdly, via ulceration, both gross and microscopic.

Investigations into the first of these mechanisms, conducted on explanted tissue from cases of IBD, are limited. Studies undertaken to examine the number and complexity of TJ strands seen by freeze-fracture electron microscopy demonstrated that both were reduced in UC and coeliac disease (Sandle et al., 1990; Schmitz et al., 1999; Schulzke et al., 1998). The functional barrier has also been assessed by measuring the tissue's overall permeability to small and large tracer molecules, such as mannitol and albumin, or by measuring its electrical conductivity (Gitter et al., 2001; Schmitz et al., 1999). These studies showed that both permeability and conductivity are markedly increased in UC, including in tissue that is only mildly inflamed and does not display any gross ulceration. This 'leakiness' concords with a report of an increase in mucosal permeability to tracer molecules seen prior to any visible inflammation in a mouse model of colitis (Kitajima et al., 1999). It remains unclear though whether these changes are due to alterations in junctional proteins, or apoptosis, or both.

Recent descriptive studies have begun to suggest that significant reductions in the expression of TJ and DJ proteins occur in both UC and CD (Gassler et al., 2001; Kucharzik et al., 2001). Whether these changes predominate in the surface or crypt epithelium is not clear, nor is the question of whether these phenomena are general, or specific to the immediate vicinity of transmigrating neutrophils (Kucharzik et al., 2001). These studies did not examine the expression of the claudins, and it also remains unclear whether the proteins of the AJ are up- or down-regulated. In addition, no such

studies have yet been performed on those at high risk of the diseases, such as first-degree relatives.

### 1.3.3 STUDIES IN CELL CULTURE

To understand the above observations at a biochemical and molecular level, a number of studies have modelled the differentiated intestinal epithelium by the use of intestinal epithelial cell culture lines. These have included the well-recognized lines HT-29 and Caco-2, and, over recent years, increasing use has been made of the cell line T84, which is derived from a malignant clone and forms a tight monolayer when cultured on a collagen type I-coated support (Madara et al., 1987). If this support contains pores, a model of separate apical and basolateral compartments can be created.

Several studies have examined the effects of particular cytokines, when applied to one or both compartments, on electrical TER and on permeability to uncharged tracers, whilst others have examined the effects on specific junctional proteins. Several of these cytokines are known to be relevant to IBD (see 1.1.1.5.4). IFNγ, for example, was shown several years ago to increase sodium-mannitol flux across T84 monolayers and to diminish TER (Madara and Stafford, 1989). The effect of IFNγ on permeability appears to involve a reduction in the transcription and protein synthesis of ZO-1 and, to a lesser extent, ZO-2, with disrupted apical actin organization (Youakim and Ahdieh, 1999). IFNγ can also reduce occludin expression and TER when applied to HT-29/B6 cells transfected with the occludin gene promotor (Mankertz et al., 2000). IFNγ has subsequently been demonstrated to increase TNFα receptor mRNA levels in T84 cells and act synergistically with TNFα to reduce TER, although TNFα alone had no effect (Fish et al., 1999). This effect on TER was not due to cytotoxicity, although TNFα has been shown to induce apoptosis in other cell lines (Soler et al., 1999), and to affect TER in Caco-2 BBE intestinal cell monolayers when applied alone (Marano et al., 1998). The detrimental effect of TNFα on barrier function in Caco2 cells has recently been confirmed to be dependent on NFkB activation (Ma et al., 2004). A recent study examined the effect of combined IFNγ and TNFα on the expression of claudins 1 and 4 in T84 cells and showed them to be internalised, with a concomitant increase in their

detergent solubility (Bruewer et al., 2003). Inhibition of apoptosis did not block these effects.

Cytokines do not always loosen epithelial TJs. The regulatory cytokine IL-10 prevents the IFNγ-induced increase in permeability across T84 cells (Madsen et al., 1997). IL-17 induces the formation of TJs, increases TER, reduces paracellular mannitol flux and upregulates transcription of claudins 1 and 2 in T84 cells (Kinugasa et al., 2000). These processes, at least with respect to claudin 2, appear to be mediated by the extracellular signal-related (ERK) mitogen-activated protein kinase (MAPK) pathway. IL-15, which is up-regulated in IBD (Liu et al., 2000b; Sakai et al., 1998), but whose role remains unclear, has been shown to mediate tightening of T84 monolayers (i.e. an increase in TER). This was associated with up-regulation of ZO-1 and ZO-2 expression, increased phosphorylation of occludin, and enhanced membrane association of claudin-1 and claudin-2 (Nishiyama et al., 2001).

In relation to the AJ, a single study of Caco-2 cells showed a marked reduction of E-cadherin and beta-catenin expression in response to TNFα, IFNγ or IL-1. In the case of E-cadherin this reduction appeared to be mediated at the transcriptional level, was maximal after 48 hours of TNFα stimulation, and was reversible on removal of the cytokine (Perry et al., 1999b).

## 1.4 HYPOTHESIS

These observations have been brought together to test the hypothesis that:

*Cytokines important in the pathogenesis of inflammatory bowel disease impair the barrier function of the intestinal epithelium by inducing alterations in the regulation of tight junction proteins.*

# CHAPTER 2

# EXPERIMENTAL METHODS

# 2 EXPERIMENTAL METHODS

## 2.1 IMMUNOHISTOCHEMISTRY

### 2.1.1 MATERIALS AND METHODS

All chemicals were obtained from Sigma (Poole, UK) unless otherwise stated. Archival human colonic biopsy specimens taken at colonoscopy and embedded in glycol methacrylate were cut into two micron (μm) sections using a Leica Reichert Ultracut S cryostat (Leica Microsystems Ltd, Milton Keynes), mounted on glass slides and stored at -20°C. Two sections per slide were utilised. At the time of the procedure, these were thawed to room temperature and supported in a humidified chamber. Endogenous peroxidases were inhibited using a solution of 0.1% sodium azide and 0.3% hydrogen peroxide in nanopure water. The sections were washed for 5 minutes three times using Tris-buffered saline solution (TBS; for constituents see appendix 1), drained, and blocked for thirty minutes in 1% bovine serum albumin (BSA) with 5% fetal bovine serum (FBS, Invitrogen Ltd, Paisley, UK) in TBS. The slides were then drained and primary antibodies at appropriate dilutions were applied. They were covered with coverslips and incubated overnight, at 4°C in the case of polyclonal antibodies, and at room temperature in the case of monoclonal antibodies. Negative controls used were either TBS or isotype-matched non-immune mouse or rabbit immunoglobulin solution at the same concentration as the primary antibody (obtained from Dako Ltd, Ely, UK). The positive control used was a mouse monoclonal antibody raised against human cytokeratin 18 (Dako Ltd). In all cases, antibodies were diluted in TBS, and 150 microlitres (μl) of solution were applied to each slide. The primary antibodies used, their species, concentrations and sources are given in table 2.1.

After overnight incubation in primary antibody the slides were washed in TBS for 5 minutes three times, drained, and 150μl of biotinylated second stage antibodies, diluted in TBS, were applied for 90 minutes at room temperature. Biotinylated rabbit anti-mouse and guinea pig anti-rabbit antibodies were used (Dako Ltd), at dilutions of 1:300 and 1:1200 respectively. After three 5-minute washes in TBS, the slides were drained and a solution of streptavidin (0.5% v/v) and biotin-peroxidase (0.5% v/v) complexes

(both from BioGenex/Menarini Diagnostics, Wokingham, UK) in Tris-HCl (48mM tris, 38mM hydrochloric acid; pH 7.6) was applied for one and a half hours. After three 5-minute washes in TBS, the slides were drained and a solution of the chromogen 3,3′-diaminobenzidine (BioGenex) was applied for 10 minutes at room temperature. The slides were then rinsed in TBS, dipped in tap water, counterstained with Mayer's haematoxylin for 90 seconds and rinsed in running tap water for 5 minutes. They were dehydrated for 4 minutes each in 70% ethanol, and twice in absolute ethanol, before three 4-minute incubations in xylene. The sections were then mounted in xylene/dibutyl phthalate (DPX) and viewed by light microscopy.

| *Antibody* | *Species (Isotype)* | *Concentration (ug/ml) or Dilution* | *Source* |
|---|---|---|---|
| Claudin 2 | Rabbit | 6.25 | Zymed |
| Claudin 3 | Rabbit | 5 | Zymed |
| Claudin 4 | Mouse (IgG1) | 1.25 | Zymed |
| Occludin | Mouse (IgG1) | 2 | Zymed |
| ZO-1 | Mouse (IgG1) | 2 | Zymed |
| Cytokeratin 18 | Mouse (IgG1) | 1:200 | Dako |

*Table 2.1. Primary antibodies used in IHC, including species, concentrations and sources (company address not given in text: Zymed, Cambridge, UK)*

### 2.1.2 ANALYSIS

The identities and diagnoses of the cases studied remained anonymous for the subsequent analysis. All the sections were examined by light microscopy on a Nikon Eclipse E600 microscope at magnifications of x200 and x400. For each antibody studied, five randomly selected fields containing surface epithelium and five containing crypt epithelium were examined for each case. Within each field the twenty leftmost

epithelial cells were examined and the number staining positive in the tight junction region was counted. Summation of the numbers from all five fields thus yielded a percentage of tight junctions staining positive. As in most cases the epithelial staining for claudins 3 and 4 also involved the lateral membranes, the percentage of crypt and surface epithelial cells staining positive at this location was also computed in the same manner. On completion of the counting, the cases were categorised into their respective diagnostic categories and compared statistically (see 2.8).

The cases used for illustration were photographed using a Nikon Coolpix 950 digital camera and processed with Adobe Photoshop 6.0 software (Adobe Systems Incorporated, California, USA).

## 2.2 EPITHELIAL CELL ISOLATION

The method used was based on that of Flint et al. (1991). Surgical specimens of human colon were used to isolate epithelial cells. Approximately $10cm^2$ of tissue was used. In cases of IBD, mildly inflamed areas were selected if possible to improve the yield of epithelial cells, which were lower in inflamed areas containing denuded mucosa. In non-IBD cases, areas distal from the abnormal lesion (usually a malignancy) were obtained and considered 'normal'. Samples were obtained fresh from surgery (i.e. without any fixative) and then placed in a medium for transport (McCoy's 5A, Invitrogen). The mucosa was then dissected from the submucosa and cut into 3-5 millimetre (mm) pieces. These were washed for 5 minutes in 50ml of ice-cold Hank's Balanced Salt Solution (HBSS, pH7.3; Invitrogen) containing 0.5mM dithiothreitol (DTT) by stirring gently at 4°C. The tissue and solution were then passed through a strainer and the tissue that collected on the strainer was then added to 150ml of ice-cold chelating buffer (appendix 1) and stirred gently for 20 minutes at 4°C. The tissue and solution were strained again, and this time the tissue was added to 25ml of chelating buffer. The solution obtained by straining was centrifuged at 1500 revolutions per minute (rpm) for 5 minutes at 4°C, producing a cell pellet and a supernatant, which was discarded. The pellet was resuspended in the small amount of residual fluid that remained around it, and 50µl were taken and mixed with an equal amount of trypan blue (Invitrogen), dropped onto a slide and viewed by light microscopy to determine, firstly, the type of tissue obtained (i.e surface epithelial islands, epithelial crypts, with an

approximate assessment of the degree of contamination by red cells), and, secondly, the viability of the epithelial cells obtained by their ability to exclude trypan blue. At this stage, surface epithelial islands were often obtained, but the amounts were often very small. The remaining tissue in 25ml of chelating buffer was gently inverted twenty times to free more cells into the chelating buffer and strained again. The tissue was again added to a fresh 25ml aliquot of chelating buffer. The strained solution, now turbid with freed cells, was treated as before (i.e. centrifuged at 1500rpm for five minutes, supernatant discarded, pellet resuspended in the small amount of residual fluid, and an aliquot stained with trypan blue). This process was repeated until either the number of surface epithelial cells being obtained was minimal, or a few crypts were beginning to emerge. At this point, the process was repeated as before except that, instead of gentle inversions of the tissue with 25ml of chelating buffer, the two were shaken vigorously together. This freed intact or partially broken crypts from the underlying matrix, which, after straining and centrifugation at 1500rpm, were resuspended and an aliquot checked by trypan blue exclusion as for the surface cells previously. The remaining crypt cell suspension was made up to 0.5ml with chelating buffer, centrifuged at 5000rpm for one minute and the cell pellet snap-frozen in liquid nitrogen before being stored at -80°C. The process was repeated until the number of crypts obtained and the size of the cellular pellet became minimal. Thus, this process generated a set of pellets containing epithelial crypts, which could be stored and utilised in experimental studies.

## 2.3 CELL CULTURE

The colonic cancer cell line T84 was cultured in 75cm$^2$ flasks (BD Biosciences, Oxford, UK) in Dulbecco's Modified Eagle Medium (DMEM) / Hams Nutrient F12 Mix, supplemented with 10% FBS, 100units/ml penicillin, 100µg/ml streptomycin and 2mM glutamine (all from Invitrogen). All cells were incubated at 37°C in 5% $CO_2$. For the experiments the cells were subcultured at a split ratio of 1:1 into various culture vessels as follows: six-well plates, each well either pre-coated with 17µl of collagen S (Roche Products Ltd, Welwyn Garden City, UK) or containing three glass 13mm diameter coverslips (each pre-coated with 2µl of collagen S); six- or twelve-well plates containing BIOCOAT Control Cell Culture Inserts (BD Biosciences), which had a filter containing 0.4µm pores. Six-well inserts were 4.2cm$^2$ in area and pre-coated with 10µl

of collagen S, whereas twelve-well inserts were 0.9cm$^2$ and precoated with 4µl of collagen S. Cells were subcultured onto the filters themselves. In the case of the filter experiments, at least one extra filter containing no cells was used to control for the characteristics of the filter and medium alone. The volumes of medium used were: 3ml per well and 1.5ml per insert in six-well plates or 2ml per well and 0.9ml per insert in twelve-well plates. Medium was changed every second day. Confluency was assessed in percentage terms by phase contrast light microscopy.

### 2.3.1 CELL CULTURE IN SERUM-FREE MEDIUM

Prior to some experiments, T84 cells were cultured in serum-free medium. In some instances the DMEM / Ham's F12 Nutrient Mix and FBS portions of the medium were replaced with Ultraculture serum-free medium (BioWhittaker, Wokingham, UK), which contains the DMEM / Ham's F12 Nutrient Mix supplemented with BSA (1%), insulin, transferrin (5ng/ml) and selenium (5ng/ml). In other cases, a serum-free medium was made from all these constituents except the insulin.

### 2.3.2 CALCIUM-SWITCH EXPERIMENTS

To expose T84 monolayers to a low calcium environment, they were rinsed twice with Dulbecco's phosphate-buffered saline (D-PBS; Invitrogen) and incubated for two hours in HBSS, which contains no calcium or magnesium. Control monolayers were rinsed twice with calcium- and magnesium-containing D-PBS (known as PBS-Ca-Mg) and incubated in HBSS containing added calcium chloride at a final concentration of 1.2mM.

### 2.3.3 CYTOKINES, ENZYME INHIBITORS AND LITHIUM CHLORIDE

The cytokines used were IFNγ, TNFα, IL-17 and IL-13 (R&D Systems Europe Ltd, Abingdon, UK). They were dissolved in PBS with 0.1% BSA to make stock solutions and stored at -20°C. The enzyme inhibitors used were Ly294002 and wortmannin (Merck Biosciences Ltd, Nottingham, UK). These were dissolved in dimethyl

sulphoxide (DMSO) to make stocks of 50mM (Ly294002) and 10mM (wortmannin), which were stored at -20°C.

Lithium chloride was dissolved in water to make a stock solution of 2M, which was stored at 4°C.

### 2.3.4 MEASUREMENT OF TRANSEPITHELIAL ELECTRICAL RESISTANCE

In filter experiments, the medium was changed at least 2 hours before measuring transepithelial epithelial resistance (TER) using an EVOM voltohmeter and an STX2 electrode (both from World Precision Instruments, Stevenage, UK). The electrode was soaked in 70% ethanol and rinsed with sterile D-PBS prior to use. The electrical resistance between the lower compartment (well) and the upper compartment (filter insert) was measured. Three measurements were taken and the mean was calculated. Three readings were also taken from a collagen-coated insert that contained medium but no cells and had been treated in exactly the same way as the experimental inserts. The mean of these was subtracted from those obtained for the inserts containing cells to give a true TER for the cell monolayer alone. The measurements were expressed as ohm.cm$^2$ by multiplying by the area of the filter inserts (0.9cm$^2$).

### 2.3.5 MEASUREMENT OF PERMEABILITY TO UNCHARGED MOLECULES

The permeability of T84 monolayers to the passage of uncharged molecules was assessed using fluorescein isothiocyanate (FITC)-conjugated 4kDa dextran with cells cultured on 0.9cm$^2$ filter inserts. A stock solution of 50mg per ml was made and stored at -20°C. The medium on the cells was changed (1ml to the basal compartment and 350µl to the apical compartment). After 1 hour the medium was replaced again; however, the apical compartment contained FITC-dextran at a final concentration of 2mg per ml. After incubation for 3 hours the basal medium was removed for the assay. Three 100µl samples were used for each monolayer examined. Fluorescence was measured in opaque 96-well Nunc™ plates (Fisher Scientific UK Ltd, Loughborough, UK) using an FLX-800 Fluorimeter (Bio-Tek Instruments Inc., Winooski, Vermont, USA) at excitation and emission wavelengths of 490nm and 520nm respectively. The fluorimeter was programmed to take ten measurements per sample and compute the

mean. A standard curve was constructed by measuring the fluorescence obtained from FITC-dextran solutions of known concentrations in cell culture medium. Thus, from a level of fluorescence obtained across a T84 monolayer, a concentration could be computed.

### 2.3.6 MEASUREMENT OF CELL TOXICITY

T84 cell toxicity was assessed by measuring lactate dehydrogenase (LDH) release into the medium using a commercially available kit (Roche). The LDH activity is determined in a two-stage enzymatic test. In the first step $NAD^+$ is reduced to $NADH/H^+$ by the LDH-catalysed conversion of lactate to pyruvate. In the second step a catalyst (diaphorase) transfers $H/H^+$ from $NADH/H^+$ to a supplied tetrazolium salt, which is reduced to formazan. This formazan is red and shows a broad absorbance maximum at a wavelength of about 500nm, whereas the tetrazolium is pale yellow and shows no significant absorption at these wavelengths. The amount of red colour formed in the assay is proportional to the number of lysed cells, and thus total LDH released, but only for a limited time (about half an hour).

Two 100µl samples were used for each monolayer examined. These were placed into a 96-well Nunc™ plate (Fisher) along with a series of standard samples of known, but differing, LDH concentrations, and the mixture of diaphorase and tetrazolium was added to each. After incubation at room temperature for twenty minutes, the absorbance of light at a wavelength of 490nm was read by an MR7000 spectrophotometric microplate reader (Dynatech, Denkendorf, Germany). A standard curve of absorbance versus concentration was constructed so that a test sample's LDH concentration could be computed from its absorbance.

## 2.4 IMMUNOFLUORESCENCE

T84 cell monolayers (on filter inserts or coverslips) had their media discarded and were then rinsed with PBS-Ca-Mg. This was discarded and the filters or coverslips were left to dry overnight in air at room temperature. They were then fixed and permeabilised in acetone for 10 minutes and then air-dried for 15 minutes, before being transferred to a glass slide and mounted in a humidified chamber. 200µl of phosphate-buffered saline

(PBS) containing 5 percent goat serum (Dako) and 1 percent BSA were applied for 30 minutes to prevent non-specific binding of the secondary antibody to the cells. Each monolayer was then incubated with a solution of a primary antibody, for either 2 hours at room temperature (coverslips) or overnight at 4 C (filters). Antibodies were diluted to appropriate concentrations, as determined by prior titration experiments (table 2.2), in a one per cent solution of BSA in PBS (known as PBS-1% BSA). PBS-1% BSA containing immunoglobulin of the same species as the primary antibody, at the same concentration, was used on separate monolayers to control for any non-specific binding by the primary antibody. Primary antibody solutions were then discarded and the monolayers washed for 5 minutes three times with PBS, discarding the solution each time with a Pasteur pipette. The monolayers were then incubated with 200µl of secondary antibody solution (table 2.2), again diluted in PBS-1% BSA, for 90 minutes at room temperature. After removing this solution, they were washed for 5 minutes twice in PBS, discarding the solution each time. The cell nuclei were then counterstained for 10 minutes with PBS-1% BSA containing either TO-PRO-3-iodide (0.67µg/ml; Molecular Probes Europe Ltd, Leiden, Netherlands) or 7-amino-actinomycin D (7-AAD; 2µg/ml) depending on the particular experiment. This was followed by two further washes with PBS. The wash solution was removed and coverslips were mounted on the slide using 0.1% mowiol mountant in Antifade (Citifluor Ltd, London, UK) and square 22mm coverslips. The slides were stored away from light at 4°C until viewing by confocal laser scanning microscopy (Leica SP2 and software).

For dual staining experiments the two primary antibodies were mixed together in a single solution and applied in the same way as described above. The two secondary antibodies were also mixed before being applied.

| *Antibody* | *Species (Isotype)* | *Concentration (µg/ml)* | *Source* |
|---|---|---|---|
| Claudin 2 | Rabbit | 1.7 | Zymed |
| Claudin 3 | Rabbit | 1.25 | Zymed |
| Claudin 4 | Mouse (IgG1) | 2.5 | Zymed |
| Ki-67 | Mouse (IgG1) | 3.2 | Dako |
| Activated β-catenin | Mouse (IgG1) | 4.3 | Upstate |
| AlexaFluor-488 anti-rabbit | Goat | 2 | Molecular Probes |
| AlexaFluor-633-anti-mouse | Goat | 10 | Molecular Probes |
| AlexaFluor-546-anti-mouse | Goat | 2 | Molecular Probes |

*Table 2.2. Primary antibodies used in immunofluorescence, including species, concentrations and sources (company address not given in text: Upstate Biotechnology, Milton Keynes, UK).*

## 2.5 PROTEIN EXTRACTION FROM CELLS

### 2.5.1 MATERIALS AND METHODS

Whole cellular protein was extracted from tissue cell pellets by adding an equal volume of 2x-concentrated SDS sample buffer with 10% v/v protease inhibitor cocktail (appendix 1) at 95°C, followed by homogenisation with an 18F gauge needle and further incubation at 95°C for 5 minutes. T84 cell monolayers were lysed with 1x SDS sample buffer with protease inhibitors, and phosphatase and kinase inhibitors (appendix 1) using the hub of a 1ml syringe. 5µl of the supernatant was retained to determine the protein concentration. The reminder of the supernatant was frozen at -80°C in 50µl aliquots until required. Once thawed, protein extracts were kept at 4°C, and their concentrations were adjusted to 2mg/ml by adding 1x SDS sample buffer. The concentration of DTT was adjusted to 100mM using a 1M DTT stock solution and

bromophenol blue (appendix 1) was added to a final concentration of 0.1%, before being heated to 95°C for 2 minutes, allowed to cool for a few seconds in air, centrifuged briefly at 200g, and then used immediately in SDS-polyacrylamide gel electrophoresis (SDS-PAGE, see below).

### 2.5.2 PROTEIN CONCENTRATION ASSAY

Protein concentrations were determined by the bicinchoninic acid (BCA; Perbio Science Ltd, Tattenhall, UK) method using a Beckman DU 530 spectrophotometer (Beckman Coulter Ltd, High Wycombe, UK). A series of standard albumin solutions of increasing dilution were created, and these, together with 10% v/v dilutions of our test protein solutions and one sample of nanopure water, were incubated at 37°C for 30 minutes with a twenty-fold larger volume of the BCA Protein Assay Reagent (a solution of sodium carbonate, sodium bicarbonate, BCA, sodium tartrate in 0.2M sodium hydroxide, mixed in a ratio of 50:1 with a solution of 4% cupric sulphate). A standard curve was then constructed by measuring absorbance of light at 562nm wavelength of the various standard albumin concentrations, relative to a sample of nanopure water. The concentrations of test protein solutions were then read off against this curve and corrected for their ten-fold initial dilution.

## 2.6 SDS-PAGE AND WESTERN BLOTTING

### 2.6.1 SDS-PAGE

SDS-PAGE and western blotting were carried out using a Hoefer MiniVE system (Amersham Biosciences, Chalfont St Giles, UK). Resolving gels for SDS-PAGE were made with either 12.5% or 10% acrylamide (National Diagnostics UK Ltd, Hessle, UK) in nanopure water (Laemmli, 1970), depending on the size of the proteins to be detected. The other constituents are listed in appendix 1. The solution was polymerised under 100µl of water-saturated n-butanol for one hour at room temperature; the butanol was then discarded, the gel surface washed with nanopure water. The resolving gel was then overlaid with the stacking gel (appendix 1) and a comb to form wells and allowed to polymerise for one hour at room temperature. The wells were washed with

electrophoresis buffer (appendix 1) and the gel was set up in a tank with electrophoresis buffer contacting top and bottom surfaces of the gel. Samples were then applied to the wells. Sixteen μg of tissue epithelial protein or 10μg of T84 cell protein was loaded into each well. One well contained 10μl of BenchMark Prestained Protein Ladder (Invitrogen), which includes pre-stained proteins at various molecular weights (9.3, 13.1, 19.2, 24.7, 36.4, 49.0, 61.3, 79.6, 111.4 and 172.6 kDa). The gel was run at a constant voltage of 150V until the bromophenol blue had reached the bottom of the gel. Before western blotting, the stacking gel was discarded, and the resolving gel was soaked in transfer buffer (appendix 1) for 10 minutes. A corner of the resolving gel was cut off to mark the orientation of the gel.

### 2.6.2 WESTERN BLOTTING

A piece of polyvinylidene difluoride (PVDF) membrane (Amersham Biosciences), slightly larger than the resolving gel, was permeabilised by soaking for a few seconds in methanol, rinsed for 5 minutes in nanopure water, and soaked in transfer buffer for 10 minutes. Western blotting was carried out by apposing the PVDF membrane and the resolving gel, and placing these two within a sandwich formed by two pieces of Whatman filter paper (Whatman International Ltd, Maidstone, UK). A set of sponges, pre-soaked in transfer buffer, was placed on top of and below the sandwich, and the entire assemblage was arranged in a module with the membrane facing the anode and the gel facing the cathode. The module was filled with transfer buffer and bubbles eliminated. A constant voltage of 25V was applied for 2¾ hours, and the module kept cool by immersing it in ice-cold water. The module was then opened and the success of transfer determined by inspecting the membrane for the pre-stained protein markers.

The membrane was incubated with blocking solution (appendix 1) for 1 hour at room temperature with gentle agitation, followed by incubation overnight with primary antibody, diluted to the appropriate concentration (as determined by prior titration experiments; table 2.3). Polyclonal antibodies were diluted in blocking solution, and monoclonal antibodies in a solution of phosphate-buffered saline and Tween20 (PBS-T; appendix 1) containing 0.1%BSA. In addition, separate strips of membrane were incubated without primary antibodies but with immunoglobulins of the same species and isotype as the primary antibodies (Dako), and at the same (or greater)

concentration, in order to control for non-specific binding of the primary antibodies to the membrane-bound proteins. Because total cellular cytokeratin expression is assumed to be invariate in epithelial cells, an antibody to cytokeratin 19 (Dako) was used on all blots to check for equivalent loading of epithelial-derived protein in each lane of the gel.

After overnight incubation, the membrane was rinsed twice in PBS-T, followed by three 15-minute washes in PBS-T, using fresh solution and agitation each time. It was then incubated for 3 hours with the appropriate HRP-conjugated secondary antibody (table 2.3), diluted in blocking solution. After two rinses and three 15-minute washes in PBS-T, the membrane was ready for detection. This involved the addition of a commercially available chemiluminescent substrate plus peroxide (ECL Plus, Amersham Biosciences) to the HRP for five minutes, followed by scanning at 430nm using a GeneGnome scanner and GeneSnap software (Syngene Corporation, Cambridge, UK). Scans were undertaken for several durations to ensure that the images were not overexposed. Images were imported into Adobe Photoshop 6 software (Adobe) for reproduction.

The blots were performed under identical conditions for each experiment. All samples were blotted at least twice. Evenness of transfer by western blotting was confirmed by incubating and developing a membrane on which the same sample had been run in all lanes, as shown in figure 2.1. The primary and secondary antibodies used, their species of origin, concentrations and sources are listed in table 2.3.

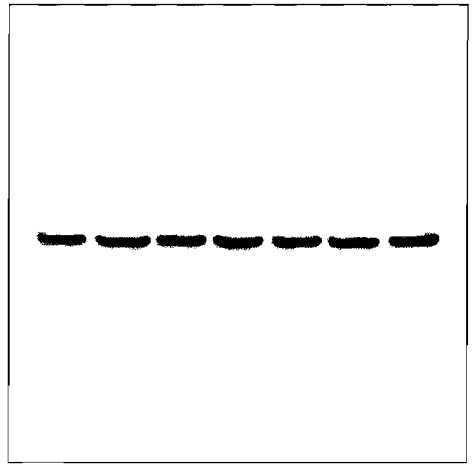

*Figure 2.1. Western blot of T84 cell protein probed for cytokeratin 19. Evenness of transfer is confirmed by the equivalence of the bands obtained across the blot.*

| *Antibody* | *Species (Isotype)* | *Concentration (ng/ml) or Dilution* | *Source* |
|---|---|---|---|
| Claudin 2 | Rabbit | 625 | Zymed |
| Claudin 3 | Rabbit | 3.125 | Zymed |
| Claudin 4 | Mouse (IgG1) | 6.25 | Zymed |
| Cytokeratin 19 | Mouse (IgG1) | 1:10000 | Dako |
| Phospho-Akt | Mouse (IgG2b) | 1:1000 | New England Biolabs |
| Akt | Rabbit | 1:1000 | New England Biolabs |
| Phospho-GSK3β | Rabbit | 1:1000 | New England Biolabs |
| GSK3β | Rabbit | 1:1000 | New England Biolabs |
| Activated β-catenin | Mouse (IgG1) | 429 | Upstate |
| β-catenin | Mouse (IgG1) | 12.5 | BD Biosciences |
| HRP-anti-mouse | Rabbit | 1300 | Dako |
| HRP-anti-rabbit | Goat | 300 | Dako |

*Table 2.3. Primary and secondary antibodies used in western blotting experiments (company addresses not given in text: New England Biolabs Ltd, Hitchin, UK).*

### 2.6.3 STRIPPING AND REPROBING OF MEMBRANES

Membranes were stripped of antibody by incubating in stripping buffer (appendix 1) for 30 minutes at 65°C, followed by two rinses and two 10-minute washes in fresh PBS-T, followed by blocking as before. In the case of the claudins, they were detected in numerical order, followed by cytokeratin 19. The success of this stripping procedure was confirmed by incubating a stripped membrane with secondary antibody and developing with ECL Plus in the usual way, as shown in figure 2.2. This was performed

on the same day that another complete blot was developed to confirm that there was no technical reason for the failure to detect bands after stripping.

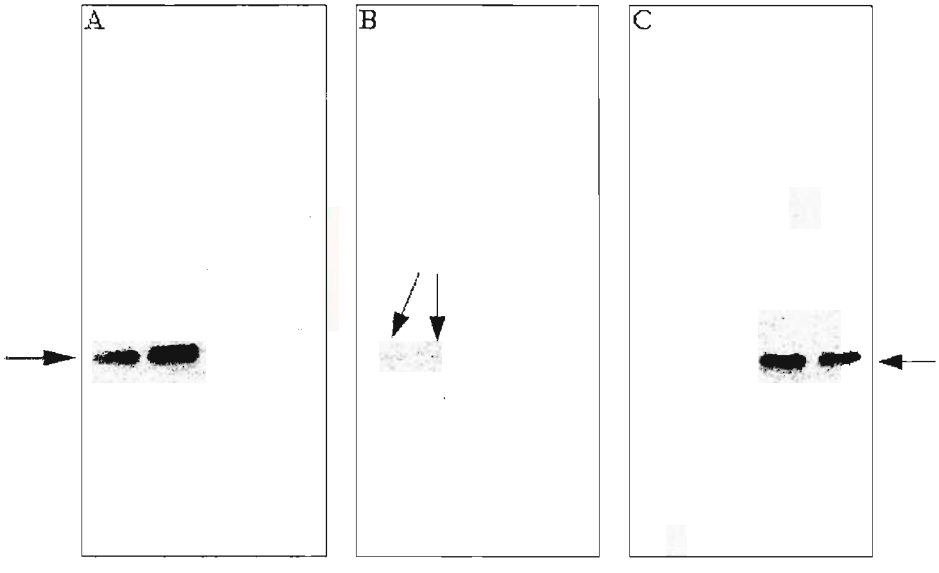


*Figure 2.2. Western blots of T84 cell protein to illustrate efficacy of stripping protocol. In panel A, the two left-hand lanes were incubated with antibody to claudin 3 and gave positive bands at this 5 second detection, whereas the two right-hand lanes were incubated with rabbit Ig only and no bands were detected. In panel B, the same membranes were stripped of antibody and incubated with only secondary antibody prior to detection. At 120 seconds only very faint bands were detected. This blot was developed at the same time as those in figure 2.3. In C, the same membranes were stripped again, but this time the left-hand lanes were incubated with rabbit Ig and the right-hand ones with claudin 3 antibody. After a 5 second detection, no bands were detected in the left-hand lanes, whereas strong bands were detected in the previously negative right-hand lanes.*

### 2.6.4 DENSITOMETRIC ANALYSIS OF WESTERN BLOTS

The intensity of the bands obtained on some western blots was analysed using QuantityOne software (Bio-Rad Laboratories Ltd, Hemel Hempstead, UK). This was performed on the blots of both isolated epithelial cell protein and T84 cell lysates, and for two reasons. Firstly, it was carried out because probing with antibody to cytokeratin 19 had shown unevenness of epithelial protein loading, and so a method was required to allow valid comparison between lanes. Secondly, the number of samples examined extended across more than one blot, and so valid comparisons between them required quantitation relative to the loading control (cytokeratin 19).

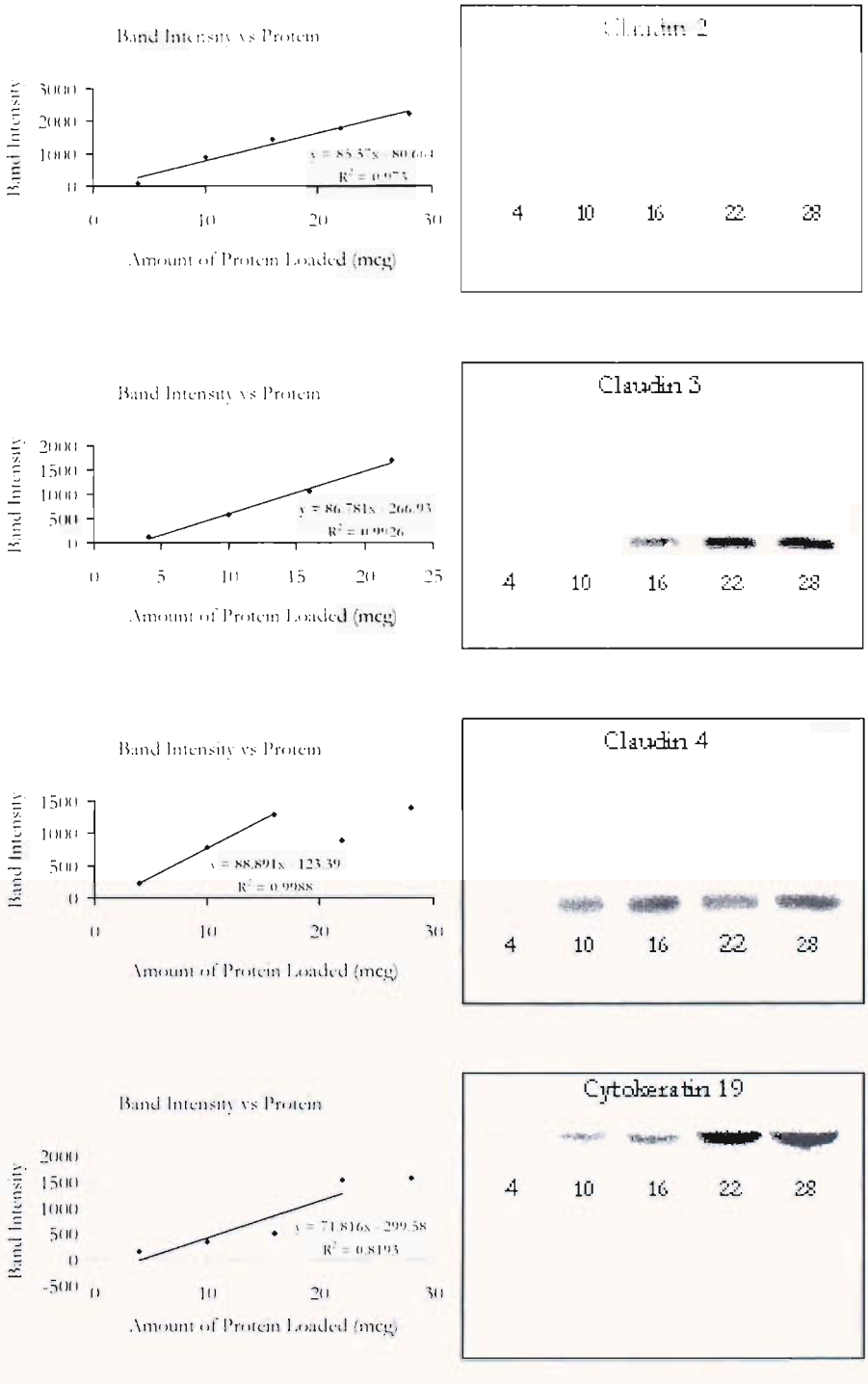


*Figure 2.3. Western blots of colonic epithelial protein in which increasing amounts of the same protein have been loaded from left to right. The right-hand panels depict blots probed for claudins 2-4 and cytokeratin 19 as marked; each number represents the amount of protein loaded in that particular lane. The left-hand panels show the relationship between band intensity, as determined using Quantity One software, and the amount of protein loaded.*

The intensity of a band obtained with, for example, the claudin 2 antibody was divided by that obtained with the cytokeratin 19 antibody (after stripping and reprobing the same membrane) to yield a ratio. This normalisation to cytokeratin 19 allowed a comparison of different samples, so long as there was a similar, and preferably linear, relationship between the amount of protein loaded in a lane and the resulting band intensity. In the blots displayed in figure 2.3, the same colonic epithelial protein sample was loaded in each lane of a blot, but in increasing amounts from left to right. The bands obtained after incubating with each of the antibodies shown are of increasing intensity with increasing amounts of protein loaded. These relationships are shown graphically in the left-hand panels, and can be seen to be both close to linear and of similar gradients to that obtained with cytokeratin 19, thus validating the use of the quantitation protocol described above.

## 2.7 QUANTIFICATION OF CLAUDIN 2 MESSENGER RNA

### 2.7.1 RNA EXTRACTION

#### *2.7.1.1 RNA Extraction Using Trizol™*

Total cellular RNA was extracted from isolated epithelial cell pellets using Trizol reagent (Invitrogen), which contains guanidine isothiocyanate (GITC) and phenol, according to the manufacturer's instructions. Each cell pellet was lysed and homogenised by adding 0.5ml of Trizol and repeatedly pipetting the mixture, followed by incubation at room temperature for 5 minutes. Chloroform (0.1ml) was added and the sample shaken vigorously by hand for 15 seconds, followed by incubation at room temperature for 2 minutes. After centrifugation at 12000g for 10 minutes at 4 C, the aqueous supernatant produced was transferred to a fresh tube and 0.25ml of isopropyl alcohol was added to it. After incubation at room temperature for 10 minutes and centrifugation at 12000g for 10 minutes at 4 C, an RNA precipitate was produced. The supernatant was removed and the precipitated RNA was washed by adding 0.5ml of 75% ethanol, vortexing and then centrifuging at 7500g for 5 minutes at 4 C. After removing the 75% ethanol, the pellet was air-dried and then redissolved in RNase-free water.

#### *2.7.1.2 RNA Extraction Using RNeasy™*

Total cellular RNA from T84 cells was extracted using an RNeasy kit (Qiagen Ltd, Crawley, UK), according to the manufacturer's instructions. Cells were lysed with the barrel of a 1ml syringe in Buffer RLT, which contains GITC and β-mercaptoethanol. Homogenisation of samples was achieved by passing the lysate five times through a 21Fr needle. After adding an equal volume of 70% ethanol, the RNA was adsorbed to the silica-gel membrane of a spin column by centrifugation at 8000g for 15 seconds. Contaminants were removed by three applications of wash buffers (Buffer RW1 once and Buffer RPE twice), each followed by centrifugation at 8000g for, successively, 15 seconds, 15 seconds and two minutes. After a further full speed centrifugation for 1 minute, the RNA was eluted into a microfuge tube by adding 45µl of RNase-free water and centrifuging for 1 minute at 8000g and then quantified.

#### *2.7.1.3 Quantification of RNA*

A 5µl aliquot of each sample was diluted ten-fold and its absorbance of light at a wavelength of 260nm was measured using a Beckman DU 530 spectrophotometer (Beckman Coulter). The concentration of RNA was calculated on the basis that 1 absorbance unit at 260nm (1 $A_{260}$ unit) equates to 40µg/ml RNA.

### 2.7.2 DNASE TREATMENT OF RNA SAMPLES

RNA samples were treated with DNase I enzyme to minimise any contamination by genomic DNA. A proprietary kit (DNA-Free™, Ambion Europe Ltd, Huntingdon, UK) was used. Up to 4µg of RNA was incubated for 30 minutes in a 37°C water bath with 2 units of DNase I in a 20µl reaction volume. DNase activity was then blocked by the addition of 5µl of DNase Inactivation Reagent at room temperature. After brief centrifugation at 10000 revolutions per minute (rpm), the supernatant containing the RNA was decanted and stored at -80°C or used directly in a reverse transcription step.

## 2.7.3 REVERSE TRANSCRIPTION

### *2.7.3.1 Synthesis of Complementary DNA (cDNA)*

After DNase treatment of an RNA sample, two 5µl aliquots were each incubated with a 5µl solution containing 0.5µg of oligo $dT_{15}$ primer (Promega UK Ltd, Southampton, UK) at 80°C for 7 minutes, in order to destroy secondary structure in the RNA that could interfere with cDNA synthesis. After the incubation period samples were placed in ice, centrifuged briefly and returned to ice to inhibit re-hybridisation of the RNA.

Each of the pair of samples was then heated to 37°C for an hour with a 10µl reverse transcription Mastermix (appendix 1) with or without reverse transcriptase (RT). Thus, for each RNA sample, aliquots were either reverse transcribed to a single strand of cDNA (denoted RT+), or subjected to the same process in the absence of the enzyme to produce a control sample in which any cDNA must have been copied from contaminating DNA (denoted RT-). The samples were then heated to 78°C for 10 minutes to inactivate the enzyme. Their concentrations were adjusted to 5ng/µl by adding nuclease-free water and they were stored at -20°C.

## 2.7.4 QUANTITATIVE POLYMERASE CHAIN REACTION

### *2.7.4.1 Quantification of Claudin 2 mRNA*

#### 2.7.4.1.1 Principle

The Polymerase Chain Reaction (PCR) was used to compare the amounts of claudin 2 cDNA (and thus mRNA) contained in different samples. PCR is a technique used to amplify a specific sequence of DNA that may otherwise be in too small an amount to quantify. Two presynthesised, short DNA sequences (primers), which are complementary to two separate sequences on the two strands of the DNA molecule of interest, are used to prime an enzyme (DNA polymerase) that synthesises a DNA strand adjacent to the primers and complementary to the pre-existing sequences. Thus, for the DNA sequence between the primers, the initial two complementary strands become two pairs of complementary strands. The reaction thus requires the four precursor nucleotides that make up DNA. Once this DNA synthesis has occurred, the products

are heated to separate the newly formed double-stranded DNA molecules, and then cooled to allow the primers to anneal to their complementary sequences on the single stranded DNA template molecules. The reaction temperature is then altered to that which permits the DNA polymerase to again synthesise the strands complementary to the templates, adjacent to the primers, before repeating the cycle of separation, annealing and synthesis. If the primers, nucleotides and enzyme are initially in excess, every cycle will lead to a doubling of the amount of DNA corresponding to the sequence between the primers on the original mRNA molecule. This amount of DNA can be compared across multiple samples after a certain number of cycles, or, as here, the cycle number at which the amount of DNA reaches a threshold can be compared.

#### 2.7.4.1.2 Primers

The basic organisation of CLDN2, the gene encoding claudin 2, is depicted in figure 2.4.

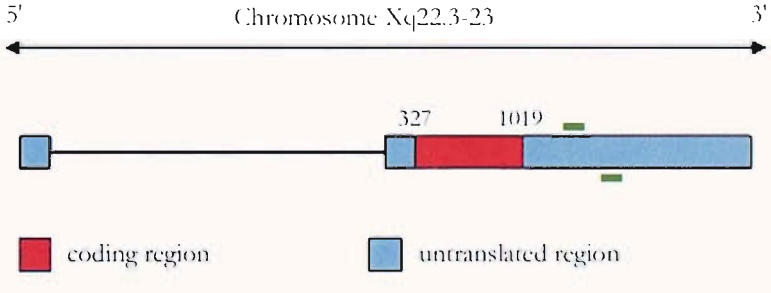


*Figure 2.4. Location and structure of CLDN2 (adapted from NCBI Gene database, GeneID 9075). The numbers 327 and 1019 represent the beginning and end of the coding region (taken from the NCBI Nucleotide Reference Sequence (RefSeq) database entry NM_020384). The green lines depict the approximate location of the primers for claudin 2.*

Sense and antisense primers to this gene (obtained from Operon Ltd, Cologne, Germany) were designed with the assistance of Dr R Powell (University of Southampton) using Beacon Designer 3 software (Premier Biosoft International, Palo Alto, California, USA). The locations of the primers in relation to CLDN2 are depicted in figure 2.4, and their sequences are shown below. The numbers represent the location of the primers on the NCBI Nucleotide Reference Sequence (RefSeq) database entry

NM_020384, which represents the coding sequence for claudin 2. Their predicted melting temperatures ($T_m$) are 59.4°C (sense) and 59.6°C (antisense).

Sense Primer: 1376- TCCCACTGACTGACCCTCTGT -1396

Antisense Primer: 1468- GCCACTGCTTCTCCTTCCCAT -1448

The PCR product (amplicon) between these primers was 93 base pairs (bp) in length, and had a predicted $T_m$ of 86.8°C.

#### 2.7.4.1.3 Reaction

The PCR reactions were performed quantitatively in an iCycler (Bio-Rad). SYBR Green was used to measure the amount of accumulating amplicons. This agent binds strongly to double-stranded DNA and fluoresces much more strongly on doing so. Fluorescein was used as a reference for this fluorescence. The DNA polymerase used was Hot Goldstar (Eurogentec Ltd, Romsey, UK).

For each initial RNA sample the reaction was performed in triplicate, i.e. three 5µl (25ng) aliquots of RT+ and one of RT- were each combined with 7.69µl of a Polymerase Chain Reaction (PCR) Mastermix. This solution contained 6.5µl of qPCR Mastermix (containing Hot Goldstar, all four dNTPs and 5mM magnesium chloride; Eurogentec), 0.0625µl of SYBR green (1% in DMSO), 0.125µl of 1mg/ml fluorescein and 1µl of a solution containing sense and antisense oligonucleotide primers to claudin 2 at 15µM each.

The samples were heated to 95°C for 9 minutes to activate the Hot Goldstar, followed by 45 or 50 cycles of separation of DNA strands (95°C for 15 seconds) and annealing and extension (60°C for 1 minute). The iCycler measured the fluorescence emitted from each sample in real-time at the peak absorbance and emission wavelengths of SYBR Green (497nm and 520nm respectively).

At the end of the reaction the Calculated Threshold (CT) for each sample was derived. During the PCR reaction the amount of accumulating amplicons, and thus fluorescence, follows an S-shaped curve. The CT is the cycle at which the degree of fluorescence reaches ten times the background level. As every cycle doubles the template, each incremental increase in CT represents a relative halving of the amount of

starting template and allows comparison of multiple samples simultaneously. Thus, a sample giving a CT of 25 contains $2^5$ less mRNA than one giving a CT of 20.

#### 2.7.4.1.4 Testing of Primers

The claudin 2 primers were tested for efficacy on a sample of T84 cell cDNA and the result is depicted in figure 2.5. The CT for claudin 2 expression in this sample was 21-22, suggesting that the primers were efficient. It can be seen that there is small variation in CT within the duplicate but wider variation in fluorescence after a higher number of cycles. One of the RT- duplicates crossed the threshold at a high cycle number (44), showing that after DNase treatment there was a negligible amount of contaminating, genomic DNA within the samples, but suggesting that no other product was being generated in the reaction. The samples of water (denoted no template or NT) generated no product, showing both that there was no general contamination of reagents with any source of claudin 2 DNA and that the primers did not form dimers.

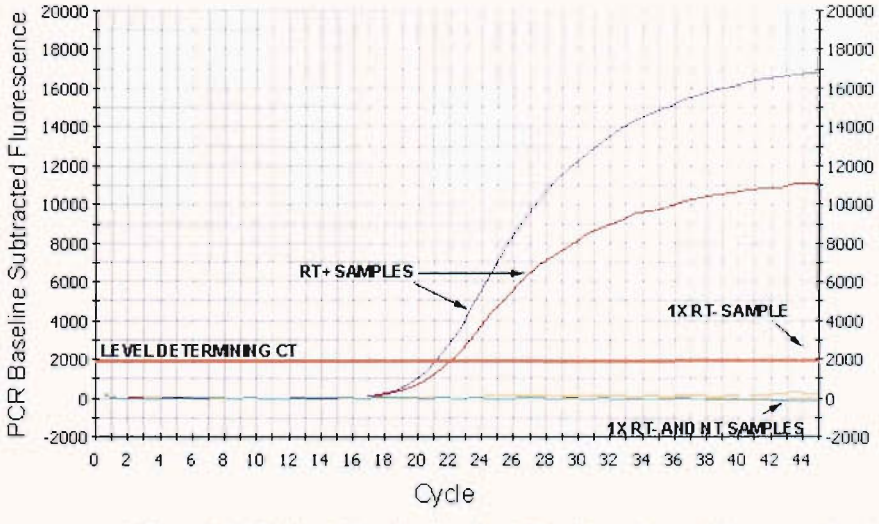


*Figure 2.5. Testing of claudin 2 primers. Baseline subtracted fluorescence is plotted against cycle number. Duplicate samples of RT+, RT- and water (no template or NT) entered the reaction.*

#### 2.7.4.1.5 Melt Curve Analysis

Although the claudin 2 primers appeared efficient above, further analysis using a melt curve analysis (figure 2.6) confirmed that a single product was being generated with a peak melting temperature corresponding to predictions. A melt curve is a graph

depicting the rate of decrease in fluorescence against temperature during a slow and controlled increase in temperature from 50°C to 90°C after completion of the PCR. As the PCR products melt with increasing temperature, bound SYBR Green is released. When the melting point of a PCR product is reached, the rate of decrease in fluorescence is high, resulting in a peak at this temperature. A single, sharp peak at or around the predicted $T_m$ of the target amplicon confirms a single product of the correct length, attesting to the specificity of the primers.

#### 2.7.4.1.6 Standard Curve and Priming Efficiency

As the accumulation of PCR products is exponential, serial four-fold dilutions of a template should lead to serial increases in CT of 2 cycles if the priming efficiency is 100%. However, this efficiency may fall if one of the primers forms hair pin structures that interfere with annealing, or because the secondary structure of the amplicon interferes with primer binding. It may exceed 100% if primer dimer formation has occurred. A plot of CT against log|dilution number| is called a Standard Curve. Its gradient should approach -3.28, which equates to an efficiency of 100%, and its correlation coefficient should exceed 0.95. Figure 2.7 depicts a Standard Curve for claudin 2 over serial four-fold dilutions. The gradient is -3.275 and the correlation coefficient is 0.99. This confirmed a priming efficiency that validated the use of the claudin 2 primers.

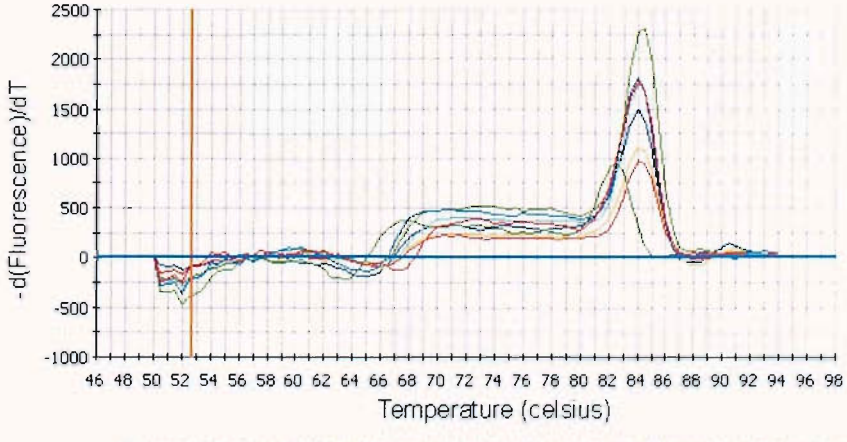


*Figure 2.6. Post-PCR melt curve of rate of decrease in fluorescence (y-axis) against temperature for a sample of T84 cDNA diluted serially by a factor of 4 . All the samples produced a single peak at around the predicted $T_m$ of the amplicon.*


*Figure 2.7. Graph of CT against log|dilution| for a single sample serially diluted by a factor of 4. The gradient=-3.275 with a correlation coefficient of 0.99.*

### *2.7.4.2 Quantification of Housekeeping Genes*

#### 2.7.4.2.1 Principle

Using the same cDNA samples as those used to compare claudin 2 expression levels, separate reactions were performed to compare the mRNA levels of genes whose expression levels are assumed to be invariant (so-called housekeeping genes or HKs). By normalising each measured expression level of claudin 2 to those for the HKs, differences could be compensated for between the samples in the amount of cDNA present in the reaction. In other words, if one sample contained more cDNA than the others in an experiment, the measured amounts of both claudin 2 and the HKs would be higher, and so normalising the claudin 2 expression levels to those for the HKs would correct for this.

Two HKs were utilised and these were the genes for glyceraldehyde 3-phosphate dehydrogenase (GAPDH) and ubiquitin C (UBC). Two were used in order to check the assumption that their expression was invariant, in which case the ratio of their expression levels would be constant. A solution containing primer pairs for both mRNAs was used (Eurogentec). In addition, this solution contained two oligonucleotide sequences of DNA complementary to part of the amplicon for each gene (known as probes). In the case of GAPDH, this probe was labelled at the 5' end with the fluorophore 5-carboxyfluorescein (FAM, Applied Biosystems, Warrington, UK), whereas the probe for UBC was labelled with VIC (Applied Biosystems). Both probes were also bound at their 3' ends to a molecule known as a quencher, which suppresses the fluorescence of the bound fluorophore in an intact probe molecule. Each probe binds to its complementary sequence in the template cDNA of a PCR reaction, but as a successfully primed DNA polymerase synthesises a new

complementary sequence of DNA at the same point, its 5' → 3' exonuclease activity cleaves the bound probe. The quencher and the fluorophore are thus physically separated and the fluorescence is no longer suppressed but can now be detected. The amount of fluorescence detected after a certain number of PCR cycles is thus proportional to the number of cleaved probe molecules and so also to the amount of DNA synthesised at the site where probe molecules were bound. It is thus a direct and highly specific measure of the amount of amplicons synthesised. Using two different fluorophores for two different genes of interest allows both genes to be analysed simultaneously in the same sample. This method does not require an intercalating agent such as SYBR Green.

#### 2.7.4.2.2 Reaction

For each cDNA sample, three 5µl aliquots of RT+ and one of RT- were each combined with 12.5µl of the qPCR Mastermix, 6.5µl of nanopure water and 1µl of a solution containing sense and antisense oligonucleotide primers (15µM each) and labelled probe (3.1µM) to both GAPDH and UBC.

The samples were heated to 95°C for 9 minutes to activate the Hot Goldstar, followed by 45 cycles of separation of DNA strands (95°C for 15 seconds) and annealing and extension (60°C for 1 minute). The iCycler measured the fluorescence emitted from each sample in real-time at the peak absorbance and emission wavelengths of FAM (494 and 522nm) and VIC (538 and 554nm).

At the end of the reaction, average CTs for each sample were derived for both GAPDH and UBC. As the CT is an exponential function, these two values were combined to give a single HK CT by calculating their geometric mean.

### 2.7.5 ANALYSIS

At the end of a series of reactions, each sample will have yielded an average CT for claudin 2 (CTCL2) and an average CT for the HKs (CTHK).

To normalise to the HKs, the relative amount of claudin 2 mRNA was divided by the relative amount of HK mRNA:

normalised claudin 2 mRNA = $2^{CTCL2} / 2^{CTHK} = 2^{CTHK - CTCL2}$

$\log_2$ normalised claudin 2 mRNA (denoted $\Delta CT$) = CTHK – CTCL2

To derive the relative amount of normalised claudin 2 mRNA in one sample compared to another, one $2^{CTHK - CTCL2}$ was divided by that for the other. A single sample was chosen as the denominator for all the other samples – usually a control sample.

Thus:

relative amount of normalised claudin 2 mRNA in sample A = $(2^{CTHK - CTCL2})_A$ / $(2^{CTHK - CTCL2})_{Control}$

$\log_2$ relative amount of normalised claudin 2 mRNA in sample A (denoted $\Delta\Delta CT$) = $(CTHK - CTCL2)_A - (CTHK - CTCL2)_{Control}$

relative amount of normalised claudin 2 mRNA in sample A = $2^{-\Delta\Delta CT}$

## 2.8 STATISTICAL ANALYSIS

### 2.8.1 METHODS

#### *2.8.1.1 Parametric Analysis*

The difference in the mean TER between two groups of filter-grown T84 cells was analysed by a group mean comparison (t-) test, using Satterthwaite's correction for unequal variances. For multiple groups compared simultaneously a One-Way Analysis of Variance (ANOVA) was performed. Statistical comparisons were performed only at the beginning and conclusion of each such experiment, and not at multiple time points in between, according to the principles described in Matthews et al. (1990).

#### *2.8.1.2 Non-parametric Analysis*

All other variables were considered to be non-parametrically distributed. Two groups of variables were compared using the Mann-Whitney U test. Comparisons of multiple groups were performed by a Kruskal-Wallis analysis, followed by comparisons of pairs of groups by the Mann-Whitney U test.

### 2.8.2 SOFTWARE AND GRAPHICAL REPRESENTATIONS

All statistical analyses were carried out using the Stata 8 software package (StataCorp LP, College Station, Texas, USA). Comparative scatterplots (dotplots) and histograms were generated using the same package. Barplots and regression plots were generated using Microsoft Excel 2002 software (Microsoft UK, Reading, UK), and the error bars depicted represent one Standard Error of the Mean (SEM) unless otherwise stated.

# CHAPTER 3

# THE TIGHT JUNCTION IN INFLAMMATORY BOWEL DISEASE

# 3 THE EXPRESSION OF TIGHT JUNCTION PROTEINS

## 3.1 INTRODUCTION AND AIMS

Previous studies of tight junctions (TJs) in IBD have shown some alterations when compared to control tissues. For example, a reduced number and a less complex pattern of TJ strands have been noted by freeze-fracture electron microscopy (Sandle et al., 1990; Schmitz et al., 1999; Schulzke et al., 1998). Increased mucosal permeability to ions and tracer molecules such as mannitol and albumin has also been demonstrated in mildly inflamed UC tissues in vitro (Gitter et al., 2001; Schmitz et al., 1999). Recently, two descriptive studies have suggested that significant reductions in the expression of certain TJ proteins (ZO-1 and occludin) may be occurring in the surface epithelium of both UC and CD (Gassler et al., 2001; Kucharzik et al., 2001). However, neither study assessed the expression of the claudins, and both were conducted on paraffin-embedded tissues. Archival GMA-embedded, colonoscopic mucosal biopsies were available for the present study. These facilitate both the long term preservation and storage of tissues, and the cutting of thin (2μm) sections that preserve tissue architecture whilst allowing the assessment of cellular detail.

The aim of this chapter was to examine the expression of claudins 2, 3 and 4, occludin and ZO-1 in the epithelium of normal and IBD colons by immunohistochemistry (IHC), western blotting and qRT-PCR, with the objective of addressing the following questions:

1. What is the staining pattern in normal colons?
2. Does the pattern differ in degree or distribution in IBD?
3. Is the total amount of protein altered in IBD?
4. If gross changes in protein expression are detected, does this involve changes in mRNA levels?

## 3.2 RESULTS

### 3.2.1 ASSESSMENT OF EXPRESSION OF CLAUDINS 2, 3 AND 4, ZO-1 AND OCCLUDIN IN COLONIC BIOPSIES BY IMMUNOHISTOCHEMISTRY

The proteins selected for examination by immunohistochemistry (IHC) were claudin 2, 3 and 4, occludin and ZO-1, together with negative and positive controls. Archival GMA-embedded endoscopic colonic biopsy specimens were sectioned and examined by IHC. Four different diagnostic groups were examined and each case was classified into one of these from the original histopathological assessment of adjacent biopsies taken at the same endoscopic procedure. The four groups were normal colon (NC), inactive ulcerative colitis (UCI), active ulcerative colitis (UC) and Crohn's disease (CD). All cases were encoded to anonymise them and to conceal their diagnoses for the subsequent analysis.

The percentage of cells staining positive in the TJ location (spot-like localisation at the subapical plasma membrane) was assessed for both crypt and surface epithelia for each antigen (as described in 2.1.2). In the cases of claudins 3 and 4, percentages of positively staining cells were also computed for the lateral membranes. These percentages were compared statistically. Following this a subjective assessment of staining patterns was made, in order to detect any trends that may have not reached statistical significance.

The number of cases examined for each antigen is shown in table 3.1.

| Antigen | NC | | UCI | | UC | | CD | |
|---|---|---|---|---|---|---|---|---|
| | *Crypt* | *Surface* | *Crypt* | *Surface* | *Crypt* | *Surface* | *Crypt* | *Surface* |
| *Claudin 2* | 4 | 4 | 4 | 4 | 12 | 12 | 5 | 5 |
| *Claudin 3* | 4 | 4 | 4 | 4 | 12 | 12 | 5 | 6 |
| *Claudin 4* | 4 | 4 | 4 | 4 | 13 | 12 | 4 | 5 |
| *Occludin* | 5 | 4 | 4 | 4 | 12 | 11 | 4 | 4 |
| *ZO-1* | 5 | 5 | 4 | 4 | 12 | 11 | 5 | 5 |

*Table 3.1. Number of cases examined by immunohistochemistry. Staining for claudins 2-4 was performed by Dr K Kankinen; all other staining and all analysis was performed by Dr S Prasad.*

### 3.2.1.1 Negative Controls

Sections were stained using rabbit immunoglobulins (Ig) and mouse Ig of isotype G1 (IgG1) in place of the primary antibodies, in order to control for any non-specific binding of the primary antibodies to the sections. No epithelial staining was observed with either control. Examples are shown in figure 3.1. This suggested that any positive staining observed with the primary antibodies was the result of their binding to protein via their antigen-specific binding sites.

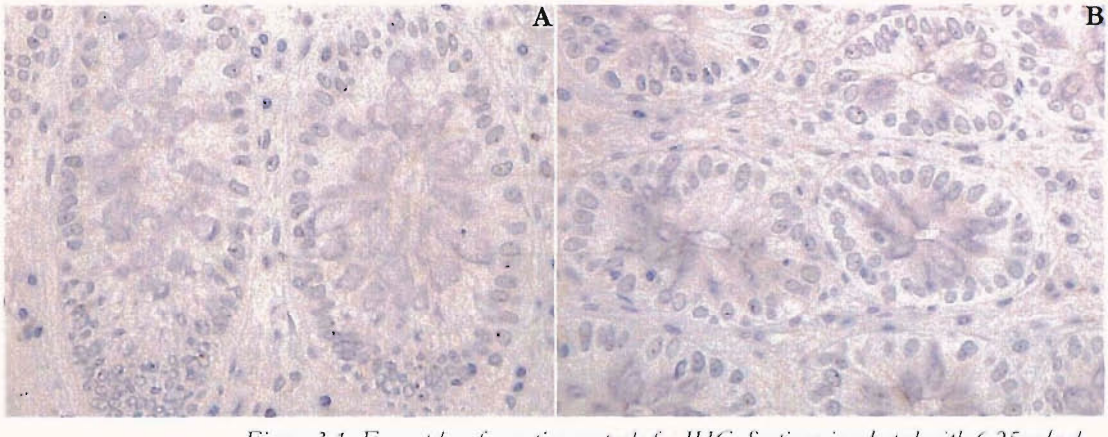


*Figure 3.1. Examples of negative controls for IHC. Sections incubated with 6.25µg/ml rabbit immunoglobulin (A) and 2µg/ml mouse immunoglobulin G1 (B) instead of primary antibodies. These concentrations were equal to the highest used for any primary antibody. Positive staining is brown.*

### 3.2.1.2 Claudin 2

Claudin 2 staining could not be detected in any of the NC cases examined, at either crypt or surface locations (figure 3.2 A,B). Staining was readily detected, however, in much of the crypt epithelium of most cases of UCI, UC and CD (figure 3.2 C,E,G). This staining was both punctate and predominantly located in the apical region of the cells, which is the area of the TJ (arrows if figure 3.2).

Claudin 2 could not be detected in the surface epithelium of most cases of IBD (examples in figure 3.2 D,F). A few cases of UC did display a little positive staining at this location, and again in the region of the TJ (arrowheads in figure 3.2 H).

The results of the analysis of this staining across all cases are depicted graphically in figure 3.3. The top graph confirms that a large proportion of crypt cells in IBD colons were positive for claudin 2 whereas normal colons were negative. The bottom graph confirms that very few surface epithelial cells stained positively for claudin 2 in any group, but also that a few cases of UC did show some staining in this location.

The results of statistical comparisons between the groups are shown in table 3.2.

| Comparison | p value | |
|---|---|---|
| | Crypt | Surface |
| NC vs UCI | **0.018** | 0.877 |
| NC vs UC | **0.009** | 0.663 |
| NC vs CD | **0.013** | 1 |
| UC vs CD | 0.889 | 0.444 |

*Table 3.2. Statistical comparisons of the percentage of crypt or surface cells displaying positive TJ staining for claudin 2. Entries in* ***bold*** *type are those that approach or reach statistical significance.*

There was thus significantly more claudin 2 detected in all three IBD groups in the epithelial crypts, but not in the surface epithelium.

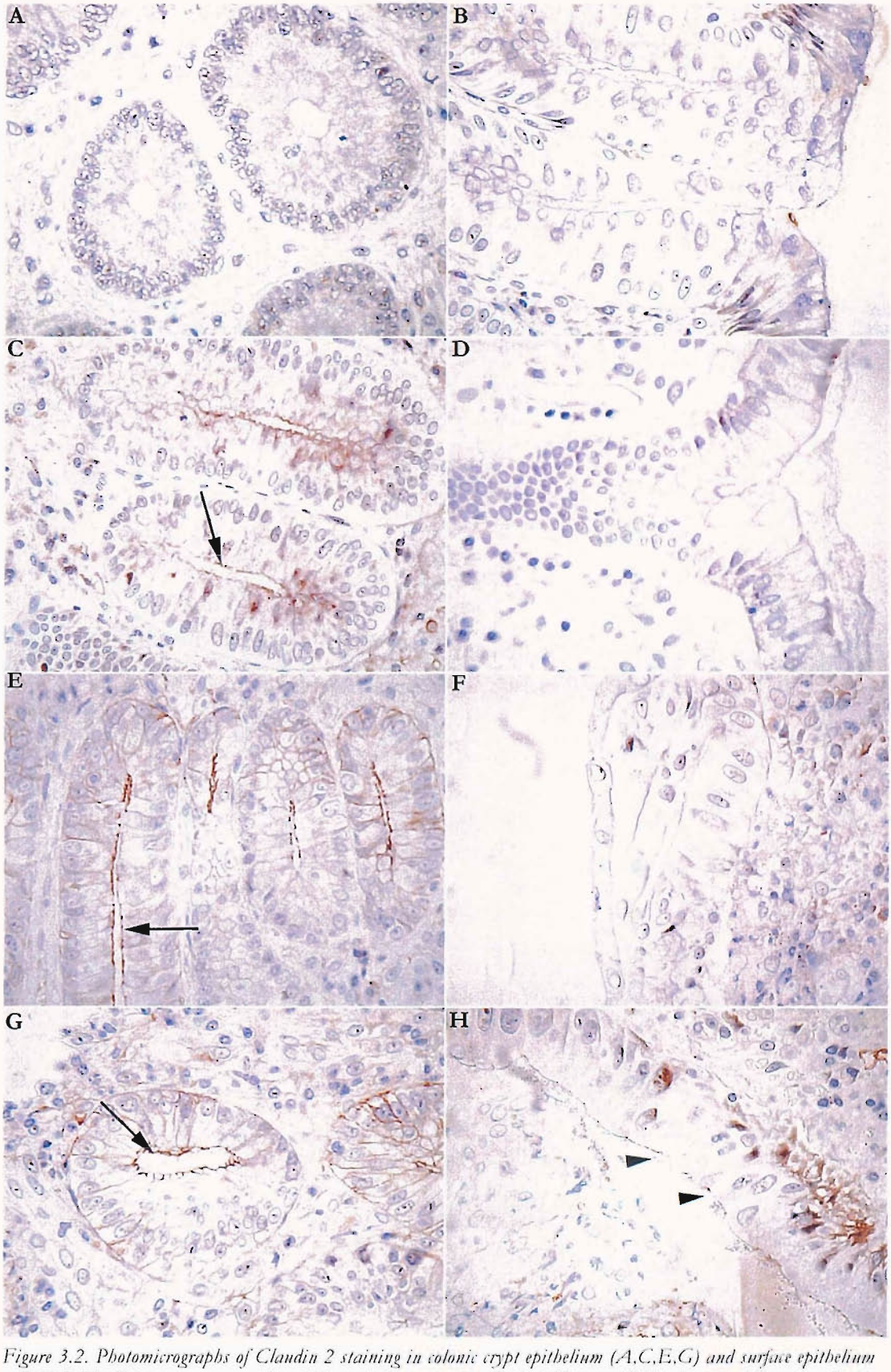


*Figure 3.2. Photomicrographs of Claudin 2 staining in colonic crypt epithelium (A,C,E,G) and surface epithelium (B,D,F,H). Depicted are examples of Normal Colon (A,B), Crohn's Disease (C,D), Inactive Ulcerative Colitis (E,F) and Active Ulcerative Colitis (G,H). Staining is not seen in normal tissue (A,B), but there is strong staining of TJs in UC and CD crypt epithelium (arrows) and UC surface epithelium (arrowheads).*

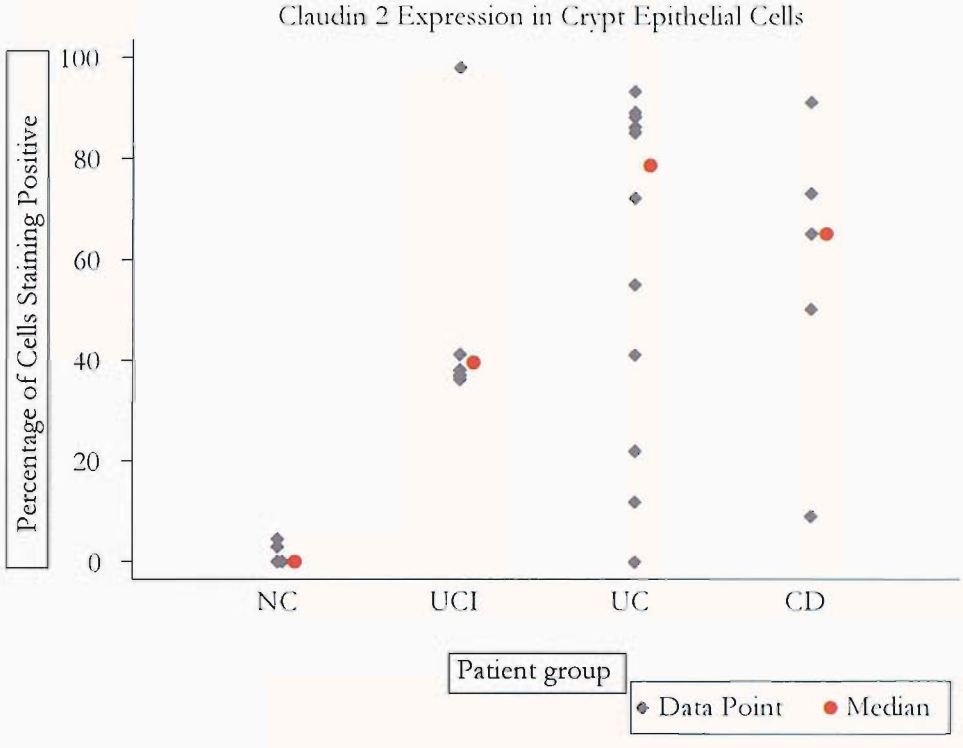


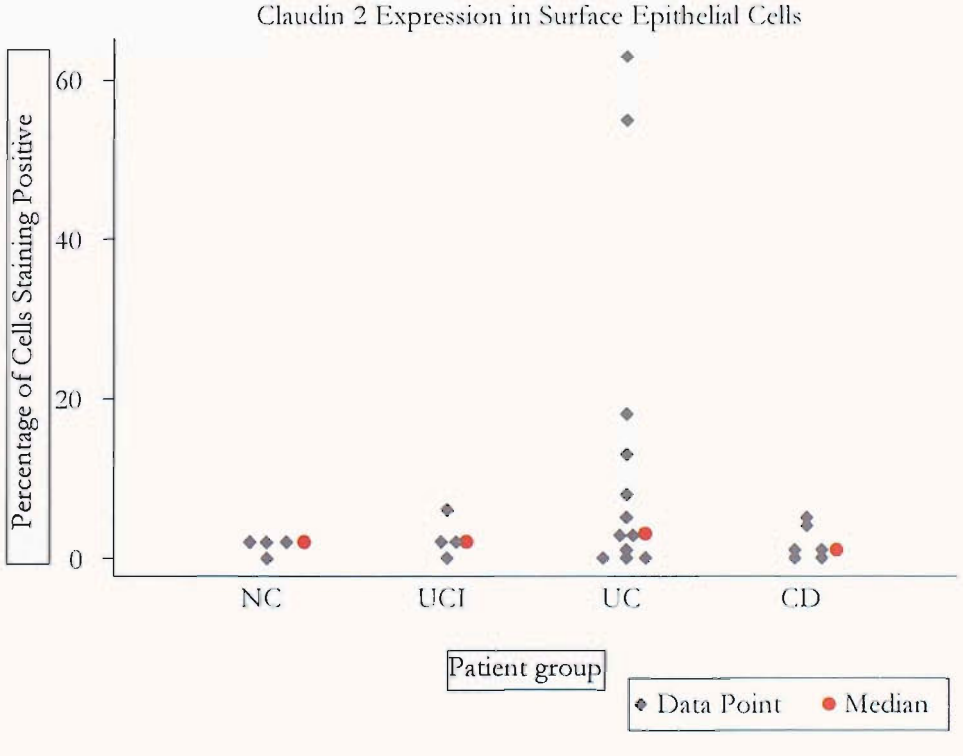


*Figure 3.3. Graphs to illustrate the percentage of epithelial cells of the crypt (top) and surface (bottom) staining positive for claudin 2 at the TJ region in normal colons (NC, n=4), inactive ulcerative colitis (UCI, n=4), active ulcerative colitis (UC, n=12) and Crohn's disease (CD, n=5). In the crypts the percentage of claudin 2 positive cells was higher in UCI (p=0.018), UC (p=0.009) and CD (p=0.013) than in NC. Differences were not statistically significant in the surface epithelium.*

### *3.2.1.3 Claudin 3*

In all NC cases strong claudin 3 staining was seen in both crypt and surface epithelia (figure 3.4 A,B). This staining was located both at the TJ, in a punctate distribution, and along the lateral membrane, where it was continuous.

In the crypts, claudin 3 staining remained strong in the TJs of all the cases of IBD examined (figure 3.4 C,E,G). However, in some cases of CD (figure 3.4 C) and particularly in UC (figure 3.4 G) there was reduced staining along the lateral membranes of the epithelial cells.

In the surface epithelium changes were more pronounced. There was marked loss of TJ staining in many cases of UCI, UC and CD (arrowheads in figure 3.4 D,F,H respectively). Furthermore, there was also a marked reduction in the staining along the lateral membranes, with sometimes complete loss (figure 3.4 F). In many of these cases staining was apparent along the basal membrane and the basal portion of the lateral membrane (arrows in figure 3.4 D,F,H), suggesting internalisation or redistribution of the antigen.

The results of the analysis of this staining across all cases are depicted graphically in figures 3.5 (crypts) and 3.6 (surface). In the crypts, the proportion of cells displaying positive staining was unchanged at the TJ (figure 3.5, top) but was smaller at the lateral membrane (figure 3.5, bottom) of some cases of UC and CD. This latter difference reached statistical significance in CD (table 3.3).

| Comparison | p value | | | |
|---|---|---|---|---|
| | *Crypt* | | *Surface* | |
| | TJ | Lat. membrane | TJ | Lat. membrane |
| NC vs UCI | 0.655 | 0.144 | **0.021** | 0.110 |
| NC vs UC | 0.457 | 0.069 | **0.004** | **0.008** |
| NC vs CD | 0.992 | **0.046** | **0.010** | 0.088 |
| UC vs CD | 0.424 | 0.792 | 0.639 | 0.673 |

*Table 3.3. Statistical comparisons of the percentage of crypt or surface cells displaying positive staining for claudin 3 at both TJ and lateral membrane locations. Entries in* ***bold*** *type are those that reach statistical significance.*

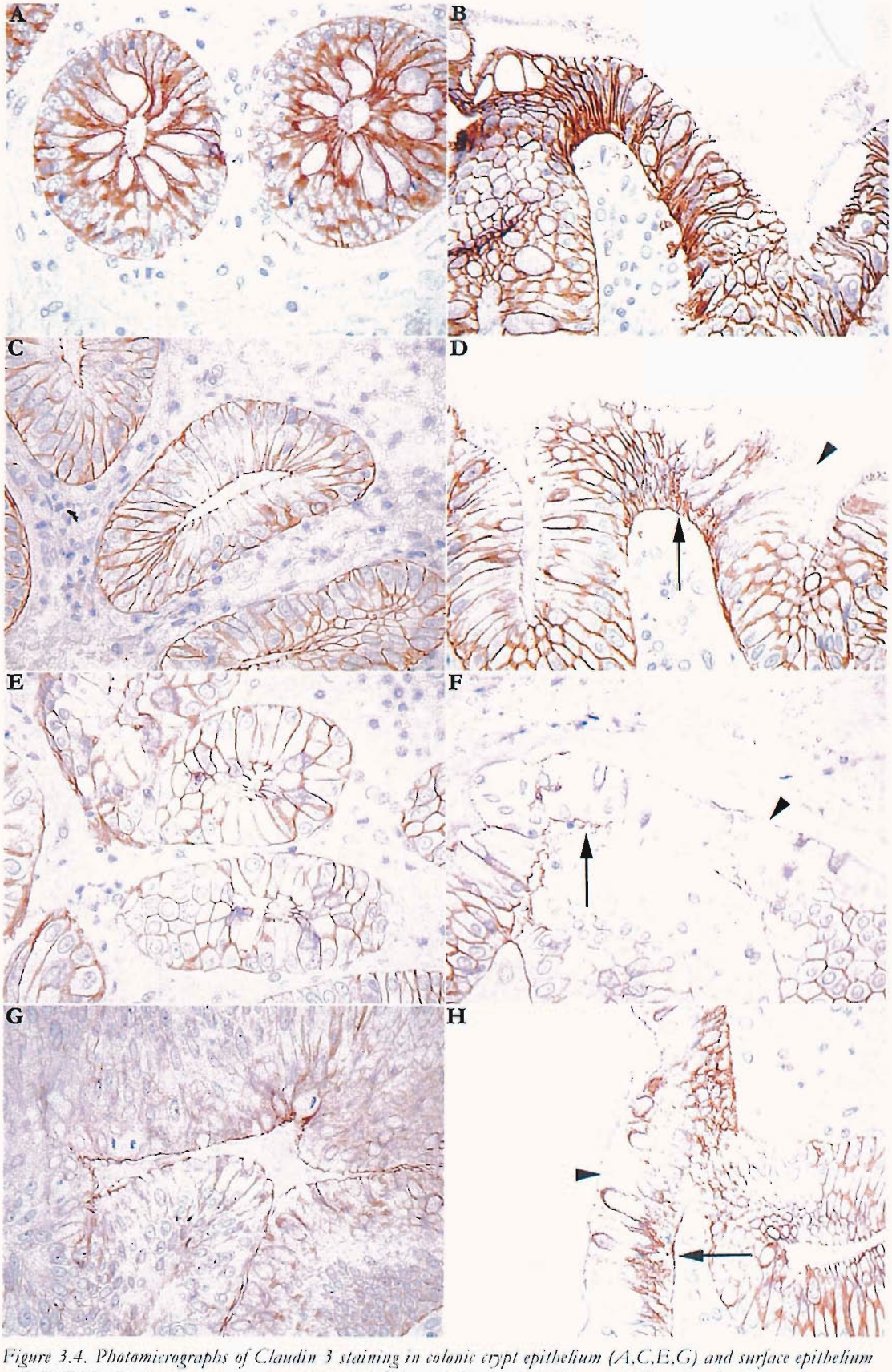


*Figure 3.4. Photomicrographs of Claudin 3 staining in colonic crypt epithelium (A,C,E,G) and surface epithelium (B,D,F,H). Depicted are examples of Normal Colon (A,B), Crohn's Disease (C,D), Inactive Ulcerative Colitis (E,F) and Active Ulcerative Colitis (G,H). Staining is present in normal colonic epithelium in TJs and lateral cell membranes, whereas in IBD staining is reduced, particularly in surface epithelia (arrowheads), whilst being retained at the basolateral membranes (arrows).*

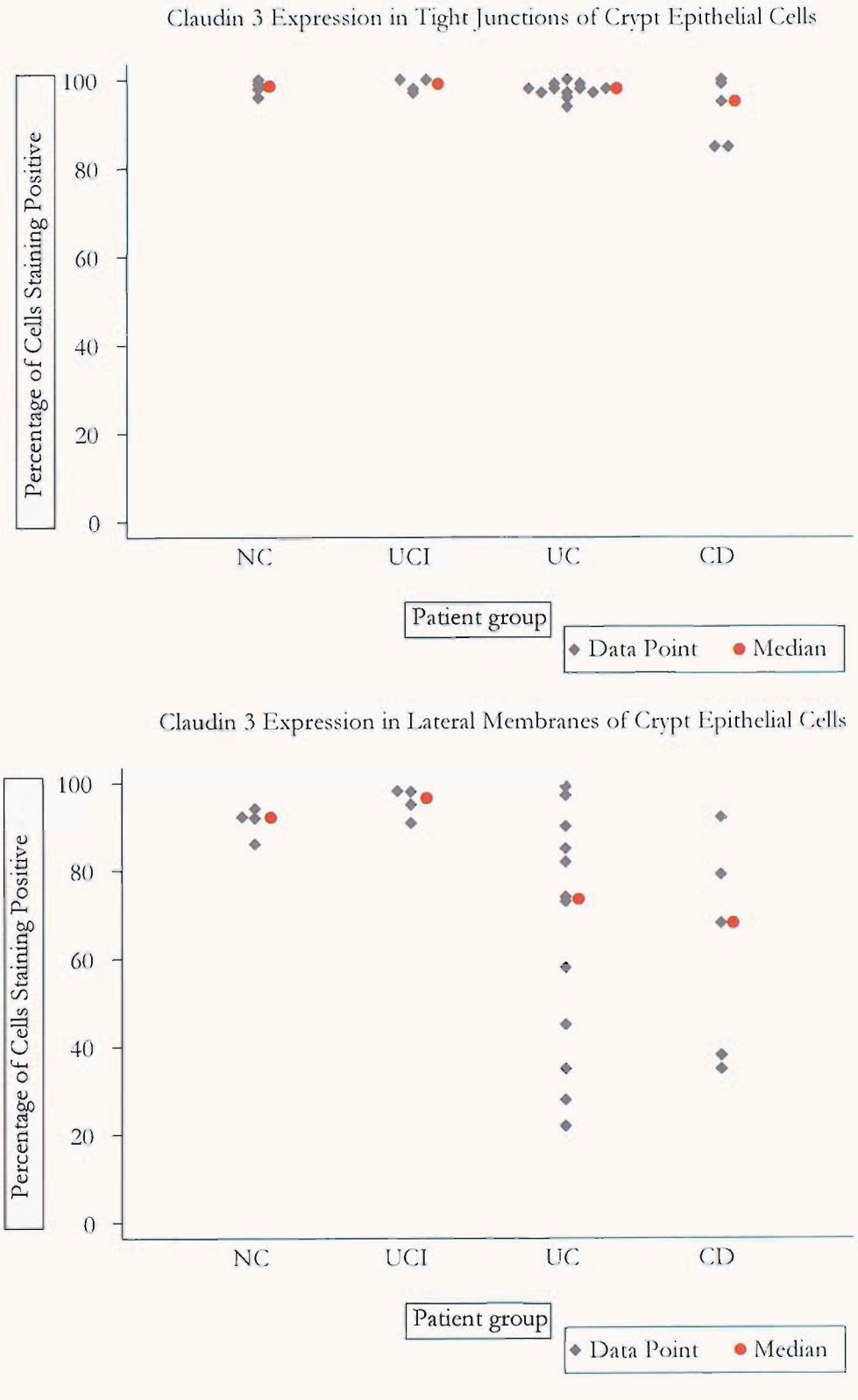


*Figure 3.5. Graphs to illustrate the percentage of crypt epithelial cells staining positive for claudin 3 at the TJ region (top) and along the lateral membrane (bottom) in normal colons (NC, n=4), inactive ulcerative colitis (UCI, n=4), active ulcerative colitis (UC, n=12) and Crohn's disease (CD, n=5). In the lateral membranes the percentage of claudin 3 positive cells was lower in UC (0.069) and CD (0.046) than in NC. All other differences were not statistically significant.*

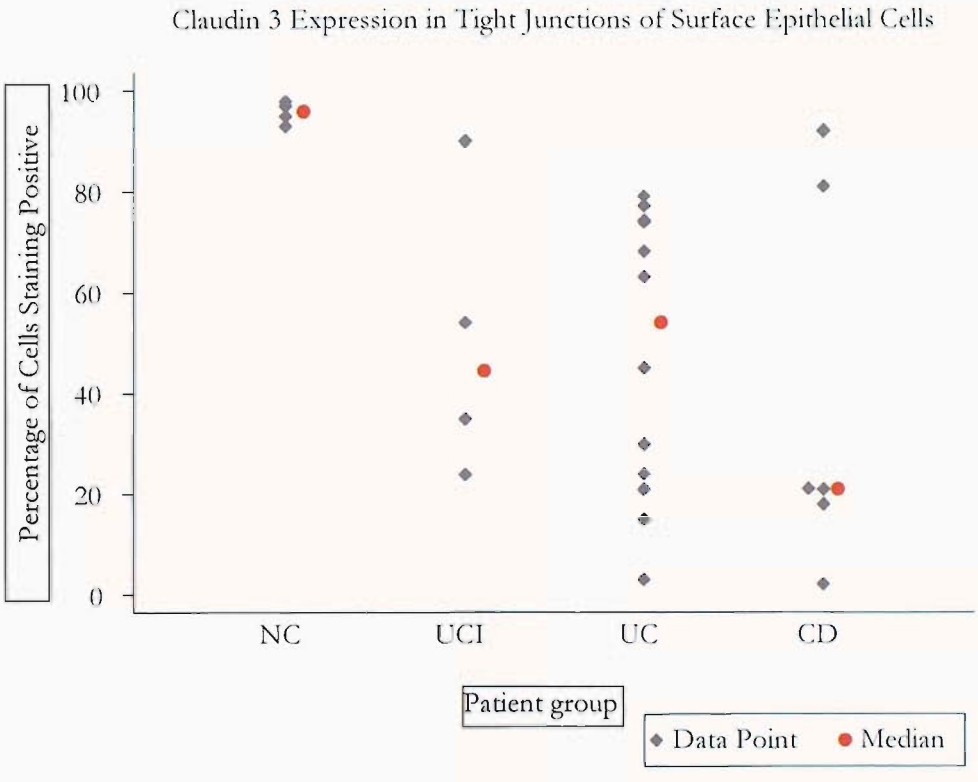


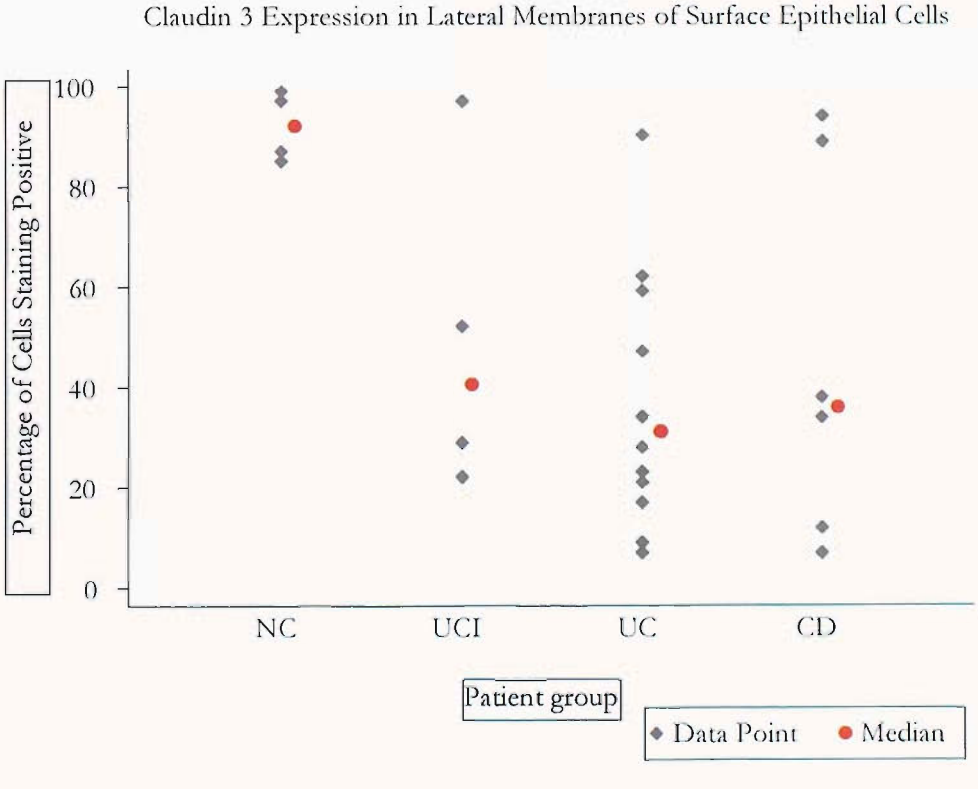


*Figure 3.6. Graphs to illustrate the percentage of surface epithelial cells staining positive for claudin 3 at the TJ region (top) and along the lateral membrane (bottom) in normal colons (NC, n=4), inactive ulcerative colitis (UCI, n=4), active ulcerative colitis (UC, n=12) and Crohn's disease (CD, n=6). At the TJ the percentage of claudin 3 positive cells was lower in UCI (p=0.021), UC (p=0.004) and CD (p=0.010) than in NC; at the lateral membrane the percentage was lower in UC than in NC (p=0.008). All other differences were not statistically significant.*

In the surface epithelium, the proportion of cells with detectable claudin 3 staining at the TJ was much smaller in most cases of UCI, UC and CD than in NC (figure 3.6, top) and reached statistical significance (table 3.3). At the lateral membrane, fewer cells were positive in many cases of IBD (figure 3.6, bottom), and this difference was statistically significant for UC and approached significance for CD (table 3.3).

### *3.2.1.4 Claudin 4*

In all NC cases strong claudin 4 staining was seen at both the TJ and the lateral membrane in both crypt and surface epithelia (figure 3.7 A,B). As was the case with claudin 3, the apical (TJ) staining was punctate, whereas the lateral membrane staining was continuous.

In the crypts, the TJ staining of claudin 4 remained strong in most cases of IBD compared to NC cases (figure 3.7 C,E,G). In many cases of IBD, however, the staining along the lateral membranes of the cells was much weaker. This was particularly the case in some UC cases (figure 3.7 G).

In the surface epithelium, claudin 4 staining was commonly weaker at both TJ and lateral membrane locations in the IBD cases. There was wide variation in the strength of staining within each diagnostic group. Thus, some CD cases displayed staining similar to that in NC cases (figure 3.7 D), while others, such as the UCI and UC cases depicted in figure 3.7 F and H, had almost total loss of TJ and lateral membrane staining (arrowheads in figure 3.7 F,H). As with claudin 3, there was often basal membrane staining in these cases (arrows in figure 3.7 F,H), which was often quite marked, suggesting loss from the TJ and redistribution basolaterally.

The results of the analysis of this staining across all cases are depicted graphically in figures 3.8 (crypts) and 3.9 (surface), and the statistical analysis is displayed in table 3.4. There was a trend towards reduced numbers of lateral membrane-positive cells in UC in both crypt and surface epithelia. In the surface epithelium the TJ was affected too in this group. Overall though, the reductions in the proportions of positive cells were less significant than was the case for claudin 3.

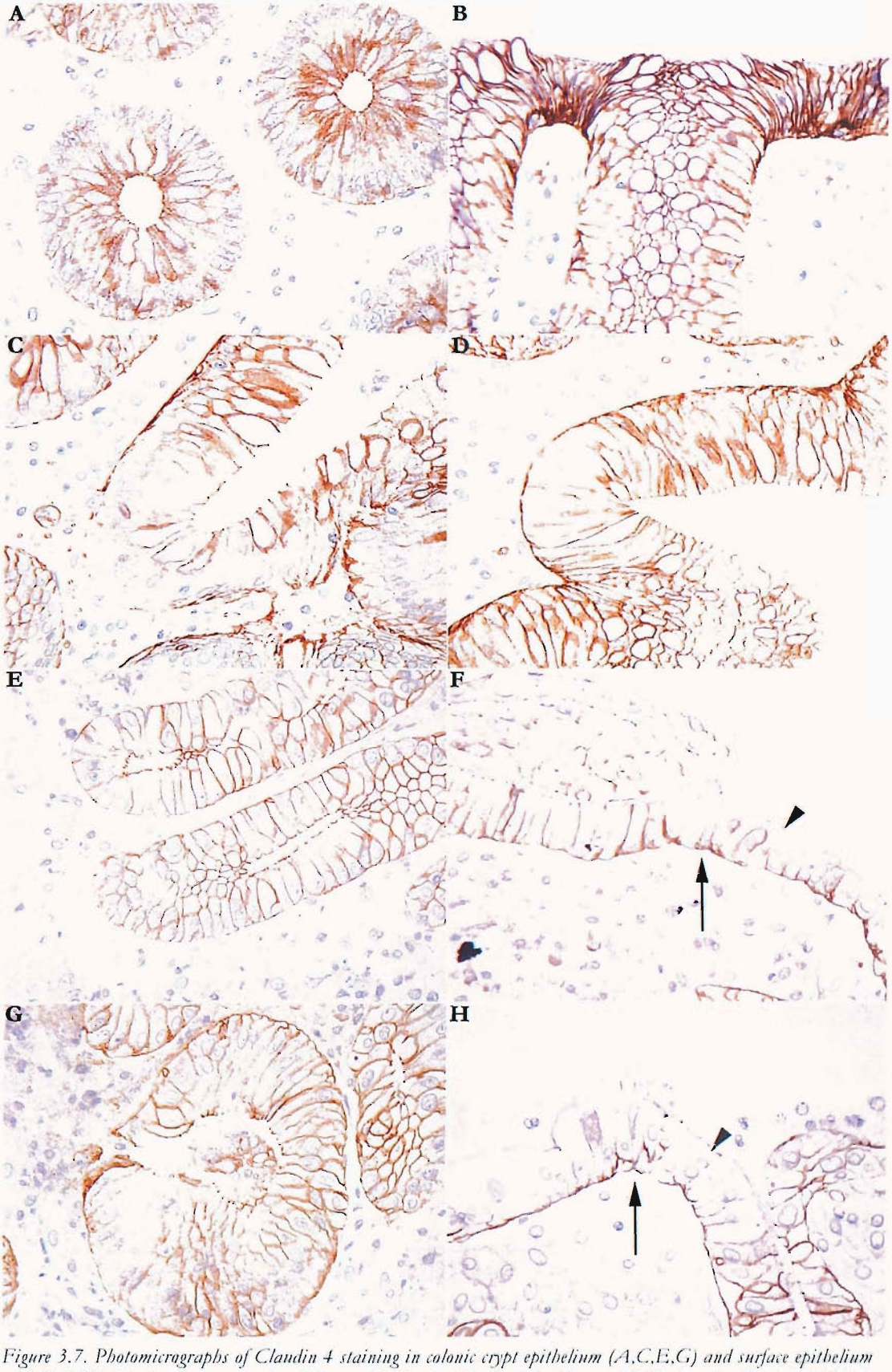


*Figure 3.7. Photomicrographs of Claudin 4 staining in colonic crypt epithelium (A,C,E,G) and surface epithelium (B,D,F,H). Depicted are examples of Normal Colon (A,B), Crohn's Disease (C,D), Inactive Ulcerative Colitis (E,F) and Active Ulcerative Colitis (G,H). Staining is strong in normal colonic epithelium, with reduced staining in IBD epithelium, particularly in the surface epithelium in UC (arrowheads), whilst being retained at the basolateral membranes (arrows).*

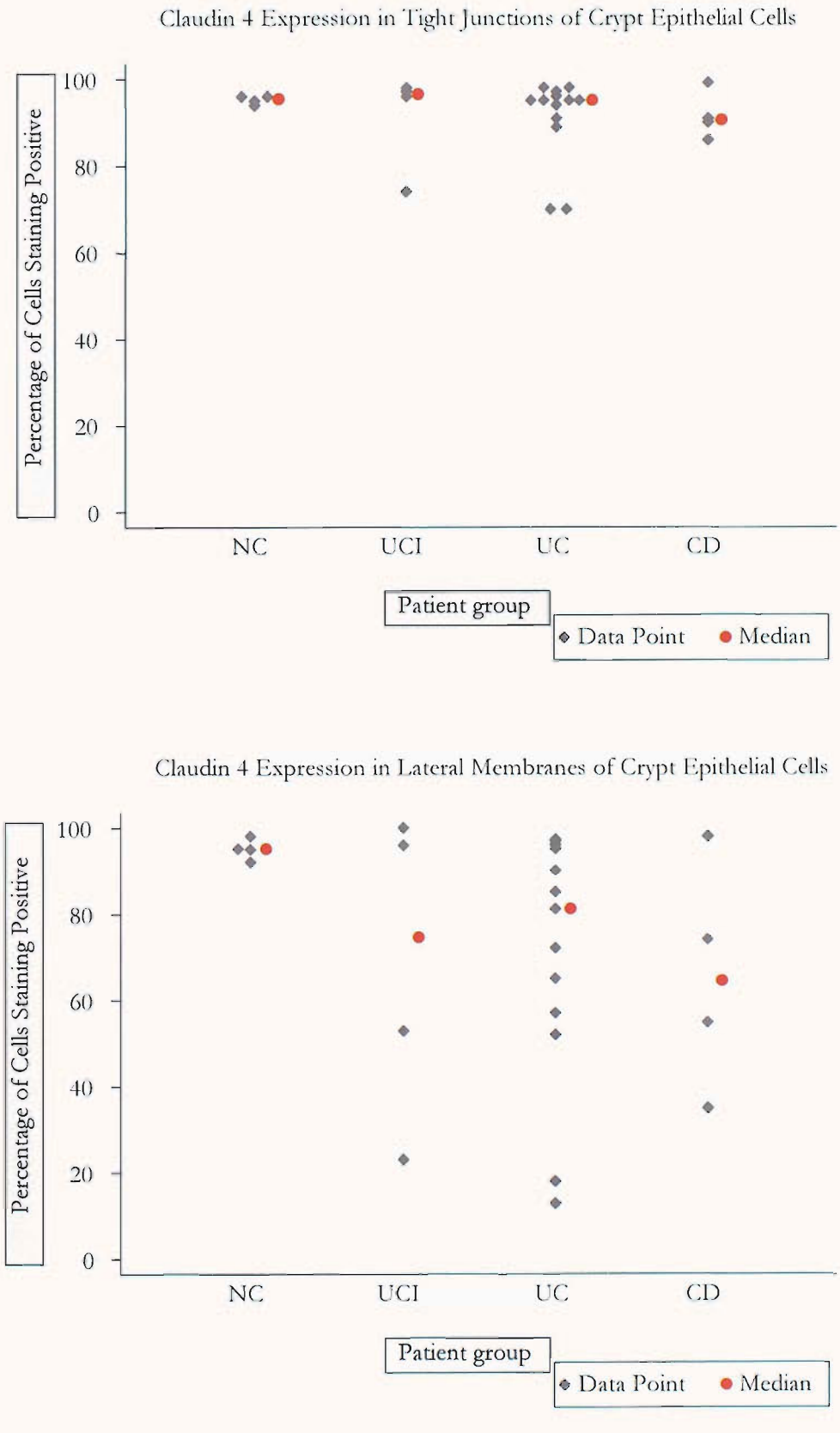


*Figure 3.8. Graphs to illustrate the percentage of crypt epithelial cells staining positive for claudin 4 at the TJ region (top) and along the lateral membrane (bottom) in normal colons (NC, n=4), inactive ulcerative colitis (UCI, n=4), active ulcerative colitis (UC, n=13) and Crohn's disease (CD, n=4). No differences were statistically significant.*

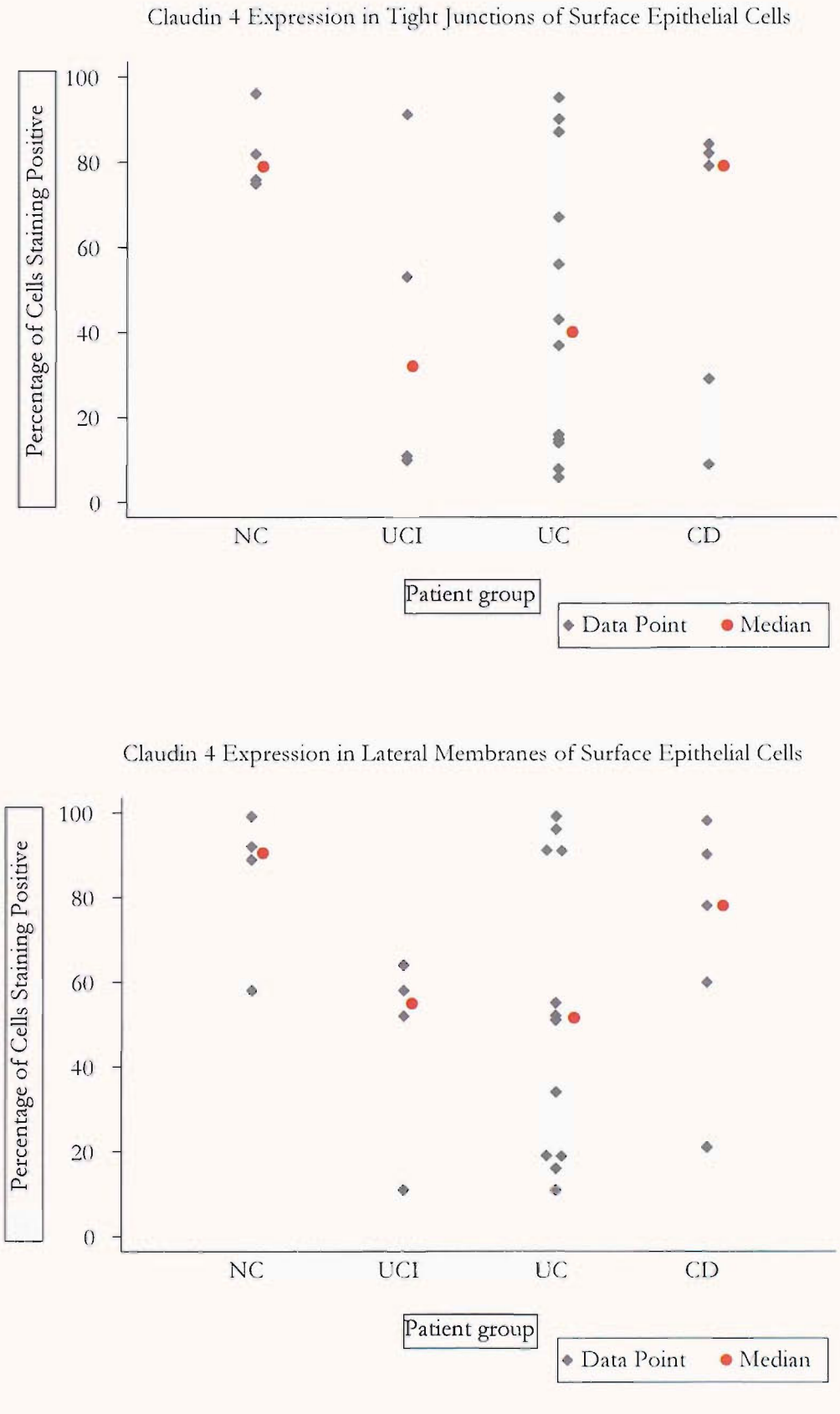


*Figure 3.9. Graphs to illustrate the percentage of surface epithelial cells staining positive for claudin 4 at the TJ region (top) and along the lateral membrane (bottom) in normal colons (NC, n=4), inactive ulcerative colitis (UCI, n=4), active ulcerative colitis (UC, n=12) and Crohn's disease (CD, n=5). No differences were statistically significant.*

| Comparison | p value | | | |
|---|---|---|---|---|
| | *Crypt* | | *Surface* | |
| | TJ | Lat. membrane | TJ | Lat. membrane |
| NC vs UCI | 0.375 | 0.772 | 0.149 | **0.059** |
| NC vs UC | 0.604 | 0.088 | 0.069 | 0.100 |
| NC vs CD | 0.245 | 0.189 | 0.539 | 0.462 |
| UC vs CD | 0.608 | 0.821 | 0.673 | 0.342 |

*Table 3.4. Statistical comparisons of the percentage of crypt or surface cells displaying positive staining for claudin 3 at both TJ and lateral membrane locations. Entries in* ***bold*** *type are those that approach or reach statistical significance.*

### *3.2.1.5 Occludin*

In NC cases punctate occludin staining was seen at the TJ cellular location both in the crypts (arrow in figure 3.10 A) and in the surface epithelium (black arrowheads in figure 3.10 B). In addition, positive staining for occludin was also seen in some cases in a continuous distribution along the lateral and basal membranes (white arrowheads in figure 3.10 B).

In the IBD cases examined, occludin staining was also seen in the TJ area in the crypt epithelium (arrows in figure 3.10 C,E,G), and no discernible differences between NC and any of the IBD diagnostic groups could be seen.

In the surface epithelium, however, there was marked loss of occludin staining from the TJ in much of the epithelium in many cases of UCI, UC and CD (figure 3.10 D,F,H). In many cases there remained a little basal membranous staining (white arrowheads in figure 3.10 D,F).

Analysis of the crypt TJ staining (figure 3.11, top) confirmed that there was no difference in the proportion of positive cells between NC and IBD groups. In the surface epithelium, however, these cell counts confirmed that in most cases of UCI, UC and CD the number of TJ-positive cells was much lower than in the NC cases (figure 3.11, bottom).

Statistical analysis of these data gave the results displayed in table 3.5. The loss of TJ staining reached statistical significance in all three IBD groups.

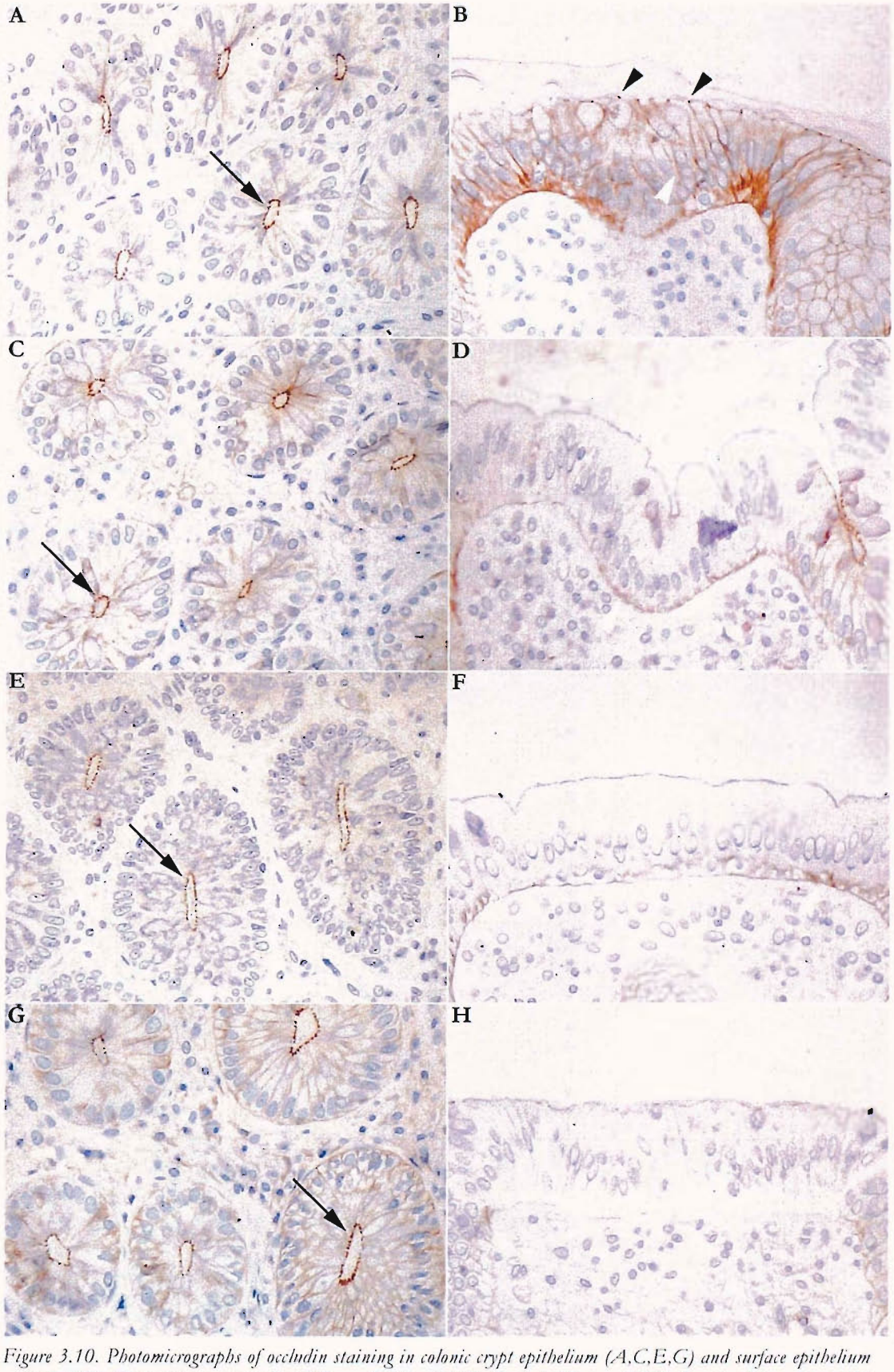


*Figure 3.10. Photomicrographs of occludin staining in colonic crypt epithelium (A,C,E,G) and surface epithelium (B,D,F,H). Depicted are examples of Normal Colon (A,B), Crohn's Disease (C,D), Inactive Ulcerative Colitis (E,F) and Active Ulcerative Colitis (G,H). Staining is strong in the TJs of both normal and IBD crypt epithelium (arrows). Staining is also seen in the TJs of normal surface epithelium (black arrowheads), whereas this is lost in IBD surface epithelia. Basolateral membrane staining is also seen in normal surface epithelium, some of which is retained in cases of IBD (white arrowheads).*

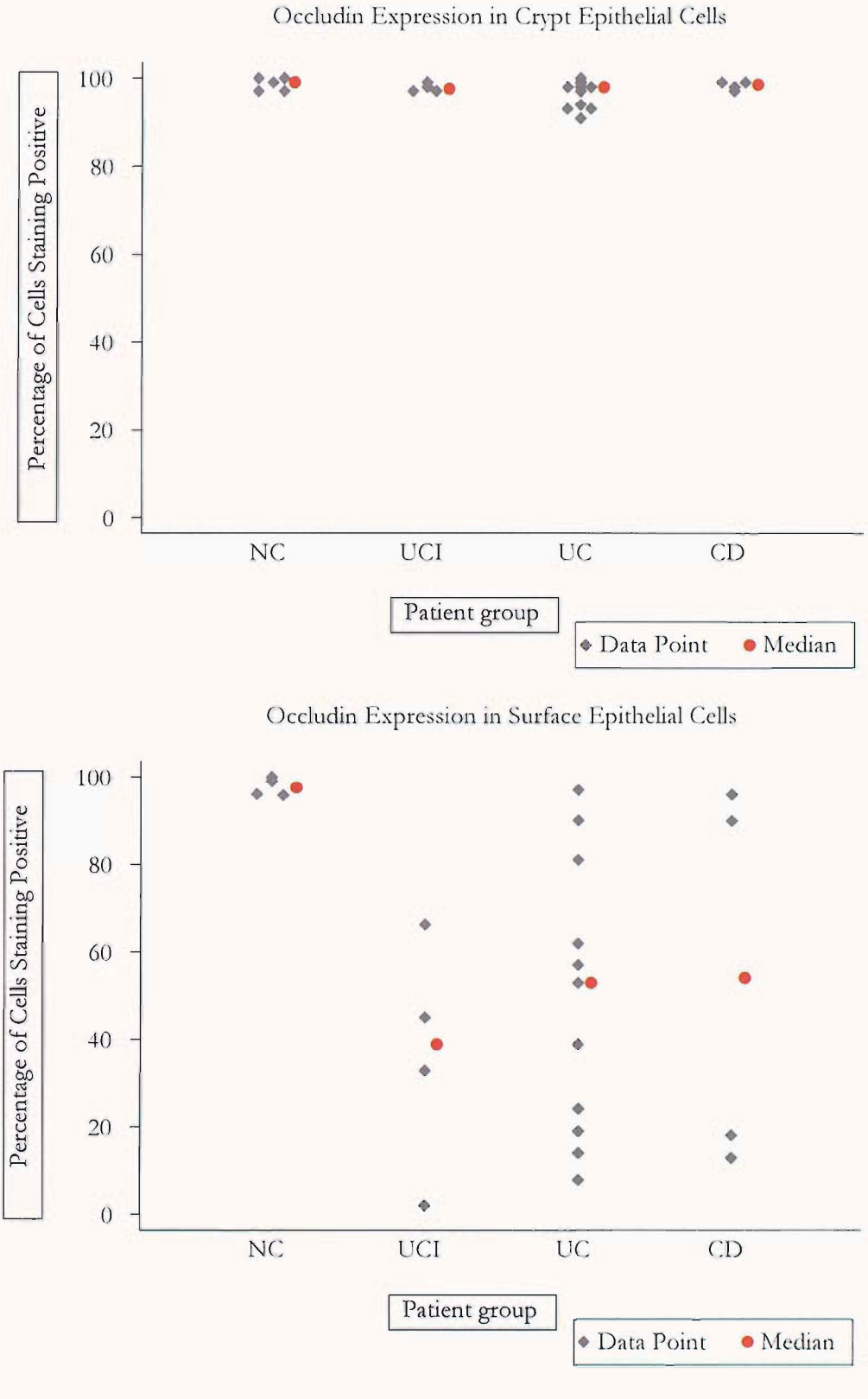


*Figure 3.11. Graphs to illustrate the percentage of epithelial cells of the crypt (top) and surface (bottom) staining positive for occludin at the TJ region in normal colons (NC, crypt:n=5, surface:n=4), inactive ulcerative colitis (UCI, crypt:n=4, surface:n=4), active ulcerative colitis (UC, crypt:n=12, surface:n=11) and Crohn's disease (CD, crypt:n=4, surface:n=4). In the surface epithelium the percentage of occludin positive cells was higher in NC than in UCI (p=0.020), UC (p=0.009) and CD (p=0.038). Differences were not statistically significant in the crypt epithelium.*

| Comparison | p value | |
|---|---|---|
| | Crypt | Surface |
| NC vs UCI | 0.366 | **0.020** |
| NC vs UC | 0.219 | **0.009** |
| NC vs CD | 0.611 | **0.038** |
| UC vs CD | 0.456 | 0.948 |

*Table 3.5. Statistical comparisons of the percentage of crypt or surface cells displaying positive TJ staining for occludin. Entries in* ***bold*** *type are those that approach or reach statistical significance.*

### *3.2.1.6 ZO-1*

Widespread punctate ZO-1 staining was seen in the region of the TJ, both in the crypts (arrow in figure 3.12 A) and in the surface epithelium (black arrowheads in figure 3.12 B) in NC cases. A small amount of basolateral membrane staining was also seen at the surface.

In the crypt epithelium of the IBD cases this pattern and distribution of staining was also seen, and no differences could be discerned between the diagnostic groups (arrows in figure 3.12 C,E,G).

In the surface epithelium, however, there was marked loss of ZO-1 staining from much of the epithelium in many cases of IBD (figure 3.12 D,F,H). Tiny amounts of basal membrane staining was seen in small patches of the affected epithelium (white arrowheads in figure 3.12 F,H).

Analysis of the crypt TJ staining (figure 3.13, top) confirmed that there was no difference in the proportion of positive cells between NC and IBD groups. In the surface epithelium, however, these cell counts showed that in most cases of UCI, UC and CD the number of TJ-positive cells was much lower than in the NC cases (figure 3.13, bottom).

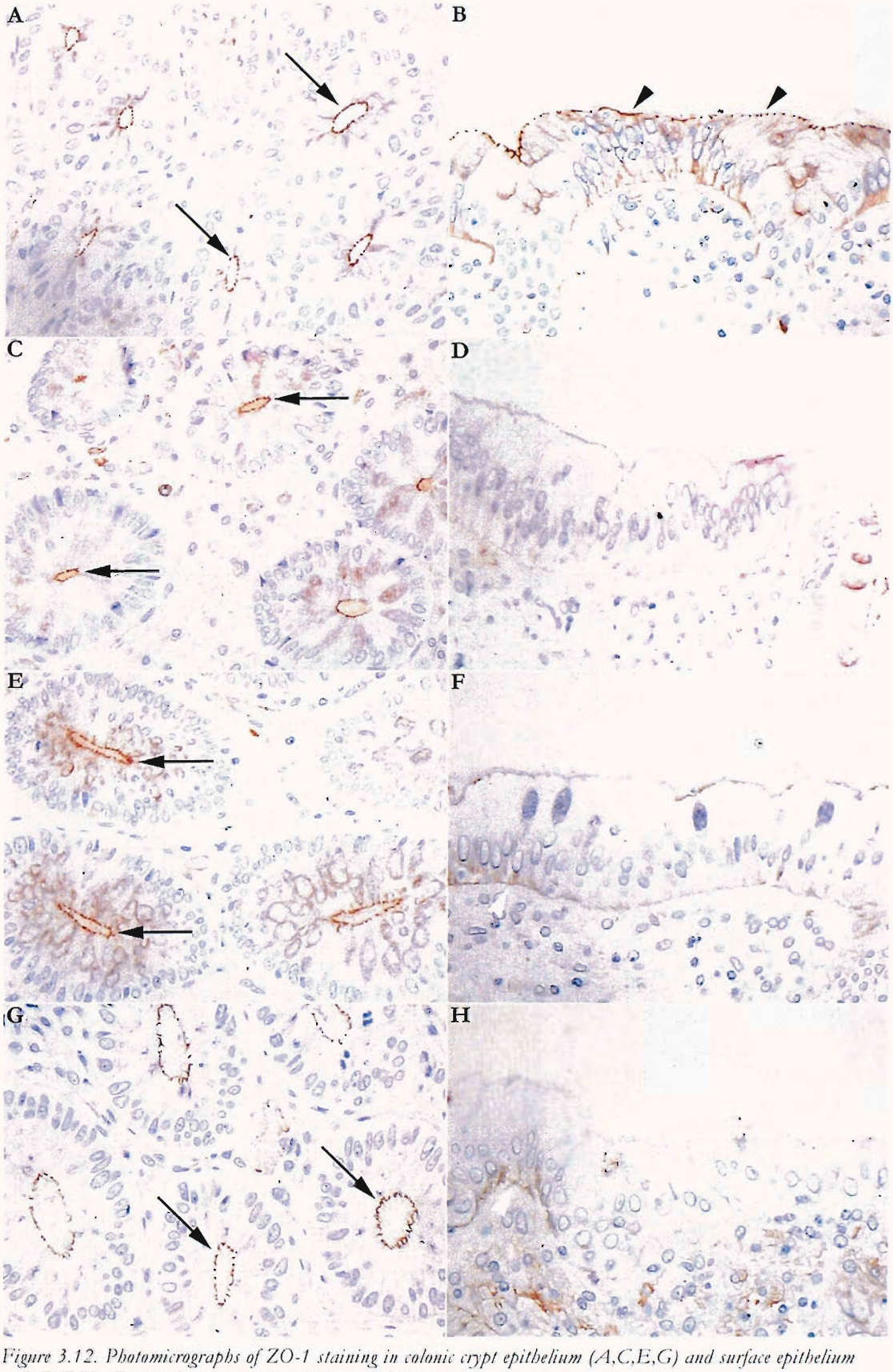


*Figure 3.12. Photomicrographs of ZO-1 staining in colonic crypt epithelium (A,C,E,G) and surface epithelium (B,D,F,H). Depicted are examples of Normal Colon (A,B), Crohn's Disease (C,D), Inactive Ulcerative Colitis (E,F) and Active Ulcerative Colitis (G,H). Staining is strong in the TJs of both normal and IBD crypt epithelium (arrows). Staining is also seen in the TJs of normal surface epithelium (black arrowheads), whereas this is lost in IBD surface epithelia. Basolateral membrane staining is also observed in normal surface epithelium, some of which is retained in cases of IBD (white arrowheads).*

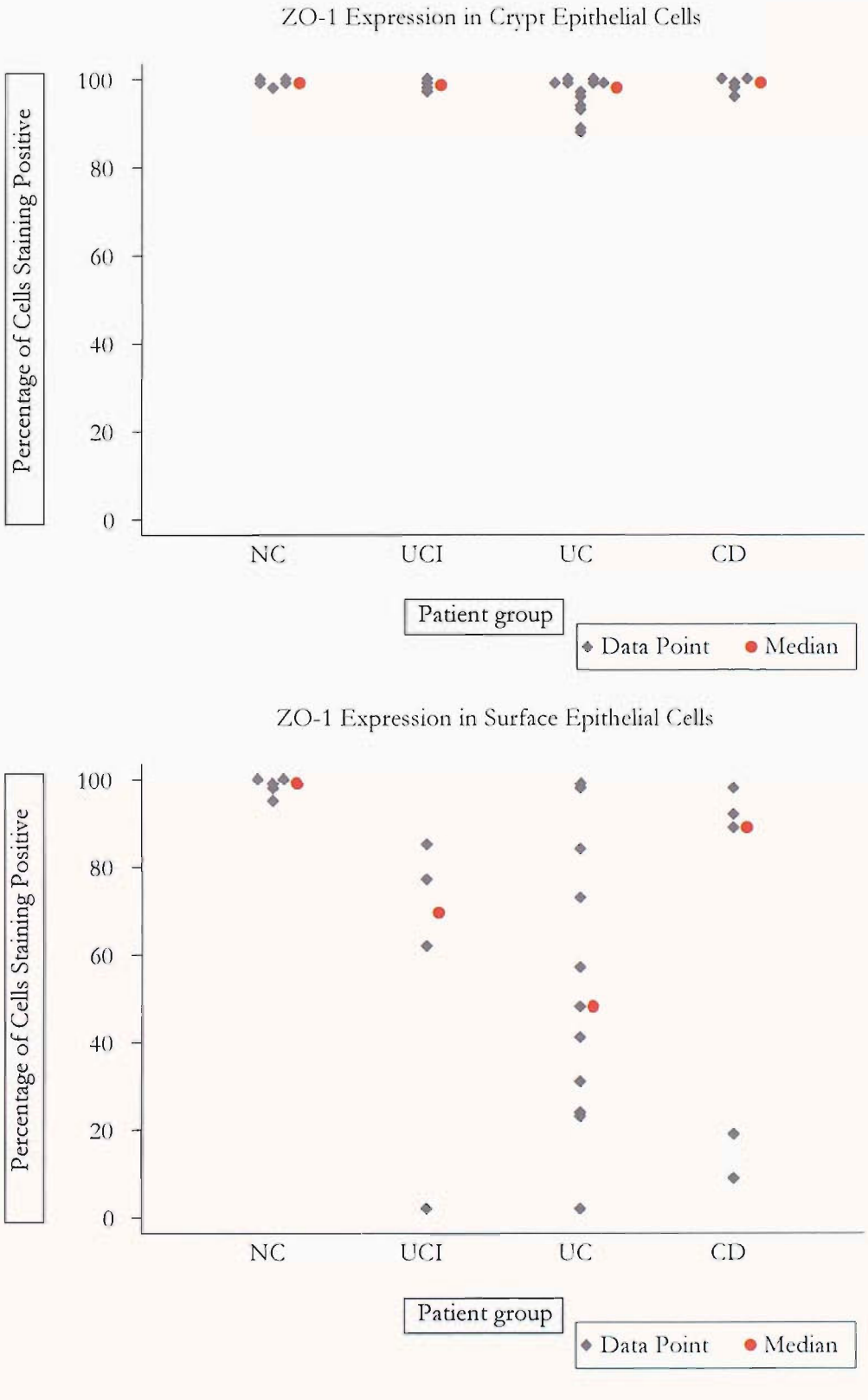


*Figure 3.13. Graphs to illustrate the percentage of epithelial cells of the crypt (top) and surface (bottom) staining positive for ZO-1 at the TJ region in normal colons (NC, crypt:n=5, surface:n=5), inactive ulcerative colitis (UCI, n=4), active ulcerative colitis (UC, crypt:n=12, surface:n=11) and Crohn's disease (CD, n=5). In the surface epithelium the percentage of ZO-1 positive cells was higher in NC than in UCI (p=0.014), UC (p=0.008) and CD (p=0.021). Differences were not statistically significant in the crypt epithelium.*

Statistical analysis of these data (table 3.6) showed that the loss of ZO-1 from surface epithelial TJs in the IBD groups was statistically significant. It also confirmed that the proportions of ZO-1-positive cells in the crypts were not significantly different between NC cases and any of the IBD groups.

| Comparison | p value | |
|---|---|---|
| | Crypt | Surface |
| NC vs UCI | 0.373 | **0.014** |
| NC vs UC | 0.129 | **0.008** |
| NC vs CD | 0.661 | **0.021** |
| UC vs CD | 0.259 | 0.821 |

*Table 3.6. Statistical comparisons of the percentage of crypt or surface cells displaying positive TJ staining for ZO-1. Entries in* ***bold*** *type are those that approach or reach statistical significance.*

### 3.2.2 ASSESSMENT OF TOTAL EXPRESSION OF CLAUDINS 2, 3 AND 4 IN ISOLATED EPITHELIAL CELLS BY SDS-PAGE AND WESTERN BLOTTING

Following the immunohistochemical examination, the expression of claudins 2, 3 and 4 was compared by SDS-PAGE and western blotting of isolated colonic crypt epithelial cell lysates. Four different diagnostic groups were examined and each case was classified into one of these from his or her diagnostic history and the result of the histopathological examination of the surgical explant. The four groups were normal colon (NC), ulcerative colitis from proximal to the affected area (UCI), active ulcerative colitis (UC) and Crohn's disease (CD). Seventeen cases were examined, comprising 6 NC cases, 2 UCI cases, 6 UC cases and 3 CD cases. The raw data are provided in appendix 2.

Validation of the blotting techniques was carried out as described in sections 2.6.2 and 2.6.3. Densitometric analysis of all blots was performed using Quantity One software, as explained in section 2.6.4. The band intensities for each claudin were normalised to those for cytokeratin 19 by computing a ratio of the former divided by the latter, as described in section 2.6.4.

### *3.2.2.1 Negative Controls*

Western blotting was performed using protein from an NC case in all lanes. Identical two-lane strips were incubated with claudin 2 antibody, rabbit Ig, claudin 4 antibody and mouse IgG1. The results are depicted in figure 3.14. No bands were detected when either primary antibody was substituted with its matching non-immune Ig. This suggested that the bands observed with the primary antibodies were the result of their binding to protein via their antigen-specific binding sites.

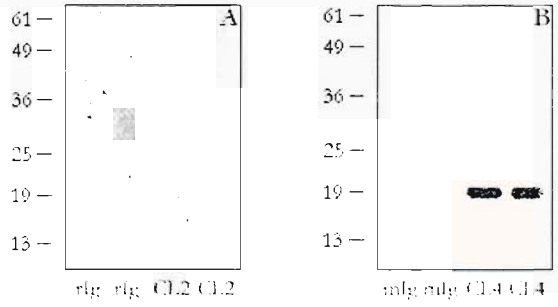


*Figure 3.14. Negative control western blots of tissue epithelial protein. In A, the right-hand pair of lanes was incubated with 6.25ng/ml of rabbit anti-claudin 2 antibody (CL2) and the left-hand pair with an equal concentration of rabbit immunoglobulin (rIg). Bands at approximately 19kDa are detected only with the CL2 antibody. In B, the right-hand pair of lanes was incubated with 6.25ng/ml of mouse anti-claudin 4 antibody (CL4) and the left-hand lanes with an equal concentration of mouse immunoglobulin (mIg) of the same subclass (IgG1). Bands at approximately 19kDa are detected only with the CL4 antibody. The chosen concentrations were the highest of the primary antibodies used on blots of tissue epithelial protein (see table 2.3).*

### *3.2.2.2 Claudin 2*

Antibody detection of claudin 2 on lysates of isolated crypt epithelial cells was carried out using a rabbit polyclonal antibody. Claudin 2 was barely detectable in most of the NC cases studied and only weakly detected in the others. Strong bands were detected in all 6 cases of UC, in all 3 cases of CD, but not in the 2 cases of UCI.

Usually a single band was apparent, which equated to a molecular weight of approximately 19,000 (19kDa). Occasionally a second band was seen at approximately 38kDa, but only in UC or CD cases in which a band was also seen at 19kDa.

An illustrative blot is depicted in figure 3.15. Faint bands can be seen in two of the three NC cases, whereas stronger bands are seen in the three UC cases and the three CD cases. Detection of cytokeratin 19 showed that protein loading was generally even (figure 3.15).

Figure 3.16 shows graphically the result of the densitometric analysis of all the cases. The results are depicted on both arithmetic and logarithmic scales as there was wide variation in the calculated ratios. It can be seen that the ratios of claudin 2 to cytokeratin 19 were much higher in the UC and CD cases than in the NC and UCI cases, showing that there was an increase in total claudin 2 protein in diseased epithelial cells from IBD patients.

Statistical analysis of these data confirmed that the increase in claudin 2 expression seen in the UC and CD cases was significant ($p=0.004$ for the comparison of NC with UC; $p=0.020$ for the comparison of NC with CD).

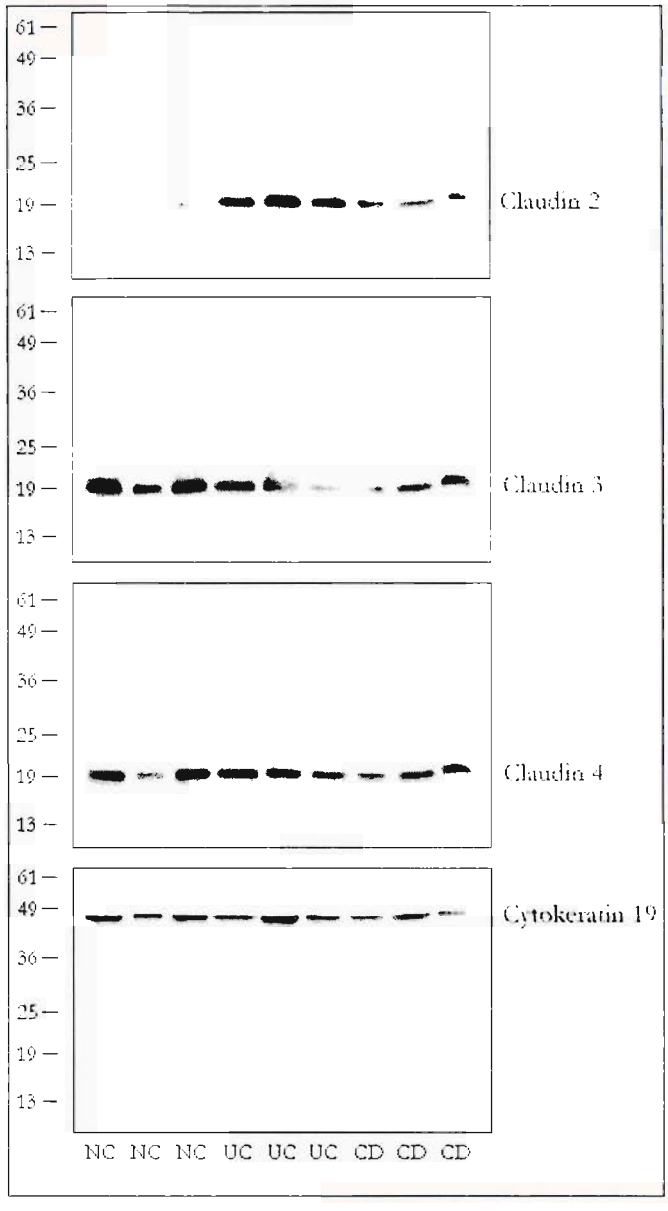


*Figure 3.15. Representative Western blots of isolated colonic crypt epithelial cell protein, probed successively for claudins 2-4 and cytokeratin 19. There is an increase in claudin 2 in IBD compared to normal epithelium. Claudins 3 and 4, detected in normal epithelium, were similar to IBD epithelium when normalised to cytokeratin 19. The numbers represent molecular mass in kiloDaltons. NC – normal colon; UC – ulcerative colitis; CD – Crohn's disease. For each antigen detected the ratios of band densities to those of cytokeratin 19 were calculated and are depicted in figures 3.16 (claudin 2), 3.17 (claudin 3) and 3.18 (claudin 4).*

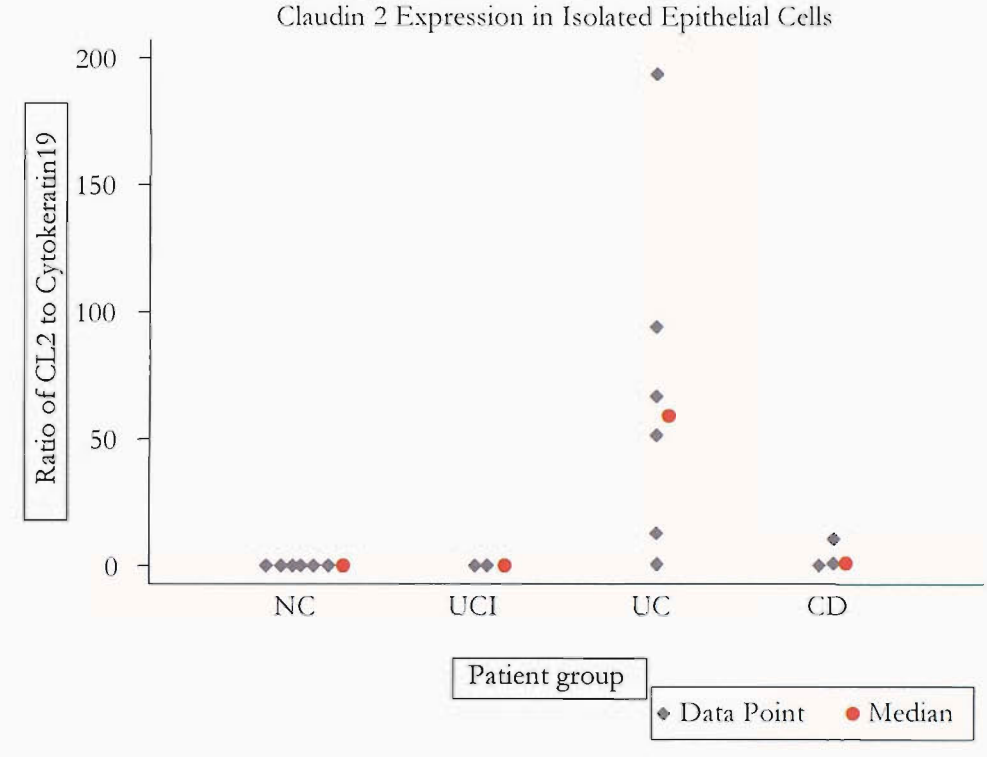


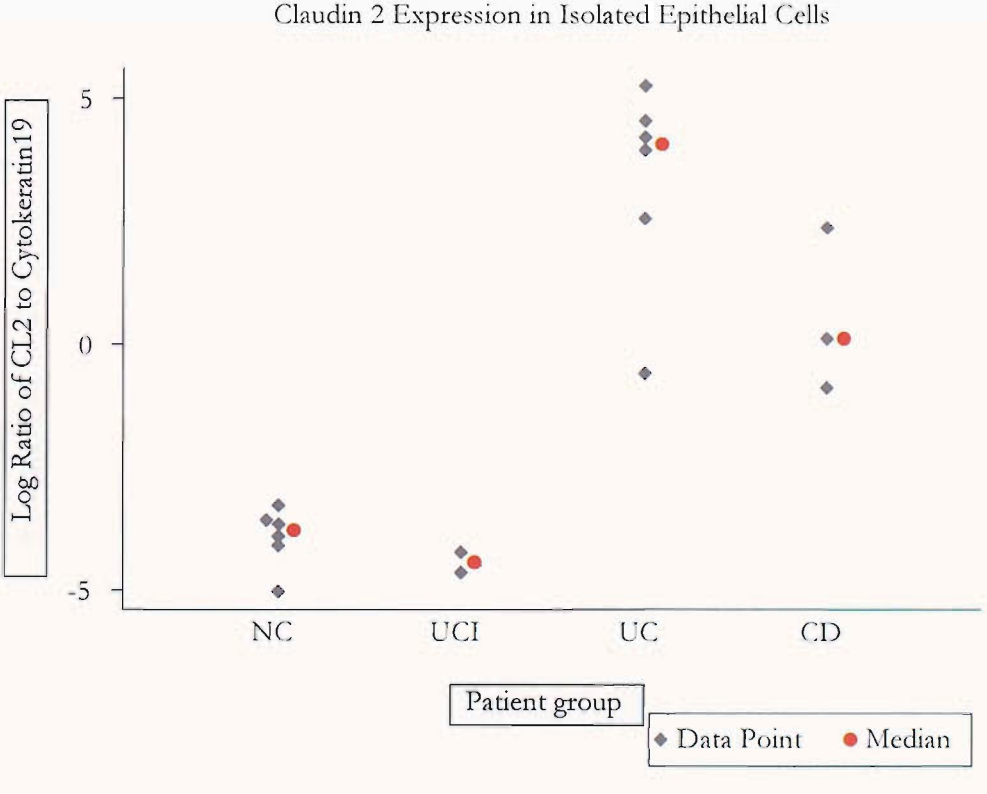


*Figure 3.16. Graphs depicting the ratio of claudin 2 to cytokeratin 19 band densities on western blots according to patient group, on both arithmetic (top) and logarithmic (bottom) scales. NC – normal colon, n=6; UCI – inactive ulcerative colitis, n=2; UC – ulcerative colitis, n=6; CD – Crohn's disease, n=3. Claudin 2 expression is increased in UC (p=0.004) and CD (p=0.020) compared to NC.*

### *3.2.2.3 Claudin 3*

Western blot studies with a rabbit polyclonal antibody to claudin 3 produced a single band in all cases, equating to a molecular weight of approximately 19kDa. There was considerable variation in the intensities of the bands produced. Some UC cases produced somewhat weaker bands than the NC cases, but there was considerable overlap between all the groups. An illustrative blot is depicted in figure 3.15. Strong bands can be seen in the NC cases, whilst there is considerable variation in the UC and CD cases, with both weak and strong bands seen.

The result of the densitometric analysis carried out on all the cases is shown graphically in figure 3.17. The variation and overlap in these normalised band densities is apparent.

There was no statistically significant difference in the expression of claudin 3 between the NC group and any of the IBD groups.

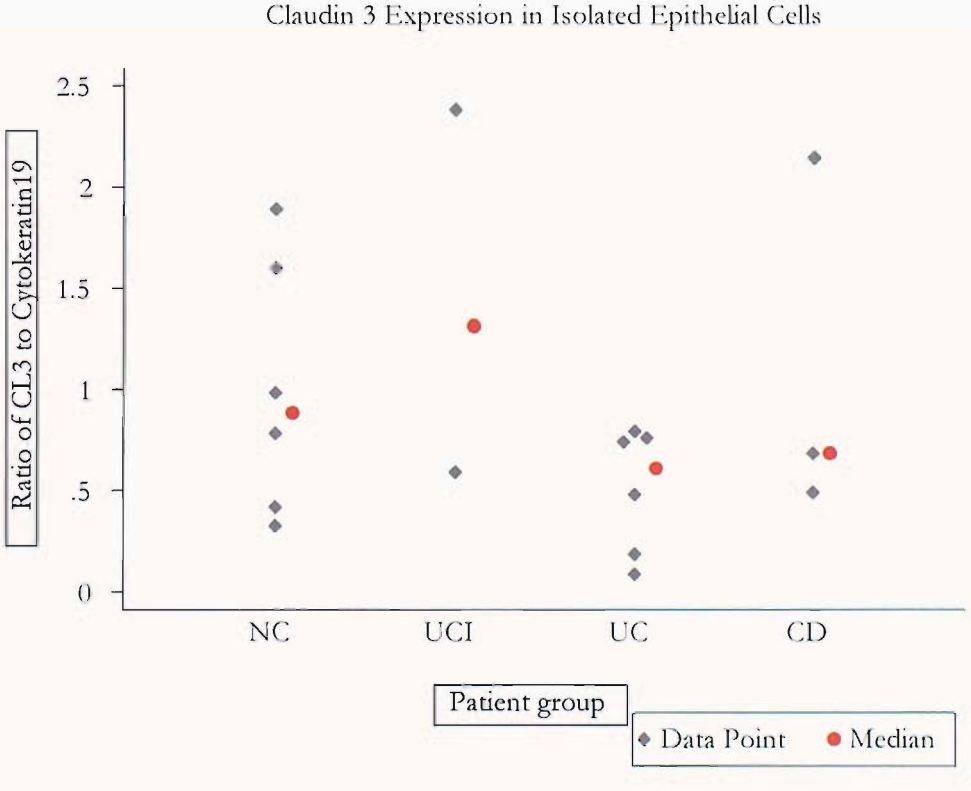


*Figure 3.17. Graph depicting the ratio of claudin 3 to cytokeratin 19 band densities on western blots according to patient group. NC – normal colon, n=6; UCI – inactive ulcerative colitis, n=2; UC – ulcerative colitis, n=6; CD – Crohn's disease, n=3. There were no differences in expression between any IBD group and NC.*

### *3.2.2.4 Claudin 4*

As was the case for claudins 2 and 3, a single band was produced on western blots probed with a mouse monoclonal antibody to claudin 4, again equating to a molecular weight of approximately 19kDa. There was, however, much less variation in the intensities of the bands seen. In the illustrative blot shown in figure 3.15, strong bands are apparent in all nine cases regardless of diagnosis.

Densitometric analysis of all the cases examined (figure 3.18) confirmed that there was little difference in claudin 4 expression in any of the IBD groups when compared to the NC group, suggesting that total protein levels were not altered.

Statistical analysis of the data showed no significant difference in claudin 4 expression between the NC group and any of the IBD groups.

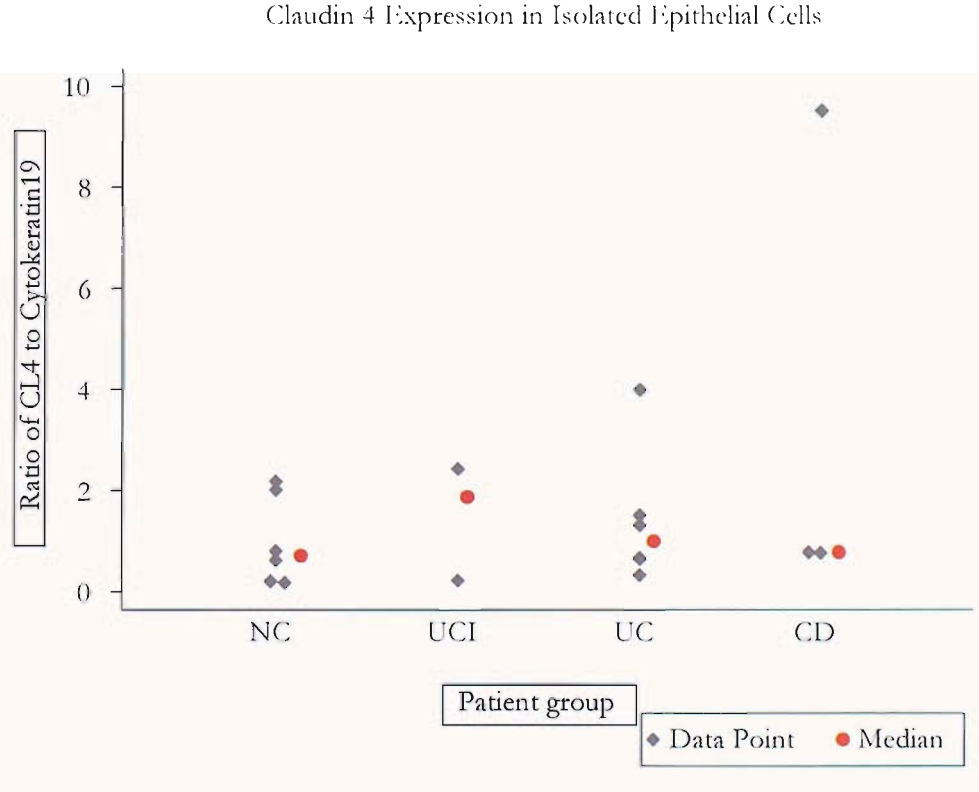


*Figure 3.18. Graph depicting the ratio of claudin 4 to cytokeratin 19 band densities on western blots according to patient group. NC – normal colon, n=6; UCI – inactive ulcerative colitis, n=2; UC – ulcerative colitis, n=6; CD – Crohn's disease, n=3. There were no differences in expression between any IBD group and NC.*

### 3.2.3 MEASUREMENT OF CLAUDIN 2 MESSENGER RNA LEVELS BY QUANTITATIVE REVERSE TRANSCRIPTASE-MEDIATED POLYMERASE CHAIN REACTION

Because the expression of claudin 2 appeared to be significantly increased in cases of IBD, the relative abundancy of claudin 2 mRNA was determined in isolated colonic crypt epithelial cells by quantitative reverse transcriptase-mediated polymerase chain reaction (qRT-PCR). Three patient groups were compared – normal colon (NC), active ulcerative colitis (UC) and Crohn's disease (CD). Abundancies were normalised to those determined for the housekeeping genes, GAPDH and UBC, as explained in sections 2.7.4 and 2.7.5.

Five NC cases were compared with four UC cases and four CD cases. For each case the relative abundancy of claudin 2 mRNA was calculated in relation to the median abundancy of the NC cases. The results for all 15 cases are displayed graphically and by patient group in figure 3.19. A logarithmic scale has been selected because of the variation in abundancies among the IBD cases. The raw data are provided in appendix 3.

All but one of the IBD cases contained more claudin 2 mRNA than the NC cases. The increase among these seven cases over the baseline ranged from 20- to 3200-fold. The remaining case (one of the CD cases) had half of the baseline level of mRNA.

Statistical analysis of these data showed the increase in claudin 2 mRNA levels among the IBD cases as a whole to be significant ($p=0.028$ for the comparison of NC with UC and CD combined). The increase among the UC cases was particularly significant ($p=0.014$ for the comparison of NC with UC), but the increase among the CD cases did not reach statistical significance ($p=0.221$ for the comparison of NC with CD).

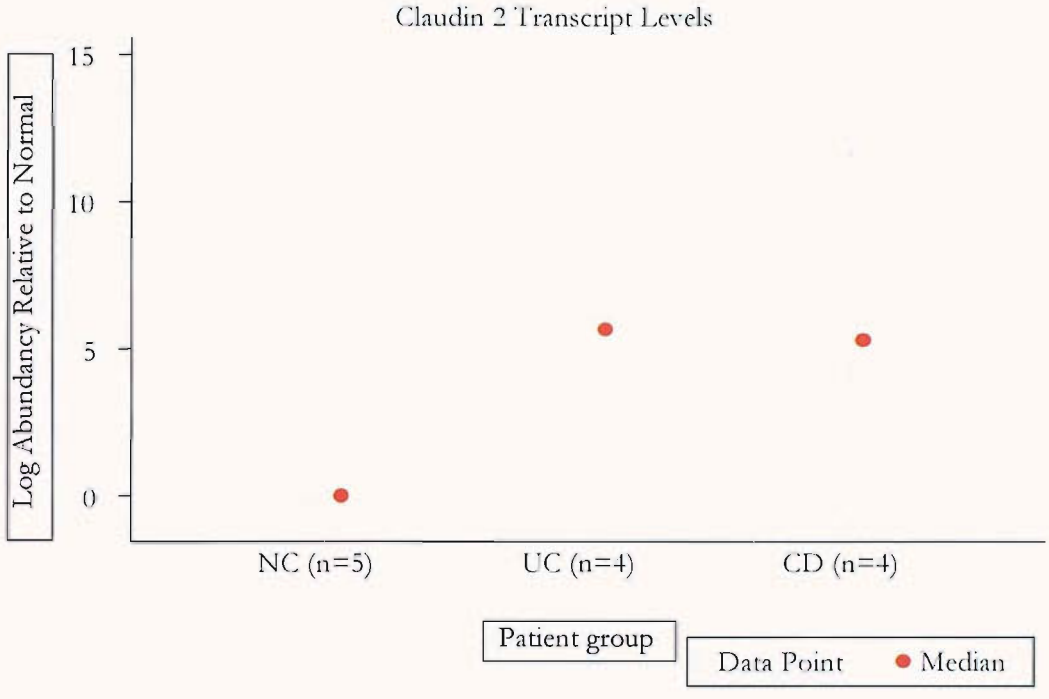


*Figure 3.19. Graph displaying the relative abundancy of claudin 2 mRNA in crypt epithelial cells by patient group. NC – normal colon, n=5; UC – ulcerative colitis, n=4; CD – Crohn's disease, n=4. Assays were performed in triplicate for each case and mean abundancies were normalised to those determined for the housekeeping genes, GAPDH and UBC. Relative abundancies were calculated in relation to the median abundancy of the NC cases. Claudin 2 mRNA levels were increased in both UC (p=0.014) and IBD as a whole (p=0.028) compared to NC, but not in CD (p=0.221).*

## 3.3 DISCUSSION

### 3.3.1 CLAUDINS

The study on the claudins has confirmed by two different methods (IHC and western blotting) that the normal human colonic epithelium expresses claudins 3 and 4, whereas claudin 2 is only barely detected by these methods. The correlation between the findings by IHC and western blotting support this conclusion. However, this experiment only examined claudins 2-4, and with twenty-three claudin subtypes now described (Katoh and Katoh, 2003; Tsukita and Furuse, 2002), it is likely that claudins other than those tested here are present in the normal and / or diseased intestine.

The specificity of the antibodies used to detect the claudins is demonstrated by the fact that all three yielded a single band at a molecular mass (19kDa) corresponding

approximately to that reported for the claudins (22kDa) (Furuse et al., 1998). The small discrepancy in apparent molecular mass when detected by western blotting may be due to difficulty in completely linearising the claudin molecules, owing to their shape and their four hydrophobic transmembrane domains (figure 1.5). Alternatively, there may be differences between the gels and molecular weight markers used in the present study and those used by Furuse et al (1998). However, the exact gel constituents utilised by Furuse et al are not clear, and using different sets of molecular weight markers also gave an apparent molecular mass for the claudins of 19kDa. It is also possible that claudins are subjected to post-translational modification (for example by phosphorylation), and that lysing cells by the method used in the present study removed more of these groups than was the case in the study by Furuse et al (1998). However, phosphorylation alone cannot account entirely for the discrepancy. It is possible that in intact cells, and after the lysis method used by Furuse et al (which attempted to keep the TJs intact), other small molecules remain bound to the claudins that are removed by the lysis method used in the present study. Immunoprecipitation of one or more claudins and assessment of their binding partners may suggest candidate molecules to explain the discrepancy.

The most striking finding among the IBD cases was the marked increase in the expression of claudin 2 seen by IHC, western blotting and RT-PCR. This increase was seen in all the cases examined, with the exception of the RT-PCR analysis of a single case of CD, which, interestingly, was the only case of IBD in which the resection was performed for a stricturing complication rather than for uncontrolled inflammation.

The RT-PCR results show that there is an increase in claudin 2 transcripts, which may result from an increase in the rate of transcription or an increase in mRNA stability (Alberts, 2002). An increase in transcript number could lead to an increase in the amount of protein synthesis (Alberts, 2002; Dever, 1999). Indeed, small increases in the amount of claudin 2 synthesis could lead to large increases in the concentration of protein detected, because the half-life of this protein is longer than 12 hours, compared, for example, to only 4 hours for claudin 4 (Van Itallie et al., 2004). In addition, these data do not exclude a contribution to the increase in protein levels from an increase in the rate of translation of claudin 2 transcripts, as regulation of protein translation is another mechanism of increasing protein concentration (Gray and Wickens, 1998)

In the western blots the increased claudin 2 expression was seen in active UC but not in proximal, uninflamed portions of colon. However, when investigated by IHC, an

increase in claudin 2 was seen both in active UC and in inactive UC cases. This is most likely to be because the proximal colon investigated by western blotting had never been inflamed or affected by the disease, whereas the inactive areas investigated by IHC had previously been very inflamed and were subsequently in the process of resolving. Some histopathological changes persist after acute inflammation has resolved in UC, such as crypt elongation or irregularities in crypt morphology. Thus, the UCI groups in the IHC experiments cannot be directly compared with the UCI group in the western blotting experiments. The findings, therefore, strongly suggests that the increase in the amount of claudin 2 is a consequence of inflammation itself rather than a predisposing factor. Increased claudin 2 was observed in both UC and CD. An increase in claudin 2 with a decrease in claudin 4 expression has also been reported in another form of colitis, collagenous colitis (Burgel et al., 2002). This suggests that the factor or factors leading to increased claudin 2 expression may be common to all these inflammatory conditions, rather than being specific to any single disease process. It is likely, therefore, to be a generic feature of inflammatory disease of the intestines.

However, the possibility cannot be excluded that a more subtle increase in level or alteration in function of claudin 2 may be present in predisposed individuals prior to their development of the disease. Confirming this would require the evaluation and long-term follow-up of a population at risk of the disease. It is also possible that the changes observed here are due to some other factor common to the cases here. For example, claudin 2 expression may change in response to drug treatments commonly taken in IBD, such as glucocorticoids, or other agents, such as non-steroidal anti-inflammatory drugs (NSAIDs), which precipitate flares of disease activity (Bjarnason and MacPherson, 1994). Treatment histories were not recorded. However, the fact that claudin 2 expression was not observed in colonic epithelial cells from proximal to diseased areas suggests that the changes are due to active disease rather than the treatments.

The predominantly crypt location of the claudin 2 detected in IBD, and its persistence in areas of resolving inflammation, may give a clue to the mechanisms involved in its upregulation. Intestinal epithelial cells arise from stem cells located in the crypt bases at positions 1-3 in the colon or 4-6 in the small intestine (figure 3.20) (Potten et al., 2002). During their lifespan, they move progressively up the crypts before emerging onto the mucosal surface, in the case of the colon, or continuing to move up

villi towards the villus tips, in the case of the small intestine, ending their lives by being shed into the intestinal lumen. As they do so, the cells differentiate and develop the characteristics of mature absorptive enterocytes (e.g. a brush border, microvilli, active transport mechanisms) and stop dividing. This whole process takes five to six days. Thus, a compartment of slowly cycling stem cells in the crypt base is topped by a larger compartment at positions 6-17 of dividing transit cells with little or no stem cell attributes, followed by non-dividing, differentiating enterocytes (Potten et al., 2002). This is illustrated in figure 3.20.

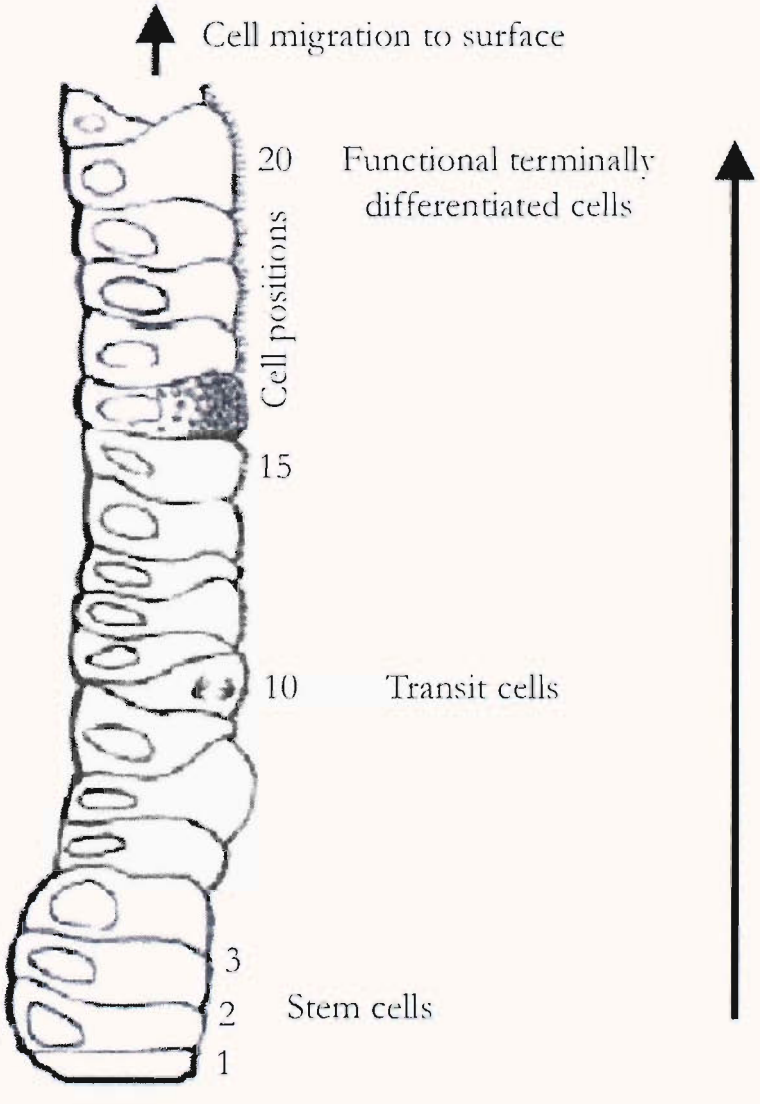


*Figure 3.20. Diagrammatic representation of the histological appearance of a longitudinal section through a crypt of the large intestine. (Adapted from Potten et al., 2002).*

In UC and CD, and indeed in other intestinal inflammations such as coeliac disease, the crypts are expanded i.e. the depth of the crypts increases considerably (MacDonald, 1992). This feature is often present even after inflammation (i.e. immune cell infiltration) has largely resolved. Logically, this expansion must arise from increased cell proliferation, which suggests, therefore, that the stem cell compartment may be expanded. Substantial evidence supports the idea of an expanded compartment of proliferating cells in CD (Kullmann et al., 1996; Noffsinger et al., 1998) and in both active and inactive UC (Arato et al., 1994; Franklin et al., 1985; Kullmann et al., 1996; Noffsinger et al., 1996). The appearance of claudin 2 in the crypt bases, with much lower expression towards the surface epithelium, suggests, therefore, one of two possibilities: firstly, that inflammation induces de novo claudin 2 expression in newly formed, less differentiated enterocytes, but as they mature and move towards the surface epithelium, this expression is reduced; or, secondly, that inflammation induces an expansion of the proliferative, stem cell compartment, which may ordinarily express claudin 2.

The other two claudins studied, claudins 3 and 4, were seen by IHC to occupy two different membrane compartments in the normal colonic epithelium – the TJ area and the lateral membrane. This pattern has also been described in rat intestine (Rahner et al., 2001). In relation to the TJ, claudin 4 is described as conferring sodium-resistance on it (Van Itallie et al., 2001), but the function of claudin 3 in the TJ is unknown. The roles of these two claudins in the lateral membrane are also unknown. It is possible that the lateral membrane claudins form a pool that exchanges with the claudins of the TJ and, perhaps, other intracellular compartments. Another explanation for this dual localisation may be that lateral membrane claudins are incorporated into other cell-cell junctions such as desmosomes, although there is no evidence at present for this. Lateral membrane claudins may participate in other physiological or pathophysiological processes, such as the transmigration of leukocytes. It is known, for example, that dendritic cells express claudins, which may allow them to pass between epithelial cells by binding to epithelial claudins (Rescigno et al., 2001).

In IBD, claudin 3 expression was reduced in the lateral membranes of the crypt cells, and reduced still further in the lateral membranes of the surface cells, where there was also loss from the TJ. Claudin 4 showed a similar pattern, although less commonly.

Western blotting of crypt cell protein did not show significant reductions in total expression of claudins 3 and 4, suggesting that the changes seen by IHC may be caused by redistribution away from cell membranes, rather than reductions in the total amounts of these proteins. The observations suggest that inflammation induces loss of claudins 3 and 4 from the lateral membrane compartment of crypt cells initially, but as these cells mature into surface cells, there is loss from the TJ compartment as well. Although cytoplasmic staining of claudins 3 and 4 was not seen, a diffuse distribution at low concentration may have been below the level of detection of the antibody concentrations used.

### 3.3.2 ZO-1 AND OCCLUDIN

A further finding of these experiments was the markedly reduced surface epithelial expression of ZO-1 and occludin, with much better preservation of expression in the crypts.

ZO-1 is a crucial structural component of TJs, forming a scaffold that supports all the other component proteins. However, evidence outlined earlier (see sections 1.2.2.1.4 and 1.2.2.2) supported the idea that its accumulation at the membrane is regulated and that this correlates with epithelial barrier function. The reduced expression of ZO-1 seen at the surface epithelium in IBD in this experiment thus implies either a reduced number or a reduced size of TJs. The inference to be drawn from this is that the surface epithelium forms a weaker barrier of reduced complexity, and it would be interesting to examine whether the many small molecules associated with ZO-1, such as small GTPases (see section 1.2.2.1.4) are relocated within the cell in this situation.

Reduced surface epithelial expression of occludin was also seen in cases of IBD. In other systems, such as the early mouse embryo (Sheth et al., 1997) or cultured epithelial cells (Furuse et al., 1994), studies have suggested that occludin and ZO-1 are intimately linked. Indeed, binding to the alpha+ isoform of ZO-1 (ZO-1α+) appears to be both necessary and sufficient for the successful clustering of occludin molecules into TJs (Medina et al., 2000; Mitic et al., 1999; Sheth et al., 2000). Therefore, the reduction in surface epithelial TJ occludin may be a consequence of the reduction in surface epithelial ZO-1α+.

If the above explanation were the case, however, it might be expected that in IBD occludin would be more readily detected in cellular locations outside the TJ, as it would no longer be clustered at the TJ by ZO-1. This was not seen in the IHC presented here, although this does not exclude the possibility that occludin freed from ZO-1 is degraded rapidly. There is as yet little evidence for this, although recently the protein Itch has been shown to bind both in vivo and in vitro to the amino-terminus of occludin and to be involved in its ubiquitination (Traweger et al., 2002).

The maintenance of strong ZO-1 and occludin staining in the crypts in the face of inflammation suggests that TJ function is largely unaltered there. However, this experiment did not examine either the expression of different splice variants of occludin or its phosphorylation state. The possibility remains, therefore, that alterations in either or both of these parameters occur in response to inflammation, and that such alterations lead to significant changes in TJ function.

Two other published studies have examined ZO-1 and occludin expression in the intestinal epithelium in IBD. In one, ZO-1 and occludin expression, as detected by western blotting of protein from whole mucosa, was significantly reduced in cases of active UC and CD, and this was also seen by immunofluorescent staining of cryosections, with more severe effects noted at the surface epithelium (Gassler et al., 2001). In the second, occludin, but not ZO-1, expression was reduced in IBD tissue, when examined by western blotting of whole mucosal protein, and immunofluorescent staining of cryosections revealed a global reduction in occludin expression, but a more patchy reduction in ZO-1 expression, which the authors associate with the presence or absence of intraepithelial neutrophils (Kucharzik et al., 2001). The method of IHC used here utilised GMA-embedded mucosal tissue, which preserves tissue architecture very accurately and permits very thin sectioning to enable closer scrutiny of cellular detail. The findings corroborate those obtained using cryosections and further support the utility of the method.

### 3.3.3 CONSEQUENCES FOR THE PATHOPHYSIOLOGY OF IBD

The findings described here may have significant consequences for the pathophysiology of the diseases. In epithelial cell culture experiments (discussed in section 1.2.2.1.1), claudin 2 has been shown to introduce a sodium ion-permeable pore

to the TJ. The implication of the finding of an increase in claudin 2 in the epithelial TJ in IBD is that it confers an increased permeability to sodium on this epithelium too. Increased sodium permeability and a reduced overall electrical resistance have indeed been demonstrated in ulcerative colitis (Sandle et al., 1990; Schmitz et al., 1999), where they are proposed to lead to diarrhoea by causing a back-leak of electrolytes and water into the intestinal lumen ('leak-flux' diarrhoea). Thus, the increase in claudin 2 demonstrated here may be one molecular basis of the leak-flux diarrhoea of IBD.

The reduced surface epithelial TJ expression of ZO-1, occludin, claudin 3 and, to some extent, claudin 4, implies a global reduction in TJ size, number, adhesiveness or all three. Of relevance to this are two observations: firstly, freeze-fracture electron microscopy has demonstrated a reduction in TJ strand number and depth, and an increase in strand breakages, in IBD specimens compared to normal colons (Schmitz et al., 1999; Schulzke et al., 1998), and, secondly, IBD specimens are more permeable than control specimens to both small and large tracer molecules (Sandle et al., 1990). Thus, reduced expression of TJ proteins could well represent the molecular correlate of this impairment of barrier function. The consequence of this impairment may be not only the leak-flux diarrhoea discussed above, but also the ability of bacteria or bacterial antigen to access immune cells, such as lymphocytes and dendritic cells, which are observed between surface epithelial cells.

### 3.3.4 RELATION OF THE FINDINGS TO THE PATHOGENESIS OF IBD

It appears that the inflammatory process may be responsible for the changes described. As discussed in 1.1.1.5.4, IBD is associated with elevations in the mucosal levels of several cytokines, such as IFNγ, TNFα, IL-17 and IL-13. Evidence from studies of cultured cells suggests that the reduced ZO-1 expression observed here may be a consequence of elevated cytokine levels. IFNγ has been shown to reduce ZO-1 levels in T84 cells by shortening its half-life and reducing the rate of its synthesis and transcription (Youakim and Ahdieh, 1999), although a recent paper that exposed T84 cells to combined IFNγ and TNFα has shown a less marked effect (Bruewer et al., 2003).

Occludin expression in vivo may also be sensitive to the elevated mucosal levels of cytokines found in IBD. There is evidence in vitro to support this. In T84 cells, IFNγ

decreases both TER and occludin expression, and leads to a more diffuse distribution of occludin within the membrane (Youakim and Ahdieh, 1999). IFNγ also causes reduced occludin expression in the human lung epithelial cell line Calu-3 (Ahdieh et al., 2001), as does combined IFNγ and TNFα application to primary human airway epithelial cells (Coyne et al., 2002). When transfected into the human intestinal cell line HT-29/B6, the occludin gene promotor displays reduced activity in the presence of either IFNγ or TNFα, and both cytokines together act synergistically (Mankertz et al., 2000). Recently, the same group discovered that the occludin gene contains an additional promoter and transcription start site, giving rise to an alternative first exon, and that this promotor also responds to TNFα (Mankertz et al., 2002).

The effects of these cytokines on the expression of claudins are largely unknown. A single study in T84 cells suggested paradoxically that IL-17 could induce both an increase in electrical resistance across a cultured epithelial monolayer and an increase in its expression of claudin 2 (Kinugasa et al., 2000). A recent study on the same cell line suggested that combined IFNγ and TNFα could induce the internalisation of claudin 4 (Bruewer et al., 2003).

### 3.3.5 SUMMARY

The assessment of the expression of key TJ proteins in colons from normal and IBD patients suggested a marked increase in claudin 2 expression in the TJs of crypt epithelial cells in IBD. Claudins 3 and 4, occludin and ZO-1 were largely unaffected in the crypts, but reductions in their expression were observed in the surface epithelium by IHC. These changes suggest functional impairments in TJs in IBD, which appear to be a consequence of inflammation.

# CHAPTER 4

# MODELLING THE INTESTINAL EPITHELIAL BARRIER

# 4 EXPRESSION OF CLAUDIN SUBTYPES DURING EPITHELIAL BARRIER FORMATION

## 4.1 INTRODUCTION AND AIMS

In the previous chapter it was observed that claudins 3 and 4 were present in the TJs and along the lateral membranes of normal colonic epithelial cells. In IBD claudin 2 expression was strongly increased in the TJs of crypt epithelial cells, and some reductions in the expression of claudins 3 and 4 were seen in the surface epithelium. It was suggested that aspects of the inflammatory response in the diseases may be responsible for inducing these alterations. In order to investigate these possible mechanisms, a model of the intestinal epithelial barrier was required.

T84 cells are used widely to investigate the properties of intestinal epithelial cells. They were derived initially from a lung metastasis of a human colonic carcinoma (Murakami and Masui, 1980). They can be cultured in both serum-containing and serum-free media (Murakami and Masui, 1980). However, when cultured for a few (3-5) days in serum-free medium, the cells pile up and form gland-like structures closely resembling the original tumour morphologically, whereas in serum-containing medium they grow as a monolayer with the morphological appearance of epithelial cells (Murakami and Masui, 1980). When grown in serum-containing medium on plastic supports, T84 cells form a monolayer of low cuboidal cells that display few structural features of mature enterocytes, such as nuclear polarity, lysosomes, TJ formation and microvilli (Dharmsathaphorn et al., 1985; Madara et al., 1987). However, when plated for a few days on type I collagen-coated supports, these cells form a highly confluent monolayer of columnar cells, which display many features of differentiated enterocytes, such as microvilli, nuclear polarity, lysosome formation, polarisation of cellular organelles and vectorial transport (Madara et al., 1987). In addition, in this situation these cells will respond to a variety of secretagogues by secreting chloride ions (Dharmsathaphorn et al., 1984; Dharmsathaphorn et al., 1985), which is reminiscent of the behaviour of crypt cells (Mandel et al., 1986). The various membrane carriers, pumps and channels responsible for this barrier are described as being very similar to that of crypt cells (Mandel et al., 1986).

Furthermore, as such a monolayer matures it develops the structural and functional correlates of TJ formation: TJs are observed by electron microscopy; a strand pattern is observed within these TJs by freeze-fracture electron microscopy; a high electrical resistance is generated across the monolayer (indicative of resistance to paracellular ion movements); and resistance to the passive passage of uncharged macromolecules develops (Dharmsathaphorn et al., 1984; Madara et al., 1987). Thus, this cell line, cultured in serum-supplemented medium on collagen type I-coated supports, has several characteristics that make it ideal for the examination of intestinal epithelial barrier function at the functional and molecular level, and it has been utilised for this purpose in numerous published studies. Other colonic cancer-derived cells, such as Caco-2 cells, have also been utilised in studies of epithelial barrier function. Cultured Caco-2 cells also form resistant monolayers of polarised cells, but their electrical properties are described as resembling partly differentiated crypt cells (Grasset et al., 1984; Grasset et al., 1985). Furthermore, they also display features of small intestinal or foetal differentiation, such as the expression of small intestinal brush border hydrolases (Zweibaum et al., 1984), and so have been utilised in the study of small intestinal epithelial properties. Whereas Caco-2 cells are hypertetraploid, with a modal number of chromosomes of 96, T84 cells have the advantage of being predominantly diploid; however, the modal number of chromosomes in T84 cells is 56 and it is not known if this affects the genes for claudins 2-4. Both cell lines are derived from malignant clones, and as abnormalities of the structure and function of AJs are common in colonic cancer (Wijnhoven et al., 2000), it is possible that these altered AJs may affect the function of TJs. Furthermore, evidence was described in 1.2.2.2.4 that suggested a possible tumour-suppressor function for TJs, so it is conceivable that TJs are inherently altered in these cancer-derived cells. In particular relation to the claudins, the expression of different claudins in T84 or Caco-2 cells had not been described.

If the collagen-coated support on which the cells are cultured is made semipermeable (e.g. by its containing 0.4μm pores), two compartments are created, an apical one and a basal one, each with access to the plasma membrane. Thus, medium placed in the apical compartment accesses the apical compartment alone, whilst medium placed in the basal compartment accesses the basolateral membrane alone. This is a very useful feature, as many cell receptors are located in one or other compartment of the plasma membrane, separated by the TJ (Dharmsathaphorn et al., 1985), and it

allows the cells to feed from the basolateral compartment after confluence is acquired and the junctions have sealed. In addition, if a known electrical current is passed across the cells between the two compartments of medium and the potential difference is measured, the electrical resistance can be easily calculated from the equation Resistance = Potential Difference/Current. Repeating this measurement without any cells, with only medium and supports in place, and subtracting this from the total resistance measured across the monolayer gives the true resistance due to the monolayer. Clearly, a culture support of larger cross-sectional area will offer lower electrical resistance than a smaller one, and therefore the resistance values are multiplied by the area of the support to give a reproducible and comparable Transepithelial Electrical Resistance (TER).

Therefore, the aims of this chapter were to:

- characterise the development of the barrier function of T84 cells by serial measurements of TER
- examine the expression of claudins 2, 3 and 4 during this development.

## 4.2 RESULTS

T84 cells were subcultured at a 1:1 split ratio onto BIOCOAT 0.4μm porous inserts, pre-coated with collagen S, on day 0, as described in section 2.3. Culture medium was replaced every two days, at least two hours before reading the TER. Three time points were selected for the examination of claudin expression: days 2, 8 and 15. At each time point monolayers were processed for analysis of expression of claudins 2, 3 and 4 by immunofluorescence. At the same time, cell monolayers were lysed for protein extraction and the lysates stored. At the end of the experiment SDS-PAGE and western blotting were performed on these samples, followed by immunodetection of claudin 2. Following this, the membranes were stripped and reprobed successively for claudin 3, claudin 4 and the loading control, cytokeratin 19. Quantity One software was used to measure band densities. The density of each claudin band was divided by that obtained with cytokeratin 19 to produce a Normalised Band Density that could be compared across lanes, as described in 2.6.4. All experiments were performed twice.

### 4.2.1 TER

Two days after plating the TER remained low, at approximately 100ohm.cm$^2$. This corresponded to the period taken for the cells to become confluent. After this the TER increased progressively, so that by 15 days it was approximately 700ohm.cm$^2$ (figure 4.1).

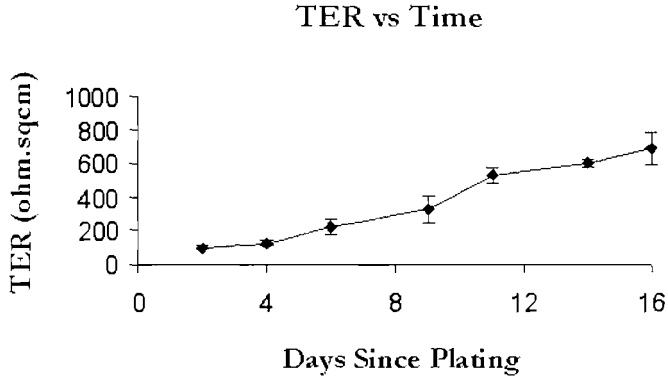


*Figure 4.1. Graph of TER vs. time for T84 cells cultured on 0.4μm pore-containing collagen S-coated filter inserts. Data points correspond to the mean of 6 separate inserts and error bars represent one Standard Error of the Mean. Duplicate experiments were performed and a representative result is depicted.*

### 4.2.2 EXPRESSION OF CLAUDINS

#### *4.2.2.1 Negative Controls*

T84 cell monolayers were stained using rabbit immunoglobulins (Ig) and mouse Ig of isotype G1 (IgG1) in place of the primary antibodies, in order to control for any non-specific binding of the primary antibodies to the sections. Almost no positive staining was observed with either non-immune globulin, suggesting that any positive staining observed with the primary antibodies was the result of their binding to protein via their antigen-specific binding sites. Examples are shown in figure 4.2.

Western blotting was performed using a single T84 whole cell lysate in all lanes. Identical two-lane strips were incubated with claudin 2 antibody, rabbit Ig, claudin 4 antibody and mouse IgG1. The results are depicted in figure 4.3. No bands were detected when either primary antibody was substituted with its matching non-immune

Ig. This suggested that the bands observed with the primary antibodies were the result of their binding to protein via their antigen-specific binding sites.

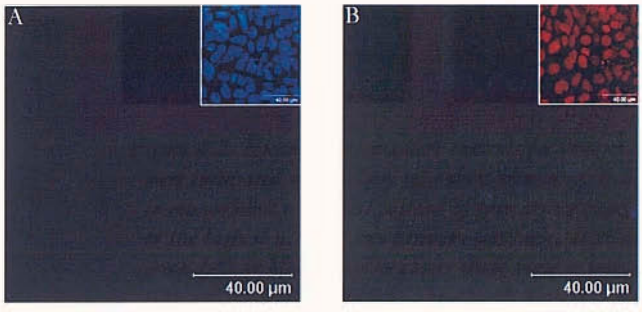


*Figure 4.2. Examples of negative controls for immunofluorescence staining. Monolayers were incubated with 1.7µg/ml rabbit immunoglobulin (A) and 4.3µg/ml mouse immunoglobulin G1 (B) instead of primary antibodies. These concentrations were equal to the highest used for any primary antibody, as shown in table 2.2. Positive staining is green (A) or blue (B). The insets show nuclear counterstaining with TO-PRO-3-iodide (A) and 7-AAD (B) of the same fields depicted in the main views, in order to confirm the presence of cells.*

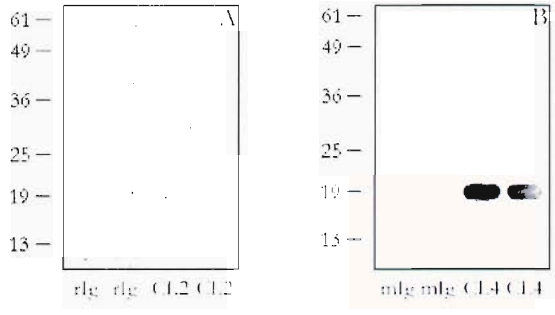


*Figure 4.3. Negative control western blots of T84 cell protein. In A, the right-hand pair of lanes was incubated with 625ng/ml of rabbit anti-claudin 2 antibody (CL2) and the left-hand pair with an equal concentration of rabbit immunoglobulin (rIg). Bands at approximately 19kDa are detected only with the CL2 antibody. In B, the right-hand pair of lanes was incubated with 6.25ng/ml of mouse anti-claudin 4 antibody (CL4) and the left-hand lanes with an equal concentration of mouse immunoglobulin (mIg) of the same subclass (IgG1). Bands at approximately 19kDa are detected only with the CL4 antibody. The chosen concentrations were the highest of the primary antibodies used on blots of T84 cell protein in the weight range depicted (see table 2.3).*

#### *4.2.2.2 Claudin 2*

Two days after the cells were plated, immunofluorescence staining of claudin 2 revealed widespread expression across the monolayer. The staining was incomplete, however, with patches of very little staining interspersed with large patches of strong fluorescence figure 4.4). At the cellular level most of this staining was observed in a sharp, 'chicken-wire' pattern suggestive of a TJ location. A small amount could be detected intracellularly, but its precise cellular location could not be determined. Computer-generated cross-sectional views (known as z-views; insets in figure 4.4) revealed an apical, punctate staining pattern, again consistent with a TJ location, with very little staining seen along the basolateral membrane.

After 8 days had elapsed immunofluorescence staining revealed a striking reduction in the amount of claudin 2 detected. Claudin 2 could still be detected, but only in very small and sparse clusters of cells. Again, the chicken-wire pattern and the punctate appearances in the z-views suggested a TJ localisation. After 15 days there were no further changes from the appearances observed at 8 days after plating.

Immunodetection of claudin 2 on western blots of whole cellular protein at these three time points produced a pattern consistent with the immunofluorescence findings (figure 4.5). A very strong band was seen after 2 days (Normalised Band Density 9.6), but the bands seen after 8 and 15 days were dramatically weaker (Normalised Band Densities 1.1 and 1.4 respectively), suggesting a marked reduction in total expression. Immunodetection of cytokeratin 19 on the same blots confirmed equal loading of protein in each lane.

#### *4.2.2.3 Claudin 3*

Two days after plating immunofluorescence staining for claudin 3 revealed widespread but somewhat patchy expression across the monolayer (figure 4.4). Most of this staining was consistent with a membranous location, but it did not resemble the chicken-wire pattern suggestive of TJ incorporation. Instead it was somewhat fuzzy and imprecise. It was also accompanied by some intracellular staining. The reconstructed z-views (insets of figure 4.4) thus show a diffuse distribution of staining within the cells and along their lateral membranes.

After 8 days, the fluorescence had become more widespread. It was now distributed in a sharp, chicken-wire pattern consistent with a TJ location, and there was much less intracellular staining. The z-views now revealed a less diffuse staining pattern, consistent with its possible incorporation into TJs. This pattern was again seen 15 days after plating. Immunodetection of claudin 3 on western blots of whole cell lysates produced only a faint band on the day 2 lysates (Normalised Band Density 0.3) but strong bands after both 8 and 15 days (Normalised Band Densities 1.5 and 1.6 respectively; figure 4.5), consistent with an increase in total expression over time.

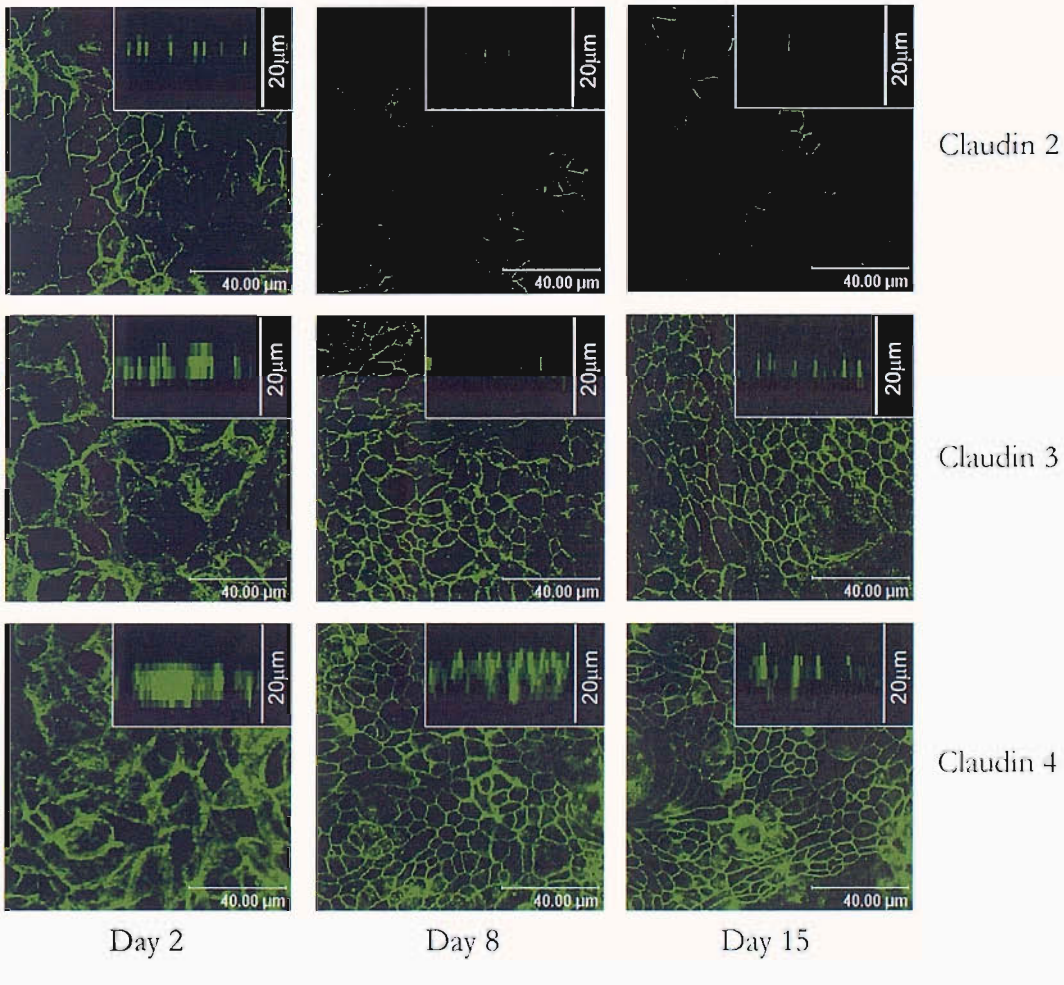


*Figure 4.4. Immunofluorescence detection of claudins 2-4 in T84 cells at 2, 8 and 15 days from the time of plating. Images were obtained by LASER confocal microscopy; insets show computer-generated cross-sectional reconstructions (side- or z-views). Each image depicts a representative field from five examined. Experiments were performed in duplicate.*

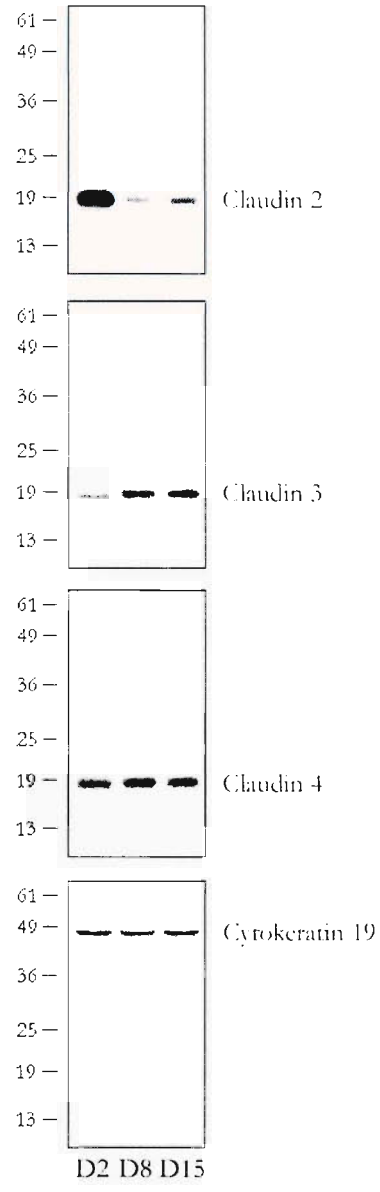


*Figure 4.5. Western blot of T84 whole cell lysates obtained 2 (D2), 8 (D8) and 15 (D15) days after plating and probed successively for claudins 2-4 and cytokeratin 19. Representative blots from duplicate experiments are depicted. Band densities normalised to cytokeratin 19 for D2, D8 and D15 were as follows: Claudin 2 – 9.6, 1.1, 1.4; Claudin 3 – 0.3, 1.5, 1.6; Claudin 4 – 1.3, 2.1, 1.8.*

### *4.2.2.4 Claudin 4*

At day 2 claudin 4 immunofluorescence staining revealed widespread expression across the monolayer (figure 4.4). The distribution was somewhat patchy, but far less so

than with claudins 2 and 3. As was the case for claudin 3 there was much expression in a membranous location, but there was also considerable intracellular expression seen. The membrane staining was very imprecise and did not suggest a TJ location. The z-views revealed a diffuse distribution of staining, both within cells and along their lateral membranes (see the depth of the staining in the insets of figure 4.4).

After 8 days most of the claudin 4 immunofluorescence was distributed in a sharp, chicken-wire pattern consistent with its incorporation into TJs, and this was spread across almost the entire monolayer. There was still some claudin 4 detectable along the lateral membranes. Thus, the z-views showed a much less diffuse distribution of staining than at day 2, but there was still considerable imprecise staining lower down the cells. By day 15 more of the claudin 4 was detected in a TJ pattern, with z-views showing a still less diffuse staining pattern, and a smaller amount could be seen lower down the cells.

Immunodetection of claudin 4 on western blots of whole cell lysates produced strong bands at all three time points examined, although the band after 2 days was somewhat weaker (Normalised Band Density 1.3) than those after 8 and 15 days (Normalised Band Densities 2.1 and 1.8 respectively; figure 4.5), consistent with an increase in total expression over time.

## 4.3 DISCUSSION

These results confirm that the T84 cell line develops phenotypic changes over time that include the development of an effective barrier to ions and alterations in both the type of claudins expressed and their cellular location. Soon after plating, electrical resistance was low. High electrical resistance took several days to develop and continued to increase for at least 15 days. This concords with those early studies that showed by electron microscopy that cellular polarisation and junction development are stimulated by several days growth on collagen-coated supports (Madara et al., 1987). Thus, in order to utilise this cell line as a model of the intestinal epithelial barrier, at least 8, and preferably 15, days must elapse from initial near confluent plating.

Confocal LASER microscopy was used to detect immunofluorescently labelled claudins in T84 cell monolayers, in order to determine both the distribution of claudin-positive cells and the likely location of positive staining within the cells. Although the

reconstructed Z-views suggested that claudin staining was occurring in either punctate apical or more diffuse patterns, making firm deductions about cellular location is problematic for two reasons. Firstly, additional staining was not carried out to determine precisely the apices and bases of the cells, and, secondly, the Z-views appear somewhat pixilated. This pixilation could be reduced by detection of staining at higher magnifications than that used (x400) and by utilising thinner optical sections than the 1μm depth used here. However, this would need to be balanced against the increased risk of fluorescence bleaching that longer exposures to LASER light would entail.

A summary of the changes observed over time is presented in table 4.1. The mature T84 monolayer was shown to express both claudin 3 and claudin 4 in most cells and in a cellular location consistent with the TJ. This correlates well with the expression pattern within human enterocytes presented in chapter 3. Furthermore, claudin 4 was also present lower down the lateral membrane in these mature cells, as was demonstrated to be the case in the human intestine, although less claudin 3 expression was seen in this location. However, during the first few days after plating less claudin 3 and claudin 4 were expressed, and both claudin 3 and claudin 4 were predominantly detected outside the TJ, either along the lateral membrane or intracellularly. This is consistent with the idea proposed in chapter 3, wherein the claudins were suggested to exist in pools in a variety of cellular locations and to move between them if stimulated to do so. Thus, in T84 cells at least, it seems most likely that the development of mature TJs is associated with the movement of claudins 3 and 4 from the cytoplasm to the lateral membrane and thence to the TJ. Studies using Green Fluorescent Protein (GFP)-labelled transfected claudins and cell fractionation experiments may be able to confirm this. The data are also consistent with a scenario in which the development of high levels of electrical resistance depends on the incorporation into TJs of those claudins that confer ionic resistance. In this instance the claudin known to confer this resistance is claudin 4 (Colegio et al., 2002; Van Itallie et al., 2001). The properties and functions of claudin 3 are, however, as yet unknown.

The most striking finding in these experiments was the high level of expression of claudin 2 found by both immunofluorescence detection and western blotting two days after plating the cells. Furthermore, claudin 2 was not observed predominantly outside the TJ (as was the case for the other claudins) but in an apical, punctate distribution in cross-section and in a chicken-wire pattern when viewed en face, which suggests a TJ

localisation. However, as stated above, mature TJs take some days to develop if electron microscopic appearances and barrier function are used as criteria. Therefore, the results obtained here suggest that claudin 2 is being expressed in immature points of apical contact between cells, which can be labelled 'immature' or 'precursor' TJs. The function of claudin 2 in this situation is unclear, but the immaturity of the TJs and the cationic permeability conferred by claudin 2 (Amasheh et al., 2002), and the observation(Colegio et al., 2003; Van Itallie et al., 2003) that claudins 3 and 4 were not detected in the same distribution, correlate well with the low electrical resistance of the monolayers at this point. By day 8 there was a marked reduction in claudin 2 expression, as detected by both immunofluorescence and western blotting, which to some extent was reciprocated by the increase in expression of claudins 3 and 4. This was associated with a rise in electrical resistance, and therefore the loss of claudin 2 may contribute to this. At days 8 and 15 the small amount of claudin 2 detected by immunofluorescence was located in small clusters of cells and in a cellular distribution consistent with the TJ.

| **Days from plating** | 2 | 8 | 15 |
|---|---|---|---|
| **Tight Junctions** | Immature | Maturing | Mature |
| **Electrical resistance$^{+}$** | Very low | Low | High |
| **CL2 expression* (*location$^{X}$*)** | High *(most in 'TJs')* | Very low *(most in TJs)* | Very low *(most in TJs)* |
| **CL3 expression* *(location$^{X}$)*** | Low *(most outside 'TJs')* | High *(most in TJs)* | High *(most in TJs)* |
| **CL4 expression* *(location$^{X}$)*** | Low *(most outside 'TJs')* | High *(some in TJs)* | High *(most in TJs)* |

*Table 4.1. Summary of changes in properties of T84 cell monolayers over time. $^{+}$ refers to the TER data depicted in figure 4.1. * refers to the western blot data depicted in figure 4.5. $^{X}$ refers to the immunofluorescence data depicted in figure 4.4.*

The function of the claudin 2 detected soon after plating is unclear, but determining more about the stimulus responsible for its upregulation may give clues to the reasons for its upregulation in IBD. A first possibility is that claudin 2 is associated with a proliferative phenotype. In other words, those cells that are proliferating also express

claudin 2. Soon after plating T84 cells do, of course, proliferate and a large amount of claudin 2 was detected at around this time. This suggests an association, but does not prove that proliferation is related to the increased claudin 2 expression. The small clusters of claudin 2-positive cells in the mature T84 cell monolayers are of interest, because if claudin 2 is upregulated in proliferating cells, these small clusters should therefore also be foci of proliferating cells. Furthermore, in IBD claudin 2 was detected in the epithelial crypts, and particularly the bases of the crypts, where it is known that cells are proliferating (see chapter 3). Both features are therefore associated anatomically. However, in normal colonic crypts there is a smaller zone of proliferating cells at the bases but claudin 2 could not be detected there by IHC. However, this does not exclude the possibility of a very low level of claudin 2 expression or that the very basal crypts were not sectioned often enough to reliably detect staining.

A second possibility is that claudin 2 is expressed in newly forming TJs, such as those in newly plated T84 cells. If this were the case it might suggest that in IBD the crypt cells remain in a more immature, less differentiated state than in normal colon as they transit towards the surface. In T84 cells it might be expected that a controlled disassembly of mature TJs, followed by reassembly, would be associated with an upregulation of claudin 2 expression reminiscent of that in recently plated cells.

A third possibility is that claudin 2 is upregulated in response to an injurious stimulus, such as the trypsinisation and resuspension during subculturing. Other possible stimuli might include signals from other cells and tissues indicating nearby injury or inflammation. Claudin 2 expression in this instance could form part of an attempted repair-and-repel strategy, with the twin aims perhaps of quickly reforming cellular contacts to help maintain tissue integrity, whilst maintaining permeability to ions and associated water. The purpose of conferring leakiness onto the epithelium may be a mechanism to help remove adherent parasites from the intestine. As claudin 2 has a relatively slow turnover compared to claudin 4 (a half-life of more than 12 hours compared to 4 hours; (Van Itallie et al., 2004)), a relatively small increase in the production of claudin 2 could lead to a significant increase in the total protein present.

In summary, the development of TJs in relation to the incorporation and expression of claudins has been described. The expression of claudins 2, 3 and 4 in mature monolayers mimicked the pattern seen in normal colon, and their incorporation into maturing TJs correlated with the acquisition of increasing TER. Therefore, this model

displayed characteristics which enabled its utilisation to study the effects of external stimuli upon the re-expression of claudin 2.

# CHAPTER 5

# EXPRESSION CHARACTERISTICS OF CLAUDIN 2 IN THE T84 CELL MODEL

# 5 EXPRESSION CHARACTERISTICS OF CLAUDIN 2 IN THE T84 CELL MODEL OF THE EPITHELIAL BARRIER

## 5.1 INTRODUCTION AND AIMS

In chapter 3 it was observed that claudin 2 expression was increased in IBD. This expression correlated with the zone of proliferation, which is known to be expanded in IBD (Arato et al., 1994; Franklin et al., 1985; Kullmann et al., 1996; Noffsinger et al., 1998; Noffsinger et al., 1996). In the T84 cell model claudin 2 expression was increased after cell plating. Therefore, it is possible that claudin 2 expression correlates with cell division and / or increased plasticity in cell-cell contacts.

The aims of this chapter were to

- examine the putative association between the expression of claudin 2 and cellular proliferation by dual antibody staining
- examine whether claudin 2 expression is upregulated when cells are reassembling TJs after calcium ion replenishment.

## 5.2 RESULTS

### 5.2.1 DUAL STAINING OF CLAUDIN 2 AND KI-67

Ki-67 was used as a marker of cells in cycle (Gerdes et al., 1983; Gerdes et al., 1984). The localisation of claudin 2 and Ki-67 in a mature monolayer of T84 cells was investigated by immunofluorescence staining and LASER confocal microscopy. The principle was that strict co-localisation of the two antigens would provide good evidence to support the hypothesis that claudin 2 is expressed by cells that are in the cell cycle.

T84 cells were cultured on collagen-coated 13mm coverslips for 15 days. They were then processed for immunofluorescence staining. Simultaneous dual staining for claudin

2 and Ki-67 was performed with appropriate negative controls according to the design given in table 5.1. The secondary antibodies used on all the coverslips were anti-rabbit-488 and anti-mouse-546. The nuclei were counterstained with ToPro-3-iodide. Detection was performed by LASER confocal microscopy. The experiment was performed twice.

| **Group of coverslips** | **Primary Antibodies (concentration)** | |
|---|---|---|
| CL2 + Ki-67 Dual Staining | Rabbit anti-human CL2 (1.7 μg/ml) | Mouse ($IgG_1$) anti-human Ki-67 (3.2 μg/ml) |
| Single negative control (1) | Rabbit anti-human CL2 (1.7 μg/ml) | Mouse $IgG_1$ (3.2 μg/ml) |
| Single negative control (2) | Rabbit immunoglobulin (1.7 μg/ml) | Mouse anti-human Ki-67 (3.2 μg/ml) |
| Double negative control | Rabbit immunoglobulin (1.7 μg/ml) | Mouse $IgG_1$ (3.2 μg/ml) |

*Table 5.1. Primary antibodies and their concentrations used in dual staining of claudin 2 (CL2) and Ki-67 and in appropriate controls.*

The results of the dual staining for claudin 2 and Ki-67 and the negative controls are depicted in figure 5.1. Figure 5.1A shows that staining for claudin 2 produced clusters of positive cells as was the case in previous experiments. There was very faint detection of the mouse immunoglobulin ($IgG_1$), which was used to detect the degree of non-specific binding of the Ki-67 antibody to the section. Figure 5.1B shows a minority of cell nuclei staining positively for Ki-67 (red), whilst the negative nuclei remain blue. There is very little fluorescence produced by the rabbit immunoglobulin, which was used to detect the degree of non-specific binding of the claudin 2 antibody to the section. Figure 5.1C shows that in the absence of the antibodies to both claudin 2 and Ki-67, the non-specific fluorescence produced by both the rabbit and mouse immunoglobulins is faint, with a small amount of bound mouse $IgG_1$ detected.

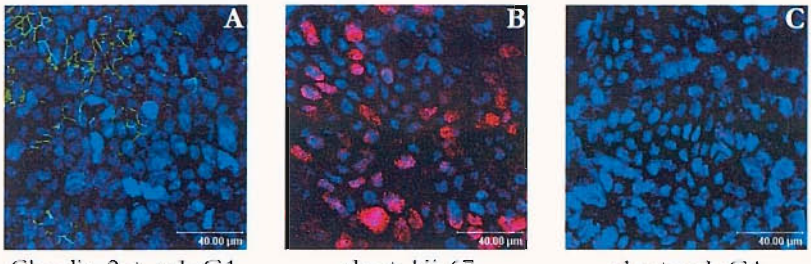


Claudin 2 + mIgG1 rIg + Ki-67 rIg + mIgG1

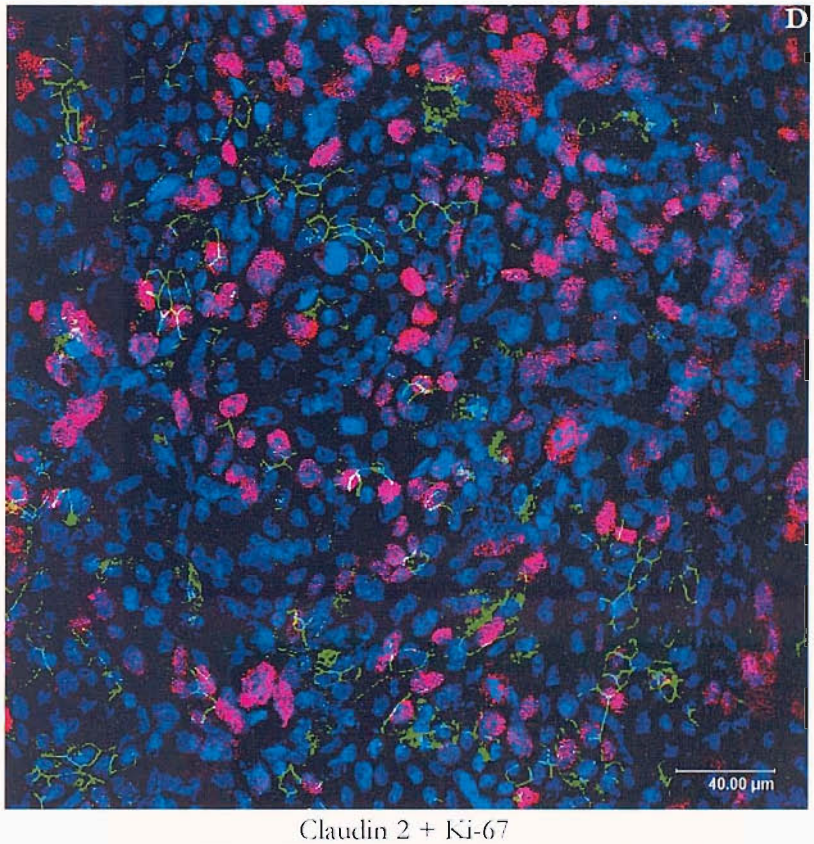


Claudin 2 + Ki-67

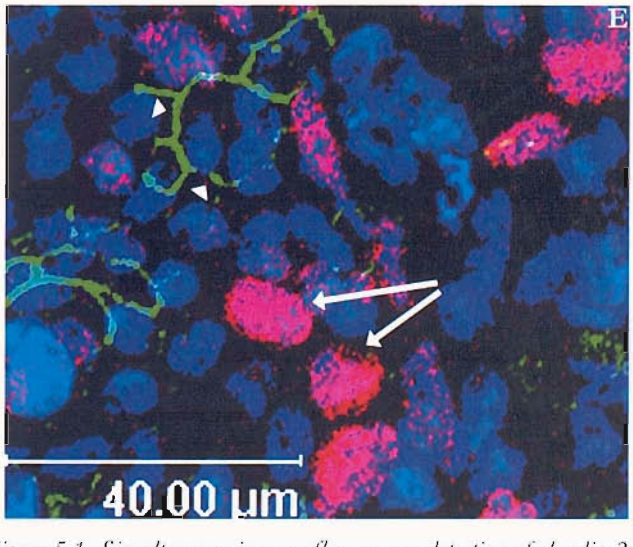


*Figure 5.1. Simultaneous immunofluorescence detection of claudin 2 and Ki-67 in T84 cells. A. Claudin 2 (green) + mouse IgG, (mIgG1, red). B. Rabbit Ig (rIg, green) + Ki-67 (red). C. rIg (green) + mIgG1 (red). D. Claudin 2 (green) + Ki-67 (red). E. Magnification of sector of D. Nuclei are blue in all cases. Five fields were examined in each of two duplicate experiments, and a representative field is depicted.*

Figure 5.1D shows a large field of T84 cells stained simultaneously with antibodies to claudin 2 and Ki-67. Minorities of cells are positive for Ki-67 (red) and claudin 2 (green). However, these groups of cells show a very small degree of overlap. There are many claudin 2 positive cells that are negative for Ki-67 and, conversely, many Ki-67-positive cells are negative for claudin 2. In the magnified section of figure 5.1D shown in 5.1E, this point is more clearly demonstrated. The Ki-67-positive cells (arrows) are distinct from the claudin 2-positive cells (arrowheads).

### 5.2.2 DETECTION OF CLAUDIN 2 AFTER CALCIUM WITHDRAWAL AND REPLACEMENT

To examine whether claudin 2 expression is increased when cells are forming new TJs, use was made of a 'calcium-switch' experiment. The integrity of TJs is dependent on extracellular calcium ions. Withdrawal of calcium from the medium therefore allows a controlled disassembly of TJs to occur. Once disassembly has occurred, replenishment of calcium permits TJ reassembly to occur. The expression of claudin 2 was investigated during this disassembly-reassembly process. The expression of the key TJ scaffold protein, ZO-1, was used to confirm simultaneously the state of assembly of the TJs.

T84 cells were cultured on collagen-coated 13mm coverslips for 15 days. They were then subjected to either withdrawal of calcium or continued exposure to calcium (1.2mmol/l) for 2 hours, before being returned to normal culture medium for up to 48 hours. Coverslips were processed for immunofluorescence staining at four time points: immediately before calcium withdrawal (0 hours), immediately after the 2 hour period of calcium withdrawal or calcium maintenance and either 24 or 48 hours after being returned to normal culture medium. Immunofluorescence staining was performed for both ZO-1 and claudin 2 at all time points. The experiment was performed twice.

The results of the immunofluorescence detection of ZO-1 and claudin 2 are depicted in figures 5.2 and 5.3 respectively. Immediately prior to the withdrawal of calcium there was widespread positive staining for ZO-1 across the T84 monolayer, in a pattern consistent with its known TJ cellular location (figure 5.2A). A two hour incubation in calcium-containing HBSS did not alter this distribution (figure 5.2B), whereas calcium withdrawal for 2 hours caused a marked and widespread redistribution

of ZO-1 into a punctate membranous and diffuse cytoplasmic pattern (figure 5.2C), consistent with TJ disassembly.

Twenty-four hours after calcium replacement most of the ZO-1 appeared to have returned to a TJ location, but some ZO-1 was still observed in the punctate distribution seen immediately after calcium withdrawal (figure 5.2E). The control monolayers, which had not experienced calcium withdrawal, continued to display the TJ-associated chicken-wire pattern of immunofluorescence at this stage (figure 5.2D) and indeed after a further 24 hours incubation in culture medium (figure 5.2F). Forty-eight hours after calcium replacement ZO-1 has almost completely returned to its original distribution (figure 5.2G).

Immediately prior to the withdrawal of calcium small clusters of cells stained positively for claudin 2, and most of this staining was distributed in the chicken-wire pattern characteristic of TJ localisation (figure 5.3A). This appearance was unchanged after 2 hours of incubation in calcium-containing HBSS (figure 5.3B). However, 2 hours of incubation in calcium-free HBSS led to the disappearance of claudin 2 from this membrane location and its appearance instead in small puncta with some more diffuse staining in the cytoplasm (figure 5.3C).

After replenishing the extracellular calcium for 24 hours, claudin 2 was detected again in a TJ pattern, but there was no increase in the total amount detected compared to the control monolayers (figure 5.3D and E). After 48 hours culture in normal medium there was also no difference between control and low calcium-treated cells (figure 5.3F and G), indicating that disassembly and reassembly using extracellular calcium withdrawal did not stimulate an increase in claudin 2 expression in a TJ pattern at these time points.

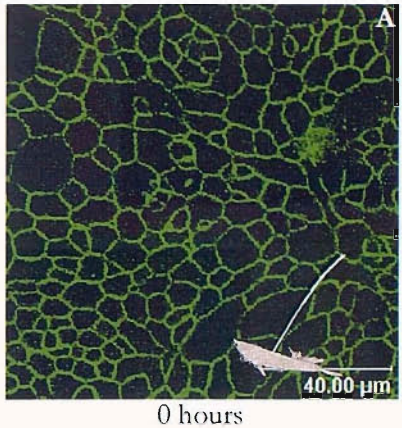


0 hours

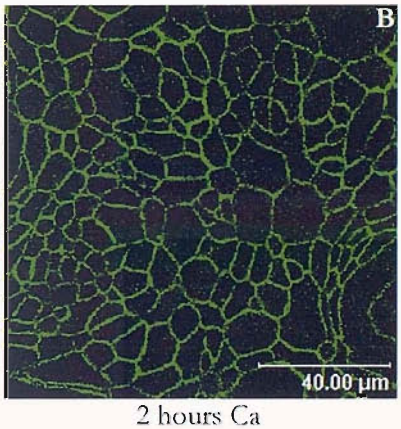


2 hours Ca

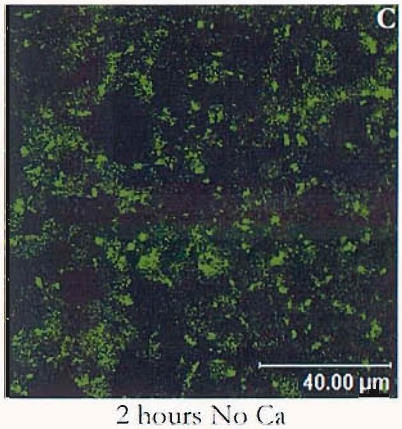


2 hours No Ca

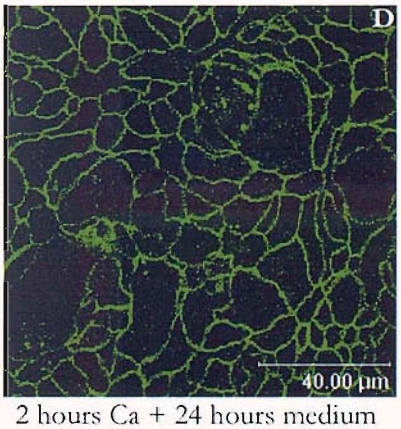


2 hours Ca + 24 hours medium

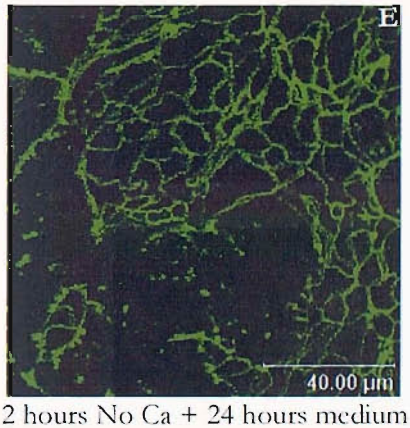


2 hours No Ca + 24 hours medium

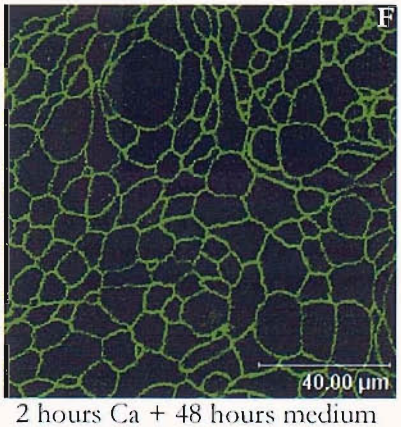


2 hours Ca + 48 hours medium

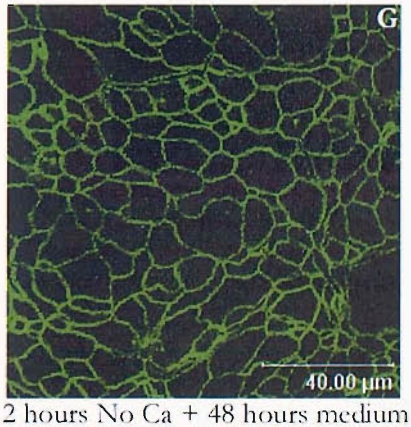


2 hours No Ca + 48 hours medium

*Figure 5.2. Immunofluorescence detection of ZO-1 in T84 cells at baseline (0 hours) or after exposure to either no calcium (No Ca) or normal calcium (Ca) for 2 hours, or after such exposures followed by replenishment of medium for either 24 hours or 48 hours. A representative field from 5 examined is depicted in each case.*

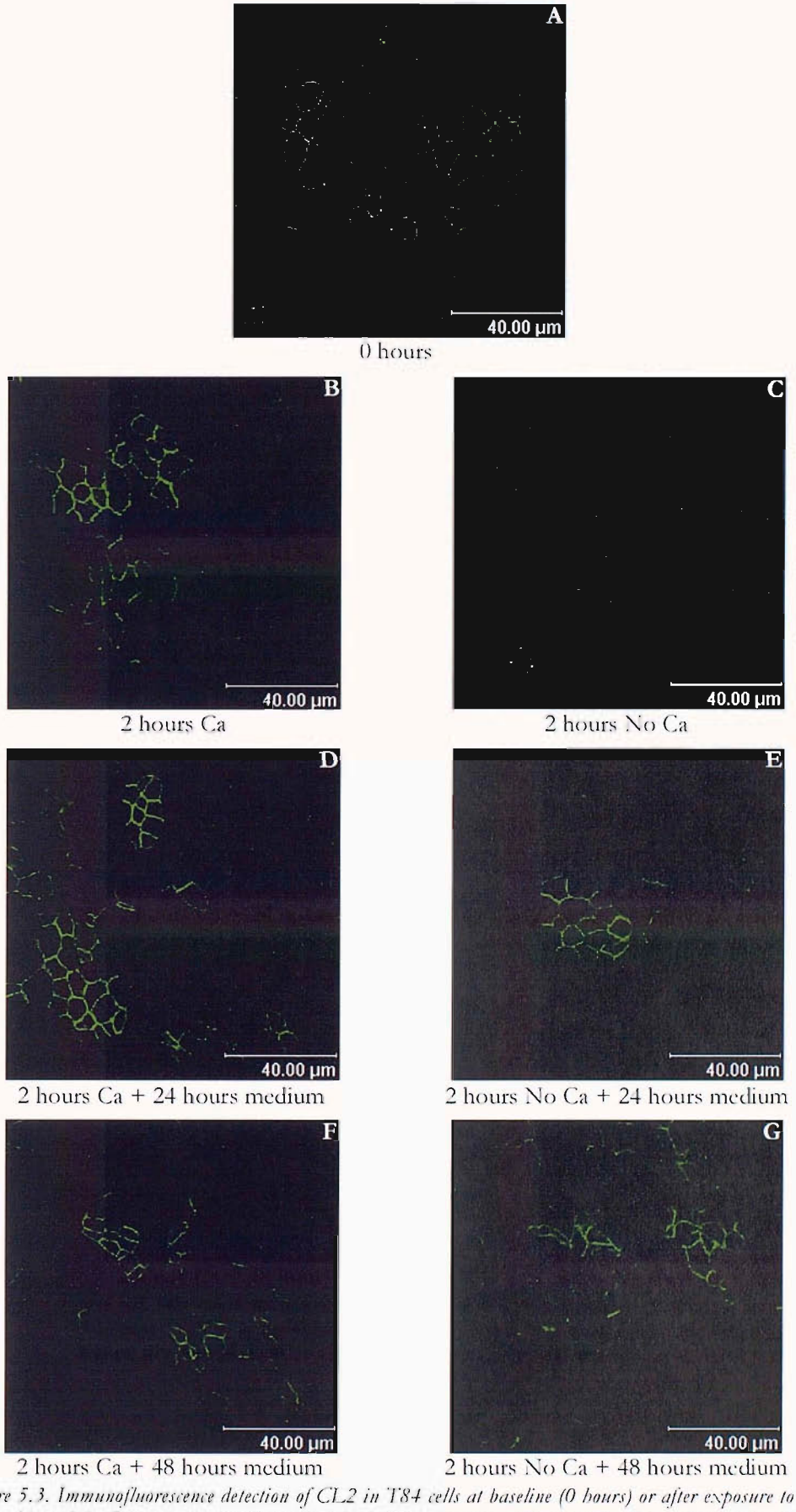


*Figure 5.3. Immunofluorescence detection of CL2 in T84 cells at baseline (0 hours) or after exposure to either no calcium (No Ca) or normal calcium (Ca) for 2 hours, or after such exposures followed by replenishment of medium for either 24 hours or 48 hours. A representative field from 5 examined is depicted in each case.*

## 5.3 DISCUSSION

Nuclear expression of Ki-67 is a frequently used and well-recognised marker of proliferating cells (Gerdes et al., 1983). It labels cells in G1-S-G2 and M phases but not those in the very early stages of re-entering G1 from G0 (Gerdes et al., 1984). Hence, it labels actively dividing cells and would be expected to label proliferating crypt cells. In the mature T84 cell monolayers examined here only a minority of cells were positive for this marker, as might be expected in a highly confluent layer of tightly adherent cells. Claudin 2 was only expressed by a small minority of cells but there was little consistent overlap between the two minorities of cells detected. If a recently plated layer of cells had been used for the experiment, it is possible that many more cells would have expressed Ki-67 as more cells would have been proliferating at this point. In the early days after plating the larger proportion of cells expressing claudin 2 may therefore have overlapped considerably with the Ki-67-positive cells, giving an impression of a correlation between cell cycle and claudin 2 expression.

Withdrawal of calcium from the medium had profound effects on TJ assembly, as evidenced by the dramatic redistribution of the TJ scaffold protein ZO-1. These effects could be completely reversed by replacing the calcium ions in the medium for 48 hours. Calcium withdrawal also caused a marked redistribution of claudin 2 away from its TJ location, and again this was reversible on restoring the extracellular calcium. However, unlike the situation in which the T84 cells had been trypsinised, resuspended and plated, there was no dramatic increase in the proportion of cells expressing claudin 2. This suggests that the reassembly of cell-cell contacts and TJs is not invariably associated with increased claudin 2 expression. It is possible, however, that other connections between cells are disrupted by trypsinisation but still present after calcium withdrawal. Furthermore, complete calcium withdrawal may not mimic any physiological or pathophysiological situation in vivo.

A third possible explanation to connect the upregulation of claudin 2 expression observed in both IBD epithelium and recently plated T84 cells is that it is a response to injury or inflammation, as discussed in chapter 4. In this regard it is known that T84 cells respond to certain inflammatory cytokines by altering their permeabilities to both ions and uncharged molecules. The cytokines examined in previous publications include combined IFNγ and TNFα (Bruewer et al., 2003; Fish et al., 1999; Madara and Stafford, 1989; Sanders et al., 1995; Youakim and Ahdieh, 1999), IL-13 (Ceponis et al., 2000;

Sanders et al., 1995; Zund et al., 1996) and IL-17 (Kinugasa et al., 2000). However, with the exception of the last study, none of these examined the expression of claudin 2. Interestingly, in this study incubation with IL-17 appeared to be associated with an increased level of claudin 2 (Kinugasa et al., 2000), suggesting that cytokines may be playing a role in the increased expression of claudin 2 in inflamed sites in vivo. Paradoxically, however, IL-17 was also associated in this study with an accelerated development of TER rather than the increased ionic permeability that might be expected with increased claudin 2 expression, and which is observed in IBD (see sections 1.3.1 and 1.3.2)

In summary, these experiments did not provide evidence to support the hypotheses that claudin 2 expression is either a feature of proliferating intestinal epithelial cells or upregulated in the early stages of TJ reassembly after calcium ion withdrawal and replenishment.

# CHAPTER 6

# THE EFFECTS OF CYTOKINES ON T84 BARRIER FUNCTION AND CLAUDIN EXPRESSION

# 6 THE EFFECTS OF CYTOKINES ON T84 BARRIER FUNCTION AND CLAUDIN EXPRESSION

## 6.1 INTRODUCTION AND AIMS

Previous chapters showed that inflammation correlates with altered expression of claudins 2, 3 and 4 and that T84 cells mimic the expression characteristics of normal bowel when allowed to develop for 8-15 days on semi-permeable supports.

The aim of this chapter was to examine the hypothesis that inflammatory cytokines thought to be important in the pathogenesis of IBD can reduce intestinal epithelial barrier function and alter the expression of the claudins. The cytokines selected for analysis were IL-17, IL-13 and the combination of IFNγ and TNFα. These were chosen because of the evidence supporting a role for them in IBD (see 1.1.1.5.4). IL-17 was chosen not only because of emerging evidence of a possible role in IBD (Fujino et al., 2003; Nielsen et al., 2003), but also because a single previous study had suggested paradoxically that it could enhance barrier function whilst stimulating an increase in claudin 2 expression in the TJ (Kinugasa et al., 2000). IFNγ and TNFα were used in combination because T84 cells do not respond to low doses of TNFα except in the presence of IFNγ, which induces the expression of membrane receptors for TNFα (Fish et al., 1999).

Therefore, the aims of this chapter were to examine the effects of IL-17, IL-13 and combined IFNγ and TNFα on:

- the expression of claudins 2, 3 and 4, by immunofluorescence staining and western blotting;
- transepithelial electrical resistance (TER);
- permeability to 4kDa FITC-dextran;
- LDH release.

## 6.2 RESULTS

T84 cells were cultured for 15 days on 0.9cm$^2$ collagen S-coated BIOCOAT Control Cell Culture Inserts. At this point either cytokines or PBS-0.1% BSA vehicle were added to the culture medium of at least six inserts, in both the apical and basolateral compartments. Cytokines and medium were replaced daily. The concentrations of cytokines used were determined from previously published evidence of their effects on T84 cells and are shown in table 6.1. In relation to IL-17, Kinugasa et al (2000) showed a concentration of 100ng/ml to affect both TER and the expression of claudins 1 and 2. Fish et al (1999) had shown that, whilst TNFα at a concentration of 1ng/ml had no effect on TER, this concentration synergised with IFNγ at 100ng/ml to profoundly diminish TER. Zund et al (1996) had previously shown that IL-13 at 2ng/ml could also markedly reduce TER. With the exception of the study by Kinugasa et al, none of these studies had examined the effects of these cytokines on the claudins.

The TER of each filter insert was measured twice daily. After three days monolayers were either processed for immunofluorescence detection of claudins 2-4, lysed to extract protein for SDS-PAGE and western blotting for claudins 2-4, or analysed for their permeability to FITC-dextran. The relative toxicity of a cytokine was determined by comparing the LDH activity within aliquots of culture medium taken from both cytokine- and vehicle-treated monolayers, as explained in 2.3.6. The mean total LDH activity within T84 monolayers was determined by lysing three monolayers by freezing and thawing, measuring the LDH activity of the lysates and calculating their average. All experiments were performed twice.

| Cytokine | Concentration (ng/ml) |
|---|---|
| IL-17 | 100 |
| IL-13 | 2 |
| IFNγ | 100 |
| TNFα | 1 |

*Table 6.1. Concentrations of cytokines to which T84 monolayers were exposed.*

## 6.2.1 IL-17

### *6.2.1.1 TER*

The change in TER observed during three days of incubation with either IL-17 or PBS-0.1%BSA vehicle (control) is illustrated by figure 6.1. IL-17 had no effect on TER when compared to control monolayers. After 3 days TER had increased by a mean of 9.0% in the control monolayers and 8.4% in the IL-17-exposed monolayers; this difference was not statistically significant (p=0.98).

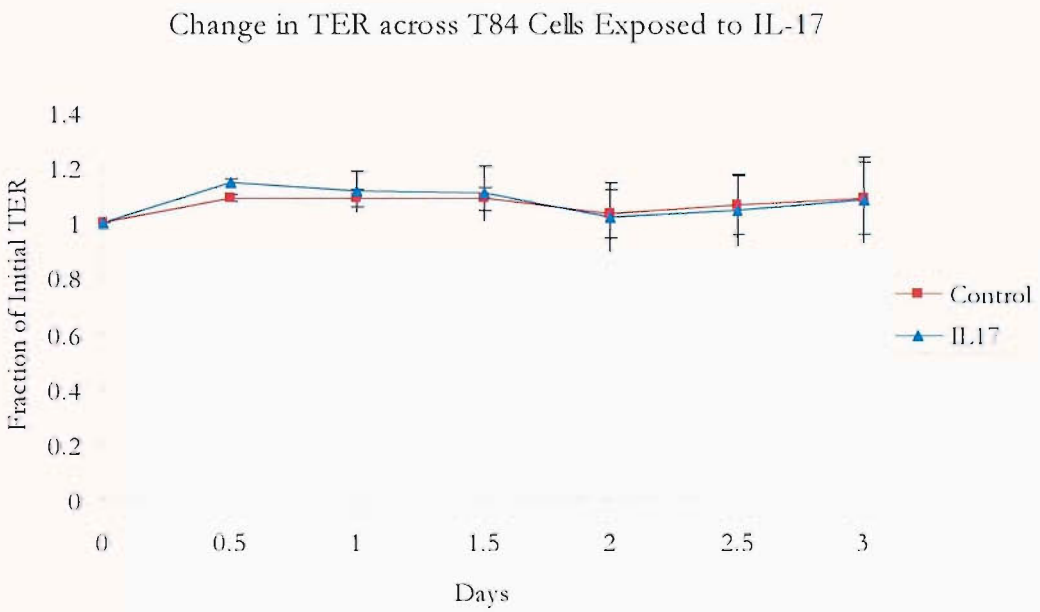


*Figure 6.1. Mean change in the TER of mature (15 day) T84 monolayers during 3 days of incubation with either IL-17 or vehicle (Control). N=6 for each group; error bars represent 1 standard deviation. A representative example from two identical experiments is depicted. p=0.98 for the comparison of Control and IL-17 groups at 3 days.*

### 6.2.1.2 *Permeability to FITC-Dextran*

The concentration of FITC-dextran in the basal culture medium was measured after 3 hours of incubation with 2mg/ml of FITC-dextran applied apically. The results are shown in figure 6.2. IL-17 did not produce a significant change in permeability to FITC-dextran (p=1).

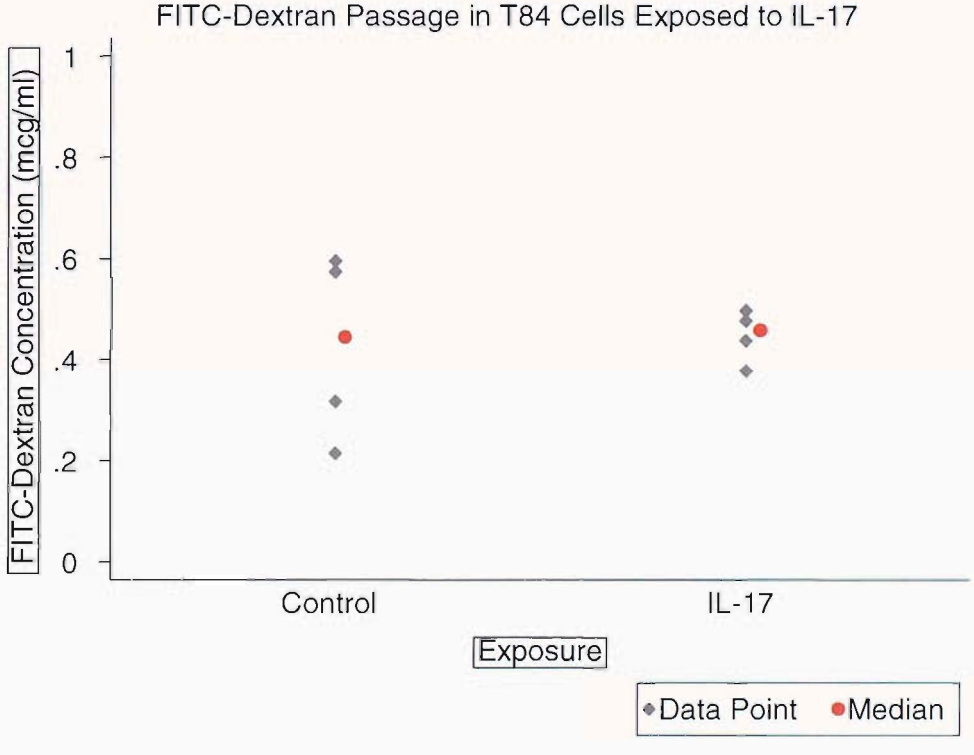


*Figure 6.2. Concentration of FITC-dextran measured in the basal medium after 3 hours incubation of T84 monolayers with apically applied FITC-dextran (2mg/ml). Mature (15 day) monolayers had previously been exposed for 3 days to either PBS-0.1%BSA (Control) or IL-17. N=4 for each group. A representative example from two identical experiments is depicted. p=1 for the comparison of Control and IL-17 groups.*

### 6.2.1.3 *Claudin Expression*

After 3 days of exposure to either IL-17 or medium plus vehicle the expression of claudins 2-4 was assessed by both immunofluorescence and western blotting. Figure 6.3 illustrates the findings of the immunofluorescence detection. IL-17 exposure was associated with a modest increase in the number of cells expressing claudin 2. This expression was observed in the chicken-wire pattern associated with TJ localisation. Cross-sectional views (so-called z-views; insets in figure 6.3) revealed apical, punctate claudin 2 expression, confirming that this expression was predominantly tight junctional. No change was discerned in the pattern of expression of claudins 3 and 4. In the case of claudin 3, detection was widespread and predominantly tight junctional after incubation with either vehicle or IL-17. This was also the case for claudin 4, except that there was also some detection lower down the lateral membranes after incubation with either vehicle or IL-17.

Three days of incubation with IL-17 was not associated with any major change in the total expression of claudins 2-4, as determined by western blotting (figure 6.4) and analysis of band densities normalised to those obtained for cytokeratin 19 (table 6.2).

| | Band densities normalised to cytokeratin 19 | |
|---|---|---|
| | Control | IL-17 |
| Claudin 2 | 0.77 | 0.50 |
| Claudin 3 | 0.32 | 0.27 |
| Claudin 4 | 0.17 | 0.16 |

*Table 6.2. Band densities normalised to cytokeratin 19 for claudins 2-4, obtained by analysis of the blots depicted in figure 6.4.*

### 6.2.1.4 *LDH Release*

The percentage of total LDH released per day is shown in figure 6.5. A very small percentage of total LDH was released from both the control and the IL-17-treated monolayers, suggesting minimal toxicity. No significant difference in this measure was observed between the IL-17-treated and control monolayers ($p=0.63$).

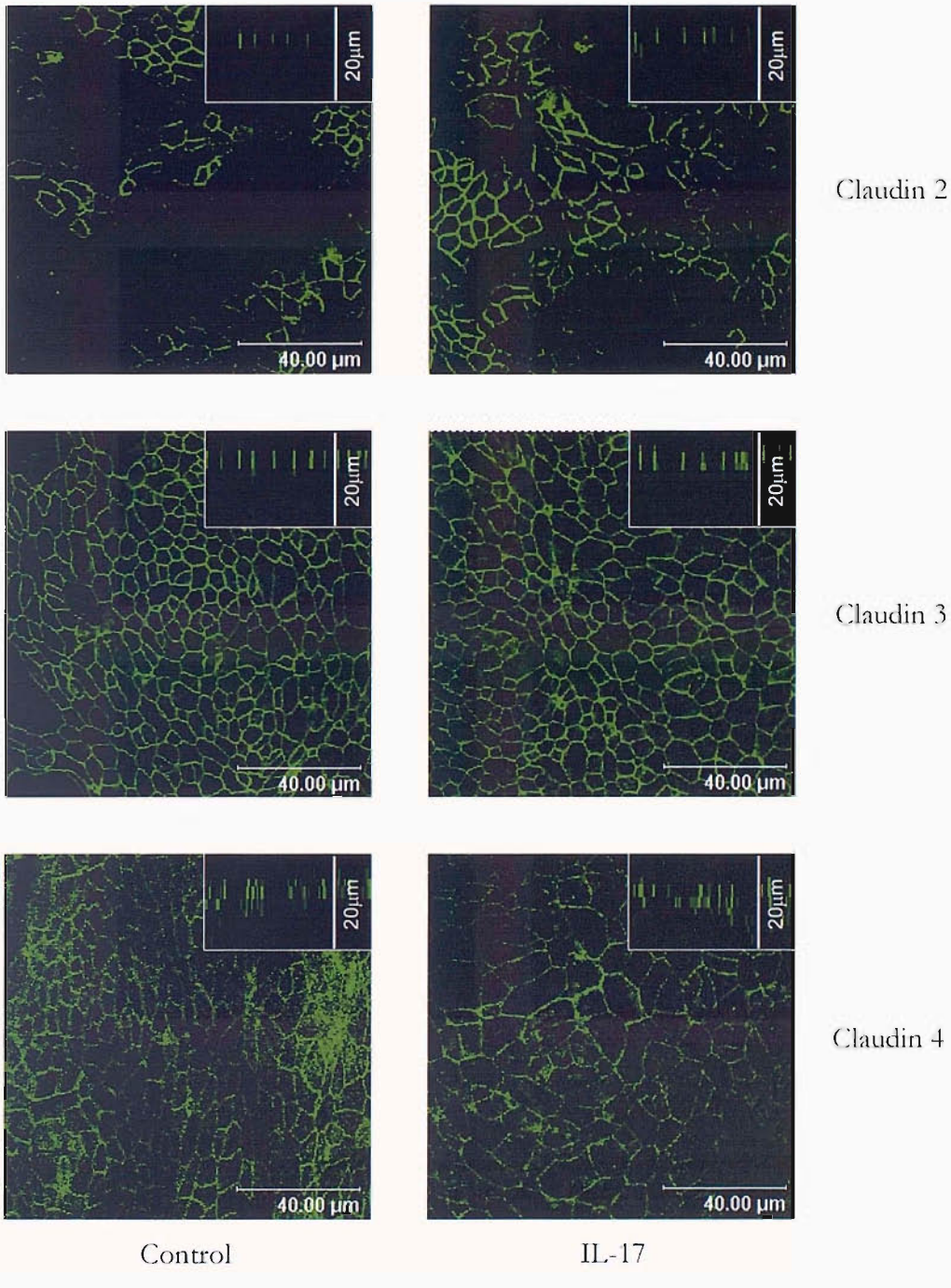


*Figure 6.3 Immunofluorescence detection of claudins 2-4 in T84 cell monolayers incubated for 3 days with either PBS-0.1%BSA vehicle (Control) or IL-17. Main views are en face (x-y) views; insets are cross-sectional (z) views. Five fields were examined in each of two identical experiments, and a representative field is depicted.*

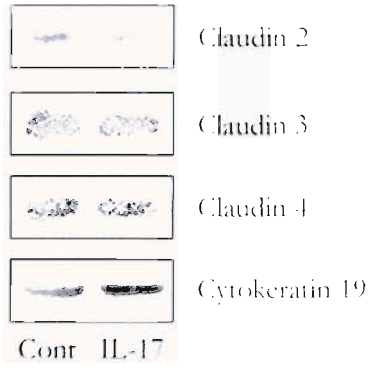


*Figure 6.4. Western blots of whole cell lysates obtained from vehicle (Cont) or IL-17-treated T84 cell monolayers and probed successively for claudins 2-4 and cytokeratin 19. See table 6.2 for the band densities measured for each claudin (normalised to those obtained for cytokeratin 19). No major change in the total expression of claudins 2-4 was observed. Representative blots from one of two identical experiments are depicted.*

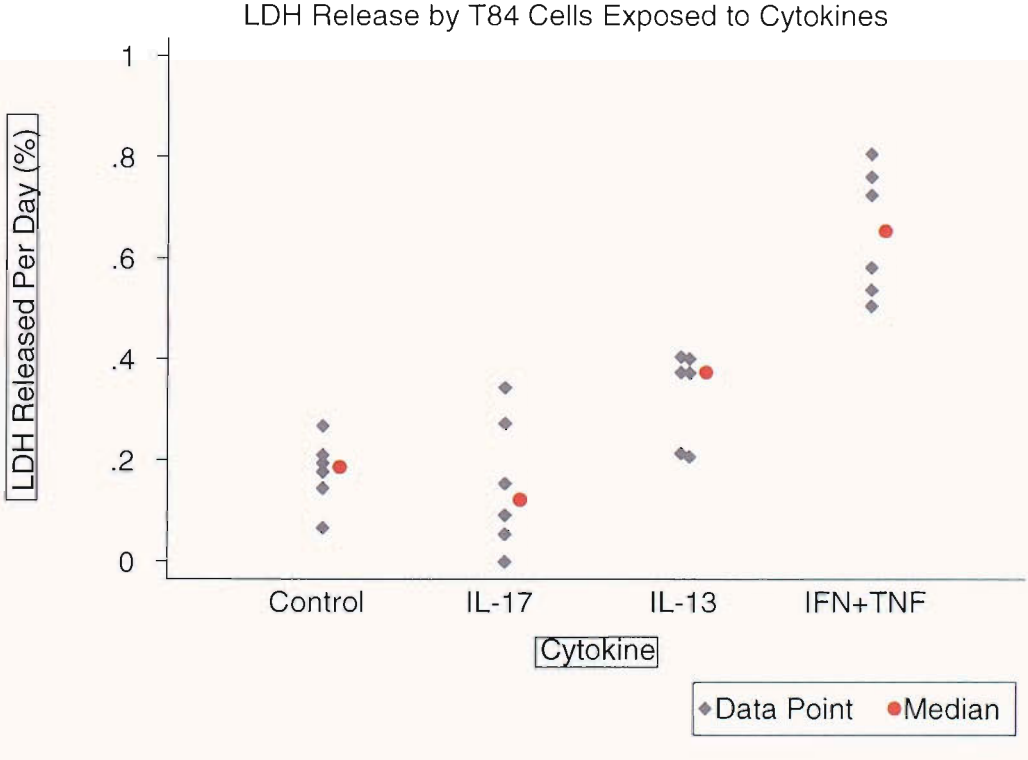


*Figure 6.5. Percentage of total LDH released per day by T84 cell monolayers exposed for 3 days to no cytokine (Control), IL-17, IL-13 or combined IFNγ and TNFα (IFN+TNF). N=6 for each group. IL-13 and IFN+TNF induced significantly more LDH release than Control (p=0.016 and 0.004 respectively), whereas IL-17 did not (p=0.63). In all cases only a very small percentage of total LDH was released per day.*

6.2.2 IL-13

### *6.2.2.1 TER*

Figure 6.6 illustrates the change in TER observed across T84 cell monolayers exposed to either IL-13 or vehicle (control) for 3 days.

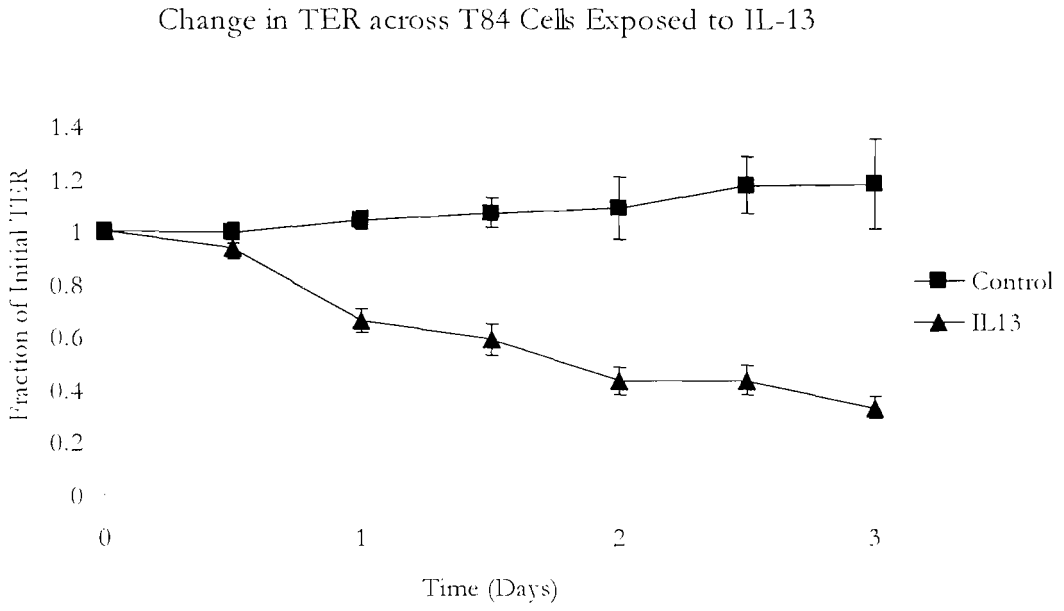


*Figure 6.6. Mean change in the TER of mature (15 day) T84 monolayers during 3 days of incubation with either IL-13 or vehicle (Control). N=6 for each group; error bars represent 1 standard deviation. A representative example from two identical experiments is depicted. p=0.002 for the comparison of Control and IL-13 groups at 3 days.*

IL-13 clearly provoked a rapid and continuing decline in TER. After 3 days the average change in TER across the control monolayers was an increase of 18%, whereas that across the IL-13-treated monolayers was a fall of 67%. This difference was highly significant statistically (p=0.002).

### *6.2.2.2 Permeability to FITC-Dextran*

The permeability of T84 cell monolayers to FITC-dextran after 3 days of exposure to either vehicle or IL-13 was compared and is illustrated in figure 6.7.

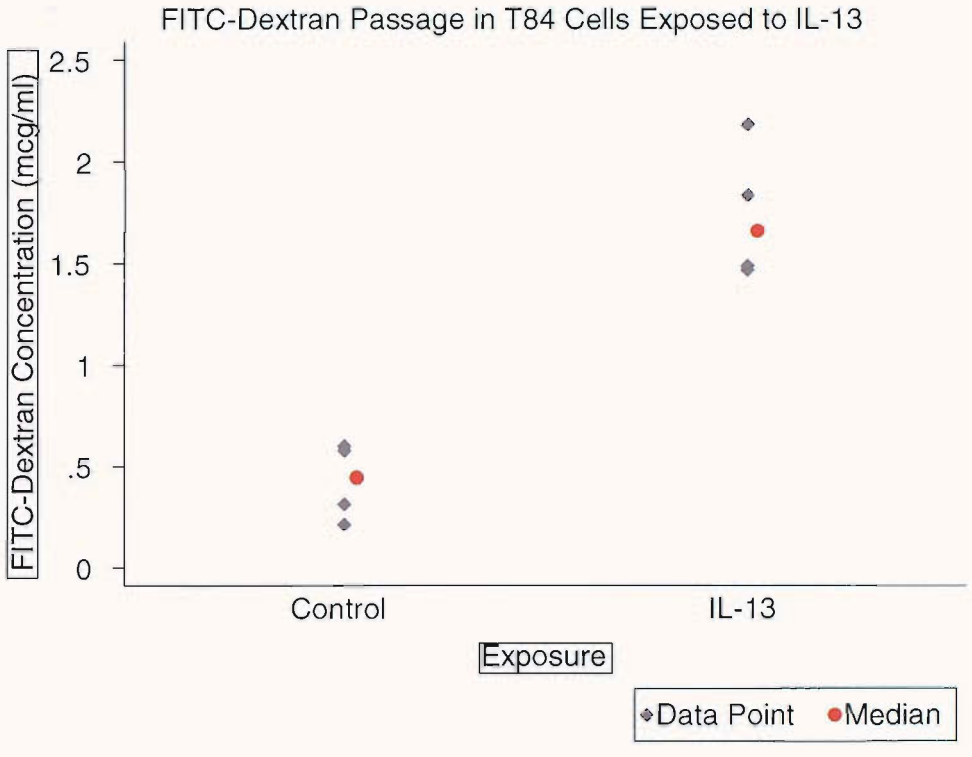


*Figure 6.7. Concentration of FITC-dextran measured in the basal medium after 3 hours incubation of T84 monolayers with apically applied FITC-dextran (2mg/ml). Mature (15 day) monolayers had previously been exposed for 3 days to either PBS-0.1%BSA (Control) or IL-13. N=4 for each group. A representative example from two identical experiments is depicted. $p<0.0001$ for the comparison of Control and IL-13 groups.*

There was a marked increase in permeability after incubation with IL-13, giving a 3.7-fold increase in the median concentration of FITC-dextran measured. This change was statistically significant ($p<0.0001$).

### *6.2.2.3 Claudin Expression*

Figure 6.8 illustrates the results of the immunofluorescence detection of claudins 2-4. Three days incubation with IL-13 produced a very large increase in the prevalence of claudin 2-positive cells when compared to control monolayers. The majority of this staining was observed in the TJs, as evidenced by the chicken-wire pattern in x-y views and the apical, punctate pattern in z-views. There were no changes in the immunofluorescence patterns for claudins 3 and 4 after exposure to IL-17. Staining of claudin 3 remained widespread and localised to the TJ. Claudin 4 was detected in both

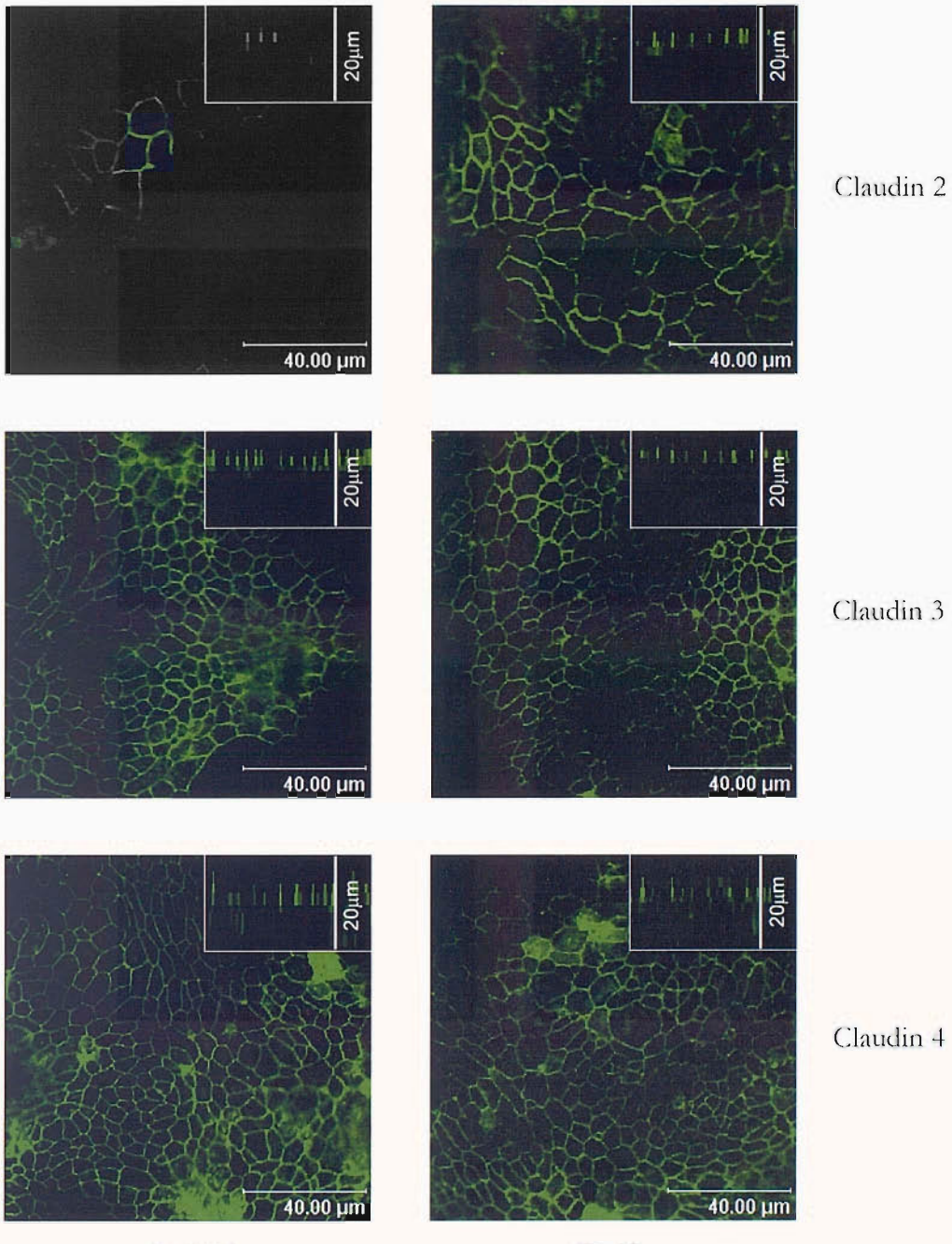


*Figure 6.8 Immunofluorescence detection of claudins 2-4 in T84 cell monolayers incubated for 3 days with either PBS-0.1%BSA vehicle (Control) or IL-13. Main views are en face (x-y) views; insets are cross-sectional (z) views. Five fields were examined in each of two identical experiments, and a representative field is depicted.*

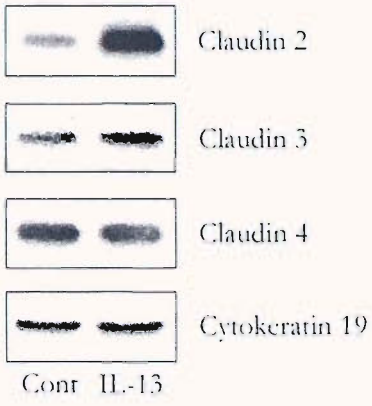


*Figure 6.9. Western blots of whole cell lysates obtained from control (Cont) or IL-13-treated T84 cell monolayers and probed successively for claudins 2-4 and cytokeratin 19. See table 6.3 for the band densities measured for each claudin (normalised to those obtained for cytokeratin 19). No major change in the total expression of claudins 3 and 4 was observed, but a large increase in claudin 2 was seen. Representative blots from one of two identical experiments are depicted.*

| | Band densities normalised to cytokeratin 19 | |
|---|---|---|
| | Control | IL-13 |
| Claudin 2 | 4.1 | 19.5 |
| Claudin 3 | 0.6 | 0.7 |
| Claudin 4 | 2.2 | 2.0 |

*Table 6.3. Band densities normalised to cytokeratin 19 for claudins 2-4, obtained by analysis of the blots depicted in figure 6.9.*

TJ and lateral membrane locations, as described previously, so that in z-views some staining was seen lower down the cells than the puncta that represent TJ localisation.

After 3 days of incubation with vehicle or IL-13, western blots of whole cell lysates underwent successive immunodetection with antibodies to claudins 2-4 and cytokeratin 19. The results are illustrated in figure 6.9. Analysis of band densities normalised to those obtained for cytokeratin 19 are depicted in table 6.3. Whilst no changes in the expression levels of claudins 3 and 4 were detected with IL-13 exposure, a much denser band was observed for claudin 2.

#### *6.2.2.4 LDH Release*

The percentage of total LDH released per day is shown in figure 6.5. The amount of LDH released during incubation with IL-13 was significantly larger than that released from control monolayers ($p=0.016$). However, this amount was still only a very small percentage (median 0.37%) of the total LDH released from a lysed monolayer, consistent with minimal toxicity.

### 6.2.3 IFN-GAMMA AND TNF-ALPHA

#### *6.2.3.1 TER*

The change in TER observed during three days of incubation with either combined IFNγ and TNFα or PBS-0.1%BSA vehicle (control) is illustrated by figure 6.10.

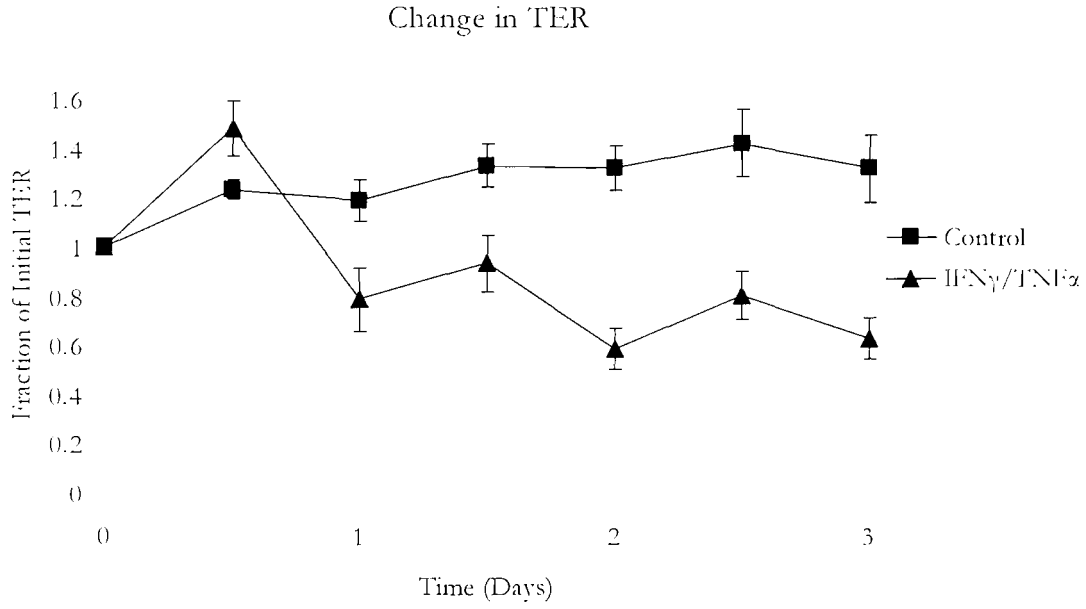


*Figure 6.10. Mean change in the TER of T84 monolayers during 3 days of incubation with either combined IFNγ and TNFα or vehicle (Control). N=6 for each group; error bars represent 1 standard deviation. A representative example from two identical experiments is depicted. $p<0.0001$ for the comparison of Control and IFNγ/TNFα groups at 3 days.*

The cytokines provoked a small initial rise in TER but by 1 day this had been rapidly superseded by a marked fall, with a continued decline seen over the subsequent 2 days. After 3 days had elapsed, the TERs across the control monolayers in the experiment depicted had increased by an average of 32%, whereas the TERs across the cytokine-treated monolayers had fallen by an average of 37%. This difference was highly statistically significant ($p<0.0001$).

### *6.2.3.2 Permeability to FITC-Dextran*

The permeability of T84 cell monolayers to FITC-dextran was compared after 3 days of exposure to either vehicle or combined IFNγ and TNFα (figure 6.11). There was a marked increase in permeability across the monolayers that had been incubated with the cytokines, giving a 4.2-fold increase in the median concentration of FITC-dextran measured. This change was statistically significant ($p=0.021$).

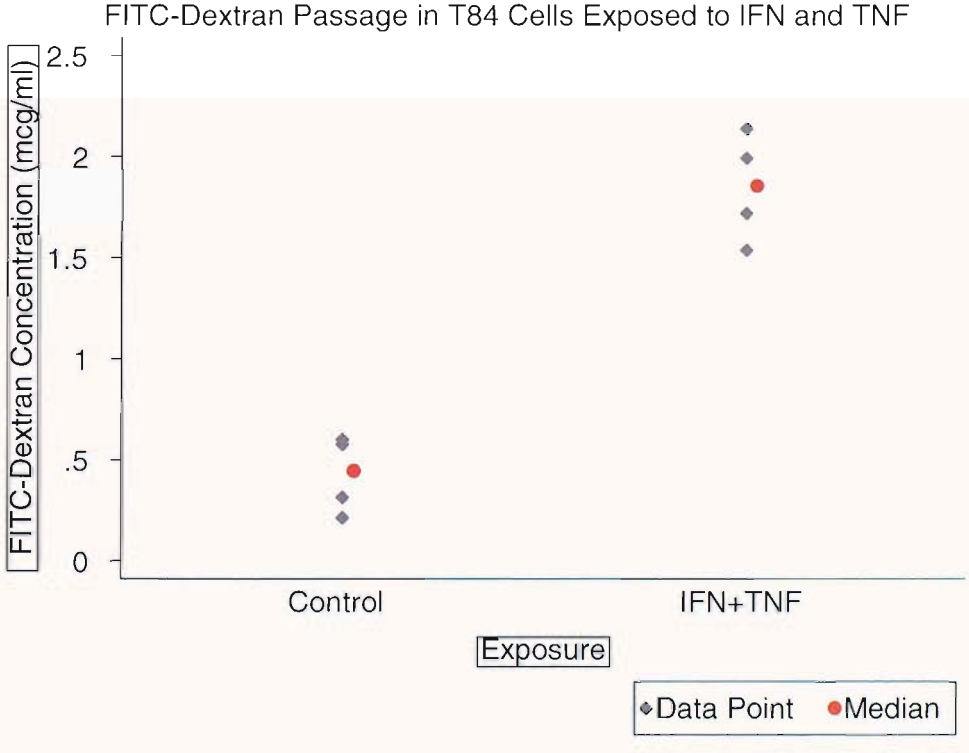


*Figure 6.11. Concentration of FITC-dextran measured in the basal medium after 3 hours incubation of T84 monolayers with apically applied FITC-dextran (2mg/ml). Mature (15 day) monolayers had previously been exposed for 3 days to either PBS-0.1%BSA (Control) or combined IFNγ and TNFα. N=4 for each group. A representative example from two identical experiments is depicted. p=0.021 for the comparison of Control and IFNγ/TNFα groups.*

### *6.2.3.3 Claudin Expression*

After 3 days of exposure to either IFNγ and TNFα or vehicle the expression of claudins 2-4 was assessed by both immunofluorescence and western blotting. Figure 6.12 illustrates the findings of the immunofluorescence detection. As before a few clusters of cells in the control monolayers expressed claudin 2. After cytokine treatment, however, even fewer such cells are detectable, and staining is very faint. It did not form the complete rings that make up the chicken-wire pattern suggestive of TJ assembly but instead was somewhat fragmented. The z-views again revealed that most of this staining was punctate and apical, which is consistent with a TJ location.

Claudin 3 was widely expressed in control monolayers, in predominantly a chicken-wire pattern on x-y views and in an apical, punctate distribution on z-views, suggesting, as previously, a TJ localisation (figure 6.12). Cytokine exposure led to a much more patchy distribution across the monolayers. Most of the remaining staining was tight junctional.

Claudin 4 was also widely expressed in control monolayers. As in previous experiments most of the fluorescence was detected in region of the TJ, with some staining seen lower down the lateral membranes. Incubation with IFNγ and TNFα led to a more patchy distribution of claudin 4 in the TJs of the monolayers and much stronger detection lower down the lateral membrane and intracellularly, leading to the imprecise and broad distribution of the staining seen in the z view (figure 6.12), and suggesting movement of antigen away from the TJ.

The expression of claudins 2-4 was examined by western blotting and an illustrative result is depicted in figure 6.13. Analysis of band densities normalised to those obtained for cytokeratin 19 are depicted in table 6.4. Incubation with IFNγ and TNFα was associated with a much less dense band when the blots were probed with antibody to claudin 2. The bands detected by antibodies to claudins 3 and 4 were of similar density whether the protein was obtained from cytokine-treated or control cells.

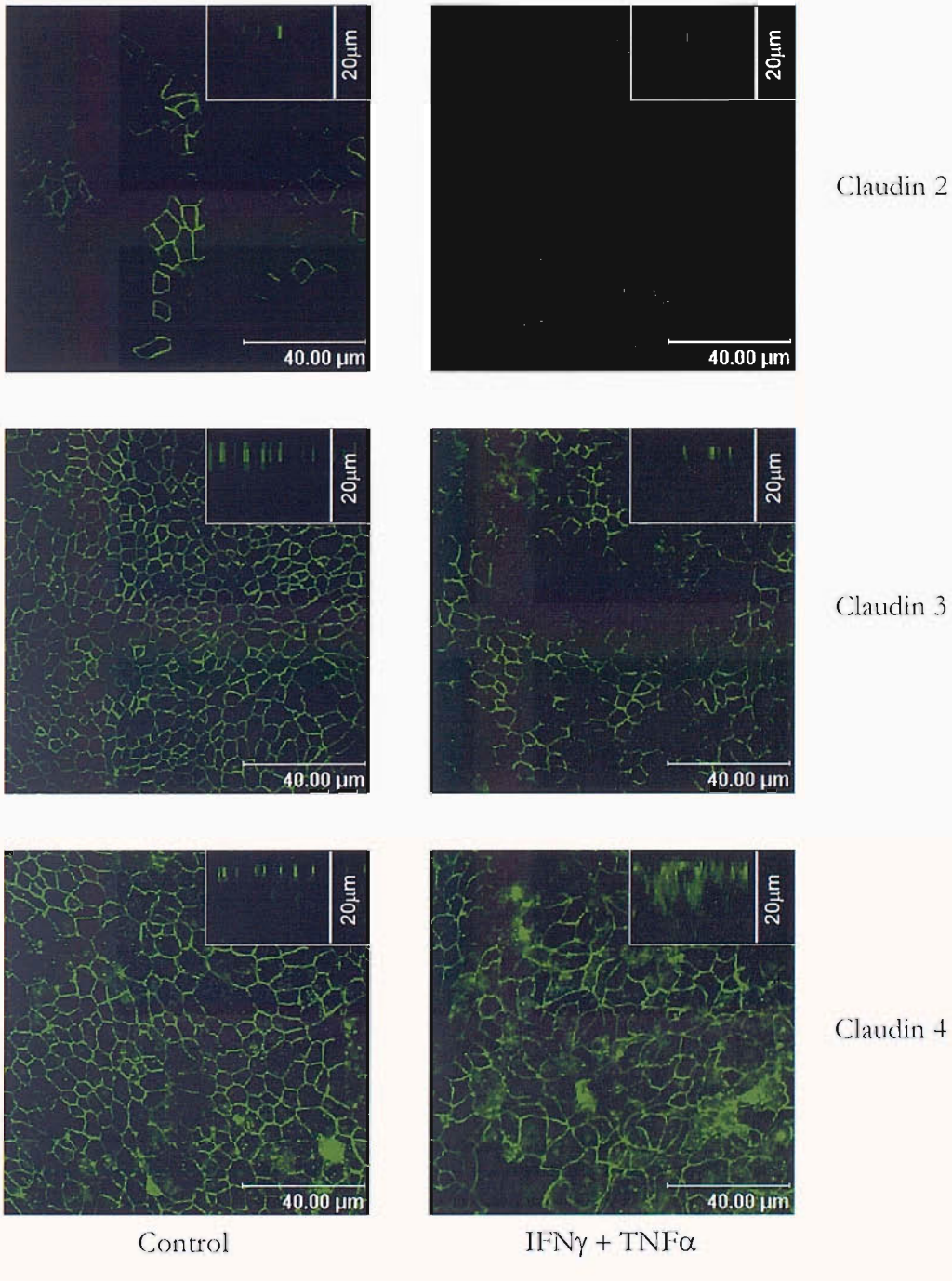


*Figure 6.12 Immunofluorescence detection of claudins 2-4 in T84 cell monolayers incubated for 3 days with either PBS-0.1%BSA vehicle (Control) or combined IFNγ and TNFα. Main views are en face (x-y) views; insets are cross-sectional (z) views. Five fields were examined in each of two identical experiments, and a representative field is depicted.*

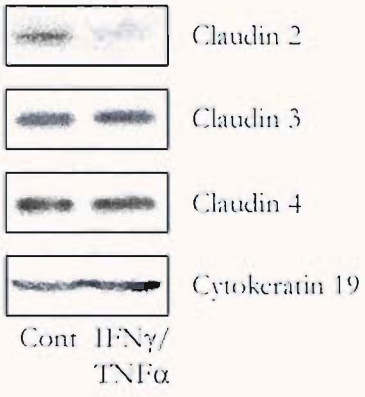


*Figure 6.13. Western blots of whole cell lysates obtained from control (Cont) or IFNγ and TNFα-treated T84 cell monolayers and probed successively for claudins 2-4 and cytokeratin 19. The latter confirms approximately equivalent loading of total protein in each lane. Representative blots from one of two identical experiments are depicted.*

| | Band densities normalised to cytokeratin 19 | |
|---|---|---|
| | Control | IFNγ and TNFα |
| Claudin 2 | 0.8 | 0.3 |
| Claudin 3 | 2.8 | 2.5 |
| Claudin 4 | 3.0 | 2.6 |

*Table 6.4. Band densities normalised to cytokeratin 19 for claudins 2-4, obtained by analysis of the blots depicted in figure 6.13.*

### *6.2.3.4 LDH Release*

The percentage of total LDH released per day is shown in figure 6.5. The amount of LDH released during incubation with IFNγ and TNFα was significantly larger than that released from control monolayers ($p=0.004$). However, this amount was still only a very small percentage (median 0.65%) of the total LDH, consistent with minimal toxicity.

## 6.3 DISCUSSION

The results described here strongly support the proposal that inflammatory cytokines induce profound alterations in the barrier function of the intestinal epithelium. They also provide evidence that cytokines can alter the profile of claudin expression in a model epithelium.

In these experiments IL-17 did not produce any effect on the T84 monolayers, in relation to either the electrical resistance or the permeability to the uncharged 4kDa dextran. It caused a modest increase in the prevalence of claudin 2-positive cells without any significant change in its total level of expression. This differed considerably from the only previously published evidence of the effects of the same concentration of IL-17 on T84 cells (Kinugasa et al., 2000). In this paper IL-17 induced an increase in TER and a fall in dextran permeability whilst at the same time upregulating the expression of claudin 2. The reasons for these discrepancies are difficult to discern. However, in the paper by Kinugasa T84 monolayers with only modest TERs (approximately 400ohm.cm$^2$) were utilised, whereas in the present study the monolayers had an average initial TER of approximately 1000ohm.cm$^2$. It is possible, therefore, that IL-17 can induce different changes in maturing and mature epithelial barriers. Even so, the lack of detectable effect of IL-17 on barrier function (compared to the other cytokines examined) suggests that it is less likely to be responsible for producing the effects seen in IBD. Ideally, experiments to determine a concentration-response relationship would have enabled the selection of an appropriate concentration of cytokine. Thus, the possibility remains that higher concentrations of IL-17 than that used here might have affected barrier function or claudin expression.

The combination of IFNγ and TNFα, on the other hand, did induce profound changes in barrier function. The resistance of T84 monolayers to both ions and the uncharged dextran was markedly impaired. Although these cytokines caused some toxicity to the cells, the amount was minimal (less than 1% per day of the average total LDH released from a lysed monolayer) and is therefore unlikely to be the reason for the major effects on resistance. The findings in relation to TER and dextran permeability confirm those published previously in T84 cells (Fish et al., 1999; Madara and Stafford, 1989; Sanders et al., 1995; Youakim and Ahdieh, 1999; Bruewer et al., 2003). One study also revealed that the barrier impairment induced in T84 cells by IFNγ is associated with a marked reduction in ZO-1 expression and the relocalisation of ZO-2 and

occludin away from the TJ, suggesting that the TJ was being disassembled (Youakim and Ahdieh, 1999). Removing the scaffold proteins ZO-1 and ZO-2 from the TJ might be expected to affect the assembly of other proteins at the TJ, or vice versa. Thus the reduction in the TJ expression of all three claudins examined here appears to correlate with the reduced expression of ZO-1 reported previously. The function of claudin 3 is unknown, but TJ expression of claudin 4 confers resistance to the paracellular passage of sodium ions (Van Itallie et al., 2001). In the present study total claudin 4 protein appeared unaffected. Importantly, however, its localisation was profoundly altered, with redistribution of claudin 4 away from the TJ and concurrent impairment of electrical resistance. Thus, the impaired barrier function induced by IFNγ and TNFα may be a correlate of global TJ disassembly. No other studies have examined the effects of IFNγ and TNFα on the expression of claudins 2 and 3 in T84 cells. One study reported a more striking internalisation of claudin 4 than seen in the present study, again without a significant change in protein detection by western blotting (Bruewer et al., 2003). This may be due to the ten-fold higher concentration of TNFα used by Bruewer et al.

IL-13 also markedly impaired the barrier function of T84 monolayers, inducing similar changes to both TER and dextran permeability as those caused by IFNγ and TNFα. Again, the toxicity of this cytokine to the cells was minimal. The effects of IL-13 on TER and dextran permeability in T84 cells are similar to those published previously (Ceponis et al., 2000; Sanders et al., 1995; Zund et al., 1996). However, the effects of IL-13 on claudin expression were not described. Unlike the effects of IFNγ and TNFα, IL-13 did not induce reductions in the amounts of all three claudins at the TJ. The expression of claudins 3 and 4 at the TJ, as detected by immunofluorescence, was unchanged. However, IL-13 induced large increases both in the total expression of claudin 2 (detected by western blotting) and in the prevalence of TJ claudin 2 expression across the monolayer (detected by immunofluorescence). The correlation between the increase in claudin 2 expression and the fall in TER suggests that they may be causally related. This is particularly so because, firstly, evidence strongly supports the idea that introducing claudin 2 into pre-existing TJs induces a marked fall in TER (as discussed in 1.2.2.1.1), and, secondly, the unchanged expression of claudins 3 and 4 in response to IL-13 strongly suggests that many components of the TJ continued to be assembled there. However, the only published examination of the effect of claudin 2 on permeability to uncharged molecules showed that its transfection into MDCK cells had no effect on the permeability to 4kDa FITC-dextran (Amasheh et al., 2002). Thus,

although it can be postulated that IL-13 impairs TER by introducing claudin 2 to TJs, a separate mechanism may have to be invoked to explain its effects on FITC-dextran permeability. A single study has suggested that occludin may be involved in the resistance of the paracellular pathway to uncharged molecules, as mutations in the molecule were shown to be capable of increasing the passage of uncharged molecules without influencing the TER (Balda et al., 2000). However, it is unclear what effects the mutated forms of occludin may have been exerting on other components of the TJ.

What are the main limitations of the approach adopted here? Firstly, an important issue is the use of serum-containing medium when evaluating the effects of cytokine stimulation. Serum was not withdrawn from the medium for several reasons. As discussed in chapter 4 (see 4.1), T84 cells form a monolayer of differentiated enterocytes when cultured in serum-containing medium on collagen-coated supports. However, when cultured in serum-free medium for a few (3-5) days there is a risk of the cells piling up and forming gland-like structures, morphologically resembling the original tumour from which the line was derived. One aim of these experiments was to attempt to recreate to a certain extent the pathophysiological situation that may exist in the intestinal mucosa in IBD. In IBD evidence points to elevated levels of key cytokines in the inflamed mucosa (see 1.1.1.5.4), but these elevations *in vivo* occur in the presence of serum. Furthermore, all the published studies that examine the effects of cytokines on T84 barrier function have included serum in the culture medium (see 1.3.3). However, there are several problems with the inclusion of serum. The exact constituents of serum are not entirely clear, but it certainly contains numerous, but poorly-defined, growth factors, cytokines and antibodies. Its inclusion means therefore that these experiments do not examine the effects of cytokines per se, but rather the effects of cytokines on the background of serum-stimulation. Certain factors in the serum may well synergise with an experimentally added cytokine to produce an effect that may not be evident when the cytokine is added alone. This could occur by many mechanisms, such as upregulation of cytokine receptors, effects on signalling pathways, modification of transcription or mRNA stability, or effects on protein translation. Growth factors in serum may promote cell cycling, and cytokines may in fact be effective only when cells are in cycle. Alternatively, other serum factors may counteract the effects produced by cytokine stimulation in the absence of serum and so obscure an important effect. Secondly, although certain cytokines were selected for application to the cells, there are many other cytokines and molecular factors present in the mucosal

inflammatory milieu that may affect the behaviour of epithelial cells and their responses to cytokines. The situation in the intestinal mucosa is likely to be much more complicated. It is possible, for example, that several cytokines act simultaneously and synergistically to exert effects, as elevated expression of several cytokines has been described in IBD (see 1.1.1.5.4). In addition, regulatory mechanisms may operate to control these effects. Thirdly, the concentrations of the cytokines used were chosen because they were known from studies elsewhere to affect the TJs of cultured cells. The actual concentrations to which epithelial cells are exposed in the diseased mucosa are not known exactly, even if total mucosal levels have been shown to be elevated. Fourthly, other agents besides cytokines may affect the behaviour of epithelial cells in vivo. For example, it is not known what effects intra-epithelial lymphocytes may exert on their neighbouring epithelial cells during disease, and it has also been proposed that neutrophils that transmigrate between crypt epithelial cells may affect TJ structure and function in those specific cells (Kucharzik et al., 2001). Fifthly, although the cellular location and total expression of the claudins were examined here, more subtle alterations in the functions of these molecules were not examined. For example, it is not known whether claudins are phosphorylated, but it is conceivable that cytokines can affect claudin function via changes in phosphorylation, whilst leaving overall expression unaltered. Sixthly, although the permeability to dextran molecules with a molecular weight of 4kDa was assessed, the permeability to larger molecules was not examined, and it remains possible that there are differential effects of cytokines on the permeability to different-sized uncharged molecules such as peptides and proteins. Seventhly, although LDH assays suggested the cytokines were only minimally cytotoxic, these assays only measure the release of cytoplasmic contents after cell death and lysis. LDH assays do not examine the functional health of cells and do not measure the extent of apoptosis. Alternative assays, such as trypan blue exclusion, can be employed to assess cell health, and there are several assays that can measure apoptosis, such as TUNEL staining or caspase expression. Incorporation of these would give a more complete assessment of the health and viability of the cells. Finally, although TER was examined at several time points during cytokine stimulation, claudin expression and dextran permeability were examined only after three days. Therefore, it is possible that changes in these parameters occurring at earlier time points have been overlooked, and the time course of these alterations has not been determined.

What is the relevance of these experimental findings to the results found in IBD tissues? The reduced expression of the claudins induced by IFNγ and TNFα, together with previously described reductions in ZO-1 and occludin expression in T84 cells exposed to these cytokines, resembles the global reduction in the expression of TJ proteins observed in the surface epithelium in IBD (see chapter 3). It is possible therefore that surface epithelial cells respond preferentially to IFNγ and TNFα, perhaps because they have more receptors for TNFα or because they are in contact with these cytokines or the cells that produce them for longer periods or at higher levels. The extent of the changes induced in cell culture systems may exceed those observed in IBD because of some of the limitations of these models listed above. However, the direction of the changes was similar in both situations, which suggests that IFNγ and TNFα may be of importance to the changes observed in vivo. Reduced TJ assembly in the surface epithelium was proposed in chapter 3 to contribute to the increased intestinal permeability observed in IBD. Indeed, a recent study has shown that treatment of Crohn's disease with a monoclonal antibody to TNFα restores the increased permeability of these patients to the levels found in healthy volunteers, suggesting that TNFα plays a role in the impairment of barrier function (Suenaert et al., 2002). However, this study does not prove that TNFα is acting directly on epithelial cells.

There is a striking resemblance between the IL-13-induced introduction of claudin 2 to the TJs of T84 cells and the increased expression of claudin 2 observed in the crypt epithelium of IBD. Furthermore, the TJ expression of claudins 3 and 4 was largely unaltered in both IL-13-exposed T84 cells and IBD crypt epithelium. Thus, it is possible that increased IL-13 expression may be the stimulant for increased claudin 2 expression in the colonic crypt cells in IBD. It is possible that crypt cells preferentially express receptors for IL-13, but there is currently no evidence to support this. It was proposed in chapter 4 that increased claudin 2 expression may be a response to injury, and therefore the logical extension of this is that IL-13 expression itself is upregulated in response to injury. The actual evidence for the role of IL-13 in intestinal immune responses is complex. Whilst it is thought to be crucial to the clearance of helminth infections as part of a T helper type 2 (Th2) immune response (McKenzie et al., 1998), IL-13 has been shown in vitro to both control and synergise with TNFα-induced epithelial responses (Artis et al., 1999; Kucharzik et al., 1998), depending on the particular response examined. Furthermore, the early phase of developing inflammation in Crohn's disease, soon after the resection of an adjacent diseased segment, is

associated with elevated IL-13 expression but the subsequent chronic inflammation is associated with increased T helper type 1 (Th1) cytokine expression (Desreumaux et al., 1997). Conversely, in the IL-10-deficient mouse model of colitis, there is a progressive increase in IL-13 expression as the inflammation becomes chronic (Spencer et al., 2002). As discussed in chapter 1, increased IL-13 expression has been demonstrated both in human UC and in the murine oxazolone colitis model of UC (Fuss et al., 2004; Heller et al., 2002). Brought together, this evidence suggests that elevated IL-13 expression is probably a feature of IBD (particularly UC), but that its expression varies with different phases of inflammation. Whether its expression fluctuates with periods of repair or in response to injury is not known, but such a situation would be consistent with the finding (described in chapter 3) that claudin 2 expression is increased during periods of quiescent or resolving UC.

In summary, these studies of the effects of inflammatory cytokines on T84 cells lead to a model of claudin responses to IL-13 and IFNγ/TNFα that could explain the patterns of claudin expression in IBD; namely, an increase in claudin 2 and unchanged claudin 3 and 4 expression in crypt cells, with reduced TJ claudin 3 and 4 and increased basolateral claudin 4 in surface cells. These changes would be expected to lead to a more permeable bowel epithelium.

# CHAPTER 7

# THE REGULATION OF INTERLEUKIN-13-INDUCED CLAUDIN 2 EXPRESSION

# THE REGULATION OF IL-13-INDUCED CLAUDIN 2 EXPRESSION

## 7.1 INTRODUCTION AND AIMS

In the previous chapter it was demonstrated that IL-13 can induce an increase in the expression of claudin 2 in mature T84 cell monolayers. The mechanisms that underlie this change are, however, unknown.

IL-13 binds to a receptor on cell membranes that also binds IL-4 and is known as the type II IL-4 receptor (Aman et al., 1996; Caput et al., 1996; Hilton et al., 1996; Miloux et al., 1997). Functional receptors comprise IL-4Rα and IL-13Rα1 subunits (Miloux et al., 1997), which dimerise upon receptor engagement, leading to the activation of at least two major signalling pathways (Kelly-Welch et al., 2003). These are known as the STAT6 and PI3K pathways (Hershey, 2003), named after the first kinases to be activated in each case: signal transducer and activator of transcription 6 and phosphatidylinositol 3-kinase respectively (see figure 7.1).

In the STAT6 pathway, receptor engagement and dimerisation leads to the enhanced activation of the Janus kinases (JAKs) (Keegan et al., 1995; Welham et al., 1995; Murata et al., 1996; Roy and Cathcart, 1998). These are tyrosine kinases that constitutively associate with the receptor subunits and their activation leads to the phosphorylation of tyrosine residues on the IL-4Rα subunit (Welham et al., 1995; Murata et al., 1996; Roy et al., 2002). This leads to the recruitment, tyrosine phosphorylation and activation of STAT6 (Mikita et al., 1996; Murata et al., 1996; Roy et al., 2002). Activated STAT6 detaches from the receptor, dimerises, migrates to the nucleus, and binds to consensus sequences found within the promoters of several genes (Mikita et al., 1998; Hershey, 2003). These include genes involved in cell survival, $Th_2$ differentiation, chemokine production and mucus production (Kelly-Welch et al., 2003).

In the PI3K pathway, receptor dimerisation and phosphorylation leads to the recruitment and tyrosine phosphorylation of members of the insulin receptor substrate (IRS) family (Keegan et al., 1994; Sun et al., 1995), so-called because they can also bind to similar sequences in receptors for insulin and the insulin-like growth factor type I (Keegan et al., 1994; White et al., 1988). This enables them to bind to the regulatory p85

subunit of PI3K, which results in the activation of the catalytic p110 subunit of PI3K (Otsu et al., 1991; Backer et al., 1992).

Activation of PI3K induces the phosphorylation and activation of at least two other kinases, known as Akt (or protein kinase B; figure 7.1) and the p70 ribosomal protein S6 kinase ($p70^{S6K}$) (Burgering and Coffer, 1995; Franke et al., 1995; Jiang et al., 2000). In the case of Akt, this occurs by the PI3K-mediated generation of the lipids phosphatidylinositol-3,4,5-triphosphate and phosphatidylinositol-3,4-biphosphate, which recruit Akt to the inner bilipid membrane, where it is phosphorylated by phosphatidylinositol-3,4,5-triphosphate-dependent kinases (PDKs) (Alessi et al., 1997). The activation of Akt depends specifically on the phosphorylation of a serine residue at position 473 and a threonine residue at position 308 (Alessi et al., 1996). Once activated, Akt (now referred to as phospho- or pAkt) can initiate any of several downstream pathways (Downward, 1998). For example, phospho-Akt has been shown to promote cell survival through the phosphorylation and inactivation of the pro-apoptotic molecule Bad (Nunez and del Peso, 1998).

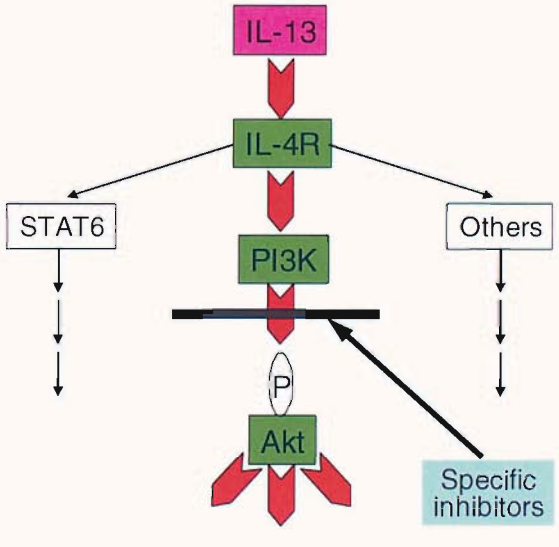


*Figure 7.1. Diagrammatic representation of the effects of IL-13 binding to its cellular receptor. Specific inhibitors such as wortmannin and Ly294002 can block the actions of activated PI3K.*

Previously published evidence has strongly implicated the PI3K pathway in the IL-13-induced impairment of TER (Ceponis et al., 2000). Specific inhibitors of STAT6 did

not inhibit this response, whereas inhibitors of the PI3K pathway significantly inhibited it. As evidence implicates the claudins in the maintenance of TER, it is therefore possible that the IL-13-induced upregulation of claudin 2 expression is mediated by the PI3K pathway.

To increase the expression of claudin 2, one or more of the following alterations in its regulation must occur: an increase in either the rate of transcription of its gene or the stability of claudin 2 mRNA, leading to elevated claudin 2 mRNA levels; an increase in the rate of translation of its mRNA; or stabilisation of any pre-existing protein, leading to an increased half-life. In IBD an increase in claudin 2 mRNA levels was demonstrated in chapter 3, and therefore an important question to be answered is whether IL-13 induces an increase in claudin 2 transcript levels and whether inhibition of PI3K affects claudin 2 mRNA levels. To help answer this question, a better understanding is needed of the time course of the increase in claudin 2 expression. A marked drop in TER was apparent after just 1 day of IL-13 exposure, and so this may be the duration necessary for the increase in claudin 2 to occur.

In summary then, the next questions to be addressed were as follows: Firstly, is PI3K involved in the increased claudin 2 expression and impaired barrier function induced by IL-13? Secondly, what is the time course of this increase in claudin 2? Thirdly, is the increase in the level of claudin 2 associated with an increase in the level of claudin 2 mRNA?

Therefore, the aims of this chapter were to:

- examine the effects of PI3K inhibitors on the increase in claudin 2 expression and impairment of barrier function of T84 cells incubated with IL-13;
- map the kinetics of the IL-13-induced increase in claudin 2 expression more closely;
- quantify claudin 2 transcripts in T84 cells in response to IL-13 or IL-13 plus a PI3K inhibitor.

## 7.2 RESULTS

### 7.2.1 THE EFFECTS OF PI3K INHIBITORS

Use was made of two small molecules, Ly294002 (2-(4-Morpholinyl)-8-phenyl-4H-1-benzopyran-4-one) and wortmannin, which are described as being highly specific inhibitors of PI3K activity (Davies et al., 2000). Because the concentrations at which they are most effective in T84 cells are not known, each was used at more than one concentration.

T84 cells were cultured for 15 days on 0.9cm$^2$ collagen S-coated BIOCOAT Control Cell Culture Inserts. At this point three inserts were allocated to each of seven experimental groups, as shown in table 7.1. Six groups of inserts were incubated with medium containing 2ng/ml of IL-13. The seventh (control) group was incubated with medium containing the equivalent amount of PBS-0.1% BSA vehicle. Inhibitors at various concentrations were added to five of the groups of inserts. As the inhibitors had been dissolved in dimethyl sulfoxide (DMSO) to make stock solutions, the amount of DMSO in the medium applied to all seven groups of inserts was adjusted to the same level (a 0.1% dilution by volume). The medium was applied to both apical and basal compartments and was replaced 12-hourly.

| Group | Concentrations in culture medium | | |
|---|---|---|---|
| | IL-13 (ng/ml) | Ly294002 (μM) | Wortmannin (μM) |
| Control | - | - | - |
| IL-13 | 2 | - | - |
| IL-13 + Ly294002 5μM | 2 | 5 | - |
| IL-13 + Ly294002 20μM | 2 | 20 | - |
| IL-13 + Ly294002 50μM | 2 | 50 | - |
| IL-13 + Wortmannin 0.1μM | 2 | - | 0.1 |
| IL-13 + Wortmannin 1μM | 2 | - | 1 |

*Table 7.1. Concentrations of IL-13, Ly294002 and wortmannin used in each experimental group.*

The TER of each filter insert was measured twice daily. After three days monolayers from each group were either processed for immunofluorescence detection of claudin 2, lysed to extract protein for detection of claudin 2 and cytokeratin 19 by SDS-PAGE and western blotting, or analysed for their permeability to FITC-dextran. The relative toxicity of each cytokine/inhibitor combination was determined by comparing the LDH activity within aliquots of culture medium. The experiment was performed three times.

As in previous experiments, the TERs of mature T84 cell monolayers fell substantially and significantly when incubated with IL-13 for 3 days ($p<0.0001$). Co-incubation with IL-13 and Ly294002 impaired this response in a dose-dependent fashion and partially, but significantly, restored the TER towards control levels (figure 7.2; $p=0.0008$ for comparison of IL-13 and IL-13 + Ly294002 50μM). Wortmannin had no significant effect on the IL-13-induced impairment of TER (figure 7.2).

Exposure to IL-13 alone for 3 days again induced a significant increase in the permeability of the monolayers to 4kDa FITC-dextran. Neither inhibitor had any significant effect on this response (figure 7.3).

As before, 3 days of IL-13 exposure induced an increase in claudin 2 expression, as detected by both immunofluorescence (figure 7.4), western blotting (figure 7.5) and analysis of band densities normalised to those obtained for cytokeratin 19 (table 7.2).. Co-incubation with IL-13 and Ly294002 impaired this increase in a dose-dependent fashion, but wortmannin had no effect at either concentration used (figures 7.4 and 7.5; table 7.2).

LDH release assays (figure 7.6) showed that both inhibitors were more cytotoxic than IL-13 alone. This increased in a dose-dependent fashion with both inhibitors and significantly exceeded that induced by IL-13 alone at concentrations of 20μM and 50μM of Ly294002 ($p=0.050$ for both) and 1μM of wortmannin ($p=0.050$). However, the proportion of cells affected remained low. Furthermore, 1μM of wortmannin and 50μM of Ly294002 were equally toxic, but claudin expression decreased and TER increased in Ly294002-treated cells, showing that these latter effects were not due to a toxic effect.

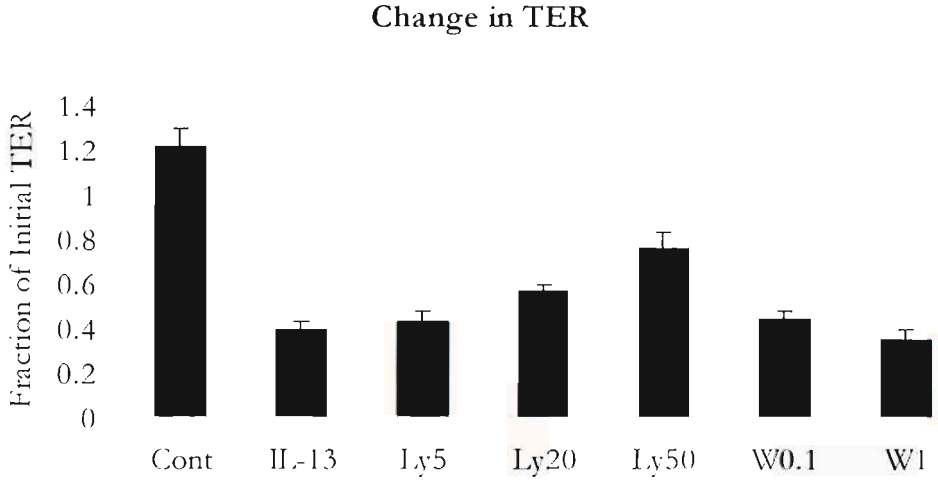


*Figure 7.2. Effect of 3 days of IL-13, in the presence or absence of PI3K inhibitors, on the TER of mature T84 monolayers. Monolayers were incubated with medium containing PBS-0.1%BSA vehicle (Cont), IL-13, IL-13 plus Ly294002 at 5μM (Ly5), 20μM (Ly20) or 50μM (Ly50), or IL-13 plus wortmannin at 0.1μM (W0.1) or 1μM (W1). The combined results of 3 experiments are shown. N=9 for each group; bars and error bars represent means and standard errors of the mean respectively. The reduction in TER after IL-13-exposure was partially reversed by Ly294002 (p=0.0008 for the comparison of IL-13 and IL-13 plus Ly294002 50μM) but not by wortmannin (p>0.05).*

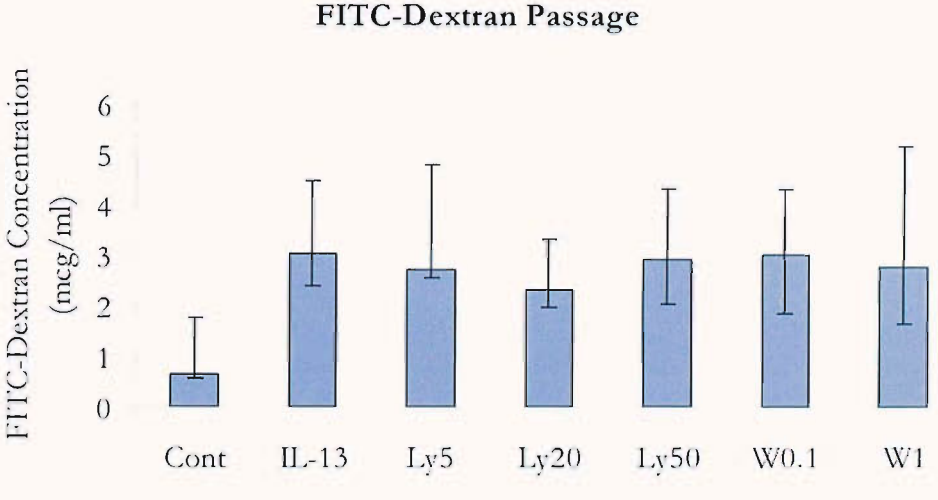


*Figure 7.3. FITC-dextran permeability of T84 monolayers incubated for 3 days with medium containing PBS-0.1%BSA vehicle (Cont), IL-13, IL-13 plus Ly294002 at 5μM (Ly5), 20μM (Ly20) or 50μM (Ly50), or IL-13 plus wortmannin at 0.1μM (W0.1) or 1μM (W1). The combined results of 3 experiments are shown. N=4 for each group; bars and error bars represent medians and ranges respectively. Permeability increased with IL-13 but showed no significant change with either inhibitor.*

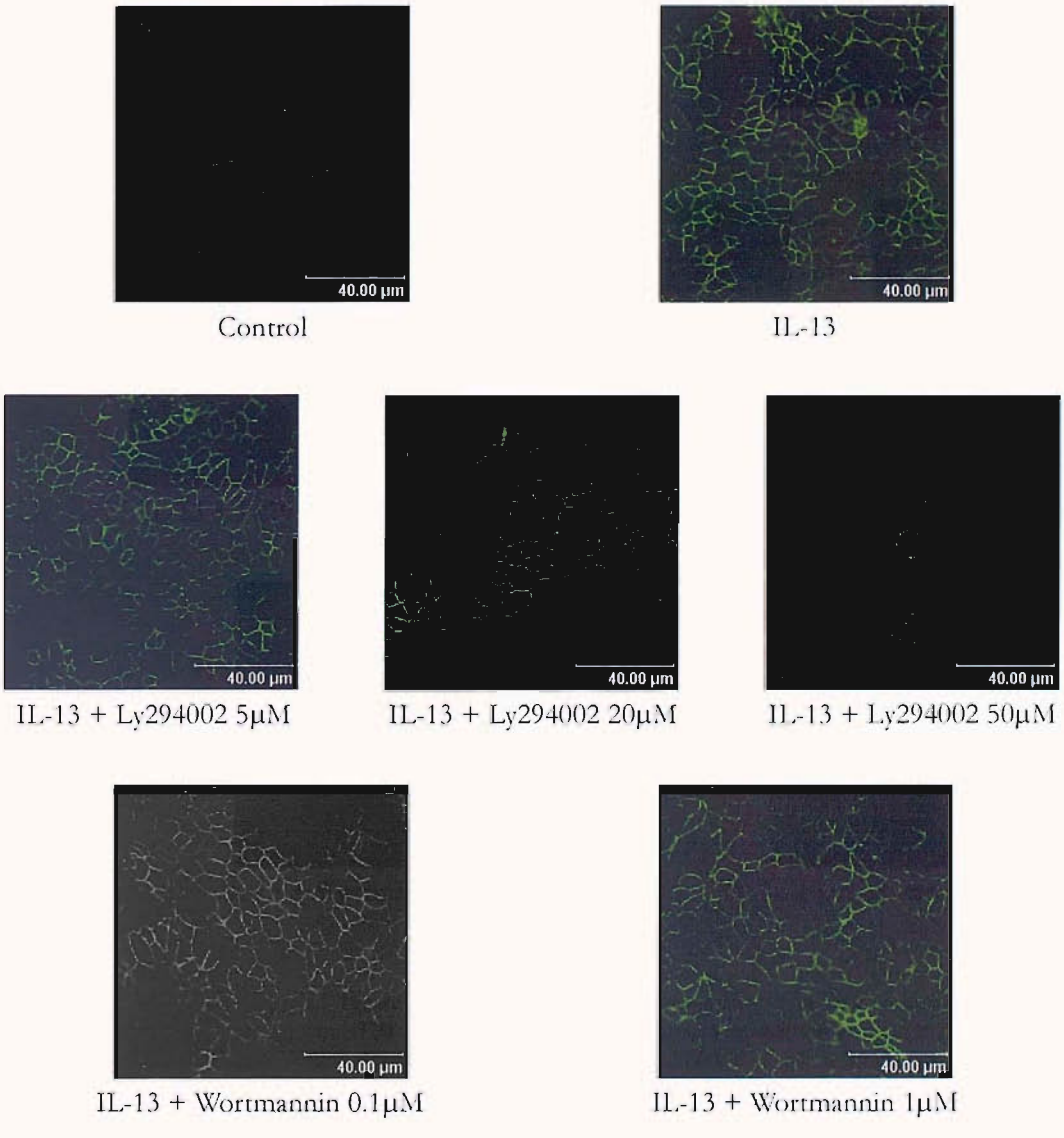


*Figure 7.4. Confocal LASER micrographs of claudin 2 immunofluorescent staining in T84 monolayers incubated for 3 days with medium containing PBS-0.1%BSA vehicle (Control), IL-13, IL-13 and Ly294002 (5, 20 or 50µM), or IL-13 and wortmannin (0.1 or 1µM). Five fields were examined in each of three experiments, and a representative field is depicted.*

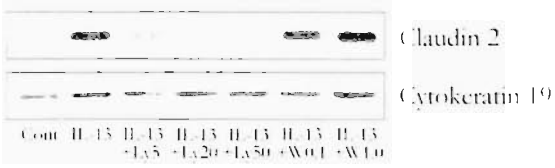


*Figure 7.5. Western blots of whole cell lysates of T84 monolayers incubated for 3 days with medium containing PBS-0.1%BSA vehicle (Cont), IL-13, IL-13 plus Ly294002 at 5μM (IL-13+Ly5), 20μM (IL-13+Ly20) or 50μM (IL-13+Ly50), or IL-13 plus wortmannin at 0.1μM (IL-13+W0.1) or 1μM (IL-13+W1.0). Blots were probed for claudin 2 and cytokeratin 19, the latter to confirm equal loading of protein in each lane. A representative blot from three separate experiments is depicted.*

| Band density normalised to cytokeratin 19 | | | | | | |
|---|---|---|---|---|---|---|
| Control | IL-13 | IL-13 + Ly5 | IL-13 + Ly20 | IL-13 + Ly50 | IL-13 + W0.1 | IL-13 + W1.0 |
| 0.18 | 1.29 | 0.54 | 0.35 | 0.08 | 1.36 | 1.32 |

*Table 7.2. Claudin 2 band densities normalised to cytokeratin 19, obtained by analysis of the blots depicted in figure 7.5.*

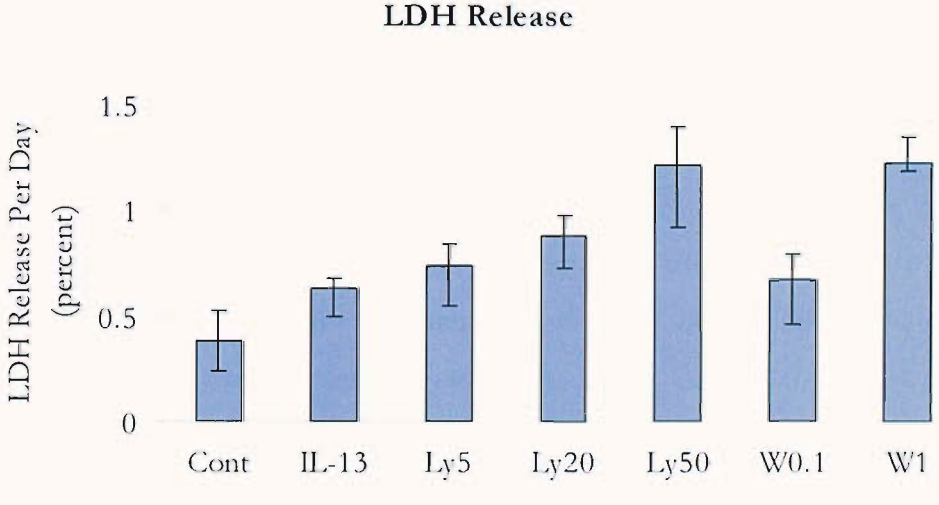


*Figure 7.6. LDH release from T84 monolayers incubated for 3 days with medium containing PBS-0.1%BSA vehicle (Cont), IL-13, IL-13 plus Ly294002 at 5μM (Ly5), 20μM (Ly20) or 50μM (Ly50), or IL-13 plus wortmannin at 0.1μM (W0.1) or 1μM (W1). N=3 for each group; bars and error bars represent medians and ranges respectively. Both inhibitors were significantly more cytotoxic than IL-13 alone ($p=0.050$ for the comparison of IL-13 with each of Ly20, Ly50 and W1), but Ly294002 50μM and wortmannin 1μM were equally toxic. In all groups the percentage of total monolayer LDH released per day was low (<1.5%).*

Further experiments were performed to confirm both that IL-13 was increasing the activity of PI3K in T84 cells and that the inhibitors were successfully inhibiting this activity. T84 cells were cultured for 14 days on collagen S-coated BIOCOAT Control Cell Culture Inserts. At this point the monolayers were rinsed with PBS-Ca-Mg and the culture medium was replaced with Ultraculture serum-free medium. After overnight incubation the inserts were allocated to one of the seven experimental groups defined in table 7.1. However, prior to incubation with IL-13 the monolayers were preincubated with their appropriate inhibitor at the appropriate concentration for 10 minutes. The medium was then replaced with fresh Ultraculture containing IL-13 and inhibitors (where appropriate), with the exception of the control monolayer, which was incubated with PBS-0.1% BSA only. As before, the concentration of DMSO was adjusted to the same level in all cases. After 10 minutes protein was extracted from monolayers using a lysis buffer that contained kinase and phosphatase inhibitors. SDS-PAGE and western blotting were carried out, and the activity of PI3K was assessed by performing immunodetections using an antibody that binds specifically to Akt that has been phosphorylated on its serine residue at position 473 (pAkt). Blots were stripped and reprobed using antibodies for both total Akt (tAkt) and cytokeratin 19, to confirm equivalent loading of protein in each lane. An identical experiment was also performed, except that, instead of using Ultraculture serum-free medium, normal serum-containing medium was used throughout. Analysis of band densities normalised to those obtained for cytokeratin 19 are depicted in table 7.3.

Total Akt expression was only slightly altered after 10 minutes of IL-13 exposure, with or without inhibitors, in either the presence or absence of serum (figure 7.7, table 7.3). However, in both cases phospho-Akt was increased after 10 minutes exposure to IL-13, and both Ly294002 and wortmannin significantly reduced phosphorylation of Akt to control levels or below (figure 7.7, table 7.3).

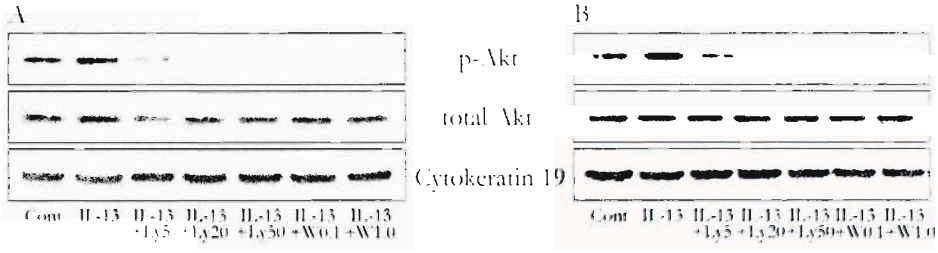


*Figure 7.7. Western blots of whole cell lysates of T84 monolayers exposed for 10 minutes to vehicle (Cont), IL-13, IL-13 plus Ly294002 at 5μM (Ly5), 20μM (Ly20) or 50μM (Ly50), or IL-13 plus wortmannin at 0.1μM (W0.1) or 1μM (W1). Blots were probed sequentially for phospho-Akt (p-Akt), total Akt and Cytokeratin 19. See table 7.3 for the band densities measured for p-Akt and total Akt (normalised to those obtained for cytokeratin 19). The experiment was performed in both serum-free (A) and serum-stimulated (B) conditions.*

| A | Band densities normalised to cytokeratin 19 | | | | | | |
|---|---|---|---|---|---|---|---|
| | Control | IL-13 | IL-13 + Ly5 | IL-13 + Ly20 | IL-13 + Ly50 | IL-13 + W0.1 | IL-13 + W1.0 |
| p-Akt | 0.78 | 1.27 | 0.23 | 0.10 | 0.04 | 0.08 | 0.05 |
| total Akt | 1.05 | 1.32 | 0.48 | 0.89 | 0.80 | 0.94 | 0.69 |

| B | Band densities normalised to cytokeratin 19 | | | | | | |
|---|---|---|---|---|---|---|---|
| | Control | IL-13 | IL-13 + Ly5 | IL-13 + Ly20 | IL-13 + Ly50 | IL-13 + W0.1 | IL-13 + W1.0 |
| p-Akt | 0.71 | 1.39 | 0.26 | 0.05 | 0.02 | 0.05 | 0.01 |
| total Akt | 1.30 | 1.32 | 0.93 | 0.91 | 1.20 | 1.33 | 1.29 |

*Table 7.3. Band densities normalised to cytokeratin 19 for p-Akt and total Akt, obtained by analysis of the blots depicted in figure 7.7.*

## 7.2.2 THE KINETICS OF THE IL-13-INDUCED INCREASE IN CLAUDIN 2 EXPRESSION

T84 cells were cultured for 15 days on 0.9cm$^2$ collagen S-coated BIOCOAT Control Cell Culture Inserts. Monolayers were then incubated with medium containing IL-13 (2ng/ml) for various durations: 0 hours, 10 minutes, 1 hour, 4 hours, 12 hours and 24

hours. The expression of claudin 2 was determined by both immunofluorescence and western blotting. Western blots were stripped and reprobed with antibody for cytokeratin 19 to confirm equal loading of protein across all lanes. Analysis of band densities normalised to those obtained for cytokeratin 19 are depicted in figure 7.4.

Very little claudin 2 was detected by either immunofluorescence or western blotting at any duration up to 4 hours (figures 7.8 and 7.9). Twelve hours of IL-13 exposure led to a very large increase in the amount of claudin 2 detected by western blotting (figure 7.9). A large increase in claudin 2 expression was observed by immunofluorescence after 24 hours of exposure to IL-13, with detection predominantly in the 'chicken-wire' distribution consistent with localisation to the TJ (figure 7.8).

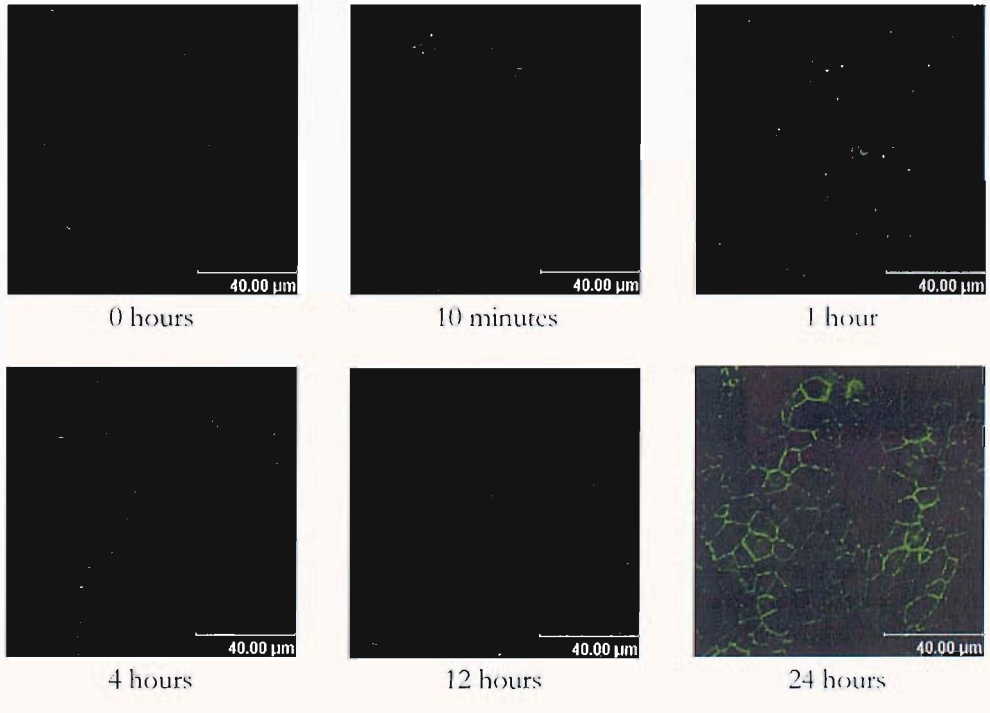


*Figure 7.8. Confocal LASER micrographs of claudin 2 immunofluorescent staining in T84 monolayers incubated for various durations with medium containing IL-13. Five fields were examined for each duration, and representative fields are depicted.*

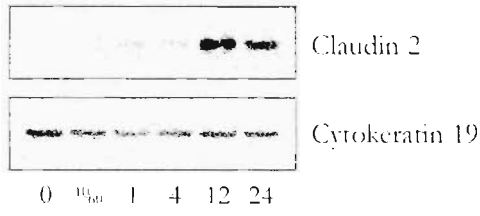


*Figure 7.9. Western blots of whole cell lysates of T84 monolayers incubated with IL-13 for 0 hours (0), 10 minutes ($^{10}/_{60}$), or 1, 4, 12 or 24 hours (1, 4, 12, 24 respectively). Blots were probed with antibodies to claudin 2 and cytokeratin 19. See table 7.4 for the band densities measured for each claudin (normalised to those obtained for cytokeratin 19).*

| Band densities normalised to cytokeratin 19 | | | | | |
|---|---|---|---|---|---|
| 0 | 10 minutes | 1 hour | 4 hours | 12 hours | 24 hours |
| 0.23 | 0.50 | 0.99 | 0.84 | 5.46 | 2.82 |

*Table 7.4. Claudin 2 band densities normalised to cytokeratin 19, obtained by analysis of the blots depicted in figure 7.9.*

### 7.2.3 QUANTITATION OF CLAUDIN 2 TRANSCRIPT NUMBER

The relative abundancy of mRNA for claudin 2 was determined in T84 cells by quantitative RT-PCR. T84 cells were cultured for 15 days on 4.2cm$^2$ collagen S-coated BIOCOAT Control Cell Culture Inserts. They were then incubated overnight (16 hours) with IL-13 (2ng/ml), IL-13 (2ng/ml) and Ly294002 (50μM), or control reagents (PBS-0.1%BSA). The level of DMSO was adjusted to 0.1% by volume in all the medium used. RNA extraction and quantitative RT-PCR were then performed. Abundancies were normalised to those determined for the housekeeping genes, GAPDH and UBC.

Insulin Receptor Substrates (IRS) stimulate PI3K activation (Backer et al., 1992), and there appeared to be a significant degree of background PI3K activation in control T84 cells cultured in Ultraculture, an insulin-containing serum-free medium, as detected by western blotting for phospho-Akt (see figure 7.7). In order to minimise this potential

background stimulation, this experiment was performed twice: in duplicate monolayers in normal medium and in triplicate monolayers in insulin-free serum-free medium.

Claudin 2 mRNA was significantly increased by exposure to IL-13 alone in all the monolayers examined ($p=0.050$). This was the case in both serum-containing and insulin-free serum-free medium (figures 7.10 and 7.11 respectively). In the latter medium the increase ranged from approximately 3- to 4-fold, whereas in serum-containing medium it ranged from 6- to 16-fold. The addition of 50μM Ly294002 abolished this increase in all but one of the monolayers examined ($p=0.050$), and indeed these levels fell below those of control monolayers, although this was not statistically significant.

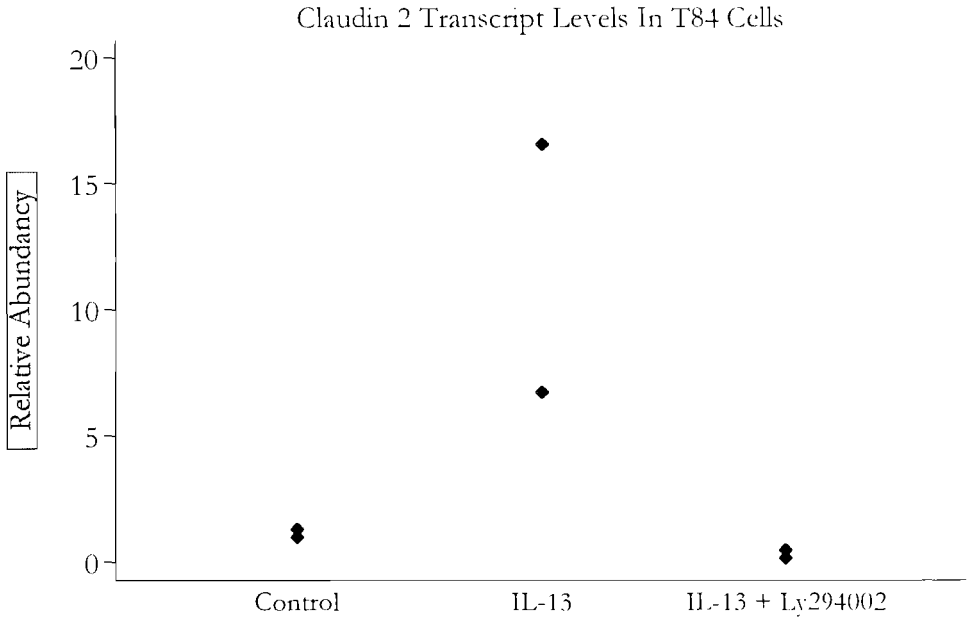


*Figure 7.10. Claudin 2 transcript (mRNA) levels in T84 monolayers cultured in normal, serum-containing, medium and exposed to vehicle (Control), IL-13 or IL-13 plus Ly294002 for 16 hours. Values have been normalised to those of housekeeping genes and then divided by the median of the control values to give a relative abundancy.*

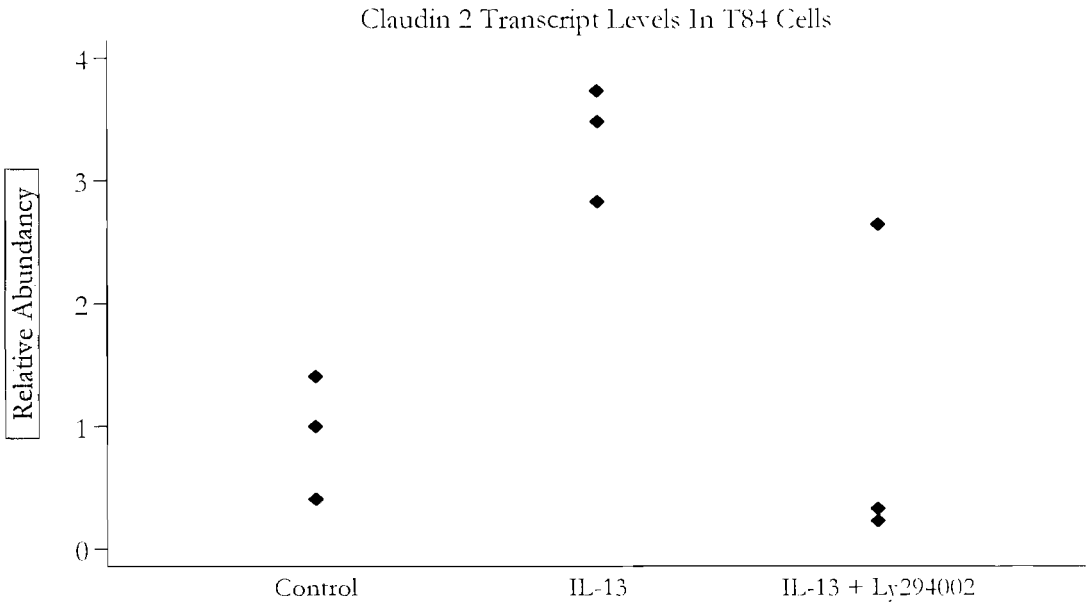


*Figure 7.11. Claudin 2 transcript (mRNA) levels in T84 monolayers cultured in insulin-free, serum-free, medium and exposed to vehicle (Control), IL-13 or IL-13 plus Ly294002 for 16 hours. Values have been normalised to those of housekeeping genes and then divided by the median of the control values to give a relative abundancy. Exposure to IL-13 increased claudin 2 transcript levels ($p=0.050$ for the comparison of Control and IL-13 groups), whereas Ly294002 prevented this increase ($p=0.050$ for the comparison of IL-13 and IL-13 + Ly294002 groups).*

## 7.3 DISCUSSION

The results presented here show that after 12 hours of exposure to IL-13 a marked increase in claudin 2 protein expression is seen on western blots of mature T84 cell lysates, and after 24 hours a marked increase is also observed in the amount of claudin 2 detected by immunofluorescence. This detection occurs in the 'chicken-wire' pattern consistent with its incorporation into the TJ. The delay in the increase seen by immunofluorescence, compared to that seen by western blotting, suggests that the incorporation of claudin 2 into the TJ follows the increase in its total expression. This correlates with the parallel fall in TER that is first noted after 24 hours and continues over subsequent days (see figure 6.6 for an example), suggesting that the two effects are related. At 12 hours it is possible that the increased claudin 2 may be distributed diffusely across the cell, and not detected by immunofluorescence because its local concentration is below that required for detection. Incorporation into the membrane compartment may greatly increase its local concentration and allow its detection by immunofluorescence.

Measurement of claudin 2 mRNA after 16 hours of IL-13 exposure showed that IL-13 had induced an increase in transcript number. It seems probable, therefore, that this mechanism contributes to the observed increase in claudin 2 protein, particularly as the relatively long half-life of claudin 2 protein (Van Itallie et al., 2004) suggests that its level within the cell would be sensitive to small changes in either its production or degradation. The mechanism leading to the increase in transcripts is not known but could be either an increase in the rate of transcription of the claudin 2 gene or stabilisation of claudin 2 transcripts. A nuclear 'run on' assay could be used to detect changes in de novo synthesis of claudin 2 mRNA transcripts and could therefore confirm whether mRNA synthesis contributes to the increase in mRNA transcript number (Lodish, 2000). The contribution of an increase in the rate of translation of claudin 2 transcripts to the increase in protein cannot be ruled out, particularly as the increase in mRNA induced by IL-13 was relatively small (3- to 15-fold). Indeed, evidence suggests that activation of PI3K can lead to an increase in protein translation by several mechanisms. Firstly, pAkt can phosphorylate and inhibit tuberin (Manning et al., 2002), preventing it from converting the G protein Rheb from an active, GTP-bound form to an inactive, GDP-bound form (Tee et al., 2003). Rheb.GTP activates the protein mammalian target of rapamycin (mTOR), which controls a number of proteins that either activate protein synthesis or increase the cellular capacity for protein synthesis (Proud, 2004). Secondly, GSK3β inhibits the eukaryotic initiation factor eIF2B (Welsh et al., 1998), which, when active, stimulates translation by replenishing eIF2.GTP from eIF.GDP to allow further cycles of translation to be initiated (Alberts, 2002). Phospho-Akt, by inhibiting GSK3β, can therefore stimulate translation by this mechanism. Further work would be required to investigate these possibilities.

It was also found that inhibition of PI3K by Ly294002 partially, but significantly, restored the IL-13 mediated drop in TER, confirming previous work (Ceponis et al., 2000). However, importantly, Ly294002 also prevented the increase in claudin 2 expression induced by IL-13, suggesting that the two effects are related. Both effects of Ly294402 were dose-dependent. Wortmannin had no effect at either concentration used.

Recommendations for the use of protein kinase inhibitors in cell-based assays were published recently (Davies et al., 2000). The 'gold-standard' for validation of a result is suggested to be the demonstration that the effects of an inhibitor disappear when an

inhibitor-resistant mutant of the protein kinase of interest is overexpressed. If such a mutant is not available, it is recommended that two different, well-described inhibitors are assayed and, further, that their cellular effects can be observed at the same concentrations that prevent the phosphorylation of a physiological substrate of the protein kinase (Davies et al., 2000). In the experiments described above two different inhibitors of PI3K were used, and their efficacies in blocking PI3K activity in vitro have been documented previously (Arcaro and Wymann, 1993; Davies et al., 2000; Kanai et al., 1993). However, only Ly294002 affected claudin 2 expression and TER. There are several possible explanations for the different effects of Ly294002 and wortmannin. Firstly, the effects of Ly294002 may have been secondary to its increasing cytotoxicity at higher concentrations, rather than due to PI3K inhibition. However, this is unlikely to explain its effects on TER and claudin 2 expression, because higher concentrations actually strengthened barrier function, whereas cell death might be expected to impair it. Furthermore, the second inhibitor used, wortmannin, was equally toxic but induced neither the increase in TER nor the reduction in claudin 2 expression. Secondly, it is possible that wortmannin was not effective in blocking PI3K activity. However, both inhibitors prevented the phosphorylation of Akt in a dose-dependent fashion, and the same concentrations were used to attempt to influence claudin 2 expression and TER. The concentration of wortmannin stated by the manufacturer to inhibit 50% of the activity of PI3K (its $IC_{50}$) is 5nM. However, the $IC_{50}$ is dependent on the concentrations of ATP and magnesium ions (Davies et al., 2000), which are not stated by the manufacturer. An independent assessment of wortmannin's activity carried out by Davies et al (2000) showed that 1μM caused 100% inhibition of PI3K in an in vitro assay, and this concentration was used here. However, the effective concentration of an inhibitor in an *in vitro* assay may be very different from the effective concentration *in vivo*. The intracellular concentration may be very different from that in the culture medium, and it will depend on several factors relating to the rates of both uptake and degradation. The rate of uptake will depend on factors such as the hydrophobicity and lipid solubility of the inhibitor, the ability of the cells to take up the inhibitor by active mechanisms, and the ability of the cells to transport the inhibitor to the intracellular location at which its activity is required. The rate at which the inhibitor's activity is degraded will depend on the ability of the cells to denature, break down or secrete the molecule, as well their ability to overcome its action by activating alternative pathways; the inhibitor's activity may also be ameliorated by substances contained within or

secreted into the culture medium. Therefore, although the concentrations of wortmannin used greatly exceeded the *in vitro* $IC_{50}$, it is possible that these concentrations were below those required to block PI3K activity *in vivo*. Furthermore, although in figure 7.7 the inhibitors were observed to inhibit Akt phosphorylation after 10 minutes, it has not been determined whether this inhibition of PI3K activity is still present after 3 days, which is the duration at which the effects on claudin 2 expression were examined. In other words, what has been demonstrated is that these inhibitors can prevent the phosphorylation of Akt by PI3K, but not that this effect is sustained throughout the time course of the experiment. The third possibility is that Ly294002 influenced TER and claudin 2 expression via effects on kinases other than PI3K. Ly294002's inhibition of PI3K is, however, highly specific, with one exception. At 50μM Ly294402 inhibits 82% of the in vitro activity of the serine threonine kinase casein kinase 2 (CK2), and indeed the $IC_{50}$ for this action (6.9μM) is similar to that for PI3K inhibition (10μM)(Davies et al., 2000). Wortmannin does not affect the activity of CK2 at doses up to 1μM. There is, however, no evidence to support a role of CK2 in either the downstream effects of IL-13 or the regulation of tight junctions, so it is unlikely that the observed effects of Ly294002 were due to any effect on CK2. The fourth possibility is that wortmannin effectively inhibited cellular PI3K activity for long enough to demonstrate inhibition of Akt phosphorylation, but that this effect was not sustained for long enough to affect claudin 2 expression and TER. Although the activity of wortmannin in aqueous solution is preserved at 0 C, it is virtually abolished after just 3 hours at 37 C (Woscholski et al., 1994). This short half-life may therefore explain the failure of wortmannin to affect TER and claudin 2 expression, as although it reduced the expression of phospho-Akt after 10 minutes, the replacement of medium and inhibitors every 12 hours may have allowed the cells several hours to recover from or overcome the effects of each dose. More frequent changes of medium and inhibitor may have led to the detection of a biological effect that was not observed with 12-hourly changes. However, the desire for more frequent changes in medium has to be balanced against their potentially deleterious effects. It has been observed that the changes in temperature associated with replacing medium can have profound effects on TER, and each replacement risks damage to the monolayer (Matter and Balda., 2003). Even if the intracellular activity of wortmannin were sustained for long enough to inhibit PI3K effectively, it is also possible that the cells could have overcome this inhibition by, for example, activating alternative pathways to bypass or overcome the

effect of wortmannin, or by increasing the synthesis of PI3K to increase the pool of uninhibited enzyme. This potential problem may be more likely during the long term *in vivo* stimulation with inhibitors or cytokines performed here and in chapter 5. In chapter 5, however, the effects of 3 days of cytokine stimulation were examined in an attempt to replicate the long term excessive cytokine stimulation observed in IBD. An increase in claudin 2 expression was observed after 3 days of IL-13 stimulation. Therefore, PI3K-inhibitors were added for the same duration in order to examine their effects on this outcome.

The IL-13-mediated increase in the passage of FITC-dextran was not reversed by Ly294002, suggesting separable regulation of TER and the passage of uncharged molecules. Separable regulation of ionic and uncharged molecular permeabilities has previously been suggested by a study in which the expression of occludin mutants that lacked its carboxy-terminus was shown to be associated with a marked increase in the paracellular flux of small molecular weight tracers, with no effect seen on electrical resistance (Balda et al., 1996a). As PI3K has been shown to bind to the carboxy-terminus of occludin (Nusrat et al., 2000), it might be expected that inhibition of PI3K would affect permeability to FITC-dextran, but this was not observed here. This implies that the mechanisms that regulate TER and FITC-dextran permeability are separate and may have different sensitivities to PI3K inhibition in T84 cells.

What alternative methods may be employed to confirm the putative involvement of PI3K in the IL-13-stimulated increase in claudin 2 expression? If the same effect on claudin 2 followed activation of PI3K by a different stimulus, this would support its involvement. Expression of a dominant-negative mutant of PI3K would be a highly specific means of inhibiting PI3K activity; if this prevented the increase in claudin 2 normally induced by IL-13, this would strongly suggest a role for PI3K in this action. As described above, the prevention of the effect of Ly294002 by the expression of an active, but Ly294002-resistant, mutant of PI3K would also provide confirmatory evidence for the involvement of PI3K in IL-13stimulated claudin 2 expression.

In summary, the evidence presented here suggests the possibility that IL-13 induces an increase in TJ claudin 2 expression in T84 cells by a PI3K-dependent mechanism. The increase in claudin 2 protein is significant after 12 hours and is associated with an increase in claudin 2 mRNA and a subsequent increase in claudin 2 assembly in a pattern consistent with TJ incorporation.

# CHAPTER 8

# THE REGULATION OF CLAUDIN 2 EXPRESSION BY THE PI3-KINASE PATHWAY

# THE REGULATION OF CLAUDIN 2 EXPRESSION BY THE PI3K PATHWAY

## 8.1 INTRODUCTION AND AIMS

In the previous chapter it was demonstrated that the PI3K inhibitor, Ly294002, can prevent the fall in TER and the increases in claudin 2 protein and mRNA which occur in T84 monolayers exposed to IL-13. It was also observed that IL-13 can increase the level of the active, phosphorylated form of Akt (pAkt), whereas Ly294002 markedly reduced it. However, a second PI3K inhibitor, wortmannin, failed to prevent either the fall in TER or the increases in claudin 2 and pAkt induced by IL-13. Therefore, further evidence was needed to support the hypothesis that IL-13 induces an increase in TJ claudin 2 expression in T84 cells by a PI3K-dependent mechanism.

The small molecule, lithium chloride (LiCl), has been shown to stimulate PI3K activity in vitro, where it has also been demonstrated to inhibit glycogen synthase kinase 3-beta (GSK3β) (Chalecka-Franaszek and Chuang, 1999). The stimulation of PI3K has been demonstrated in disparate cell types, such as cerebellar granule cells (Chalecka-Franaszek and Chuang, 1999; Mora et al., 2002) and cardiomyoblasts (Kashour et al., 2003). Therefore, if LiCl were able to stimulate PI3K in T84 cells, a subsequent increase in claudin 2 protein expression would provide further evidence to support a role for PI3K in regulating claudin 2 expression.

In addition, pAkt has been shown to inactivate glycogen synthase kinase 3-beta (GSK3β) by phosphorylating it on a serine residue at position 9 (Cross et al., 1995), and evidence suggests that this is the result of a direct interaction between the two molecules (van Weeren et al., 1998). GSK3β is a key regulator of the Wnt signalling pathway. Activation of this pathway leads to the stabilisation of free β-catenin i.e. that which is cytosolic and not bound in the adherens junction to E-cadherin. Normally the level of free beta-catenin is tightly regulated by its forming a complex with two proteins, APC and axin, which allow it to be phosphorylated and designated for ubiquitinaton (Huelsken and Behrens, 2002; Nelson and Nusse, 2004). This phosphorylation takes place on four residues at the N-terminus of the molecule (Staal et al., 2002), and three of these phosphorylations are performed by GSK3β (Doble and Woodgett, 2003). If

this complex cannot form because, for example, of a mutation to one of these components or the delivery of a signal via the Wnt pathway that phosphorylates and inactivates GSK3β, then beta-catenin remains unphosphorylated (Giles et al., 2003; van Noort et al., 2002). This form of β-catenin (sometimes referred to as active β-catenin or ABC) is not degraded and instead is able to enter the nucleus and bind to the transcription factor lymphoid-enhancing factor-1/T-cell factor-4 (Lef-1/TCF-4), where this complex then increases transcription of many pro-proliferative genes and genes involved in tissue remodelling (e.g. matrix metalloproteinase-7, fibronectin) (Giles et al., 2003; Polakis, 2000).

The promoter region of the human claudin 2 gene (CLDN2) was cloned recently and was demonstrated to contain binding sites for the transcription factors hepatocyte nuclear factor (HNF)-1 and the caudal-related homeodomain (Cdx) proteins (Sakaguchi et al., 2002). More recently still, measurements of the activity of the claudin 2 gene promoter in vitro, coupled with further analysis of the sequence and the effects of targeted mutations therein, have revealed that Lef-1/TCF-4 binds to the promoter and enhances its activity (Mankertz et al., 2004). Further analysis of the promoter region has shown that it contains several Lef-1/TCF-4 binding sites in addition to those studied by Mankertz et al. (J.E.Collins, personal communication). Furthermore, transcriptionally active β-catenin has also been shown to activate transcription of Cdx1 (Domon-Dell and Freund, 2002; Lickert et al., 2000). Thus, it is possible that β-catenin can enhance the transcription of claudin 2 by both direct and indirect mechanisms.

The model to be tested in this chapter, therefore, is that IL-13, by inducing the phosphorylation and activation of Akt, inactivates GSK3β, leading to the stabilisation and nuclear accumulation of active β-catenin and an increase in the transcription of the gene for claudin 2. This putative pathway is illustrated in figure 8.1.

Therefore, the aims of this chapter were to address the following questions:

- Does lithium chloride, an activator of PI3K, stimulate claudin 2 expression in mature T84 cells with the same time course as IL-13?
- Do IL-13 and lithium chloride activate Akt and alter the downstream signalling proteins GSK3β and β-catenin prior to increased claudin 2 expression in T84 cells?

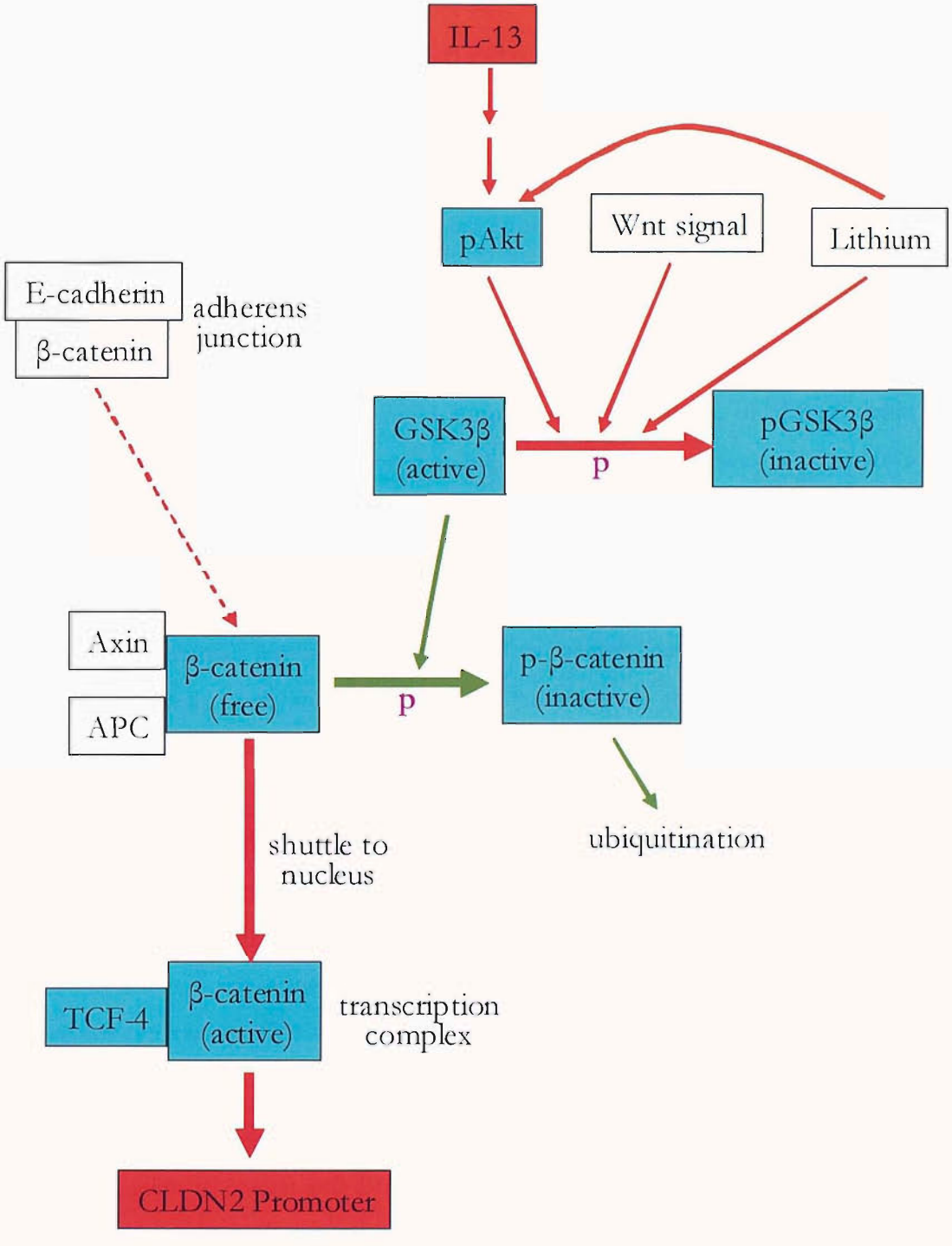


*Figure 8.1. Proposed mechanism for the IL-13-stimulated increase in claudin 2 expression. In adherent epithelia most β-catenin is bound to E-cadherin within the adherens junction of the cell membrane. The level of free β-catenin is tightly regulated by the pathway represented by the green arrows: if bound to APC and axin it is phosphorylated by GSK3β, which marks it for ubiquitination and degradation. The red arrows represent the suggested pathways to increased expression of claudin 2. IL-13 binding or the addition of exogenous lithium chloride lead to the phosphorylation and activation of Akt, which, like a Wnt signal, may inactivate GSK3β. β-catenin would thus remain unphosphorylated and would accumulate and enter the nucleus, where it would form a complex with the transcription factor TCF-4 and bind to and enhance the activity of the promoter of the claudin 2 gene (CLDN2).*

## 8.2 RESULTS

### 8.2.1 THE EFFECTS OF LITHIUM CHLORIDE ON CLAUDIN 2 EXPRESSION, AKT PHOSPHORYLATION, GSK3-BETA PHOSPHORYLATION AND BETA-CATENIN EXPRESSION

T84 cells were cultured for 15 days on either 4.2cm$^2$ BIOCOAT Control Cell Culture Inserts or 6-well plates, all of which had been pre-coated with collagen S. On the day before experiments were performed, monolayers were rinsed twice with PBS-Ca-Mg, and the medium was replaced for 16 hours with insulin-free serum-free medium to minimise the level of any background stimulation of the PI3K or Wnt pathways. Fresh insulin-free serum-free medium containing LiCl (20mmol/l) was then added for various durations: 0, 1, 4, 12 and 24 hours. The time course of any response to LiCl was not known prior to this experiment, but some evidence from other cell culture models had suggested that approximately 6 hours of exposure to 20mmol/l of LiCl was necessary for maximal inhibition of GSK3β to occur (van Noort et al., 2002). Monolayers in wells were then lysed in the presence of kinase and phosphatase inhibitors, and SDS-PAGE and western blotting were performed on the lysates. Specific antibodies to the following were used to detect their relative expression levels on these blots: claudin 2, pAkt, tAkt, GSK3β phosphorylated on its serine residue at position 9 (pGSK), total GSK3β (tGSK), β-catenin that is unphosphorylated on two of the four N-terminal residues (active β-catenin or ABC), total β-catenin and cytokeratin 19. Band densities were measured using Quantity One software and were normalised to those obtained for cytokeratin 19. Monolayers cultured on filter inserts were processed for the detection of claudin 2 expression by immunofluorescence. All experiments were performed twice.

At the baseline (0 hours) and after 1 hour of LiCl exposure, claudin 2-positive cells were observed infrequently by immunofluorescence detection (figure 8.2). After 4, 12 and, especially, 24 hours larger clusters of claudin 2-positive cells were observed, interspersed with large areas of cells in which claudin 2 could not be detected. The claudin 2 was distributed in the characteristic chicken-wire pattern of junctional localisation. Detection of claudin 2 on western blots of whole cell lysates yielded much stronger bands after 12 and 24 hours than after shorter durations of LiCl exposure, the strongest band being detected at the 12 hour time point (figure 8.3; table 8.1).

LiCl induced a very marked increase in the expression of phospho-Akt, which peaked at 4 hours (figure 8.3; table 8.1), accompanied by some increase in total Akt expression (peaking at 12 hours). This suggested not only that LiCl was stimulating PI3K activity, but also that this increase preceded the increase in claudin 2 expression.

Western blotting for pGSK produced very weak bands at 0 and 1 hour time points, but much stronger bands after 4, 12 and 24 hours, with the strongest band observed after 12 hours of LiCl (figure 8.3; table 8.1). Interestingly, the level of total GSK3β also increased with time (figure 8.3; table 8.1). These increases appeared to parallel that of claudin 2.

β-catenin expression was assessed by western blotting using two different antibodies. Only a small increase in expression was observed over time, and this did not appear to parallel that of claudin 2, suggesting that there had not been a marked accumulation of either unphosphorylated or total β-catenin (figure 8.3).

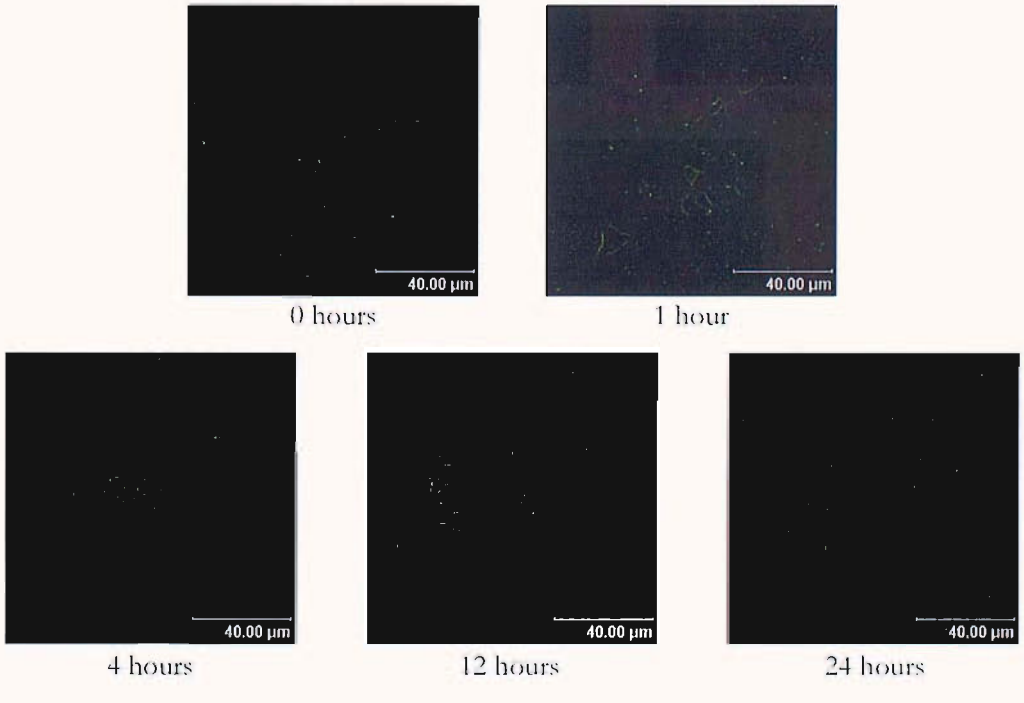


*Figure 8.2. Confocal LASER micrographs of claudin 2 immunofluorescent staining in T84 monolayers incubated for various durations with lithium chloride. Five fields were examined for each duration, and representative fields are depicted.*

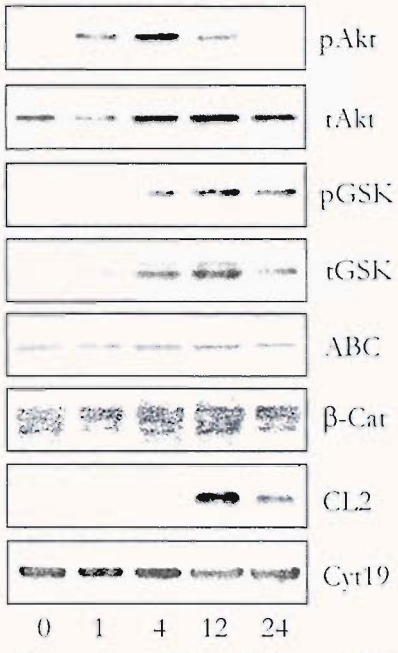


*Figure 8.3. Western blots of whole cell lysates of T84 monolayers incubated with LiCl for 0, 1, 4, 12 and 24 hours and probed with antibodies to phospho-Akt (pAkt), total Akt (tAkt), phosphorylated GSK3β (pGSK), total GSK3β (tGSK), active β-catenin (ABC), total β-catenin, claudin 2 (CL2) and cytokeratin 19 (Cyt19). See table 8.1 for the band densities measured for each antibody (normalised to those obtained for cytokeratin 19).*

| | Band densities normalised to cytokeratin 19 | | | | |
|---|---|---|---|---|---|
| | 0 | 1 hour | 4 hours | 12 hours | 24 hours |
| pAkt | 0.56 | 1.25 | 8.01 | 1.99 | 0.62 |
| tAkt | 3.79 | 1.78 | 10.66 | 11.31 | 7.24 |
| pGSK | 0.12 | 0.19 | 0.86 | 1.13 | 0.75 |
| tGSK | 0.41 | 0.42 | 2.66 | 2.77 | 1.34 |
| ABC | 0.69 | 0.51 | 1.47 | 1.18 | 0.82 |
| β-Cat | 0.56 | 0.50 | 1.33 | 1.09 | 0.75 |
| CL2 | 0.37 | 0.35 | 0.46 | 5.50 | 1.92 |

*Table 8.1. Band densities normalised to cytokeratin 19 for phospho-Akt (pAkt), total Akt (tAkt), phosphorylated GSK3β (pGSK), total GSK3β (tGSK), active β-catenin (ABC), total β-catenin and claudin 2 (CL2), obtained by analysis of the blots depicted in figure 8.3.*

### 8.2.2 THE KINETICS OF IL-13-INDUCED AKT PHOSPHORYLATION, AND THE EFFECTS OF IL-13 ON GSK3-BETA PHOSPHORYLATION AND BETA-CATENIN EXPRESSION

T84 cells were cultured for 15 days on 0.9cm$^2$ collagen S-coated BIOCOAT Control Cell Culture Inserts before 16 hours serum and insulin starvation, followed by incubation with insulin-free serum-free medium containing IL-13 (2ng/ml) for various durations: 0 hours, 10 minutes, 1 hour, 4 hours, 12 hours and 24 hours. The relative expression levels of the following were determined at each time point by SDS-PAGE/western blotting: claudin 2, pAkt, tAkt, pGsk, tGsk, active β-catenin (ABC), total β-catenin and cytokeratin 19. As before, band densities were measured using Quantity One software and normalised to those obtained for cytokeratin 19. The expression and distribution of claudin 2 and ABC were also determined by immunofluorescence.

When assessed by both immunofluorescence staining (figure 8.4) and western blotting (figure 8.5; table 8.2), a small increase in claudin 2 expression was observed after 4 hours but a much more marked increase was noted after 12 and, especially, 24 hours, similar to that observed without serum-starvation, and to that observed in LiCl-treated cells.

Western blotting for pAkt suggested a marked increase in expression after 1 hour of incubation with IL-13, with expression falling off by 4 hours (figure 8.5; table 8.2). Therefore, as in LiCl-treated cells, peak pAkt expression preceded the increase in claudin 2; however, peak pAkt expression occurred after 1 hour of IL-13 treatment but after 4 hours of LiCl treatment. There was no significant change in the expression of tAkt. Unlike the case with LiCl exposure, however, no increase was observed in the expression of either pGSK or total GSK expression (figure 8.5; table 8.2). Detection of β-catenin with either antibody did not show any marked change in expression with different durations of exposure to IL-13 (figure 8.5; table 8.2).

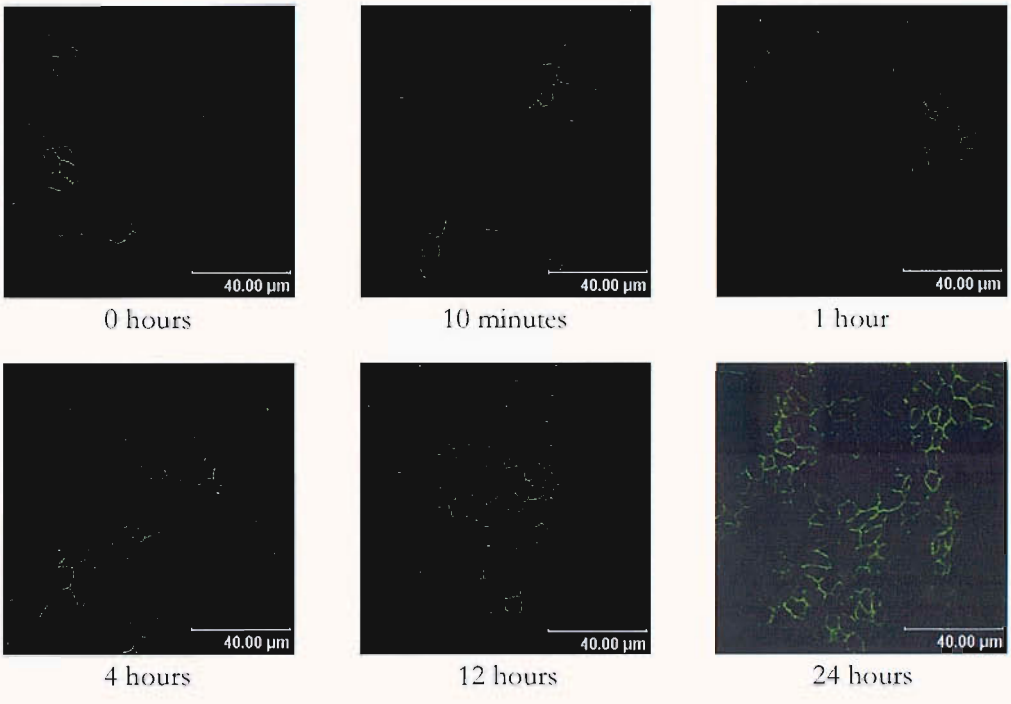


*Figure 8.4. Confocal LASER micrographs of claudin 2 immunofluorescent staining in T84 monolayers incubated for various durations with insulin-free serum-free medium containing IL-13. Five fields were examined for each duration, and representative fields are depicted.*

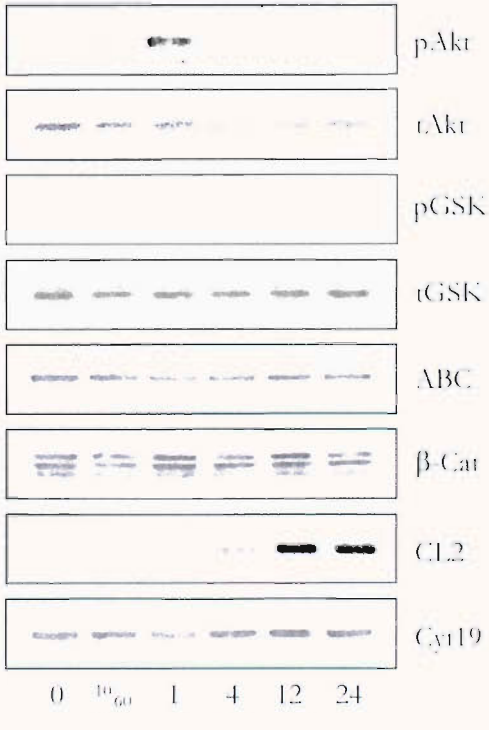


*Figure 8.5. Western blots of whole cell lysates of T84 monolayers incubated with IL-13 for 0, 1, 4, 12 and 24 hours and 10 minutes ($^{10}/_{60}$). Blots were probed with antibodies to phosphorylated Akt (pAkt), total Akt (tAkt), phosphorylated GSK3β (pGSK), total GSK3β (tGSK), active β-catenin (ABC), total β-catenin (β-cat), claudin 2 (CL2) and cytokeratin 19 (Cyt19). See table 8.2 for the band densities measured for each antibody (normalised to those obtained for cytokeratin 19).*

| | Band densities normalised to cytokeratin 19 | | | | | |
|---|---|---|---|---|---|---|
| | 0 | 10 minutes | 1 hour | 4 hours | 12 hours | 24 hours |
| pAkt | 0.30 | 0.39 | 1.02 | 0.37 | 0.22 | 0.29 |
| tAkt | 10.30 | 7.08 | 9.35 | 6.51 | 5.11 | 6.24 |
| pGSK | 0.26 | 0.33 | 0.41 | 0.37 | 0.32 | 0.40 |
| tGSK | 1.41 | 1.07 | 1.65 | 1.39 | 1.10 | 1.17 |
| ABC | 0.71 | 0.63 | 0.65 | 0.61 | 0.58 | 0.49 |
| B-Cat | 1.16 | 0.68 | 2.02 | 2.30 | 1.27 | 1.18 |
| CL2 | 0.44 | 2.32 | 0.53 | 6.41 | 20.70 | 20.44 |

*Table 8.2. Band densities normalised to cytokeratin 19 for phospho-Akt (pAkt), total Akt (tAkt), phosphorylated GSK3β (pGSK), total GSK3β (tGSK), active β-catenin (ABC), total β-catenin and claudin 2 (CL2), obtained by analysis of the blots depicted in figure 8.5.*

Because the western blots provided no evidence for an accumulation of either pGSK or ABC prior to or simultaneous with that of claudin 2, the antibody to ABC was used to examine the expression and cellular localisation of β-catenin by immunofluorescence staining of 15 day T84 monolayers that had been insulin- and serum-starved for 16 hours and then exposed to IL-13 for different durations. ABC was detected strongly in a junctional distribution at all time points examined (figure 8.6). No nuclear staining was seen at any time point. Furthermore, even after 24 hours there was no apparent increase in cell density that might suggest a proliferative response.

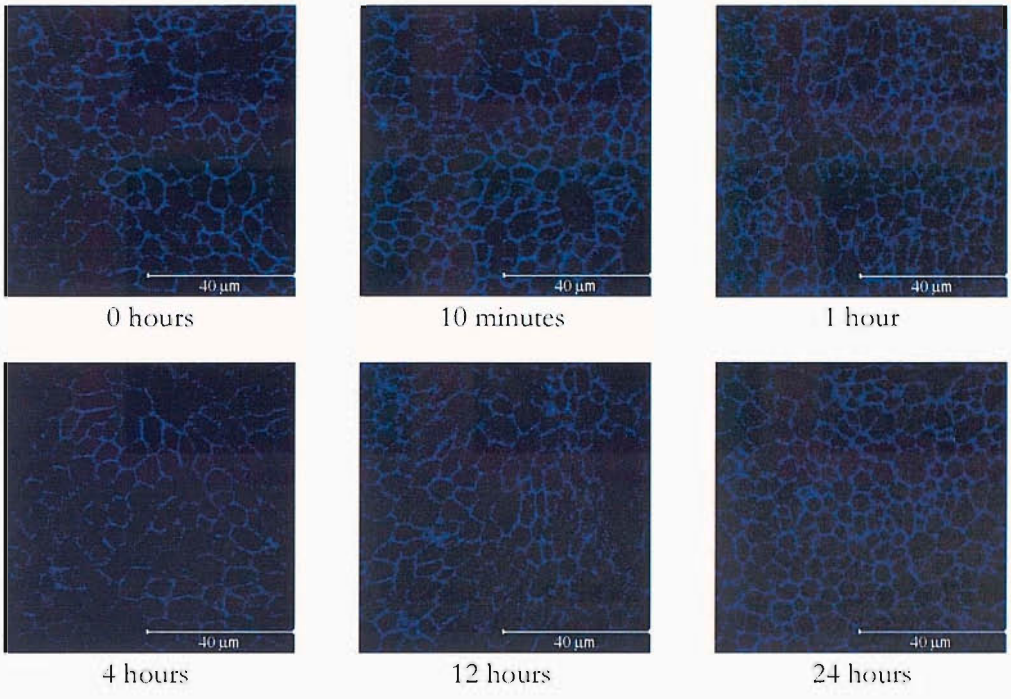


*Figure 8.6. Confocal LASER micrographs of hypophosphorylated β-catenin immunofluorescent staining in T84 monolayers incubated for various durations with insulin-free serum-free medium containing IL-13. Five fields were examined for each duration, and representative fields are depicted.*

## 8.3 DISCUSSION

These results provide further evidence to support the role of PI3K activation in the induction of claudin 2 expression. LiCl stimulated both an increase in the level of pAkt and a subsequent increase in claudin 2 expression. IL-13 also stimulated an increase in the level of pAkt that preceded an increase in claudin 2. However, there were differences in the kinetics of the LiCl- and IL-13-induced changes.

LiCl-mediated increases in PI3K activity have been observed in cerebellar granule cells and in cardiomyoblasts (Chalecka-Franaszek and Chuang, 1999; Kashour et al., 2003; Mora et al., 2002), but not in intestinal epithelial cells. The dose-response relationship for this effect is not known, but at physiological intracellular concentrations of magnesium and potassium ions (0.5 and 150mM respectively) the $IC_{50}$ of LiCl for GSK3β inhibition in vitro is 2mM (Davies et al., 2000). Published studies of cell-based assays have suggested that LiCl is effective at 20mM, with a peak effect recorded after

5-6 hours exposure (van Noort et al., 2002). This concords with the present finding of an increase in the level of pGSK that began at 4 hours and peaked at 12 hours of exposure to 20mM LiCl.

The increase in claudin 2 expression induced by IL-13 was clear after 12 hours of exposure and possibly began by 4 hours. It was preceded by an increase in the level of pAkt, indicating increased PI3K activity. Interestingly, an increase in the level of pAkt was seen after 10 minutes exposure to IL-13 in Ultraculture (an insulin-containing serum-free medium; figure 7.7), whereas in insulin-free serum-free medium only a small increase was noted after 10 minutes, with a much larger increase after 1 hour (figure 8.5). These changes are difficult to compare, however, as the amount of pAkt detected in control monolayers was significantly greater when insulin was present, suggesting a degree of background stimulation of PI3K by insulin. It is also possible that insulin synergised with IL-13 to produce an accelerated activation of PI3K.

Although IL-13 and LiCl induced increases in both claudin 2 expression and PI3K activity, more evidence is required to confirm that PI3K activation leads to increased claudin 2 expression. As discussed in chapter 7, expression of a dominant-negative mutant of PI3K would be a highly specific means of inhibiting PI3K activity; if this prevented the increase in claudin 2 induced by IL-13 and LiCl, this would strongly suggest a role for PI3K in this action. Similar methods could be utilised to investigate the role of Akt downstream of PI3K. An ideal approach would be to transfect T84 cells with an Akt mutant in which the serine residue at position 473 had been replaced with an amino acid that cannot be phosphorylated, thus making it resistant to activation. Failure of these cells to increase claudin 2 expression in response to IL-13 or LiCl would provide strong evidence for the involvement of Akt in this response.

The LiCl-stimulated increase in pAkt preceded the increase in pGSK, which itself coincided with the increase in claudin 2 expression. However, no accumulation of pGSK was observed during IL-13 treatment. Thus, although both LiCl and IL-13 led to increases in pAkt and claudin 2, only LiCl induced an increase in pGSK. It must be concluded, therefore, that pGSK does not play a role in the stimulation of claudin 2 expression.

Furthermore, no accumulation of total or hypophosphorylated β-catenin was observed by western blotting during either IL-13 or LiCl treatment. These findings do

not support the proposed model depicted in figure 8.1 and suggest that β-catenin is not transcriptionally activated in T84 cells by treatment with either IL-13 or LiCl.

The methods utilised here have significant limitations for adequately investigating the role of β-catenin in this pathway. Western blotting for an increase in total or hypophosphorylated β-catenin may not be feasible against the high background of total cellular protein. Western blotting of nuclear extracts or a more specific and sensitive method, such as an electromobility shift assay (EMSA), may be more useful in demonstrating whether an increase in transcriptionally-active, nuclear β-catenin occurs in response to IL-13 or LiCl and could detect binding to specific sequences within the claudin 2 promoter. Alternatively, the cells could be transfected with a construct comprising a promoter with β-catenin/TCF-4 consensus sequences in front of the coding sequence of a reporter gene such as luciferase, such as the Topflash TCF reporter gene (Korinek et al., 1997). TCF-stimulated transcription could then be determined by measuring the luciferase activity in the presence or absence of IL-13 or LiCl in the culture medium. An alternative approach would be to investigate the pathway with the use of dominant negative β-catenin constructs to activate β-catenin signalling or altered TCFs to block β-catenin-mediated transcription (DasGupta et al., 2002). In this context it is of interest that Ly294002 treatment of embryonic stem cells has recently been demonstrated to lead to decreases in hypophosphorylated β-catenin only after long term inhibition (4-6 days), suggesting that the β-catenin pathway does not play a major role downstream of PI3K and pAkt (Paling et al., 2004).

In summary, LiCl stimulation of T84 cells led to increases in both PI3K activity and claudin 2 expression. This further supports a role for PI3K in the regulation of claudin 2 expression. The results presented here do not support roles for either GSK3β or β-catenin in the IL-13-induced increase in claudin 2 expression.

# CHAPTER 9

# FINAL DISCUSSION

# 9 CONCLUSIONS

The work presented in this thesis adds to what is currently known about TJ structure and function in the colonic epithelium:

1. Initially, it was shown by two methods (IHC and western blotting) that the normal colonic epithelium contains claudins 3 and 4, and that these can be observed in both TJ and lateral membrane locations. However, no claudin 2 could be detected by IHC and very little by western blotting of epithelial whole cell lysates. The TJ expression of occludin and ZO-1 was confirmed by IHC. In IBD colons alterations in the expression pattern of these proteins were observed. Total claudin 2 expression was markedly increased, and this was observed in the TJs of the crypt epithelium, where the expression of claudins 3 and 4, occludin and ZO-1 was largely unaltered. This suggested that claudin 2 had been introduced into pre-existing TJs. The increase in claudin 2 mRNA levels in IBD suggested that this could be contributing to the increase in protein levels. In the surface epithelium, marked reductions in occludin and ZO-1 and some reductions in claudins 3 and 4 were observed, suggesting that the TJs at this location had to some extent been disassembled. These alterations were observed in areas of resolving inflammation but not in areas of colon proximal to inflammation, suggesting that they are consequences of the inflammatory process.

2. Monolayers of T84 cells, cultured for 8 to 15 days on collagen S-coated supports, were utilised to model the colonic epithelial barrier. They were shown to develop significant and measurable electrical resistances and to express both claudins 3 and 4, whilst expressing claudin 2 in only a small proportion of cells. This model therefore resembled the situation in the normal colonic epithelium. Evidence was also presented that suggested that claudin 2 expression in T84 cells was not associated with either proliferation or plasticity.

3. The inflammatory cytokine IL-17 had previously been shown to induce claudin 2 expression and accelerate the development of TER in partially matured monolayers of T84 cells. Exposure of mature monolayers to this cytokine, however, produced no change in barrier function and only a minor increase in claudin 2 expression, and so did not appear to replicate the situation in IBD described above. Exposing T84 cell

monolayers to either IL-13 or combined IFNγ and TNFα for three days produced only minor toxicity but marked impairments in barrier function, as determined by both falls in TER and increases in permeability to a 4kDa uncharged dextran. Although these impairments were similar, very different changes in claudin expression were observed after exposure to these cytokines. IL-13 did not alter the expression of claudins 3 and 4 but induced a marked increase in claudin 2 expression, which was observed predominantly in the subapical lateral membrane, consistent with its incorporation into TJs. This resembled the increased claudin 2 observed in the crypt epithelium of IBD cases. IFNγ and TNFα on the other hand induced reductions in the TJ expression of claudins 2, 3 and 4. Previous studies had also shown the expression of occludin and ZO-1 to be reduced in IFNγ/TNFα-exposed T84 cells (Bruewer et al., 2003; Mankertz et al., 2000; Mankertz et al., 2002; Youakim and Ahdieh, 1999). Thus, these alterations appeared to resemble the situation observed in the surface epithelium of IBD cases.

4. The binding of IL-13 to its cellular receptor activates several signalling pathways (Hershey, 2003). The IL-13-induced increases in claudin 2 protein expression and claudin 2 mRNA levels could be prevented by the addition of Ly294002, an inhibitor of PI3-kinase. Stimulation of PI3-kinase by lithium chloride led to increased claudin 2 expression. Hence, both IL-13 and lithium chloride stimulate increases in both PI3K activity and claudin 2 expression.

These findings have implications for the pathophysiology of IBD. Both UC and CD are associated with increases in mucosal permeability to ions and small molecules in affected areas of intestine (Gitter et al., 2001; Schmitz et al., 1999), and the reduced TJ strand number and complexity observed by freeze-fracture electron microscopy has been proposed to be the structural correlate of this (Sandle et al., 1990; Schmitz et al., 1999; Schulzke et al., 1998). Claudins have been proposed to form paracellular pores for small ions (Tsukita and Furuse, 2000), with claudin 2 in particular implicated as being leaky to sodium ions (Amasheh et al., 2002; Colegio et al., 2003; Van Itallie et al., 2003). The reduced expression of claudins 3 and 4, occludin and ZO-1 in the surface epithelium may thus be the molecular basis for both the increased permeability and the reduced TJ strand number and complexity. The increased expression of claudin 2 in the TJs of the crypt epithelium would also be expected to increase the permeability of the epithelium to sodium ions (and thus water). Fluid loss due to increased permeability in IBD is one of the major contributors to the predominant symptom of the diseases,

namely diarrhoea (Schmitz et al., 1999). Hence, the results suggest that alterations in claudin expression may contribute to this leak-flux diarrhoea. Indeed, altered TJ structure and function contributes to the diarrhoea caused by many intestinal pathogens, either by altering the cellular cytoskeleton or by affecting specific TJ proteins (Berkes et al., 2003). For example, toxins produced by the bacterium *Clostridium difficile* induce the degradation of filamentous actin, leading to increases in paracellular permeability and diarrhoea (Hecht et al., 1988; Hecht et al., 1992; Nusrat et al., 2001). Alternatively, pathogenic, diarrhoea-producing strains of *Clostridium perfringens* produce an enterotoxin that binds to intestinal epithelial cells by using claudins 3 and 4 as specific receptors (Katahira et al., 1997a; Katahira et al., 1997b). Binding induces reduced claudin 4 expression and disrupted TJ fibrils and function in cultured cells (Sonoda et al., 1999), and increased paracellular permeability in rat intestine (Kondoh et al., 2004). Different mechanisms are involved in the disruption of intestinal TJs by *Vibrio cholera*, *Bacteroides fragilis* and enteropathogenic, enterohaemorrhagic and enterotoxigenic forms of *Escherichia coli*, but all result in diarrhoeal illness (Berkes et al., 2003).

The findings in T84 cells also suggest that the alterations in TJs observed in IBD are mediated by inflammatory cytokines acting directly on epithelial cells. Therefore, treating or preventing the diarrhoea of IBD may be possible by any of the following approaches:

1. Blocking the binding of cytokines to their receptors on epithelial cells using specific inhibitors, such as monoclonal antibodies. A monoclonal antibody to TNFα (infliximab) is already used to treat IBD and is effective in ameliorating the inflammation and symptoms of the disease (Gordon and MacDonald, 2003). It is not known if it reverses the reductions in occludin, ZO-1, claudin 3 and claudin 4 expression in the surface epithelium.

2. Inhibiting or activating the signalling pathways that are activated or inhibited by cytokines. For example, IL-13 activates PI3-kinase, and blocking this with Ly294002 prevented the increase in claudin 2 expression and the fall in TER induced by IL-13.

3. Blocking the translation of the increased claudin 2 mRNA observed in IBD, for example by stimulating RNA interference using specific double-stranded RNA oligonucleotides (Sharp, 2001).

4. Blocking the function of individual claudins by the use of specific molecules. For example, a C-terminal fragment of Clostridium perfringens enterotoxin has recently been shown to reduce the membrane expression of claudin 4 and increase the dextran permeability of rat jejunum in vivo (Kondoh et al., 2004). Construction of a molecule that binds specifically to claudin 2 may have beneficial effects in relation to inflammatory or infective diarrhoea.

Several questions arising from the results presented in this thesis provide the basis for future experimental work:

1. Which other claudins are expressed in the colon and are they affected by inflammation? There are now known to be at least 24 claudins (Schneeberger and Lynch, 2004). The tissue distributions and functions of many of these are not yet known (Turksen and Troy, 2004). It is possible that several of these are expressed in the colonic epithelium and that their expression or functions are altered by inflammation. A comprehensive assessment of colonic claudin expression by IHC and western blotting may be possible, as specific antibodies to most are now available (Zymed).

2. What is the pattern of claudin expression in the various segments of the small intestine, and is this pattern altered in small bowel CD or other small bowel inflammatory conditions, such as celiac disease? In the rat claudins 3 and 4 are expressed in both small and large intestines, but claudin 2 may be expressed at a higher level in the crypts of the small intestine (Rahner et al., 2001). If a similar pattern exists in the human, it might be expected that mucosal permeability to ions is higher in the small intestine, and it would be interesting to examine the effects of inflammation on this pattern in normal and CD-affected ileum and in normal and coeliac disease-affected jejunum by IHC, western blotting and RT-PCR.

3. Why is claudin 2 expression increased in the crypt epithelium of colonic CD? Claudin 2 expression was increased in both UC and CD. As discussed in section 1.1.1.5.4, UC is associated with increased activity of IL-13 and IL-13 was shown in chapter 6 to induce increased claudin 2 expression. However, there is no evidence as yet of increased levels of IL-13 in the mucosa of CD-affected intestine, whereas there is strong evidence of increased levels of Th1 cytokines such as IFNγ and IL-12 (see section 1.1.1.5.4). There are several possible explanations for this: IL-13 expression may in fact be increased in CD mucosa but this may not yet have been observed experimentally, for example increased IL-13 release may occur during distinct phases of

inflammation or in specific regions of the mucosa, such as the deep lamina propria or deeper muscularis layers. In this context it is of interest that IL-4 protein and T cells have been shown to be increased in deeper muscle in CD, and smooth muscle cells contract in response to IL-4 and IL-13 (Akiho et al., 2004). This could be investigated by examining IL-13 expression at several time points during acute, resolving and inactive phases of disease. This could be achieved by IHC for IL-13, or by mounting and culturing endoscopic mucosal biopsies and assaying IL-13 activity in the culture supernatant. Alternatively, there may in CD be an enhanced sensitivity to low and unaltered levels of IL-13. For example, the increase in mucosal IFNγ may stimulate an increase in the crypt epithelial expression of receptors for IL-13, similar to the way in which IFNγ can induce increased expression of TNFα receptors (Fish et al., 1999). Using specific antibodies for IL-13 receptor in both IHC on biopsies and western blotting on isolated epithelial cells may answer this question. Also, one could examine the effects of IFNγ on both IL-13 receptor expression and responses to IL-13 in T84 cells. Another possibility is that the downstream effects of IL-13 on signalling pathways are enhanced by other factors in the inflammatory response that activate the same pathways. It may of course be the case that other cytokines important to the immune and inflammatory responses in CD stimulate epithelial expression of claudin 2, such as IL-17, IL-2 and IL-12. IL-17 provoked a minor increase in claudin 2 expression in mature T84 cell monolayers, but other cytokines have not yet been studied in this regard. It is also possible that increased claudin 2 expression in CD is stimulated by other, non-cytokine-mediated mechanism. In chapter 2 T84 cells were shown to respond to trypsinisation, resuspension and plating by increasing their expression of claudin 2, although the mechanisms which mediate this are unclear. It is possible that epithelial cells in vivo respond to injurious stimuli in a similar way. It may be the case that cleavage of all cell-cell contacts stimulates this expression, and one way of investigating this would be to wound part of a monolayer of mature T84 cells and examine claudin 2 expression along the edge of the wound and distally at various time points. Interestingly, a single study has suggested that several claudins can promote the processing of the protease matrix metalloproteinase-2 from a precursor to an active form (Miyamori et al., 2001), but whether claudins are themselves targets for this protease is not known.

4. Does activated PI3-kinase stimulate an increase in claudin 2 mRNA and protein levels and via what mechanisms? Expression of a dominant-negative mutant of PI3K

would be a highly specific means of inhibiting PI3K activity; if this prevented the increase in claudin 2 induced by IL-13 and LiCl, this would strongly suggest a role for PI3K in this action. The prevention of the effect of Ly294002 by the expression of an active, but Ly294002-resistant, mutant of PI3K would also provide confirmatory evidence for the involvement of PI3K in IL-13stimulated claudin 2 expression. Similar methods could be utilised to investigate the role of Akt downstream of PI3K. An ideal approach would be to transfect T84 cells with an Akt mutant in which the serine residue at position 473 had been replaced with an amino acid that cannot be phosphorylated, thus making it resistant to activation. Failure of these cells to increase claudin 2 expression in response to IL-13 or LiCl would provide strong evidence for the involvement of Akt in this response.

The mechanism leading to the increase in claudin 2 transcripts is not known but could be either an increase in the rate of transcription of the claudin 2 gene or stabilisation of claudin 2 transcripts. The most frequent mechanism leading to an increase in transcript levels is an increase in transcription (Alberts, 2002). A nuclear 'run on' assay could be used to detect changes in de novo synthesis of claudin 2 mRNA transcripts and could therefore confirm whether mRNA synthesis contributes to the increase in mRNA transcript number (Lodish, 2000). The contribution of an increase in the rate of translation of claudin 2 transcripts to the increase in protein cannot be ruled out, particularly as the increase in mRNA induced by IL-13 was relatively small (3- to 15-fold). Increases in the rate of translation of an mRNA tend to lead to reduced degradation and increased stability of that mRNA (Alberts, 2002). Indeed, evidence suggests that activation of PI3K can lead to an increase in protein translation. For example, pAkt can phosphorylate and inhibit tuberin (Manning et al., 2002), preventing it from converting the G protein Rheb from an active, GTP-bound form to an inactive, GDP-bound form (Tee et al., 2003). Rheb.GTP activates the protein mammalian target of rapamycin (mTOR), which controls a number of proteins that either activate protein synthesis or increase the cellular capacity for protein synthesis (Proud, 2004). Using an inhibitor of protein translation, such as cycloheximide, may assist in delineating the contribution of this process to the increased claudin 2 protein expression induced by IL-13.

5. By what mechanism does IL-13 induce an increase in permeability to 4kDa dextran? As discussed earlier, a specific role has been suggested for occludin in

regulating permeability to uncharged molecules. The effects of IL-13 on occludin expression could be examined by immunofluorescence and western blotting. As the removal of occludin from the TJ has been shown to be associated with reduced phosphorylation, the effects of phosphatase inhibitors on IL-13-induced changes could be examined. In a broader context, it would be of value to study how permeability to uncharged molecules, such as sugars, peptides and proteins, and immune cells is affected by cytokines. The movement of neutrophils and dendritic cells across epithelia has been shown to occur without an associated increase in ionic permeability (Huber et al., 2000; Michail et al., 2003; Rescigno et al., 2001), suggesting that they are regulated separately. Changes in TJ protein expression may permit such transmigration, and, therefore, one major goal of research could be to understand how this is regulated and how this could be prevented by therapeutic intervention. Changes in TJ protein expression were observed in areas of colon where inflammation had largely resolved, suggesting that persistent alterations in permeability had occurred. As IBD is characterised by recurrent relapses, inhibiting these permeability changes may reduce the level of exposure of immune cells to foreign antigens and commensals and help to reduce the level of persistent activation of the immune system.

In summary, this thesis has shown that tight junctions are consistently and reproducibly altered in inflammatory bowel disease. IBD-related cytokines induce alterations in both the permeability and the TJ protein expression of cultured colonic epithelial cells. The cytokine-mediated changes appear to be amenable to alteration by drugs, suggesting a future therapeutic strategy that might improve the prognosis for patients with these debilitating diseases.

# APPENDICES

# APPENDIX 1 CONSTITUENTS OF REAGENTS

All reagents obtained from Sigma (Poole, UK) unless otherwise stated.

## TRIS-BUFFERED SALINE SOLUTION (TBS)

| | |
|---|---|
| Tris | 5mM |
| Sodium chloride | 137mM |
| pH 7.60 | |

## CHELATING BUFFER

| | |
|---|---|
| Tri-sodium citrate | 27mM |
| Di-sodium hydrogen orthophosphate | 5mM |
| Sodium chloride | 96mM |
| Potassium hydrogen orthophosphate | 8mM |
| Potassium chloride | 1.5mM |
| Sorbitol | 55mM |
| Sucrose | 44mM |
| Dithiothreitol (DTT) | 0.5mM |
| pH7.3 | |

## SDS SAMPLE BUFFER

| | |
|---|---|
| Tris HCl | 100mM |
| Sodium dodecyl sulphate (SDS) | 5% w/v |
| Glycerol | 20% v/v |
| DTT | 5mM |

PROTEASE INHIBITOR COCKTAIL

| | |
|---|---|
| (4-(2-aminoethyl-)benzenesulfonyl fluoride, pepstatin A, transepoxysuccinyl-L-leucylamido(4-guanidino)butane, bestatin, leupeptin, aprotinin) | 10% v/v |

PHOSPHATASE AND KINASE INHIBITORS

| | |
|---|---|
| EDTA | 1mM |
| EGTA | 1mM |
| Sodium pyrophosphate | 20mM |
| Sodium fluoride | 1mM |
| Activated sodium orthovanadate | 1mM |

RESOLVING GELS

| | |
|---|---|
| Tris HCl (pH 8.8) | 375mM |
| SDS | 0.1% w/v |
| Ammonium persulphate | 0.05% w/v |
| N,N,N′,N′-tetramethylethylenediamine (TEMED) | 0.05% v/v |
| Bis:mono acrylamide (29:1)(40%)(National Diagnostics) | |

STACKING GEL

| | |
|---|---|
| Tris HCl (pH6.8) | 125mM |
| SDS | 0.1% w/v |
| Ammonium persulphate | 0.05% w/v |
| TEMED | 0.1% v/v |
| Bis:mono acrylamide (29:1)(40%)(National Diagnostics) | 10% v/v |

BROMOPHENOL BLUE

| | |
|---|---|
| Bromophenol blue | 5% w/v in absolute ethanol |

ELECTROPHORESIS BUFFER

| | |
|---|---|
| Tris | 25mM |
| Glycine | 192mM |
| SDS | 0.1% w/v |

TRANSFER BUFFER

| | |
|---|---|
| Tris | 25mM |
| Glycine | 192mM |
| Methanol | 20% v/v |

BLOCKING SOLUTION

| | |
|---|---|
| Milk powder | 5% w/v |
| Sodium chloride | 120mM |
| Di-sodium hydrogen orthophosphate | 24.2mM |
| Potassium hydrogen orthophosphate | 5.8mM |
| Tween-20 | 0.1% v/v |

PHOSPHATE-BUFFERED SALINE AND TWEEN20 (PBS-T)

| | |
|---|---|
| Sodium chloride | 120mM |
| Di-sodium hydrogen orthophosphate | 24.2mM |
| Potassium hydrogen orthophosphate | 5.8mM |
| Tween-20 | 0.1% v/v |

STRIPPING BUFFER

| | |
|---|---|
| SDS | 2% w/v |
| Tris HCl | 62.5mM |
| 2-mercaptoethanol | 100mM |
| pH 6.7 | |

REVERSE TRANSCRIPTION MASTERMIX (ALL FROM PROMEGA)

RT Buffer (final concentrations)

| | |
|---|---|
| Tris-HCl (pH 8.3) | 50mM |
| Potassium chloride | 75mM |
| Magnesium chloride | 3mM |
| DTT | 10mM |

Deoxynucleotide triphosphates (dNTPs) mixture

| | |
|---|---|
| Adenosine | 500µM |
| Thymidine | 500µM |
| Guanosine | 500µM |
| Cytidine | 500µM |

| | |
|---|---|
| RNasin RNAse inhibitor | 1000 units/ml |
| Moloney Monkey Reverse Transcriptase | 5000 units/ml |

# APPENDIX 2 DENSITOMETRIC ANALYSIS OF WESTERN BLOTS OF TISSUE EPITHELIAL PROTEIN

## CLAUDIN 2

| Case | Diagnosis | Claudin 2 Band Density | Cytokeratin 19 Band Density | Ratio |
|---|---|---|---|---|
| N47 | NC | 706 | 108137 | 0.007 |
| N60 | NC | 6235 | 165928 | 0.038 |
| N61 | NC | 2321 | 141556 | 0.016 |
| N62 | NC | 8912 | 347766 | 0.026 |
| N44 | NC | 11421 | 410821 | 0.028 |
| N592 | NC | 8300 | 417110 | 0.020 |
| UC17N | UCI | 1028 | 107289 | 0.010 |
| UC13 | UCI | 1331 | 92370 | 0.014 |
| UC8 | UC | 11234421 | 167761 | 66.967 |
| UC9 | UC | 10836085 | 209249 | 51.786 |
| UC10 | UC | 347393 | 627659 | 0.553 |
| UC11 | UC | 42518050 | 451287 | 94.215 |
| UC15 | UC | 67568985 | 349068 | 193.570 |
| UC17 | UC | 2041160 | 157244 | 12.981 |
| CD12 | CD | 60733 | 54824 | 1.108 |
| CD3 | CD | 77018 | 186484 | 0.413 |
| CD8 | CD | 433102 | 40917 | 10.585 |

# CLAUDIN 3

| Case | Diagnosis | Claudin 3 Band Density | Cytokeratin 19 Band Density | Ratio |
|---|---|---|---|---|
| N592 | NC | 399648 | 417110 | 0.958 |
| N47 | NC | 392255 | 108137 | 3.627 |
| N60 | NC | 370490 | 165928 | 2.233 |
| N44 | NC | 136562 | 410821 | 0.332 |
| N61 | NC | 267724 | 141556 | 1.891 |
| N62 | NC | 269969 | 347766 | 0.776 |
| UC13 | UCI | 275419 | 92370 | 2.982 |
| UC17N | UCI | 579617 | 107289 | 5.402 |
| UC7 | UC | 399818 | 221738 | 1.803 |
| UC9 | UC | 352301 | 209249 | 1.684 |
| UC15 | UC | 147515 | 349068 | 0.423 |
| UC8 | UC | 126872 | 167761 | 0.756 |
| UC11 | UC | 214868 | 451287 | 0.476 |
| UC17 | UC | 14066 | 157244 | 0.089 |
| CD12 | CD | 26666 | 54824 | 0.486 |
| CD3 | CD | 126914 | 186484 | 0.681 |
| CD8 | CD | 87580 | 40917 | 2.140 |

# CLAUDIN 4

| Case | Diagnosis | Claudin 4 Band Density | Cytokeratin 19 Band Density | Ratio |
|---|---|---|---|---|
| N592 | NC | 199783 | 417110 | 0.479 |
| N47 | NC | 545834 | 108137 | 5.048 |
| N60 | NC | 239858 | 165928 | 1.446 |
| N44 | NC | 333526 | 410821 | 0.812 |
| N61 | NC | 26392 | 141556 | 0.186 |
| N62 | NC | 696126 | 347766 | 2.002 |
| UC13 | UCI | 400504 | 92370 | 4.336 |
| UC17N | UCI | 604225 | 107289 | 5.632 |
| UC7 | UC | 334952 | 221738 | 1.511 |
| UC9 | UC | 328977 | 209249 | 1.572 |
| UC15 | UC | 276625 | 349068 | 0.792 |
| UC8 | UC | 667957 | 167761 | 3.982 |
| UC11 | UC | 592463 | 451287 | 1.313 |
| UC17 | UC | 237499 | 157244 | 1.510 |
| CD12 | CD | 42407 | 54824 | 0.774 |
| CD3 | CD | 145845 | 186484 | 0.782 |
| CD8 | CD | 389312 | 40917 | 9.515 |

# APPENDIX 3 CLAUDIN 2 Q-RT-PCR DATA IN TISSUE EPITHELIAL CELLS

| Diagnosis | NC | | | | | UC | | | | CD | | | |
|---|---|---|---|---|---|---|---|---|---|---|---|---|---|
| Case | N28 | N30 | N44 | N60 | N61 | UC7 | UC9 | UC17 | UC18 | CD2 | CD3 | CD8 | CD12 |
| $CT_{CL2}$ | 44.0 | 43.4 | 38.8 | 44.2 | 45.3 | 33.1 | 34.8 | 31.2 | 33.8 | 38.1 | 30.5 | 44.4 | 33.4 |
| $CT_{GAPDH}$ | 27.7 | 28.7 | 23.1 | 28.0 | 30.9 | 22.3 | 22.9 | 23.3 | 23.4 | 26.7 | 26.7 | 27.0 | 23.4 |
| $CT_{UBC}$ | 25.8 | 26.0 | 20.4 | 25.6 | 28.0 | 20.4 | 21.2 | 20.1 | 22.1 | 24.0 | 23.5 | 25.7 | 21.8 |
| $CT_{HK}$ | 26.7 | 27.3 | 21.7 | 26.8 | 29.4 | 21.3 | 22.0 | 21.6 | 22.7 | 25.3 | 25.0 | 26.3 | 22.6 |
| -ΔCT | 17.3 | 16.1 | 17.1 | 17.4 | 15.9 | 11.8 | 12.8 | 9.6 | 11.1 | 12.8 | 5.5 | 18.1 | 10.8 |
| ΔΔCT | -0.2 | 1.0 | 0 | -0.3 | 1.2 | 5.3 | 4.3 | 7.5 | 6.0 | 4.3 | 11.6 | -1.0 | 6.3 |
| Rel abun | 0.9 | 2.0 | 1 | 0.8 | 2.3 | 40.2 | 20.2 | 186.2 | 65.8 | 19.9 | 3211.3 | 0.5 | 78.0 |

*Analysis of qRT-PCR data for claudin 2 in tissue samples. Rel abun – relative abundancy.*

# REFERENCES

# REFERENCE LIST

Akiho,H., Lovato,P., Deng,Y., Ceponis,P.J., Blennerhassett,P., and Collins,S.M. (2004). Interleukin-4 and 13-induced hypercontractility of human intestinal muscle cells - implication for motility changes in Crohn's disease. Am. J. Physiol Gastrointest. Liver Physiol.

Alberts,B. (2002). Molecular biology of the cell. New York : Garland Science).

Alessi,D.R., Andjelkovic,M., Caudwell,B., Cron,P., Morrice,N., Cohen,P., and Hemmings,B.A. (1996). Mechanism of activation of protein kinase B by insulin and IGF-1. EMBO J. 15, 6541-6551.

Alessi,D.R., James,S.R., Downes,C.P., Holmes,A.B., Gaffney,P.R., Reese,C.B., and Cohen,P. (1997). Characterization of a 3-phosphoinositide-dependent protein kinase which phosphorylates and activates protein kinase Balpha. Curr. Biol. 7, 261-269.

Almer,S., Franzen,L., Olaison,G., Smedh,K., and Strom,M. (1993). Increased absorption of polyethylene glycol 600 deposited in the colon in active ulcerative colitis. Gut 34, 509-513.

Aman,M.J., Tayebi,N., Obiri,N.I., Puri,R.K., Modi,W.S., and Leonard,W.J. (1996). cDNA cloning and characterization of the human interleukin 13 receptor alpha chain. J. Biol. Chem. 271, 29265-29270.

Amasheh,S., Meiri,N., Gitter,A.H., Schoneberg,T., Mankertz,J., Schulzke,J.D., and Fromm,M. (2002). Claudin-2 expression induces cation-selective channels in tight junctions of epithelial cells. J. Cell Sci. 115, 4969-4976.

Ament,M.E. (1975). Inflammatory disease of the colon: ulcerative colitis and Crohn's colitis. J. Pediatr. 86, 322-334.

Anderson,J.M., Stevenson,B.R., Jesaitis,L.A., Goodenough,D.A., and Mooseker,M.S. (1988). Characterization of ZO-1, a protein component of the tight junction from mouse liver and Madin-Darby canine kidney cells. J. Cell Biol. 106, 1141-1149.

Ando-Akatsuka,Y., Yonemura,S., Itoh,M., Furuse,M., and Tsukita,S. (1999). Differential behavior of E-cadherin and occludin in their colocalization with ZO-1 during the establishment of epithelial cell polarity. J. Cell Physiol 179, 115-125.

Andoh,A., Fujino,S., Bamba,S., Araki,Y., Okuno,T., Bamba,T., and Fujiyama,Y. (2002). IL-17 selectively down-regulates TNF-alpha-induced RANTES gene expression in human colonic subepithelial myofibroblasts. J. Immunol. 169, 1683-1687.

Andre,F., Andre,C., Emery,Y., Forichon,J., Descos,L., and Minaire,Y. (1988). Assessment of the lactulose-mannitol test in Crohn's disease. Gut 29, 511-515.

Andreeva,A.Y., Krause,E., Muller,E.C., Blasig,I.E., and Utepbergenov,D.I. (2001). Protein kinase C regulates the phosphorylation and cellular localization of occludin. J. Biol. Chem. 276, 38480-38486.

Andus,T., Targan,S.R., Deem,R., and Toyoda,H. (1993). Measurement of tumor necrosis factor alpha mRNA in small numbers of cells by quantitative polymerase chain reaction. Reg Immunol. 5, 11-17.

Arato,A., Savilahti,E., and Paszti,I. (1994). Crypt hyperplasia related to increased lymphocyte activation in the rectal mucosa of children with ulcerative colitis. Z. Gastroenterol. 32, 483-487.

Arcaro,A. and Wymann,M.P. (1993). Wortmannin is a potent phosphatidylinositol 3-kinase inhibitor: the role of phosphatidylinositol 3,4,5-trisphosphate in neutrophil responses. Biochem. J. 296 ( Pt 2) , 297-301.

Artis,D., Humphreys,N.E., Bancroft,A.J., Rothwell,N.J., Potten,C.S., and Grencis,R.K. (1999). Tumor necrosis factor alpha is a critical component of interleukin 13-mediated protective T helper cell type 2 responses during helminth infection. J. Exp. Med. 190, 953-962.

Awane,M., Andres,P.G., Li,D.J., and Reinecker,H.C. (1999). NF-kappa B-inducing kinase is a common mediator of IL-17-, TNF-alpha-, and IL-1 beta-induced chemokine promoter activation in intestinal epithelial cells. J. Immunol. 162, 5337-5344.

Backer,J.M., Myers,M.G., Jr., Shoelson,S.E., Chin,D.J., Sun,X.J., Miralpeix,M., Hu,P., Margolis,B., Skolnik,E.Y., Schlessinger,J., and . (1992). Phosphatidylinositol 3'-kinase is activated by association with IRS-1 during insulin stimulation. EMBO J. 11, 3469-3479.

Balda,M.S. and Anderson,J.M. (1993). Two classes of tight junctions are revealed by ZO-1 isoforms. Am. J. Physiol 264, C918-C924.

Balda,M.S., Anderson,J.M., and Matter,K. (1996b). The SH3 domain of the tight junction protein ZO-1 binds to a serine protein kinase that phosphorylates a region C-terminal to this domain. FEBS Lett. 399, 326-332.

Balda,M.S., Flores-Maldonado,C., Cereijido,M., and Matter,K. (2000). Multiple domains of occludin are involved in the regulation of paracellular permeability. J. Cell Biochem. 78, 85-96.

Balda,M.S., Garrett,M.D., and Matter,K. (2003). The ZO-1-associated Y-box factor ZONAB regulates epithelial cell proliferation and cell density. J. Cell Biol. 160, 423-432.

Balda,M.S. and Matter,K. (2000). The tight junction protein ZO-1 and an interacting transcription factor regulate ErbB-2 expression. EMBO J. 19, 2024-2033.

Balda,M.S. and Matter,K. (2003). Epithelial cell adhesion and the regulation of gene expression. Trends Cell Biol. 13, 310-318.

Balda,M.S., Whitney,J.A., Flores,C., Gonzalez,S., Cereijido,M., and Matter,K. (1996a). Functional dissociation of paracellular permeability and transepithelial electrical resistance and disruption of the apical-basolateral intramembrane diffusion barrier by expression of a mutant tight junction membrane protein. J. Cell Biol. 134, 1031-1049.

Bamforth,S.D., Kniesel,U., Wolburg,H., Engelhardt,B., and Risau,W. (1999). A dominant mutant of occludin disrupts tight junction structure and function. J. Cell Sci. 112 ( Pt 12), 1879-1888.

Barton,J.R., Gillon,S., and Ferguson,A. (1989). Incidence of inflammatory bowel disease in Scottish children between 1968 and 1983; marginal fall in ulcerative colitis, three-fold rise in Crohn's disease. Gut 30, 618-622.

Batlle,E., Sancho,E., Franci,C., Dominguez,D., Monfar,M., Baulida,J., and Garcia,D.H. (2000). The transcription factor snail is a repressor of E-cadherin gene expression in epithelial tumour cells. Nat. Cell Biol. 2, 84-89.

Batsche,E., Muchardt,C., Behrens,J., Hurst,H.C., and Cremisi,C. (1998). RB and c-Myc activate expression of the E-cadherin gene in epithelial cells through interaction with transcription factor AP-2. Mol. Cell Biol. 18, 3647-3658.

Bayless,T.M., Tokayer,A.Z., Polito,J.M., Quaskey,S.A., Mellits,E.D., and Harris,M.L. (1996). Crohn's disease: concordance for site and clinical type in affected family members--potential hereditary influences. Gastroenterology 111, 573-579.

Bazzoni,G. (2003). The JAM family of junctional adhesion molecules. Curr. Opin. Cell Biol. 15, 525-530.

Bazzoni,G., Martinez-Estrada,O.M., Orsenigo,F., Cordenonsi,M., Citi,S., and Dejana,E. (2000). Interaction of junctional adhesion molecule with the tight junction components ZO-1, cingulin, and occludin. J. Biol. Chem. 275, 20520-20526.

Behrens,J., Lowrick,O., Klein-Hitpass,L., and Birchmeier,W. (1991). The E-cadherin promoter: functional analysis of a G.C-rich region and an epithelial cell-specific palindromic regulatory element. Proc. Natl. Acad. Sci. U. S. A 88, 11495-11499.

Benais-Pont,G., Punn,A., Flores-Maldonado,C., Eckert,J., Raposo,G., Fleming,T.P., Cereijido,M., Balda,M.S., and Matter,K. (2003). Identification of a tight junction-associated guanine nucleotide exchange factor that activates Rho and regulates paracellular permeability. J. Cell Biol. 160, 729-740.

Berkes,J., Viswanathan,V.K., Savkovic,S.D., and Hecht,G. (2003). Intestinal epithelial responses to enteric pathogens: effects on the tight junction barrier, ion transport, and inflammation. Gut 52, 439-451.

Betanzos,A., Huerta,M., Lopez-Bayghen,E., Azuara,E., Amerena,J., and Gonzalez-Mariscal,L. (2004). The tight junction protein ZO-2 associates with Jun, Fos and C/EBP transcription factors in epithelial cells. Exp. Cell Res. 292, 51-66.

Bjarnason,I. and MacPherson,A.J. (1994). Intestinal toxicity of non-steroidal anti-inflammatory drugs. Pharmacol. Ther. 62, 145-157.

Blaschuk,O.W., Oshima,T., Gour,B.J., Symonds,J.M., Park,J.H., Kevil,C.G., Trocha,S.D., Michaud,S., Okayama,N., Elrod,J.W., and Alexander,J.S. (2002). Identification of an occludin cell adhesion recognition sequence. Inflammation 26, 193-198.

Blumberg,R.S., Saubermann,L.J., and Strober,W. (1999). Animal models of mucosal inflammation and their relation to human inflammatory bowel disease. Curr. Opin. Immunol. 11 , 648-656.

Bonen,D.K. and Cho,J.H. (2003). The genetics of inflammatory bowel disease. Gastroenterology 124, 521-536.

Breese,E., Braegger,C.P., Corrigan,C.J., Walker-Smith,J.A., and MacDonald,T.T. (1993). Interleukin-2- and interferon-gamma-secreting T cells in normal and diseased human intestinal mucosa. Immunology 78, 127-131.

Breslin,N.P., Nash,C., Hilsden,R.J., Hershfield,N.B., Price,L.M., Meddings,J.B., and Sutherland,L.R. (2001). Intestinal permeability is increased in a proportion of spouses of patients with Crohn's disease. Am. J. Gastroenterol. 96, 2934-2938.

Bruewer,M., Hopkins,A.M., Hobert,M.E., Nusrat,A., and Madara,J.L. (2004). RhoA, Rac1, and Cdc42 exert distinct effects on epithelial barrier via selective structural and biochemical modulation of junctional proteins and F-actin. Am. J. Physiol Cell Physiol 287, C327-C335.

Bruewer,M., Luegering,A., Kucharzik,T., Parkos,C.A., Madara,J.L., Hopkins,A.M., and Nusrat,A. (2003). Proinflammatory cytokines disrupt epithelial barrier function by apoptosis-independent mechanisms. J. Immunol. 171, 6164-6172.

Burgel,N., Bojarski,C., Mankertz,J., Zeitz,M., Fromm,M., and Schulzke,J.D. (2002). Mechanisms of diarrhea in collagenous colitis. Gastroenterology 123, 433-443.

Burgering,B.M. and Coffer,P.J. (1995). Protein kinase B (c-Akt) in phosphatidylinositol-3-OH kinase signal transduction. Nature 376, 599-602.

Caput,D., Laurent,P., Kaghad,M., Lelias,J.M., Lefort,S., Vita,N., and Ferrara,P. (1996). Cloning and characterization of a specific interleukin (IL)-13 binding protein structurally related to the IL-5 receptor alpha chain. J. Biol. Chem. 271, 16921-16926.

Ceponis,P.J., Botelho,F., Richards,C.D., and McKay,D.M. (2000). Interleukins 4 and 13 increase intestinal epithelial permeability by a phosphatidylinositol 3-kinase pathway. Lack of evidence for STAT 6 involvement. J. Biol. Chem. 275, 29132-29137.

Chalecka-Franaszek,E. and Chuang,D.M. (1999). Lithium activates the serine/threonine kinase Akt-1 and suppresses glutamate-induced inhibition of Akt-1 activity in neurons. Proc. Natl. Acad. Sci. U. S. A 96, 8745-8750.

Chen,Y., Lu,Q., Schneeberger,E.E., and Goodenough,D.A. (2000). Restoration of tight junction structure and barrier function by down-regulation of the mitogen-activated protein kinase pathway in ras-transformed Madin-Darby canine kidney cells. Mol. Biol. Cell 11, 849-862.

Chen,Y.H. and Lu,Q. (2003). Association of nonreceptor tyrosine kinase c-yes with tight junction protein occludin by coimmunoprecipitation assay. Methods Mol. Biol. 218, 127-132.

Chen,Y.H., Lu,Q., Goodenough,D.A., and Jeansonne,B. (2002). Nonreceptor tyrosine kinase c-Yes interacts with occludin during tight junction formation in canine kidney epithelial cells. Mol. Biol. Cell 13, 1227-1237.

Citi,S., Sabanay,H., Jakes,R., Geiger,B., and Kendrick-Jones,J. (1988). Cingulin, a new peripheral component of tight junctions. Nature 333, 272-276.

Clarke,H., Soler,A.P., and Mullin,J.M. (2000). Protein kinase C activation leads to dephosphorylation of occludin and tight junction permeability increase in LLC-PK1 epithelial cell sheets. J. Cell Sci. 113 ( Pt 18), 3187-3196.

Colegio,O.R., Van Itallie,C., Rahner,C., and Anderson,J.M. (2003). Claudin Extracellular Domains Determine Paracellular Charge Selectivity and Resistance but not Tight Junction Fibril Architecture. Am. J. Physiol Cell Physiol.

Colegio,O.R., Van Itallie,C.M., McCrea,H.J., Rahner,C., and Anderson,J.M. (2002). Claudins create charge-selective channels in the paracellular pathway between epithelial cells. Am. J. Physiol Cell Physiol 283, C142-C147.

Collins,J.E. (2002). Adhesion between dendritic cells and epithelial cells maintains the gut barrier during bacterial sampling. Gut 50, 449-450.

Cominelli,F. (2004). Cytokine-based therapies for Crohn's disease--new paradigms. N. Engl. J. Med. 351, 2045-2048.

Cordenonsi,M., D'Atri,F., Hammar,E., Parry,D.A., Kendrick-Jones,J., Shore,D., and Citi,S. (1999). Cingulin contains globular and coiled-coil domains and interacts with ZO-1, ZO-2, ZO-3, and myosin. J. Cell Biol. 147, 1569-1582.

Cross,D.A., Alessi,D.R., Cohen,P., Andjelkovich,M., and Hemmings,B.A. (1995). Inhibition of glycogen synthase kinase-3 by insulin mediated by protein kinase B. Nature 378, 785-789.

Danese,S., Sans,M., and Fiocchi,C. (2004). Inflammatory bowel disease: the role of environmental factors. Autoimmun. Rev. 3, 394-400.

Darfeuille-Michaud,A., Boudeau,J., Bulois,P., Neut,C., Glasser,A.L., Barnich,N., Bringer,M.A., Swidsinski,A., Beaugerie,L., and Colombel,J.F. (2004). High prevalence of

adherent-invasive Escherichia coli associated with ileal mucosa in Crohn's disease. Gastroenterology 127, 412-421.

Darfeuille-Michaud,A., Neut,C., Barnich,N., Lederman,E., Di Martino,P., Desreumaux,P., Gambiez,L., Joly,B., Cortot,A., and Colombel,J.F. (1998). Presence of adherent Escherichia coli strains in ileal mucosa of patients with Crohn's disease. Gastroenterology 115, 1405-1413.

Das,K.M., Dasgupta,A., Mandal,A., and Geng,X. (1993). Autoimmunity to cytoskeletal protein tropomyosin. A clue to the pathogenetic mechanism for ulcerative colitis. J. Immunol. 150, 2487-2493.

DasGupta,R., Rhee,H., and Fuchs,E. (2002). A developmental conundrum: a stabilized form of beta-catenin lacking the transcriptional activation domain triggers features of hair cell fate in epidermal cells and epidermal cell fate in hair follicle cells. J. Cell Biol. 158, 331-344.

Davies,S.P., Reddy,H., Caivano,M., and Cohen,P. (2000). Specificity and mechanism of action of some commonly used protein kinase inhibitors. Biochem. J. 351, 95-105.

Desreumaux,P., Brandt,E., Gambiez,L., Emilie,D., Geboes,K., Klein,O., Ectors,N., Cortot,A., Capron,M., and Colombel,J.F. (1997). Distinct cytokine patterns in early and chronic ileal lesions of Crohn's disease. Gastroenterology 113, 118-126.

Dever,T.E. (1999). Translation initiation: adept at adapting. Trends Biochem. Sci. 24, 398-403.

Dharmsathaphorn,K., Mandel,K.G., Masui,H., and McRoberts,J.A. (1985). Vasoactive intestinal polypeptide-induced chloride secretion by a colonic epithelial cell line. Direct participation of a basolaterally localized Na+,K+,Cl- cotransport system. J. Clin. Invest 75, 462-471.

Dharmsathaphorn,K., McRoberts,J.A. , Mandel,K.G., Tisdale,L.D., and Masui,H. (1984). A human colonic tumor cell line that maintains vectorial electrolyte transport. Am. J. Physiol 246, G204-G208.

Dieckgraefe,B.K. and Korzenik,J.R. (2002). Treatment of active Crohn's disease with recombinant human granulocyte-macrophage colony-stimulating factor. Lancet 360, 1478-1480.

Doble,B.W. and Woodgett,J.R. (2003). GSK-3: tricks of the trade for a multi-tasking kinase . J. Cell Sci. 116, 1175-1186.

Domon-Dell,C. and Freund,J.N. (2002). Stimulation of Cdx1 by oncogenic beta-catenin/Tcf4 in colon cancer cells: opposite effect of the CDX2 homeoprotein. FEBS Lett. 518, 83-87.

Downward,J. (1998). Mechanisms and consequences of activation of protein kinase B/Akt. Curr. Opin. Cell Biol. 10, 262-267.

Duchmann,R., Kaiser,I., Hermann,E., Mayet,W., Ewe,K., and Meyer zum Buschenfelde,K.H. (1995). Tolerance exists towards resident intestinal flora but is broken in active inflammatory bowel disease (IBD). Clin. Exp. Immunol. 102, 448-455.

Ebnet,K., Schulz,C.U., Meyer Zu Brickwedde,M.K., Pendl,G.G., and Vestweber,D. (2000). Junctional adhesion molecule interacts with the PDZ domain-containing proteins AF-6 and ZO-1. J. Biol. Chem. 275, 27979-27988.

Ebnet,K., Suzuki,A., Horikoshi,Y., Hirose,T., Meyer Zu Brickwedde,M.K., Ohno,S., and Vestweber,D. (2001). The cell polarity protein ASIP/PAR-3 directly associates with junctional adhesion molecule (JAM). EMBO J. 20, 3738-3748.

Edmiston,C.E., Jr., Avant,G.R., and Wilson,F.A. (1982). Anaerobic bacterial populations on normal and diseased human biopsy tissue obtained at colonoscopy. Appl. Environ. Microbiol. 43, 1173-1181.

Escaffit,F., Boudreau,F., and Beaulieu,J.F. (2004). Differential expression of claudin-2 along the human intestine: Implication of GATA-4 in the maintenance of claudin-2 in differentiating cells. J. Cell Physiol.

Evans,W.H. and Martin,P.E. (2002). Gap junctions: structure and function (Review). Mol. Membr. Biol. 19, 121-136.

Fais,S., Capobianchi,M.R., Pallone,F., Di Marco,P., Boirivant,M., Dianzani,F., and Torsoli,A. (1991). Spontaneous release of interferon gamma by intestinal lamina propria lymphocytes in Crohn's disease. Kinetics of in vitro response to interferon gamma inducers. Gut 32, 403-407.

Fanning,A.S., Jameson,B.J., Jesaitis,L.A., and Anderson,J.M. (1998). The tight junction protein ZO-1 establishes a link between the transmembrane protein occludin and the actin cytoskeleton. J. Biol. Chem. 273, 29745-29753.

Fanning,A.S., Ma,T.Y., and Anderson,J.M. (2002). Isolation and functional characterization of the actin-binding region in the tight junction protein ZO-1. FASEB J.

Farmer,M., Petras,R.E., Hunt,L.E., Janosky,J.E., and Galandiuk,S. (2000). The importance of diagnostic accuracy in colonic inflammatory bowel disease. Am. J. Gastroenterol. 95, 3184-3188.

Farquhar,M.G. and Palade,G.E. (1965). Cell junctions in amphibian skin. J. Cell Biol. 26, 263-291.

Farrell,R.J. and Peppercorn,M.A. (2002). Ulcerative colitis. Lancet 359, 331-340.

Farshori,P. and Kachar,B. (1999). Redistribution and phosphorylation of occludin during opening and resealing of tight junctions in cultured epithelial cells. J. Membr. Biol. 170, 147-156.

Fish,S.M., Proujansky,R., and Reenstra,W.W. (1999). Synergistic effects of interferon gamma and tumour necrosis factor alpha on T84 cell function . Gut 45, 191-198.

Fleming,T.P. and Hay,M.J. (1991). Tissue-specific control of expression of the tight junction polypeptide ZO-1 in the mouse early embryo. Development 113, 295-304.

Fleming,T.P., Papenbrock,T., Fesenko,I., Hausen,P., and Sheth,B. (2000). Assembly of tight junctions during early vertebrate development. Semin. Cell Dev. Biol. 11, 291-299.

Flint,N., Cove,F.L., and Evans,G.S. (1991). A low-temperature method for the isolation of small-intestinal epithelium along the crypt-villus axis. Biochem. J. 280 ( Pt 2) , 331-334.

Forrest,J.C., Campbell,J.A., Schelling,P., Stehle,T., and Dermody,T.S. (2003). Structure-function analysis of reovirus binding to junctional adhesion molecule 1. Implications for the mechanism of reovirus attachment. J. Biol. Chem. 278, 48434-48444.

Franchimont,D., Vermeire,S., El Housni,H., Pierik,M., Van Steen,K., Gustot,T., Quertinmont,E., Abramowicz,M., Van Gossum,A., Deviere,J., and Rutgeerts,P. (2004). Deficient host-bacteria interactions in inflammatory bowel disease? The toll-like receptor (TLR)-4 Asp299gly polymorphism is associated with Crohn's disease and ulcerative colitis. Gut 53, 987-992.

Franke,T.F., Yang,S.I., Chan,T.O., Datta,K., Kazlauskas,A., Morrison,D.K., Kaplan,D.R., and Tsichlis,P.N. (1995). The protein kinase encoded by the Akt proto-oncogene is a target of the PDGF-activated phosphatidylinositol 3-kinase. Cell 81, 727-736.

Franklin,W.A., McDonald,G.B., Stein,H.O., Gatter,K.C., Jewell,D.P., Clarke,L.C., and Mason,D.Y. (1985). Immunohistologic demonstration of abnormal colonic crypt cell kinetics in ulcerative colitis. Hum. Pathol. 16, 1129-1132.

Fujino,S., Andoh,A., Bamba,S., Ogawa,A., Hata,K., Araki,Y., Bamba,T., and Fujiyama,Y. (2003). Increased expression of interleukin 17 in inflammatory bowel disease. Gut 52, 65-70.

Furuse,M., Fujita,K., Hiiragi,T., Fujimoto,K., and Tsukita,S. (1998a). Claudin-1 and -2: novel integral membrane proteins localizing at tight junctions with no sequence similarity to occludin. J. Cell Biol. 141, 1539-1550.

Furuse,M., Hata,M., Furuse,K., Yoshida,Y., Haratake,A., Sugitani,Y., Noda,T., Kubo,A., and Tsukita,S. (2002). Claudin-based tight junctions are crucial for the mammalian epidermal barrier: a lesson from claudin-1-deficient mice. J. Cell Biol. 156, 1099-1111.

Furuse,M., Hirase,T., Itoh,M., Nagafuchi,A., Yonemura,S., Tsukita,S., and Tsukita,S. (1993). Occludin: a novel integral membrane protein localizing at tight junctions. J. Cell Biol. 123, 1777-1788.

Furuse,M., Itoh,M., Hirase,T., Nagafuchi,A., Yonemura,S., Tsukita,S., and Tsukita,S. (1994). Direct association of occludin with ZO-1 and its possible involvement in the localization of occludin at tight junctions. J. Cell Biol. 127, 1617-1626.

Furuse,M., Sasaki,H., Fujimoto,K., and Tsukita,S. (1998b). A single gene product, claudin-1 or -2, reconstitutes tight junction strands and recruits occludin in fibroblasts. J. Cell Biol. 143, 391-401.

Furuse,M., Sasaki,H., and Tsukita,S. (1999). Manner of interaction of heterogeneous claudin species within and between tight junction strands. J. Cell Biol. 147, 891-903.

Fuss,I.J., Heller,F., Boirivant,M., Leon,F., Yoshida,M., Fichtner-Feigl,S., Yang,Z., Exley,M., Kitani,A., Blumberg,R.S., Mannon,P., and Strober,W. (2004). Nonclassical CD1d-restricted NK T cells that produce IL-13 characterize an atypical Th2 response in ulcerative colitis. J. Clin. Invest 113, 1490-1497.

Fuss,I.J., Neurath,M., Boirivant,M., Klein,J.S., de la,M.C., Strong,S.A., Fiocchi,C., and Strober,W. (1996). Disparate CD4+ lamina propria (LP) lymphokine secretion profiles in inflammatory bowel disease. Crohn's disease LP cells manifest increased secretion of IFN-gamma, whereas ulcerative colitis LP cells manifest increased secretion of IL-5. J. Immunol. 157, 1261-1270.

Garrod,D.R., Merritt,A.J., and Nie,Z. (2002). Desmosomal adhesion: structural basis, molecular mechanism and regulation (Review). Mol. Membr. Biol. 19, 81-94.

Gassler,N., Rohr,C., Schneider,A., Kartenbeck,J., Bach,A., Obermuller,N., Otto,H.F., and Autschbach,F. (2001). Inflammatory bowel disease is associated with changes of enterocytic junctions. Am. J. Physiol Gastrointest. Liver Physiol 281, G216-G228.

Gerdes,J., Lemke,H., Baisch,H., Wacker,H.H., Schwab,U., and Stein,H. (1984). Cell cycle analysis of a cell proliferation-associated human nuclear antigen defined by the monoclonal antibody Ki-67. J. Immunol. 133, 1710-1715.

Gerdes,J., Schwab,U., Lemke,H., and Stein,H. (1983). Production of a mouse monoclonal antibody reactive with a human nuclear antigen associated with cell proliferation. Int. J. Cancer 31, 13-20.

Ghassemifar,M.R., Sheth,B., Papenbrock,T., Leese,H.J., Houghton,F.D., and Fleming,T.P. (2002). Occludin TM4(-): an isoform of the tight junction protein present in primates lacking the fourth transmembrane domain. J. Cell Sci. 115, 3171-3180.

Giles,R.H., van Es,J.H., and Clevers,H. (2003). Caught up in a Wnt storm: Wnt signaling in cancer. Biochim. Biophys. Acta 1653, 1-24.

Gitter,A.H., Wullstein,F., Fromm,M., and Schulzke,J.D. (2001). Epithelial barrier defects in ulcerative colitis: characterization and quantification by electrophysiological imaging. Gastroenterology 121, 1320-1328.

Glasser,A.L., Boudeau,J., Barnich,N., Perruchot,M.H., Colombel,J.F., and Darfeuille-Michaud,A. (2001). Adherent invasive Escherichia coli strains from patients with Crohn's disease survive and replicate within macrophages without inducing host cell death. Infect. Immun. 69, 5529-5537.

Gonzalez-Mariscal,L., Betanzos,A., Nava,P., and Jaramillo,B.E. (2003). Tight junction proteins. Prog. Biophys. Mol. Biol. 81, 1-44.

Gonzalez-Mariscal,L., Islas,S., Contreras,R.G., Garcia-Villegas,M.R., Betanzos,A., Vega,J., Diaz-Quinonez,A., Martin-Orozco,N., Ortiz-Navarrete,V., Cereijido,M., and Valdes,J. (1999). Molecular characterization of the tight junction protein ZO-1 in MDCK cells. Exp. Cell Res. 248, 97-109.

Gonzalez-Mariscal,L., Namorado,M.C., Martin,D., Luna,J., Alarcon,L., Islas,S., Valencia,L., Muriel,P., Ponce,L., and Reyes,J.L. (2000). Tight junction proteins ZO-1, ZO-2, and occludin along isolated renal tubules. Kidney Int. 57, 2386-2402.

Gopalakrishnan,S., Raman,N., Atkinson,S.J., and Marrs,J.A. (1998). Rho GTPase signaling regulates tight junction assembly and protects tight junctions during ATP depletion. Am. J. Physiol 275, C798-C809.

Gordon,J.N. and MacDonald,T.T. (2003). Biological therapy in Crohn's disease. Hosp. Med. 64, 708-712.

Gottardi,C.J., Arpin,M., Fanning,A.S., and Louvard,D. (1996). The junction-associated protein, zonula occludens-1, localizes to the nucleus before the maturation and during the remodeling of cell-cell contacts. Proc. Natl. Acad. Sci. U. S. A 93, 10779-10784.

Gray,N.K. and Wickens,M. (1998). Control of translation initiation in animals. Annu. Rev. Cell Dev. Biol. 14, 399-458.

Green,K.J. and Gaudry,C.A. (2000). Are desmosomes more than tethers for intermediate filaments? Nat. Rev. Mol. Cell Biol. 1, 208-216.

Grindstaff,K.K., Yeaman,C., Anandasabapathy,N., Hsu,S.C., Rodriguez-Boulan,E., Scheller,R.H., and Nelson,W.J. (1998). Sec6/8 complex is recruited to cell-cell contacts and specifies transport vesicle delivery to the basal-lateral membrane in epithelial cells. Cell 93, 731-740.

Gumbiner,B., Stevenson,B., and Grimaldi,A. (1988). The role of the cell adhesion molecule uvomorulin in the formation and maintenance of the epithelial junctional complex. J. Cell Biol. 107, 1575-1587.

Hamazaki,Y., Itoh,M., Sasaki,H., Furuse,M., and Tsukita,S. (2002). Multi-PDZ domain protein 1 (MUPP1) is concentrated at tight junctions through its possible interaction with claudin-1 and junctional adhesion molecule. J. Biol. Chem. 277, 455-461.

Hampe,J., Cuthbert,A., Croucher,P.J., Mirza,M.M., Mascheretti,S., Fisher,S., Frenzel,H., King,K., Hasselmeyer,A., MacPherson,A.J., Bridger,S., van Deventer,S., Forbes,A., Nikolaus,S., Lennard-Jones,J.E., Foelsch,U.R., Krawczak,M., Lewis,C., Schreiber,S., and Mathew,C.G. (2001). Association between insertion mutation in NOD2 gene and Crohn's disease in German and British populations. Lancet 357, 1925-1928.

Hartley,M.G., Hudson,M.J., Swarbrick,E.T., Hill,M.J., Gent,A.E., Hellier,M.D., and Grace,R.H. (1992). The rectal mucosa-associated microflora in patients with ulcerative colitis. J. Med. Microbiol. 36, 96-103.

Haskins,J., Gu,L., Wittchen,E.S., Hibbard,J., and Stevenson,B.R. (1998). ZO-3, a novel member of the MAGUK protein family found at the tight junction, interacts with ZO-1 and occludin. J. Cell Biol. 141, 199-208.

Hecht,G., Koutsouris,A., Pothoulakis,C., LaMont,J.T., and Madara,J.L. (1992). Clostridium difficile toxin B disrupts the barrier function of T84 monolayers. Gastroenterology 102, 416-423.

Hecht,G., Pothoulakis,C., LaMont,J.T., and Madara,J.L. (1988). Clostridium difficile toxin A perturbs cytoskeletal structure and tight junction permeability of cultured human intestinal epithelial monolayers. J. Clin. Invest 82, 1516-1524.

Heller,F., Fuss,I.J., Nieuwenhuis,E.E., Blumberg,R.S., and Strober,W. (2002). Oxazolone colitis, a Th2 colitis model resembling ulcerative colitis, is mediated by IL-13-producing NK-T cells. Immunity. 17, 629-638.

Hennig,G., Lowrick,O., Birchmeier,W., and Behrens,J. (1996). Mechanisms identified in the transcriptional control of epithelial gene expression. J. Biol. Chem. 271, 595-602.

Hershey,G.K. (2003). IL-13 receptors and signaling pathways: an evolving web. J. Allergy Clin. Immunol. 111, 677-690.

Hilsden,R.J., Meddings,J.B., and Sutherland,L.R. (1996). Intestinal permeability changes in response to acetylsalicylic acid in relatives of patients with Crohn's disease. Gastroenterology 110, 1395-1403.

Hilton,D.J., Zhang,J.G., Metcalf,D., Alexander,W.S., Nicola,N.A., and Willson,T.A. (1996). Cloning and characterization of a binding subunit of the interleukin 13 receptor that is also a component of the interleukin 4 receptor. Proc. Natl. Acad. Sci. U. S. A 93, 497-501.

Hirabayashi,S., Tajima,M., Yao,I., Nishimura,W., Mori,H., and Hata,Y. (2003). JAM4, a Junctional Cell Adhesion Molecule Interacting with a Tight Junction Protein, MAGI-1. Mol. Cell Biol. 23, 4267-4282.

Hisamatsu,T., Suzuki,M., Reinecker,H.C., Nadeau,W.J., McCormick,B.A., and Podolsky,D.K. (2003). CARD15/NOD2 functions as an antibacterial factor in human intestinal epithelial cells. Gastroenterology 124, 993-1000.

Hollander,D. (2003). Inflammatory bowel diseases and brain-gut axis. J. Physiol Pharmacol. 54 Suppl 4, 183-190.

Hollander,D., Vadheim,C.M., Brettholz,E., Petersen,G.M., Delahunty,T., and Rotter,J.I. (1986). Increased intestinal permeability in patients with Crohn's disease and their relatives. A possible etiologic factor. Ann. Intern. Med. 105, 883-885.

Hosono,S., Gross,I., English,M.A., Hajra,K.M., Fearon,E.R., and Licht,J.D. (2000). E-cadherin is a WT1 target gene. J. Biol. Chem. 275, 10943-10953.

Huber,D., Balda,M.S., and Matter,K. (2000). Occludin modulates transepithelial migration of neutrophils. J. Biol. Chem. 275, 5773-5778.

Hudson,M.J., Hill,M.J., Elliott,P.R., Berghouse,L.M., Burnham,W.R., and Lennard-Jones,J.E. (1984). The microbial flora of the rectal mucosa and faeces of patients with Crohn's disease before and during antimicrobial chemotherapy. J. Med. Microbiol. 18, 335-345.

Huelsken,J. and Behrens,J. (2002). The Wnt signalling pathway. J. Cell Sci. 115, 3977-3978.

Hughes,K., Nikolakaki,E., Plyte,S.E., Totty,N.F., and Woodgett,J.R. (1993). Modulation of the glycogen synthase kinase-3 family by tyrosine phosphorylation. EMBO J. 12, 803-808.

Hugot,J.P., Chamaillard,M., Zouali,H., Lesage,S., Cezard,J.P., Belaiche,J., Almer,S., Tysk,C., O'Morain,C.A., Gassull,M., Binder,V., Finkel,Y., Cortot,A., Modigliani,R., Laurent-Puig,P., Gower-Rousseau,C., Macry,J., Colombel,J.F., Sahbatou,M., and Thomas,G. (2001). Association of NOD2 leucine-rich repeat variants with susceptibility to Crohn's disease. Nature 411, 599-603.

Humbert,P., Russell,S., and Richardson,H. (2003). Dlg, Scribble and Lgl in cell polarity, cell proliferation and cancer. Bioessays 25, 542-553.

Inai,T., Kobayashi,J., and Shibata,Y. (1999). Claudin-1 contributes to the epithelial barrier function in MDCK cells. Eur. J. Cell Biol. 78, 849-855.

Inohara,N., Ogura,Y., Fontalba,A., Gutierrez,O., Pons,F., Crespo,J., Fukase,K., Inamura,S., Kusumoto,S., Hashimoto,M., Foster,S.J., Moran,A.P., Fernandez-Luna,J.L., and Nunez,G.

(2003). Host recognition of bacterial muramyl dipeptide mediated through NOD2. Implications for Crohn's disease. J. Biol. Chem. 278 , 5509-5512.

Inoue,S., Matsumoto,T., Iida,M., Mizuno,M., Kuroki,F., Hoshika,K., and Shimizu,M. (1999). Characterization of cytokine expression in the rectal mucosa of ulcerative colitis: correlation with disease activity . Am. J. Gastroenterol. 94, 2441-2446.

Irvine,E.J. and Marshall,J.K. (2000). Increased intestinal permeability precedes the onset of Crohn's disease in a subject with familial risk. Gastroenterology 119, 1740-1744.

Islas,S., Vega,J., Ponce,L., and Gonzalez-Mariscal,L. (2002). Nuclear localization of the tight junction protein ZO-2 in epithelial cells. Exp. Cell Res. 274, 138-148.

Itoh,M., Furuse,M., Morita,K., Kubota,K., Saitou,M., and Tsukita,S. (1999a). Direct binding of three tight junction-associated MAGUKs, ZO-1, ZO-2, and ZO-3, with the COOH termini of claudins. J. Cell Biol. 147, 1351-1363.

Itoh,M., Morita,K., and Tsukita,S. (1999b). Characterization of ZO-2 as a MAGUK family member associated with tight as well as adherens junctions with a binding affinity to occludin and alpha catenin. J. Biol. Chem. 274, 5981-5986.

James,S.P. (1988). Cellular immune mechanisms in the pathogenesis of Crohn's disease. In Vivo 2, 1-7.

James,S.P., Strober,W., Quinn,T.C., and Danovitch,S.H. (1987). Crohn's disease. New concepts of pathogenesis and current approaches to treatment. Dig. Dis. Sci. 32, 1297-1310.

Jamora,C. and Fuchs,E. (2002). Intercellular adhesion, signalling and the cytoskeleton. Nat. Cell Biol. 4, E101-E108.

Jeansonne,B., Lu,Q., Goodenough,D.A., and Chen,Y.H. (2003). Claudin-8 interacts with multi-PDZ domain protein 1 (MUPP1) and reduces paracellular conductance in epithelial cells. Cell Mol. Biol. (Noisy. -le-grand) 49, 13-21.

Jiang,H., Harris,M.B., and Rothman,P. (2000). IL-4/IL-13 signaling beyond JAK/STAT. J. Allergy Clin. Immunol. 105, 1063-1070.

Johnson-Leger,C.A., Aurrand-Lions,M., Beltraminelli,N., Fasel,N., and Imhof,B.A. (2002). Junctional adhesion molecule-2 (JAM-2) promotes lymphocyte transendothelial migration. Blood 100, 2479-2486.

Jordan,M.S., Boesteanu,A., Reed,A.J., Petrone,A.L., Holenbeck,A.E., Lerman,M.A., Naji,A., and Caton,A.J. (2001). Thymic selection of CD4+CD25+ regulatory T cells induced by an agonist self-peptide. Nat. Immunol. 2, 301-306.

Jou,T.S., Schneeberger,E.E., and Nelson,W.J. (1998). Structural and functional regulation of tight junctions by RhoA and Rac1 small GTPases. J. Cell Biol. 142, 101-115.

Jovanovic,D.V., Di Battista,J.A., Martel-Pelletier,J., Jolicoeur,F.C., He,Y., Zhang,M., Mineau,F., and Pelletier,J.P. (1998). IL-17 stimulates the production and expression of proinflammatory cytokines, IL-beta and TNF-alpha, by human macrophages. J. Immunol. 160, 3513-3521.

Kadivar,K., Ruchelli,E.D., Markowitz,J.E., Defelice,M.L., Strogatz,M.L., Kanzaria,M.M., Reddy,K.P., Baldassano,R.N., von Allmen,D., and Brown,K.A. (2004). Intestinal interleukin-13 in pediatric inflammatory bowel disease patients. Inflamm. Bowel. Dis. 10, 593-598.

Kanai,F., Ito,K., Todaka,M., Hayashi,H., Kamohara,S., Ishii,K., Okada,T., Hazeki,O., Ui,M., and Ebina,Y. (1993). Insulin-stimulated GLUT4 translocation is relevant to the phosphorylation of IRS-1 and the activity of PI3-kinase. Biochem. Biophys. Res. Commun. 195, 762-768.

Kashour,T., Burton,T., Dibrov,A., and Amara,F. (2003). Myogenic signaling by lithium in cardiomyoblasts is Akt independent but requires activation of the beta-catenin-Tcf/Lef pathway. J. Mol. Cell Cardiol. 35, 937-951.

Katahira,J., Inoue,N., Horiguchi,Y., Matsuda,M., and Sugimoto,N. (1997b). Molecular cloning and functional characterization of the receptor for Clostridium perfringens enterotoxin. J. Cell Biol. 136, 1239-1247.

Katahira,J., Sugiyama,H., Inoue,N., Horiguchi,Y., Matsuda,M., and Sugimoto,N. (1997a). Clostridium perfringens enterotoxin utilizes two structurally related membrane proteins as functional receptors in vivo. J. Biol. Chem. 272, 26652-26658.

Katoh,M. and Katoh,M. (2003). CLDN23 gene, frequently down-regulated in intestinal-type gastric cancer, is a novel member of CLAUDIN gene family. Int. J. Mol. Med. 11, 683-689.

Kawabe,H., Nakanishi,H., Asada,M., Fukuhara,A., Morimoto,K., Takeuchi,M., and Takai,Y. (2001). Pilt, a novel peripheral membrane protein at tight junctions in epithelial cells. J. Biol. Chem. 276, 48350-48355.

Keegan,A.D., Johnston,J.A., Tortolani,P.J., McReynolds,L.J., Kinzer,C., O'Shea,J.J., and Paul,W.E. (1995). Similarities and differences in signal transduction by interleukin 4 and interleukin 13: analysis of Janus kinase activation. Proc. Natl. Acad. Sci. U. S. A 92, 7681-7685.

Keegan,A.D., Nelms,K., White,M., Wang,L.M., Pierce,J.H., and Paul,W.E. (1994). An IL-4 receptor region containing an insulin receptor motif is important for IL-4-mediated IRS-1 phosphorylation and cell growth. Cell 76, 811-820.

Kelly-Welch,A.E., Hanson,E.M., Boothby,M.R., and Keegan,A.D. (2003). Interleukin-4 and interleukin-13 signaling connections maps. Science 300, 1527-1528.

Keon,B.H., Schafer,S., Kuhn,C., Grund,C., and Franke,W.W. (1996). Symplekin, a novel type of tight junction plaque protein. J. Cell Biol. 134, 1003-1018.

Kett,K., Rognum,T.O., and Brandtzaeg,P. (1987). Mucosal subclass distribution of immunoglobulin G-producing cells is different in ulcerative colitis and Crohn's disease of the colon. Gastroenterology 93, 919-924.

Kiliaan,A.J., Saunders,P.R., Bijlsma,P.B., Berin,M.C., Taminiau,J.A., Groot,J.A., and Perdue,M.H. (1998). Stress stimulates transepithelial macromolecular uptake in rat jejunum. Am. J. Physiol 275, G1037-G1044.

Kinugasa,T., Sakaguchi,T., Gu,X., and Reinecker,H.C. (2000). Claudins regulate the intestinal barrier in response to immune mediators. Gastroenterology 118, 1001-1011.

Kitajima,S., Takuma,S., and Morimoto,M. (1999). Changes in colonic mucosal permeability in mouse colitis induced with dextran sulfate sodium. Exp. Anim 48, 137-143.

Kiuchi-Saishin,Y., Gotoh,S., Furuse,M., Takasuga,A., Tano,Y., and Tsukita,S. (2002). Differential expression patterns of claudins, tight junction membrane proteins, in mouse nephron segments. J. Am. Soc. Nephrol. 13, 875-886.

Knust,E. and Bossinger,O. (2002). Composition and formation of intercellular junctions in epithelial cells. Science 298, 1955-1959.

Kohler,K., Louvard,D., and Zahraoui,A. (2004). Rab13 regulates PKA signaling during tight junction assembly. J. Cell Biol. 165, 175-180.

Kojima,T., Sawada,N., Chiba,H., Kokai,Y., Yamamoto,M., Urban,M., Lee,G.H., Hertzberg,E.L., Mochizuki,Y., and Spray,D.C. (1999). Induction of tight junctions in human

connexin 32 (hCx32)-transfected mouse hepatocytes: connexin 32 interacts with occludin. Biochem. Biophys. Res. Commun. 266, 222-229.

Kondoh,M., Masuyama,A., Takahashi,A., Asano,N., Mizuguchi,H., Koizumi,N., Fujii,M., Hayakawa,T., Horiguchi,Y., and Watanabe,Y. (2004). A novel strategy for the enhancement of drug absorption using a claudin modulator. Mol. Pharmacol.

Korinek,V., Barker,N., Morin,P.J., van Wichen,D., de Weger,R., Kinzler,K.W., Vogelstein,B., and Clevers,H. (1997). Constitutive transcriptional activation by a beta-catenin-Tcf complex in APC-/- colon carcinoma. Science 275, 1784-1787.

Korzenik,J.R. and Dieckgraefe,B.K. (2000). Is Crohn's disease an immunodeficiency? A hypothesis suggesting possible early events in the pathogenesis of Crohn's disease. Dig. Dis. Sci. 45, 1121-1129.

Kubota,K., Furuse,M., Sasaki,H., Sonoda,N., Fujita,K., Nagafuchi,A., and Tsukita,S. (1999). Ca(2+)-independent cell-adhesion activity of claudins, a family of integral membrane proteins localized at tight junctions. Curr. Biol. 9, 1035-1038.

Kucharzik,T., Lugering,N., Pauels,H.G., Domschke,W., and Stoll,R. (1998). IL-4, IL-10 and IL-13 down-regulate monocyte-chemoattracting protein-1 (MCP-1) production in activated intestinal epithelial cells. Clin. Exp. Immunol. 111, 152-157.

Kucharzik,T., Walsh,S.V., Chen,J., Parkos,C.A., and Nusrat,A. (2001). Neutrophil transmigration in inflammatory bowel disease is associated with differential expression of epithelial intercellular junction proteins. Am. J. Pathol. 159, 2001-2009.

Kullmann,F., Fadaie,M., Gross,V., Knuchel,R., Bocker,T., Steinbach,P., Scholmerich,J., and Ruschoff,J. (1996). Expression of proliferating cell nuclear antigen (PCNA) and Ki-67 in dysplasia in inflammatory bowel disease. Eur. J. Gastroenterol. Hepatol. 8, 371-379.

Kyle,J. (1992). Crohn's disease in the northeastern and northern Isles of Scotland: an epidemiological review. Gastroenterology 103, 392-399.

La Ferla,K., Seegert,D., and Schreiber,S. (2004). Activation of NF-kappaB in intestinal epithelial cells by E. coli strains isolated from the colonic mucosa of IBD patients. Int. J. Colorectal Dis. 19, 334-342.

Lacaz-Vieira,F., Jaeger,M.M., Farshori,P., and Kachar,B. (1999). Small synthetic peptides homologous to segments of the first external loop of occludin impair tight junction resealing. J. Membr. Biol. 168, 289-297.

Laemmli,U.K. (1970). Cleavage of structural proteins during the assembly of the head of bacteriophage T4. Nature 227, 680-685.

Langholz,E., Munkholm,P., Davidsen,M., and Binder,V. (1992). Colorectal cancer risk and mortality in patients with ulcerative colitis. Gastroenterology 103, 1444-1451.

Lapierre,L.A., Tuma,P.L., Navarre,J., Goldenring,J.R., and Anderson,J.M. (1999). VAP-33 localizes to both an intracellular vesicle population and with occludin at the tight junction. J. Cell Sci. 112 ( Pt 21), 3723-3732.

Larue,L., Ohsugi,M., Hirchenhain,J., and Kemler,R. (1994). E-cadherin null mutant embryos fail to form a trophectoderm epithelium. Proc. Natl. Acad. Sci. U. S. A 91, 8263-8267.

Lickert,H., Domon,C., Huls,G., Wehrle,C., Duluc,I., Clevers,H., Meyer,B.I., Freund,J.N., and Kemler,R. (2000). Wnt/(beta)-catenin signaling regulates the expression of the homeobox gene Cdx1 in embryonic intestine. Development 127, 3805-3813.

Liu,Y., Nusrat,A., Schnell,F.J., Reaves,T.A., Walsh,S., Pochet,M., and Parkos,C.A. (2000a). Human junction adhesion molecule regulates tight junction resealing in epithelia. J. Cell Sci. 113 ( Pt 13), 2363-2374.

Liu,Z., Geboes,K., Colpaert,S., D'Haens,G.R., Rutgeerts,P., and Ceuppens,J.L. (2000b). IL-15 is highly expressed in inflammatory bowel disease and regulates local T cell-dependent cytokine production. J. Immunol. 164, 3608-3615.

Lodish,H.F. (2000). Molecular cell biology. New York : W.H.Freeman, c2000).

Ma,T.Y., Iwamoto,G.K., Hoa,N.T., Akotia,V., Pedram,A., Boivin,M.A., and Said,H.M. (2004). TNF-alpha-induced increase in intestinal epithelial tight junction permeability requires NF-kappa B activation. Am. J. Physiol Gastrointest. Liver Physiol 286, G367-G376.

MacDonald,T.T. (1992). Epithelial proliferation in response to gastrointestinal inflammation. Ann. N. Y. Acad. Sci. 664, 202-209.

MacDonald,T.T. (2003). The mucosal immune system. Parasite Immunol. 25, 235-246.

MacDonald,T.T., Hutchings,P., Choy,M.Y., Murch,S., and Cooke,A. (1990). Tumour necrosis factor-alpha and interferon-gamma production measured at the single cell level in normal and inflamed human intestine. Clin. Exp. Immunol. 81, 301-305.

Madara,J.L. and Stafford,J. (1989). Interferon-gamma directly affects barrier function of cultured intestinal epithelial monolayers. J. Clin. Invest 83, 724-727.

Madara,J.L., Stafford,J., Dharmsathaphorn,K., and Carlson,S. (1987). Structural analysis of a human intestinal epithelial cell line. Gastroenterology 92, 1133-1145.

Madsen,K.L., Doyle,J.S., Tavernini,M.M., Jewell,L.D., Rennie,R.P., and Fedorak,R.N. (2000). Antibiotic therapy attenuates colitis in interleukin 10 gene-deficient mice. Gastroenterology 118, 1094-1105.

Madsen,K.L., Lewis,S.A., Tavernini,M.M., Hibbard,J., and Fedorak,R.N. (1997). Interleukin 10 prevents cytokine-induced disruption of T84 monolayer barrier integrity and limits chloride secretion. Gastroenterology 113, 151-159.

Mahida,Y.R. and Johal,S. (2001). NF-kappa B may determine whether epithelial cell--microbial interactions in the intestine are hostile or friendly. Clin. Exp. Immunol. 123, 347-349.

Malhotra,S.K. (1996). Advances in structural biology. Greenwich, Conn. ; London : JAI).

Mandel,K.G., Dharmsathaphorn,K., and McRoberts,J.A. (1986). Characterization of a cyclic AMP-activated Cl-transport pathway in the apical membrane of a human colonic epithelial cell line. J. Biol. Chem. 261, 704-712.

Mankertz,J., Hillenbrand,B., Tavalali,S., Huber,O., Fromm,M., and Schulzke,J.D. (2004). Functional crosstalk between Wnt signaling and Cdx-related transcriptional activation in the regulation of the claudin-2 promoter activity. Biochem. Biophys. Res. Commun. 314, 1001-1007.

Mankertz,J., Stefan,W.J., Hillenbrand,B., Tavalali,S., Florian,P., Schoneberg,T., Fromm,M., and Dieter,S.J. (2002). Gene expression of the tight junction protein occludin includes differential splicing and alternative promoter usage. Biochem. Biophys. Res. Commun. 298, 657-666.

Mankertz,J., Tavalali,S., Schmitz,H., Mankertz,A., Riecken,E.O., Fromm,M., and Schulzke,J.D. (2000). Expression from the human occludin promoter is affected by tumor necrosis factor alpha and interferon gamma. J. Cell Sci. 113 ( Pt 11), 2085-2090.

Manning,B.D., Tee,A.R., Logsdon,M.N., Blenis,J., and Cantley,L.C. (2002). Identification of the tuberous sclerosis complex-2 tumor suppressor gene product tuberin as a target of the phosphoinositide 3-kinase/akt pathway. Mol. Cell 10, 151-162.

Marano,C.W., Lewis,S.A., Garulacan,L.A., Soler,A.P., and Mullin,J.M. (1998). Tumor necrosis factor-alpha increases sodium and chloride conductance across the tight junction of CACO-2 BBE, a human intestinal epithelial cell line. J. Membr. Biol. 161, 263-274.

Martin-Padura,I., Lostaglio,S., Schneemann,M., Williams,L., Romano,M., Fruscella,P., Panzeri,C., Stoppacciaro,A., Ruco,L., Villa,A., Simmons,D., and Dejana,E. (1998). Junctional adhesion molecule, a novel member of the immunoglobulin superfamily that distributes at intercellular junctions and modulates monocyte transmigration. J. Cell Biol. 142, 117-127.

Martin,H.M., Campbell,B.J., Hart,C.A., Mpofu,C., Nayar,M., Singh,R., Englyst,H., Williams,H.F., and Rhodes,J.M. (2004). Enhanced Escherichia coli adherence and invasion in Crohn's disease and colon cancer. Gastroenterology 127, 80-93.

Marzesco,A.M., Dunia,I., Pandjaitan,R., Recouvreur,M., Dauzonne,D., Benedetti,E.L., Louvard,D., and Zahraoui,A. (2002). The small GTPase Rab13 regulates assembly of functional tight junctions in epithelial cells. Mol. Biol. Cell 13, 1819-1831.

Masuda,H., Iwai,S., Tanaka,T., and Hayakawa,S. (1995). Expression of IL-8, TNF-alpha and IFN-gamma m-RNA in ulcerative colitis, particularly in patients with inactive phase. J. Clin. Lab Immunol. 46, 111-123.

Matter,K. and Balda,M.S. (1998). Biogenesis of tight junctions: the C-terminal domain of occludin mediates basolateral targeting. J. Cell Sci. 111 ( Pt 4), 511-519.

Matter,K. and Balda,M.S. (2003). Functional analysis of tight junctions. Methods 30, 228-234.

Matthews,J.N., Altman,D.G., Campbell,M.J., and Royston,P. (1990). Analysis of serial measurements in medical research. BMJ 300, 230-235.

May,G.R., Sutherland,L.R., and Meddings,J.B. (1993). Is small intestinal permeability really increased in relatives of patients with Crohn's disease? Gastroenterology 104, 1627-1632.

McCarthy,K.M., Skare,I.B., Stankewich,M.C., Furuse,M., Tsukita,S., Rogers,R.A., Lynch,R.D., and Schneeberger,E.E. (1996). Occludin is a functional component of the tight junction. J. Cell Sci. 109 ( Pt 9), 2287-2298.

McKenzie,G.J., Bancroft,A., Grencis,R.K., and McKenzie,A.N. (1998). A distinct role for interleukin-13 in Th2-cell-mediated immune responses. Curr. Biol. 8, 339-342.

Meddings,J.B. and Swain,M.G. (2000). Environmental stress-induced gastrointestinal permeability is mediated by endogenous glucocorticoids in the rat. Gastroenterology 119, 1019-1028.

Medina,R., Rahner,C., Mitic,L.L., Anderson,J.M., and Van Itallie,C.M. (2000). Occludin localization at the tight junction requires the second extracellular loop. J. Membr. Biol. 178, 235-247.

Meucci,G., Bortoli,A., Riccioli,F.A., Girelli,C.M., Radaelli,F., Rivolta,R., and Tatarella,M. (1999). Frequency and clinical evolution of indeterminate colitis: a retrospective multi-centre study in northern Italy. GSMII (Gruppo di Studio per le Malattie Infiammatorie Intestinali). Eur. J. Gastroenterol. Hepatol. 11, 909-913.

Meyer,T.N., Schwesinger,C., and Denker,B.M. (2002). Zonula occludens-1 is a scaffolding protein for signaling molecules. Galpha(12) directly binds to the Src homology 3 domain and regulates paracellular permeability in epithelial cells. J. Biol. Chem. 277, 24855-24858.

Michail,S.K., Halm,D.R., and Abernathy,F. (2003). Enteropathogenic Escherichia coli: stimulating neutrophil migration across a cultured intestinal epithelium without altering transepithelial conductance. J. Pediatr. Gastroenterol. Nutr. 36, 253-260.

Mikita,T., Campbell,D., Wu,P., Williamson,K., and Schindler,U. (1996). Requirements for interleukin-4-induced gene expression and functional characterization of Stat6. Mol. Cell Biol. 16, 5811-5820.

Mikita,T., Daniel,C., Wu,P., and Schindler,U. (1998). Mutational analysis of the STAT6 SH2 domain. J. Biol. Chem. 273, 17634-17642.

Miloux,B., Laurent,P., Bonnin,O., Lupker,J., Caput,D., Vita,N., and Ferrara,P. (1997). Cloning of the human IL-13R alpha1 chain and reconstitution with the IL4R alpha of a functional IL-4/IL-13 receptor complex. FEBS Lett. 401, 163-166.

Mitic,L.L., Schneeberger,E.E., Fanning,A.S., and Anderson,J.M. (1999). Connexin-occludin chimeras containing the ZO-binding domain of occludin localize at MDCK tight junctions and NRK cell contacts. J. Cell Biol. 146, 683-693.

Miyamori,H., Takino,T., Kobayashi,Y., Tokai,H., Itoh,Y., Seiki,M., and Sato,H. (2001). Claudin promotes activation of pro-matrix metalloproteinase-2 mediated by membrane-type matrix metalloproteinases. J. Biol. Chem. 276, 28204-28211.

Monteleone,G., Kumberova,A., Croft,N.M., McKenzie,C., Steer,H.W., and MacDonald,T.T. (2001). Blocking Smad7 restores TGF-beta1 signaling in chronic inflammatory bowel disease. J. Clin. Invest 108, 601-609.

Monteleone,G. and MacDonald,T.T. (2000). Manipulation of cytokines in the management of patients with inflammatory bowel disease. Ann. Med. 32, 552-560.

Mora,A., Sabio,G., Risco,A.M., Cuenda,A., Alonso,J.C., Soler,G., and Centeno,F. (2002). Lithium blocks the PKB and GSK3 dephosphorylation induced by ceramide through protein phosphatase-2A. Cell Signal. 14, 557-562.

Morimoto,S., Nishimura,N., Terai,T., Manabe,S., Yamamoto,Y., Shinahara,W., Miyake,H., Tashiro,S., Shimada,M., and Sasaki,T. (2004). Rab13 mediates the continuous endocytic recycling of occludin to the cell-surface. J. Biol. Chem.

Mueller,S.L., Portwich,M., Schmidt,A., Utepbergenov,D.I., Huber,O., Blasig,I.E., and Krause,G. (2004). The tight junction protein occludin and the adherens junction protein alpha -catenin share a common interaction mechanism with ZO-1. J. Biol. Chem.

Mullin,G.E., Lazenby,A.J., Harris,M.L., Bayless,T.M., and James,S.P. (1992). Increased interleukin-2 messenger RNA in the intestinal mucosal lesions of Crohn's disease but not ulcerative colitis. Gastroenterology 102, 1620-1627.

Munkholm,P., Langholz,E., Davidsen,M., and Binder,V. (1993). Intestinal cancer risk and mortality in patients with Crohn's disease. Gastroenterology 105, 1716-1723.

Murata,T., Noguchi,P.D., and Puri,R.K. (1996). IL-13 induces phosphorylation and activation of JAK2 Janus kinase in human colon carcinoma cell lines: similarities between IL-4 and IL-13 signaling. J. Immunol. 156, 2972-2978.

Murch,S.H., Braegger,C.P., Walker-Smith,J.A., and MacDonald,T.T. (1993). Location of tumour necrosis factor alpha by immunohistochemistry in chronic inflammatory bowel disease. Gut 34, 1705-1709.

Muresan,Z., Paul,D.L., and Goodenough,D.A. (2000). Occludin 1B, a variant of the tight junction protein occludin. Mol. Biol. Cell 11, 627-634.

Nagafuchi,A. (2001). Molecular architecture of adherens junctions. Curr. Opin. Cell Biol. 13, 600-603.

Nagar,B., Overduin,M., Ikura,M., and Rini,J.M. (1996). Structural basis of calcium-induced E-cadherin rigidification and dimerization. Nature 380, 360-364.

Nakamura,K., Kitani,A., and Strober,W. (2001). Cell contact-dependent immunosuppression by CD4(+)CD25(+) regulatory T cells is mediated by cell surface-bound transforming growth factor beta. J. Exp. Med. 194, 629-644.

Nelson,W.J. and Nusse,R. (2004). Convergence of Wnt, beta-catenin, and cadherin pathways. Science 303, 1483-1487.

Netea,M.G., Kullberg,B.J., de Jong,D.J., Franke,B., Sprong,T., Naber,T.H., Drenth,J.P., and Van der Meer,J.W. (2004). NOD2 mediates anti-inflammatory signals induced by TLR2 ligands: implications for Crohn's disease. Eur. J. Immunol. 34, 2052-2059.

Nielsen,O.H., Brynskov,J., and Bendtzen,K. (1993). Circulating and mucosal concentrations of tumour necrosis factor and inhibitor(s) in chronic inflammatory bowel disease. Dan. Med. Bull. 40, 247-249.

Nielsen,O.H., Kirman,I., Rudiger,N., Hendel,J., and Vainer,B. (2003). Upregulation of interleukin-12 and -17 in active inflammatory bowel disease. Scand. J. Gastroenterol. 38, 180-185.

Niemann,C., Brinkmann,V., Spitzer,E., Hartmann,G., Sachs,M., Naundorf,H., and Birchmeier,W. (1998). Reconstitution of mammary gland development in vitro: requirement of c-met and c-erbB2 signaling for branching and alveolar morphogenesis. J. Cell Biol. 143, 533-545.

Nishiyama,R., Sakaguchi,T., Kinugasa,T., Gu,X., MacDermott,R.P., Podolsky,D.K., and Reinecker,H.C. (2001). Interleukin-2 receptor beta subunit-dependent and -independent regulation of intestinal epithelial tight junctions. J. Biol. Chem. 276, 35571-35580.

Noffsinger,A., Unger,B., and Fenoglio-Preiser,C.M. (1998). Increased cell proliferation characterizes Crohn's disease. Mod. Pathol. 11, 1198-1203.

Noffsinger,A.E., Miller,M.A., Cusi,M.V., and Fenoglio-Preiser,C.M. (1996). The pattern of cell proliferation in neoplastic and nonneoplastic lesions of ulcerative colitis. Cancer 78, 2307-2312.

Nunbhakdi-Craig,V., Machleidt,T., Ogris,E., Bellotto,D., White,C.L., III, and Sontag,E. (2002). Protein phosphatase 2A associates with and regulates atypical PKC and the epithelial tight junction complex. J. Cell Biol. 158, 967-978.

Nunez,G. and del Peso,L. (1998). Linking extracellular survival signals and the apoptotic machinery. Curr. Opin. Neurobiol. 8, 613-618.

Nusrat,A., Chen,J.A., Foley,C.S., Liang,T.W., Tom,J., Cromwell,M., Quan,C. , and Mrsny,R.J. (2000). The coiled-coil domain of occludin can act to organize structural and functional elements of the epithelial tight junction. J. Biol. Chem. 275, 29816-29822.

Nusrat,A., Eichel-Streiber,C., Turner,J.R., Verkade,P., Madara,J.L., and Parkos,C.A. (2001). Clostridium difficile toxins disrupt epithelial barrier function by altering membrane microdomain localization of tight junction proteins. Infect. Immun. 69, 1329-1336.

O'Neill,L.A. (2004). How NOD-ing off leads to Crohn disease. Nat. Immunol. 5, 776-778.

Ogura,Y., Bonen,D.K., Inohara,N., Nicolae,D.L., Chen,F.F., Ramos,R., Britton,H., Moran,T., Karaliuskas,R., Duerr,R.H., Achkar,J.P., Brant,S.R., Bayless,T.M., Kirschner,B.S., Hanauer,S.B., Nunez,G., and Cho,J.H. (2001). A frameshift mutation in NOD2 associated with susceptibility to Crohn's disease. Nature 411, 603-606.

Orholm,M., Binder,V., Sorensen,T.I., Rasmussen,L.P., and Kyvik,K.O. (2000). Concordance of inflammatory bowel disease among Danish twins. Results of a nationwide study. Scand. J. Gastroenterol. 35, 1075-1081.

Ostermann,G., Weber,K.S., Zernecke,A., Schroder,A., and Weber,C. (2002). JAM-1 is a ligand of the beta(2) integrin LFA-1 involved in transendothelial migration of leukocytes. Nat. Immunol. 3, 151-158.

Otsu,M., Hiles,I., Gout,I., Fry,M.J., Ruiz-Larrea,F., Panayotou,G., Thompson,A., Dhand,R., Hsuan,J., Totty,N., and . (1991). Characterization of two 85 kd proteins that associate with receptor tyrosine kinases, middle-T/pp60c-src complexes, and PI3-kinase. Cell 65, 91-104.

Ozawa,M., Baribault,H., and Kemler,R. (1989). The cytoplasmic domain of the cell adhesion molecule uvomorulin associates with three independent proteins structurally related in different species. EMBO J. 8, 1711-1717.

Paling,N.R., Wheadon,H., Bone,H.K., and Welham,M.J. (2004). Regulation of embryonic stem cell self-renewal by phosphoinositide 3-kinase-dependent signaling. J. Biol. Chem. 279, 48063-48070.

Peltekova,V.D., Wintle,R.F., Rubin,L.A., Amos,C.I., Huang,Q., Gu,X., Newman,B., Van Oene,M., Cescon,D., Greenberg,G., Griffiths,A.M., George-Hyslop,P.H., and Siminovitch,K.A. (2004). Functional variants of OCTN cation transporter genes are associated with Crohn disease. Nat. Genet. 36, 471-475.

Perry,I., Hardy,R., Tselepis,C., and Jankowski,J.A. (1999a). Cadherin adhesion in the intestinal crypt regulates morphogenesis, mitogenesis, motogenesis, and metaplasia formation. Mol. Pathol. 52, 166-168.

Perry,I., Tselepis,C., Hoyland,J., Iqbal,T.H., Scott,D., Sanders,S.A., Cooper,B.T., and Jankowski,J.A. (1999b). Reduced cadherin/catenin complex expression in celiac disease can be reproduced in vitro by cytokine stimulation. Lab Invest 79, 1489-1499.

Pickard,K.M., Bremner,A.R., Gordon,J.N., and MacDonald,T.T. (2004). Microbial-gut interactions in health and disease. Immune responses. Best. Pract. Res. Clin. Gastroenterol. 18, 271-285.

Polakis,P. (2000). Wnt signaling and cancer. Genes Dev. 14, 1837-1851.

Potten,C.S., Owen,G., and Booth,D. (2002). Intestinal stem cells protect their genome by selective segregation of template DNA strands. J. Cell Sci. 115, 2381-2388.

Poxton,I.R., Brown,R., Sawyerr,A., and Ferguson,A. (1997). Mucosa-associated bacterial flora of the human colon. J. Med. Microbiol. 46, 85-91.

Prota,A.E., Campbell,J.A., Schelling,P., Forrest,J.C., Watson,M.J., Peters,T.R., Aurrand-Lions,M., Imhof,B.A., Dermody,T.S., and Stehle,T. (2003). Crystal structure of human junctional adhesion molecule 1: implications for reovirus binding. Proc. Natl. Acad. Sci. U. S. A 100, 5366-5371.

Proud,C.G. (2004). Ras, PI3-kinase and mTOR signaling in cardiac hypertrophy. Cardiovasc. Res. 63, 403-413.

Rahner,C., Mitic,L.L., and Anderson,J.M. (2001). Heterogeneity in expression and subcellular localization of claudins 2, 3, 4, and 5 in the rat liver, pancreas, and gut. Gastroenterology 120, 411-422.

Rath,H.C., Herfarth,H.H., Ikeda,J.S., Grenther,W.B., Hamm,T.E., Jr., Balish,E., Taurog,J.D., Hammer,R.E., Wilson,K.H., and Sartor,R.B. (1996). Normal luminal bacteria, especially Bacteroides species, mediate chronic colitis, gastritis, and arthritis in HLA-B27/human beta2 microglobulin transgenic rats. J. Clin. Invest 98, 945-953.

Rath,H.C., Schultz,M., Freitag,R., Dieleman,L.A., Li,F., Linde,H.J., Scholmerich,J., and Sartor,R.B. (2001). Different subsets of enteric bacteria induce and perpetuate experimental colitis in rats and mice. Infect. Immun. 69, 2277-2285.

Rath,H.C., Wilson,K.H., and Sartor,R.B. (1999). Differential induction of colitis and gastritis in HLA-B27 transgenic rats selectively colonized with Bacteroides vulgatus or Escherichia coli. Infect. Immun. 67, 2969-2974.

Reinecker,H.C., Steffen,M., Witthoeft,T., Pflueger,I., Schreiber,S., MacDermott,R.P., and Raedler,A. (1993). Enhanced secretion of tumour necrosis factor-alpha, IL-6, and IL-1 beta by isolated lamina propria mononuclear cells from patients with ulcerative colitis and Crohn's disease. Clin. Exp. Immunol. 94, 174-181.

Rescigno,M., Urbano,M., Valzasina,B., Francolini,M., Rotta,G., Bonasio,R., Granucci,F., Kraehenbuhl,J.P., and Ricciardi-Castagnoli,P. (2001). Dendritic cells express tight junction proteins and penetrate gut epithelial monolayers to sample bacteria. Nat. Immunol. 2, 361-367.

Reuter,B.K. and Pizarro,T.T. (2004). Commentary: the role of the IL-18 system and other members of the IL-1R/TLR superfamily in innate mucosal immunity and the pathogenesis of inflammatory bowel disease: friend or foe? Eur. J. Immunol. 34, 2347-2355.

Riethmacher,D., Brinkmann,V., and Birchmeier,C. (1995). A targeted mutation in the mouse E-cadherin gene results in defective preimplantation development. Proc. Natl. Acad. Sci. U. S. A 92, 855-859.

Rodrigo,I., Cato,A.C., and Cano,A. (1999). Regulation of E-cadherin gene expression during tumor progression: the role of a new Ets-binding site and the E-pal element. Exp. Cell Res. 248, 358-371.

Roh,M.H., Liu,C.J., Laurinec,S., and Margolis,B. (2002a). The carboxyl terminus of zona occludens-3 binds and recruits a mammalian homologue of discs lost to tight junctions. J. Biol. Chem. 277, 27501-27509.

Roh,M.H., Makarova,O., Liu,C.J., Shin,K., Lee,S., Laurinec,S., Goyal,M., Wiggins,R., and Margolis,B. (2002b). The Maguk protein, Pals1, functions as an adapter, linking mammalian homologues of Crumbs and Discs Lost. J. Cell Biol. 157, 161-172.

Rose,J.D., Roberts,G.M., Williams,G., Mayberry,J.F., and Rhodes,J. (1988). Cardiff Crohn's disease jubilee: the incidence over 50 years. Gut 29, 346-351.

Roy,B., Bhattacharjee,A., Xu,B., Ford,D., Maizel,A.L., and Cathcart,M.K. (2002). IL-13 signal transduction in human monocytes: phosphorylation of receptor components, association with Jaks, and phosphorylation/activation of Stats. J. Leukoc. Biol. 72, 580-589.

Roy,B. and Cathcart,M.K. (1998). Induction of 15-lipoxygenase expression by IL-13 requires tyrosine phosphorylation of Jak2 and Tyk2 in human monocytes. J. Biol. Chem. 273, 32023-32029.

Russel,M.G., Dorant,E., Volovics,A., Brummer,R.J., Pop,P., Muris,J.W., Bos,L.P., Limonard,C.B., and Stockbrugger,R.W. (1998). High incidence of inflammatory bowel disease in The Netherlands: results of a prospective study. The South Limburg IBD Study Group. Dis. Colon Rectum 41, 33-40.

Saitou,M., Ando-Akatsuka,Y., Itoh,M., Furuse,M., Inazawa,J., Fujimoto,K., and Tsukita,S. (1997). Mammalian occludin in epithelial cells: its expression and subcellular distribution. Eur. J. Cell Biol. 73, 222-231.

Saitou,M., Fujimoto,K., Doi,Y., Itoh,M., Fujimoto,T., Furuse,M., Takano,H., Noda,T., and Tsukita,S. (1998). Occludin-deficient embryonic stem cells can differentiate into polarized epithelial cells bearing tight junctions. J. Cell Biol. 141, 397-408.

Saitou,M., Furuse,M., Sasaki,H., Schulzke,J.D., Fromm,M., Takano,H., Noda,T., and Tsukita,S. (2000). Complex phenotype of mice lacking occludin, a component of tight junction strands. Mol. Biol. Cell 11, 4131-4142.

Sakaguchi,S., Sakaguchi,N., Asano,M., Itoh,M., and Toda,M. (1995). Immunologic self-tolerance maintained by activated T cells expressing IL-2 receptor alpha-chains (CD25). Breakdown of a single mechanism of self-tolerance causes various autoimmune diseases. J. Immunol. 155, 1151-1164.

Sakaguchi,T., Gu,X., Golden,H.M., Suh,E., Rhoads,D.B., and Reinecker,H.C. (2002). Cloning of the human claudin-2 5'-flanking region revealed a TATA-less promoter with

conserved binding sites in mouse and human for caudal-related homeodomain proteins and hepatocyte nuclear factor-1alpha. J. Biol. Chem. 277, 21361-21370.

Sakai,T., Kusugami,K., Nishimura,H., Ando,T., Yamaguchi,T., Ohsuga,M., Ina,K., Enomoto,A., Kimura,Y. , and Yoshikai,Y. (1998). Interleukin 15 activity in the rectal mucosa of inflammatory bowel disease. Gastroenterology 114, 1237-1243.

Sakakibara,A., Furuse,M., Saitou,M., Ando-Akatsuka,Y., and Tsukita,S. (1997). Possible involvement of phosphorylation of occludin in tight junction formation. J. Cell Biol. 137, 1393-1401.

Sanders,S.E., Madara,J.L., McGuirk,D.K., Gelman,D.S., and Colgan,S.P. (1995). Assessment of inflammatory events in epithelial permeability: a rapid screening method using fluorescein dextrans. Epithelial Cell Biol. 4, 25-34.

Sandle,G.I., Higgs,N., Crowe,P., Marsh,M.N., Venkatesan,S., and Peters,T.J. (1990). Cellular basis for defective electrolyte transport in inflamed human colon. Gastroenterology 99, 97-105.

Sartor,R.B. (1997). Review article: Role of the enteric microflora in the pathogenesis of intestinal inflammation and arthritis. Aliment. Pharmacol. Ther. 11 Suppl 3, 17-22.

Saxon,A., Shanahan,F., Landers,C., Ganz,T., and Targan,S. (1990). A distinct subset of antineutrophil cytoplasmic antibodies is associated with inflammatory bowel disease. J. Allergy Clin. Immunol. 86, 202-210.

Schmidt,A., Utepbergenov,D.I., Mueller,S.L., Beyermann,M., Schneider-Mergener,J., Krause,G., and Blasig,I.E. (2004). Occludin binds to the SH3-hinge-GuK unit of zonula occludens protein 1: potential mechanism of tight junction regulation. Cell Mol. Life Sci. 61, 1354-1365.

Schmitz,H., Barmeyer,C., Fromm,M., Runkel,N., Foss,H.D., Bentzel,C.J., Riecken,E.O., and Schulzke,J.D. (1999). Altered tight junction structure contributes to the impaired epithelial barrier function in ulcerative colitis. Gastroenterology 116, 301-309.

Schneeberger,E.E. and Lynch,R.D. (2004). The tight junction: a multifunctional complex. Am. J. Physiol Cell Physiol 286, C1213-C1228.

Schreiber,S., Nikolaus,S., and Hampe,J. (1998). Activation of nuclear factor kappa B inflammatory bowel disease. Gut 42, 477-484.

Schulzke,J.D., Bentzel,C.J., Schulzke,I., Riecken,E.O., and Fromm,M. (1998). Epithelial tight junction structure in the jejunum of children with acute and treated celiac sprue . Pediatr. Res. 43, 435-441.

Secondulfo,M., de Magistris,L., Fiandra,R., Caserta,L., Belletta,M., Tartaglione,M.T., Riegler,G., Biagi,F., Corazza,G.R., and Carratu,R. (2001). Intestinal permeability in Crohn's disease patients and their first degree relatives. Dig. Liver Dis. 33, 680-685.

Shanahan,F. (2002). Crohn's disease. Lancet 359, 62-69.

Sharp,P.A. (2001). RNA interference--2001. Genes Dev. 15, 485-490.

Shepherd,N.A. (1991). Pathological mimics of chronic inflammatory bowel disease. J. Clin. Pathol. 44, 726-733.

Sheth,B., Fesenko,I., Collins,J.E., Moran,B., Wild,A.E., Anderson,J.M., and Fleming,T.P. (1997). Tight junction assembly during mouse blastocyst formation is regulated by late expression of ZO-1 alpha+ isoform. Development 124, 2027-2037.

Sheth,B., Fontaine,J.J., Ponza,E., McCallum,A., Page,A., Citi,S., Louvard,D., Zahraoui,A., and Fleming,T.P. (2000a). Differentiation of the epithelial apical junctional complex during mouse preimplantation development: a role for rab13 in the early maturation of the tight junction. Mech. Dev. 97, 93-104.

Sheth,B., Moran,B., Anderson,J.M., and Fleming,T.P. (2000b). Post-translational control of occludin membrane assembly in mouse trophectoderm: a mechanism to regulate timing of tight junction biogenesis and blastocyst formation. Development 127, 831-840.

Sheth,P., Basuroy,S., Li,C., Naren,A.P., and Rao,R.K. (2003). Role of phosphatidylinositol 3-kinase in oxidative stress-induced disruption of tight junctions. J. Biol. Chem. 278, 49239-49245.

Shivananda,S., Hordijk,M.L., Ten Kate,F.J., Probert,C.S., and Mayberry,J.F. (1991). Differential diagnosis of inflammatory bowel disease. A comparison of various diagnostic classifications. Scand. J. Gastroenterol. 26, 167-173.

Shivananda,S., Lennard-Jones,J., Logan,R., Fear,N., Price,A., Carpenter,L., and van Blankenstein,M. (1996). Incidence of inflammatory bowel disease across Europe: is there a difference between north and south? Results of the European Collaborative Study on Inflammatory Bowel Disease (EC-IBD). Gut 39, 690-697.

Simon,D.B., Lu,Y., Choate,K.A., Velazquez,H., Al Sabban,E., Praga,M., Casari,G., Bettinelli,A., Colussi,G. , Rodriguez-Soriano,J., McCredie,D., Milford,D., Sanjad,S., and Lifton,R.P. (1999). Paracellin-1, a renal tight junction protein required for paracellular Mg2+ resorption. Science 285, 103-106.

Simonovic,I., Rosenberg,J., Koutsouris,A., and Hecht,G. (2000). Enteropathogenic Escherichia coli dephosphorylates and dissociates occludin from intestinal epithelial tight junctions. Cell Microbiol. 2, 305-315.

Snook,J.A., de Silva,H.J., and Jewell,D.P. (1989). The association of autoimmune disorders with inflammatory bowel disease. Q. J. Med. 72, 835-840.

Soderholm,J.D., Olaison,G., Lindberg,E., Hannestad,U., Vindels,A., Tysk,C., Jarnerot,G., and Sjodahl,R. (1999). Different intestinal permeability patterns in relatives and spouses of patients with Crohn's disease: an inherited defect in mucosal defence? Gut 44, 96-100.

Soderholm,J.D. and Perdue,M.H. (2001). Stress and gastrointestinal tract. II. Stress and intestinal barrier function. Am. J. Physiol Gastrointest. Liver Physiol 280, G7-G13.

Soler,A.P., Marano,C.W., Bryans,M., Miller,R.D., Garulacan,L.A., Mauldin,S.K., Stamato,T.D., and Mullin,J.M. (1999). Activation of NF-kappaB is necessary for the restoration of the barrier function of an epithelium undergoing TNF-alpha-induced apoptosis. Eur. J. Cell Biol. 78, 56-66.

Sonoda,N., Furuse,M., Sasaki,H., Yonemura,S., Katahira,J., Horiguchi,Y., and Tsukita,S. (1999). Clostridium perfringens enterotoxin fragment removes specific claudins from tight junction strands: Evidence for direct involvement of claudins in tight junction barrier. J. Cell Biol. 147, 195-204.

Spencer,D.M., Veldman,G.M., Banerjee,S., Willis,J., and Levine,A.D. (2002). Distinct inflammatory mechanisms mediate early versus late colitis in mice. Gastroenterology 122, 94-105.

Staal,F.J., Noort,M.M., Strous,G.J., and Clevers,H.C. (2002). Wnt signals are transmitted through N-terminally dephosphorylated beta-catenin. EMBO Rep. 3, 63-68.

Stevenson,B.R., Anderson,J.M., Braun,I.D., and Mooseker,M.S. (1989). Phosphorylation of the tight-junction protein ZO-1 in two strains of Madin-Darby canine kidney cells which differ in transepithelial resistance. Biochem. J. 263, 597-599.

Stevenson,B.R., Anderson,J.M., Goodenough,D.A., and Mooseker,M.S. (1988). Tight junction structure and ZO-1 content are identical in two strains of Madin-Darby canine kidney cells which differ in transepithelial resistance. J. Cell Biol. 107, 2401-2408.

Stevenson,B.R., Siliciano,J.D., Mooseker,M.S., and Goodenough,D.A. (1986). Identification of ZO-1: a high molecular weight polypeptide associated with the tight junction (zonula occludens) in a variety of epithelia. J. Cell Biol. 103, 755-766.

Stoll,M., Corneliussen,B., Costello,C.M., Waetzig,G.H., Mellgard,B., Koch,W.A., Rosenstiel,P., Albrecht,M., Croucher,P.J., Seegert,D., Nikolaus,S., Hampe,J., Lengauer,T., Pierrou,S., Foelsch,U.R., Mathew,C.G., Lagerstrom-Fermer,M., and Schreiber,S. (2004). Genetic variation in DLG5 is associated with inflammatory bowel disease. Nat. Genet. 36, 476-480.

Strober,W., Fuss,I.J., and Blumberg,R.S. (2002). The immunology of mucosal models of inflammation. Annu. Rev. Immunol. 20, 495-549.

Strober,W., Fuss,I.J., Nakamura,K., and Kitani,A. (2003). Recent advances in the understanding of the induction and regulation of mucosal inflammation. J. Gastroenterol. 38 Suppl 15, 55-58.

Strober,W. and James,S.P. (1986). The immunologic basis of inflammatory bowel disease. J. Clin. Immunol. 6, 415-432.

Stuart,R.O. and Nigam,S.K. (1995). Regulated assembly of tight junctions by protein kinase C. Proc. Natl. Acad. Sci. U. S. A 92, 6072-6076.

Suenaert,P., Bulteel,V., Lemmens,L., Noman,M., Geypens,B., Van Assche,G., Geboes,K., Ceuppens,J.L., and Rutgeerts,P. (2002). Anti-tumor necrosis factor treatment restores the gut barrier in Crohn's disease. Am. J. Gastroenterol. 97, 2000-2004.

Sun,X.J., Wang,L.M., Zhang,Y., Yenush,L., Myers,M.G., Jr., Glasheen,E., Lane,W.S., Pierce,J.H., and White,M.F. (1995). Role of IRS-2 in insulin and cytokine signalling. Nature 377, 173-177.

Swidsinski,A., Ladhoff,A., Pernthaler,A., Swidsinski,S., Loening-Baucke,V., Ortner,M., Weber,J., Hoffmann,U., Schreiber,S., Dietel,M., and Lochs,H. (2002). Mucosal flora in inflammatory bowel disease. Gastroenterology 122, 44-54.

Tamura,G., Yin,J., Wang,S., Fleisher,A.S., Zou,T., Abraham,J.M., Kong,D. , Smolinski,K.N., Wilson,K.T., James,S.P., Silverberg,S.G., Nishizuka,S., Terashima,M.,

Motoyama,T., and Meltzer,S.J. (2000). E-Cadherin gene promoter hypermethylation in primary human gastric carcinomas. J. Natl. Cancer Inst. 92, 569-573.

Tanabe,T., Chamaillard,M., Ogura,Y., Zhu,L., Qiu,S., Masumoto,J., Ghosh,P. , Moran,A., Predergast,M.M., Tromp,G., Williams,C.J., Inohara,N., and Nunez,G. (2004). Regulatory regions and critical residues of NOD2 involved in muramyl dipeptide recognition. EMBO J. 23, 1587-1597.

Tanaka,M. and Riddell,R.H. (1990). The pathological diagnosis and differential diagnosis of Crohn's disease. Hepatogastroenterology 37, 18-31.

Teahon,K., Smethurst,P., Levi,A.J., Menzies,I.S., and Bjarnason,I. (1992). Intestinal permeability in patients with Crohn's disease and their first degree relatives. Gut 33, 320-323.

Teahon,K., Smethurst,P., Pearson,M., Levi,A.J., and Bjarnason,I. (1991). The effect of elemental diet on intestinal permeability and inflammation in Crohn's disease. Gastroenterology 101, 84-89.

Tee,A.R., Manning,B.D., Roux,P.P., Cantley,L.C., and Blenis,J. (2003). Tuberous sclerosis complex gene products, Tuberin and Hamartin, control mTOR signaling by acting as a GTPase-activating protein complex toward Rheb. Curr. Biol. 13, 1259-1268.

Thomas,F.C., Sheth,B., Eckert,J.J., Bazzoni,G., Dejana,E., and Fleming,T.P. (2004). Contribution of JAM-1 to epithelial differentiation and tight-junction biogenesis in the mouse preimplantation embryo. J. Cell Sci. 117, 5599-5608.

Thompson,N.P., Driscoll,R., Pounder,R.E., and Wakefield,A.J. (1996). Genetics versus environment in inflammatory bowel disease: results of a British twin study. BMJ 312, 95-96.

Traweger,A., Fang,D., Liu,Y.C., Stelzhammer,W., Krizbai,I.A., Fresser,F., Bauer,H.C., and Bauer,H. (2002a). The tight junction-specific protein occludin is a functional target of the E3 ubiquitin-protein ligase itch. J. Biol. Chem. 277, 10201-10208.

Traweger,A., Fuchs,R., Krizbai,I.A., Weiger,T.M., Bauer,H.C., and Bauer,H. (2002b). The tight junction protein ZO-2 localizes to the nucleus and interacts with the hnRNP protein SAF-B. J. Biol. Chem.

Troyanovsky,S.M. (1999). Mechanism of cell-cell adhesion complex assembly. Curr. Opin. Cell Biol. 11, 561-566.

Tsukamoto,T. and Nigam,S.K. (1999). Role of tyrosine phosphorylation in the reassembly of occludin and other tight junction proteins. Am. J. Physiol 276, F737-F750.

Tsukita,S. and Furuse,M. (2000b). Pores in the wall: claudins constitute tight junction strands containing aqueous pores. J. Cell Biol. 149, 13-16.

Tsukita,S. and Furuse,M. (2000a). The structure and function of claudins, cell adhesion molecules at tight junctions. Ann. N. Y. Acad. Sci. 915, 129-135.

Tsukita,S. and Furuse,M. (2002). Claudin-based barrier in simple and stratified cellular sheets. Curr. Opin. Cell Biol. 14, 531.

Turksen,K. and Troy,T.C. (2002). Permeability barrier dysfunction in transgenic mice overexpressing claudin 6. Development 129, 1775-1784.

Turksen,K. and Troy,T.C. (2004). Barriers built on claudins. J. Cell Sci. 117, 2435-2447.

Turunen,U.M., Farkkila,M.A., Hakala,K., Seppala,K., Sivonen,A., Ogren,M., Vuoristo,M., Valtonen,V.V., and Miettinen,T.A. (1998). Long-term treatment of ulcerative colitis with ciprofloxacin: a prospective, double-blind, placebo-controlled study. Gastroenterology 115, 1072-1078.

Tysk,C., Lindberg,E., Jarnerot,G., and Floderus-Myrhed,B. (1988). Ulcerative colitis and Crohn's disease in an unselected population of monozygotic and dizygotic twins. A study of heritability and the influence of smoking. Gut 29, 990-996.

Umeda,K., Matsui,T., Nakayama,M., Furuse,K., Sasaki,H., Furuse,M., and Tsukita,S. (2004). Establishment and characterization of cultured epithelial cells lacking expression of ZO-1. J. Biol. Chem.

Unno,N. and Fink,M.P. (1998). Intestinal epithelial hyperpermeability. Mechanisms and relevance to disease. Gastroenterol. Clin. North Am. 27, 289-307.

Vainer,B., Nielsen,O.H., Hendel,J., Horn,T., and Kirman,I. (2000). Colonic expression and synthesis of interleukin 13 and interleukin 15 in inflammatory bowel disease. Cytokine 12, 1531-1536.

Van Heel,D.A., McGovern,D.P., and Jewell,D.P. (2001). Crohn's disease: genetic susceptibility, bacteria, and innate immunity. Lancet 357, 1902-1904.

Van Itallie,C., Rahner,C., and Anderson,J.M. (2001). Regulated expression of claudin-4 decreases paracellular conductance through a selective decrease in sodium permeability. J. Clin. Invest 107, 1319-1327.

Van Itallie,C.M. and Anderson,J.M. (1997). Occludin confers adhesiveness when expressed in fibroblasts. J. Cell Sci. 110 ( Pt 9), 1113-1121.

Van Itallie,C.M., Balda,M.S., and Anderson,J.M. (1995). Epidermal growth factor induces tyrosine phosphorylation and reorganization of the tight junction protein ZO-1 in A431 cells. J. Cell Sci. 108 ( Pt 4), 1735-1742.

Van Itallie,C.M., Colegio,O.R., and Anderson,J.M. (2004). The cytoplasmic tails of claudins can influence tight junction barrier properties through effects on protein stability. J. Membr. Biol. 199, 29-38.

Van Itallie,C.M., Fanning,A.S., and Anderson,J.M. (2003). Reversal of charge selectivity in cation or anion-selective epithelial lines by expression of different claudins. Am. J. Physiol Renal Physiol 285, F1078-F1084.

van Noort,M., Meeldijk,J., van der,Z.R., Destree,O., and Clevers,H. (2002). Wnt signaling controls the phosphorylation status of beta-catenin. J. Biol. Chem. 277, 17901-17905.

van Weeren,P.C., de Bruyn,K.M., Vries-Smits,A.M., van Lint,J., and Burgering,B.M. (1998). Essential role for protein kinase B (PKB) in insulin-induced glycogen synthase kinase 3 inactivation. Characterization of dominant-negative mutant of PKB. J. Biol. Chem. 273, 13150-13156.

Wakabayashi,M., Ito,T., Mitsushima,M., Aizawa,S., Ueda,K., Amachi,T., and Kioka,N. (2003). Interaction of lp-dlg/KIAA0583, a membrane-associated guanylate kinase family protein, with vinexin and beta-catenin at sites of cell-cell contact. J. Biol. Chem. 278, 21709-21714.

Ward,P.D., Klein,R.R., Troutman,M.D., Desai,S., and Thakker,D.R. (2002). Phospholipase C-gamma modulates tight junction permeability through hyperphosphorylation of tight junction proteins. J. Biol. Chem.

Weber,E., Berta,G., Tousson,A., St John,P., Green,M.W., Gopalokrishnan,U., Jilling,T., Sorscher,E.J., Elton,T.S., Abrahamson,D.R., and . (1994). Expression and polarized targeting of a rab3 isoform in epithelial cells. J. Cell Biol. 125, 583-594.

Weber,S., Schneider,L., Peters,M., Misselwitz,J., Ronnefarth,G., Boswald,M., Bonzel,K.E., Seeman,T., Sulakova,T., Kuwertz-Broking,E., Gregoric,A., Palcoux,J.B., Tasic,V., Manz,F., Scharer,K., Seyberth,H.W., and Konrad,M. (2001). Novel paracellin-1 mutations in 25 families with familial hypomagnesemia with hypercalciuria and nephrocalcinosis. J. Am. Soc. Nephrol. 12, 1872-1881.

Weiler,F., Marbe,T., Scheppach,W., and Schauber,J. (2004). Influence of protein kinase C on transcription of the tight junction elements ZO-1 and occludin. J. Cell Physiol.

Welham,M.J., Learmonth,L., Bone,H., and Schrader,J.W. (1995). Interleukin-13 signal transduction in lymphohemopoietic cells. Similarities and differences in signal transduction with interleukin-4 and insulin. J. Biol. Chem. 270, 12286-12296.

Welsh,G.I., Miller,C.M., Loughlin,A.J., Price,N.T., and Proud,C.G. (1998). Regulation of eukaryotic initiation factor eIF2B: glycogen synthase kinase-3 phosphorylates a conserved serine which undergoes dephosphorylation in response to insulin. FEBS Lett. 421, 125-130.

White,M.F., Livingston,J.N., Backer,J.M., Lauris,V., Dull,T.J., Ullrich,A., and Kahn,C.R. (1988). Mutation of the insulin receptor at tyrosine 960 inhibits signal transmission but does not affect its tyrosine kinase activity. Cell 54, 641-649.

Wijnhoven,B.P., Dinjens,W.N., and Pignatelli,M. (2000). E-cadherin-catenin cell-cell adhesion complex and human cancer. Br. J. Surg. 87, 992-1005.

Williams,L.A., Martin-Padura,I., Dejana,E., Hogg,N., and Simmons,D.L. (1999). Identification and characterisation of human Junctional Adhesion Molecule (JAM). Mol. Immunol. 36, 1175-1188.

Willott,E., Balda,M.S., Heintzelman,M., Jameson,B., and Anderson,J.M. (1992). Localization and differential expression of two isoforms of the tight junction protein ZO-1. Am. J. Physiol 262, C1119-C1124.

Winkelstein,J.A., Marino,M.C., Johnston,R.B., Jr., Boyle,J., Curnutte,J., Gallin,J.I., Malech,H.L., Holland,S.M., Ochs,H., Quie,P., Buckley,R.H., Foster,C.B., Chanock,S.J., and Dickler,H. (2000). Chronic granulomatous disease. Report on a national registry of 368 patients. Medicine (Baltimore) 79, 155-169.

Wirtz,S. and Neurath,M.F. (2000). Animal models of intestinal inflammation: new insights into the molecular pathogenesis and immunotherapy of inflammatory bowel disease. Int. J. Colorectal Dis. 15, 144-160.

Wittchen,E.S., Haskins,J., and Stevenson,B.R. (1999). Protein interactions at the tight junction. Actin has multiple binding partners, and ZO-1 forms independent complexes with ZO-2 and ZO-3. J. Biol. Chem. 274, 35179-35185.

Wong,V. (1997). Phosphorylation of occludin correlates with occludin localization and function at the tight junction. Am. J. Physiol 273, C1859-C1867.

Wong,V. and Gumbiner,B.M. (1997). A synthetic peptide corresponding to the extracellular domain of occludin perturbs the tight junction permeability barrier. J. Cell Biol. 136, 399-409.

Woscholski,R., Kodaki,T., McKinnon,M., Waterfield,M.D., and Parker,P.J. (1994). A comparison of demethoxyviridin and wortmannin as inhibitors of phosphatidylinositol 3-kinase. FEBS Lett. 342, 109-114.

Woywodt,A., Neustock,P., Kruse,A., Schwarting,K., Ludwig,D., Stange,E.F., and Kirchner,H. (1994). Cytokine expression in intestinal mucosal biopsies. In situ hybridisation of the mRNA for interleukin-1 beta, interleukin-6 and tumour necrosis factor-alpha in inflammatory bowel disease. Eur. Cytokine Netw. 5, 387-395.

Wright,R. (1970). Ulcerative colitis. Gastroenterology 58, 875-897.

Yamamoto,T., Harada,N., Kano,K., Taya,S., Canaani,E., Matsuura,Y., Mizoguchi,A., Ide,C., and Kaibuchi,K. (1997). The Ras target AF-6 interacts with ZO-1 and serves as a peripheral component of tight junctions in epithelial cells. J. Cell Biol. 139, 785-795.

Yamamoto,T., Harada,N., Kawano,Y., Taya,S., and Kaibuchi,K. (1999). In vivo interaction of AF-6 with activated Ras and ZO-1. Biochem. Biophys. Res. Commun. 259, 103-107.

Yamamoto,Y., Nishimura,N., Morimoto,S., Kitamura,H., Manabe,S., Kanayama,H.O., Kagawa,S., and Sasaki,T. (2003). Distinct roles of Rab3B and Rab13 in the polarized transport of apical, basolateral, and tight junctional membrane proteins to the plasma membrane. Biochem. Biophys. Res. Commun. 308, 270-275.

Yao,Z., Painter,S.L., Fanslow,W.C., Ulrich,D., Macduff,B.M., Spriggs,M.K., and Armitage,R.J. (1995). Human IL-17: a novel cytokine derived from T cells. J. Immunol. 155, 5483-5486.

Yao,Z., Spriggs,M.K., Derry,J.M., Strockbine,L., Park,L.S., Vandenbos,T., Zappone,J.D., Painter,S.L., and Armitage,R.J. (1997). Molecular characterization of the human interleukin (IL)-17 receptor. Cytokine 9, 794-800.

Youakim,A. and Ahdieh,M. (1999). Interferon-gamma decreases barrier function in T84 cells by reducing ZO-1 levels and disrupting apical actin. Am. J. Physiol 276, G1279-G1288.

Zahraoui,A., Joberty,G., Arpin,M., Fontaine,J.J., Hellio,R., Tavitian,A., and Louvard,D. (1994). A small rab GTPase is distributed in cytoplasmic vesicles in non polarized cells but colocalizes with the tight junction marker ZO-1 in polarized epithelial cells. J. Cell Biol. 124, 101-115.

Zamora,S.A., Hilsden,R.J., Meddings,J.B., Butzner,J.D., Scott,R.B., and Sutherland,L.R. (1999). Intestinal permeability before and after ibuprofen in families of children with Crohn's disease. Can. J. Gastroenterol. 13, 31-36.

Zeissig,S., Bojarski,C., Buergel,N., Mankertz,J., Zeitz,M., Fromm,M., and Schulzke,J.D. (2004). Downregulation of epithelial apoptosis and barrier repair in active Crohn's disease by tumour necrosis factor alpha antibody treatment. Gut 53 , 1295-1302.

Zhong,Y., Saitoh,T., Minase,T., Sawada,N., Enomoto,K., and Mori,M. (1993). Monoclonal antibody 7H6 reacts with a novel tight junction-associated protein distinct from ZO-1, cingulin and ZO-2. J. Cell Biol. 120, 477-483.

Zuckerman,M.J. and Watts,M.T. (1993). Intestinal permeability to 51Cr-ethylenediaminetetraacetate in patients with ulcerative colitis. Am. J. Gastroenterol. 88, 1978-1979.

Zund,G., Madara,J.L., Dzus,A.L., Awtrey,C.S., and Colgan,S.P. (1996). Interleukin-4 and interleukin-13 differentially regulate epithelial chloride secretion. J. Biol. Chem. 271, 7460-7464.